STATUS OF GROUNDWATER QUALITY IN LUDHIANA DISTRICT OF PUNJAB, INDIA

A Thesis Submitted
In Partial Fulfilment of the Requirements
for the Degree of

DOCTOR OF PHILOSOPHY

by

DEEPALI GOYAL
(Roll No. 2K18/PHDEN/02)

Under the supervision of

Prof. S.K. SINGH

and

Prof. A.K. HARITASH

To the

Department of Environmental Science and Engineering

DELHI TECHNOLOGICAL UNIVERSITY
Delhi-110042, India

May, 2026

STATUS OF GROUNDWATER QUALITY IN LUDHIANA DISTRICT OF PUNJAB, INDIA

A Thesis Submitted
In Partial Fulfilment of the Requirements
for the Degree of

DOCTOR OF PHILOSOPHY

in

ENVIRONMENTAL ENGINEERING

by

DEEPALI GOYAL
(Roll No. 2K18/PHDEN/02)

Under the supervision of

Prof. S.K. SINGH

and

Prof. A.K. HARITASH

To the

Department of Environmental Science and Engineering

DELHI TECHNOLOGICAL UNIVERSITY
(Formerly Delhi College of Engineering)
Shahbad Daulatpur, Main Bawana Road, Delhi-110042, India

May, 2026

..... ********** .....

Dedicated to

My pillars of strength

My Father

Mr. Bharat Bhushan Goyal

and

My Husband

Mr. Piyush Ranjan

..... ********** .....

ACKNOWLEDGEMENTS

Reflecting upon the arduous and intellectually challenging journey of my doctoral research, I am profoundly aware of the invaluable contributions of numerous individuals whose steadfast support and guidance were essential to the successful completion of this scholarly pursuit. At this pivotal juncture of academic accomplishment, it is my privilege to formally acknowledge and extend my deepest gratitude to all those who have played a seminal role in enabling my progress towards this significant milestone.

At the forefront of this acknowledgement, I wish to express my deepest gratitude to my esteemed research supervisor, Prof. S. K. Singh, whose astute guidance, discerning insights, and unwavering encouragement served as a constant beacon throughout the rigorous and demanding journey of my doctoral research. His thoughtful counsel, constructive critique, and enduring patience instilled in me a profound sense of intellectual confidence and scholarly direction. Prof. Singh's mentorship has been instrumental in shaping the trajectory of my academic endeavours, for which I remain sincerely and deeply indebted.

Equally deserving of recognition is my esteemed co-supervisor, Prof. A. K. Haritash, whose consistent guidance, expert counsel, and generous cooperation have left a lasting and profound impact on my academic journey. His extensive expertise, insightful perspective, and unwavering commitment to scholarly excellence provided invaluable support at critical junctures of my research, significantly enhancing the rigor, depth, and quality of this work and contributing greatly to its successful completion.

I gratefully acknowledge Delhi Technological University for providing essential institutional support for my doctoral research. I sincerely thank the Hon'ble Vice-Chancellor, DTU, for strengthening the research infrastructure and facilitating access to laboratory facilities and analytical instruments. I also express my gratitude to Dr. Geeta Singh, Head of the Department of Environmental Science and Engineering, and all faculty members of the department for their support and encouragement. I am deeply thankful to the University Grants Commission (UGC) for providing financial assistance under the Junior Research Fellowship (JRF) Scheme (No. 3710 / NET-NOV 2017), which enabled me to carry out my research with dedication.

I wish to place on record my sincere appreciation for the guidance and encouragement received from my seniors—Dr. Vandana Shan, Dr. Sakshi, Dr. Manisha Verma, Dr. Amrit Kumar, and Dr. Shailendra Kumar Yadav—as well as for the invaluable academic companionship and collaborative support of my colleagues—Ms. Riki

Sarma, Dr. Ali Reza Noori, Ms. Chitrakshi, Ms. Rachna Garg, Ms. Mallika Vashist, Mr. Kulvendra Patel, Ms. Lavi Dhiman, Dr. Monika Sharma, Dr. Vighnesh Mohan, Dr. Kanagraj Rajgopal, Mr. Ravi Pratap Singh Jadon, and Ms. Ankita Gupta. Their scholarly discussions, collaborative spirit, and moral support were instrumental in sustaining my academic resolve, particularly during challenging phases of this journey.

I further acknowledge with deep gratitude the support received during data collection and analytical interpretation from Mr. Darshan Singh; Prof. Rakesh Sharda, HOD, Dept. of Soil and Water Engineering, Punjab Agricultural University; Prof. Samanpreet Kaur, Professor, Dept. of Soil and Water Engineering, Punjab Agricultural University; Dr. Kriti Mishra, Senior Scientist, Central Ground Water Board; and Mr. Manoj Shrivastav, Former Regional Director, Central Ground Water Board. Their cooperation in facilitating access to relevant datasets, coupled with their invaluable guidance in the theoretical understanding and execution of modelling analyses, significantly strengthened the scientific rigor, analytical depth, and overall quality of the present research.

I extend my sincere gratitude to Mr. Vishal Goyal, Ms. Gurpreet Kaur, Mr. Kishan Singh, Mr. Rajinder Singh, Mr. Jagdev Singh, and Mr. Pawan for their invaluable assistance during sampling activities, and I gratefully acknowledge the cooperation and goodwill of the local community. I also thank Mr. Harshit Chawla and Mr. Anthony Nimely Chea, Jr. for their assistance during laboratory analysis. My sincere appreciation is extended to the laboratory staff—Ms. Navita, Mr. Sunil, Mr. Sahil, and Ms. Sita—for their diligent and tireless support during experimental work, and to the departmental office staff, Mr. Jaiveer and Mr. Ajit Pandey, for their efficient administrative assistance.

I respectfully express my gratitude to my spiritual guide, H.H. Sri Sri Ravi Shankar, whose wisdom and teachings provided inner strength and clarity during the course of my doctoral studies. Finally, and most importantly, I express my profound and heartfelt gratitude to my family, whose enduring faith, patience, and encouragement formed the bedrock of my perseverance. I am deeply indebted to my father, Mr. Bharat Bhushan Goyal; my mother, Ms. Anju Goyal; my father-in-law, Mr. Ram Chandra Singh; my mother-in-law, Ms. Kiran Singh; and my paternal uncle, Late Mr. S. K. Goyal, for their constant support and belief in my aspirations. Above all, I offer my deepest gratitude to my husband, Mr. Piyush Ranjan, whose unwavering encouragement, personal sacrifices, and unfailing faith in me made this scholarly pursuit possible. I also wish to acknowledge the encouragement and support of my friends, particularly Dr. Viruja Ummat, whose presence remained a source of motivation throughout this journey.

Deepali Goyal

DELHI TECHNOLOGICAL UNIVERSITY

(Formerly Delhi College of Engineering)
Shahbad Daulatpur, Main Bawana Road, Delhi-42

CANDIDATE'S DECLARATION

I, Deepali Goyal, hereby certify that the work which is being presented in the thesis entitled **"Status of Groundwater Quality in Ludhiana District of Punjab, India"** in partial fulfilment of the requirements for the award of the Degree of Doctor of Philosophy, submitted to the Department of Environmental Science and Engineering, Delhi Technological University is an authentic record of my own work carried out during the period Aug 2018 to May 2026 under the joint supervision of Prof. S.K. Singh (Supervisor) and Prof. A.K. Haritash (Co-Supervisor).

The matter presented in the thesis has not been submitted by me for the award of any other degree from this or any other institution.

Candidate's Signature
(Deepali Goyal)

This is to certify that the student has incorporated all the corrections suggested by the examiners in the thesis, and the statement made by the candidate is correct to the best of our knowledge.

Signature of Supervisor(s)

Signature of External Examiner
(Prof. D.K. Singh,
Principal Scientist, IARI)

DELHI TECHNOLOGICAL UNIVERSITY

(Formerly Delhi College of Engineering)
Shahbad Daulatpur, Main Bawana Road, Delhi-42

CERTIFICATE BY THE SUPERVISOR

Certified that **Deepali Goyal** (Roll No. 2K18/PHDEN/02) has carried out her research work presented in this thesis entitled **"Status of Groundwater Quality in Ludhiana District of Punjab, India"** for the award of **Doctor of Philosophy** from the Department of Environmental Science and Engineering, Delhi Technological University, Delhi, under our supervision. The thesis embodies the results of original work, and studies were carried out by the student herself. The contents of the thesis have not formed the basis for the award of any other degree to the candidate or to any other person at this or any other University/Institution.

(Signature of Supervisor)

Prof. S.K. Singh,
Professor,
Department of Environmental Science and Engineering,
Delhi Technological University;
Former-Vice Chancellor,
Rajasthan Technical University,
Kota, Rajasthan – 324010

(Signature of Co- Supervisor)

Prof. A.K. Haritash,
Professor,
Department of Environmental Science and Engineering,
Delhi Technological University

Date:

DELHI TECHNOLOGICAL UNIVERSITY

(Formerly Delhi College of Engineering)
Shahbad Daulatpur, Main Bawana Road, Delhi-42

PLAGIARISM VERIFICATION

Title of the Thesis: **Status of Groundwater Quality in Ludhiana District of Punjab, India.**

Total Pages:

Name of the Research Scholar: Deepali Goyal

Supervisor (s)

(1) Prof. S.K. Singh

(2) Prof. A.K. Haritash

Department of Environmental Science and Engineering

This is to report that the above thesis was scanned for similarity detection. Process and outcome are given below:

Software used: Similarity Index: Total Word Count:

Date:

Candidate's Signature **Signature of Supervisor(s)**

Table of Contents

CHAPTER 3
METHODOLOGY

List of Tables

List of Figures

List of Abbreviations

ANN	Artificial Neural Network
APHA	American Public Health Association
AVI	Aquifer Vulnerability Index
CAI	Chloro-Alkaline Index
CBE	Charge Balance Error
CGWB	Central Ground Water Board
COP	Concentration of flow, Overlying layers, and Precipitation regime
DI	DRASTIC Index
DRASTIC	Depth to Water table, Recharge, Aquifer media, Soil media, Topography, Impact of vadose zone, Hydraulic Conductivity
EC	Electrical Conductivity
EPIK	Epikarst, Protective cover, Infiltration conditions, Karst network
FAO	Food and Agriculture Organization
FGI	Flow Guided Interpolation
GALDIT	Groundwater occurrence, Aquifer hydraulic conductivity, Level of water table above sea level, Distance from shore, Impact of existing seawater intrusion, Thickness of aquifer
GEC-15	Groundwater Estimation Committee (2015 methodology)
GIS	Geographic Information System
GOD	Groundwater occurrence, Overlying strata, Depth to groundwater
GPS	Global Positioning System
IAP	Ion Activity Product
IDW	Inverse Distance Weighted
IWQI	Irrigation Water Quality Index
LULC	Land Use Land Cover
MODFLOW	Modular Finite Difference Groundwater Flow Model
MT3DMS	Modular Three-Dimensional Multi-Species Transport Model
NRSC	National Remote Sensing Centre
PCA	Principal Component Analysis
PI	Permeability Index
RMSE	Root Mean Square Error
SAR	Sodium Adsorption Ratio
SDG	Sustainable Development Goal

SI	Saturation Index
SINTACS	Soggiacenza, Infiltrazione, Nonsaturo, Tipologia della copertura, Acquifero, Conducibilità idraulica, Superficie topografica
SSP	Soluble Sodium Percentage
TA	Total Alkalinity
TDS	Total Dissolved Solids
TH	Total Hardness
USEPA	United States Environmental Protection Agency
WQI	Water Quality Index
WWQA	World Water Quality Alliance

Abstract

The present study provides an integrated assessment of groundwater quality in Ludhiana district, Punjab, based on 152 groundwater samples characterized by 18 physicochemical parameters. These were synthesized into a Drinking Water Quality Index (WQI) to evaluate potable suitability. The WQI classification shows that 2.6% of samples are "excellent" and 57.9% "good," whereas 32.9%, 4.0%, and 2.6% fall into "poor," "very poor," and "unsuitable" categories, respectively, indicating spatially heterogeneous degradation in groundwater quality.

Hydrogeochemical characterization, supported by facies diagrams, ionic diagnostics, saturation indices, and multivariate statistics, indicates that groundwater chemistry is primarily governed by carbonate and silicate weathering, with active cation exchange. Saturation indices show that groundwater is generally supersaturated with respect to calcite, dolomite, and aragonite, and undersaturated with respect to halite, fluorite, and sylvite. Spatial variability in nitrate and other key parameters reflects localized agricultural and urban influences, while IDW interpolation in QGIS has been used to generate spatial distribution maps of major ions.

In the present study, irrigation suitability has been evaluated using salinity, sodicity, and carbonate–bicarbonate hazard indices, including EC, %Na, SAR, and PI. In addition, an Irrigation Water Quality Index (IWQI) is computed using EC, SAR, Na^+, Cl^-, and HCO_3^- concentrations. Salinity classification indicates that 62.5% of samples fall within the "medium" EC range (250–750 µS/cm), while 37.5% fall within the "high" category. Hazard assessment indicates that 75% of samples fall within the excellent-to-permissible range based on %Na, 97.4% belong to the S1 class (low sodicity) based on SAR, and all samples fall within PI Classes I–II. However, IWQI-based classification indicates irrigation constraints, with 21.7% of samples under "severe restriction" (IWQI < 40), 37.5% under "high restriction" (40–55), 33.6% under "moderate restriction" (55–70), and only 7.2% under "low restriction" (70–85). IDW-based GIS mapping delineates zones of elevated irrigation risk, particularly in eastern Samrala and Khanna, parts of Ludhiana II and Machhiwara, and southern to western

Pakhowal and Sidhwan Bet, whereas low-restriction pockets are confined to limited villages such as Sherpur Kalan, Bardeke, Hathur, and Dholanwal.

An ANN-based predictive model for IWQI is developed using the multilayer perceptron architecture in IBM SPSS with standardized inputs. The optimal network includes five input neurons (EC, SAR, Na^+, Cl^-, HCO_3^-), two hidden layers, and one sigmoid-activated output neuron, trained using batch learning and gradient-descent backpropagation. The model achieved RMSE values of 0.09 for training and 0.07 for testing, indicating strong predictive performance and close agreement between observed and simulated IWQI values. Sensitivity analysis shows that Cl^- has the highest normalized importance (100%), followed by SAR (59.7%), Na^+ (58.5%), HCO_3^- (53.1%), and EC (27.2%), confirming the dominant influence of salinity and sodicity on irrigation water quality.

Additionally, nitrate distribution has been examined to distinguish regional hydrogeological controls from localized anthropogenic influences. The weak statistical association between nitrate concentration and hydraulic parameters indicates that regional groundwater flow is not the principal control on nitrate occurrence. The lack of a coherent downgradient nitrate plume suggests that nitrate distribution is governed mainly by localized recharge and anthropogenic inputs. A conservative nitrate-transport scenario simulated by coupling the calibrated transient MODFLOW flow model with MT3D-USGS shows a decline in mean nitrate concentration from 8.86 mg/l in Year 1 to 6.51 mg/l in Year 10 (~27% reduction), contraction of the >45 mg/l footprint from ~1.70% to ~0.88%, and a reduction in peak concentrations to a maximum simulated value of ~69.95 mg/l after 10 years.

Keywords: *Hydrogeochemical characterization, Spatial interpolation, Principal component analysis, Water quality index, Groundwater flow and transport modelling*

CHAPTER 1

INTRODUCTION

1.1 Background

Recent times have seen a relentless increase in the freshwater demand all over the world due to the rapid development in agricultural, commercial, industrial and residential spheres of human life. Groundwater forms an important part of global freshwater supply, contributing roughly one quarter of global renewable freshwater resources (Food and Agriculture Organization of the United Nations [FAO], 2003). This essential resource plays a pivotal role in supplying nearly half of the world's drinking water and accounts for 43% of global consumptive irrigation usage (World Water Quality Alliance [WWQA], 2021). Also, within the natural environment, groundwater significantly contributes to baseflow in rivers and provides crucial support to ecosystems dependent on it. However, there is over reliance of communities on groundwater to meet their needs. It has resulted in lowering of groundwater levels in large parts of the world (Rodell et al., 2009). It has increasingly become vulnerable to over-exploitation especially in areas where surface water sources are either not available (arid and semi-arid areas) or are polluted (Jha & Sinha, 2010).

Groundwater is a complex resource. Its residence time can range from months to millions of years as the natural cycles of its recharge and flow are considerably slower than surface water. It is thus, not able to replenish as quickly as would be needed in this current situation of overwhelming withdrawal in many cities (World Bank, 2010; Jasechko et al., 2017). Also, other than over-utilisation, another major concern surrounding groundwater is its growing quality deterioration (Reddy, 2008). Human activities such as excessive overdraft of water for industrial and agricultural requirements, use of fertilizers and pesticides, and discharge of industrial effluents can enhance dissolution of salts and promote the spread of pollutants in aquifers. This has resulted in widespread groundwater quality deterioration across India (Central Ground Water Board [CGWB], 2018). Therefore, similar to over-exploitation, the reason for

unbridled groundwater quality degradation lies in the rapid development and expansion of human life (Dhillon et al., 2019; Haritash et al., 2017).

1.2 Concerns related to groundwater quality

The general belief related to groundwater is that it is qualitatively safe, as it is formed by water that percolates downwards through the layers of sediments which tend to remove different pathogenic and chemical constituents from it. Although, it is only deeper, confined groundwater bodies, which are often better protected from recent contamination because longer travel times and low-permeability layers can attenuate pollutants (Schmoll et al., 2013). However, they are not immune to contamination, as groundwater can still be affected by various geogenic sources, as well as multiple pollution pathways and transport processes (Lapworth et al., 2022). Beneath the surface, the evolution of groundwater takes place through a variety of processes such as rock mineral reactions, redox processes and cationic exchanges; which are affected by recharge sources, hydrological setting, the mineralogy of the watersheds and geological structure of the aquifers (Duan et al., 2022; Liu et al., 2022a; Wei et al., 2022). Therefore, Aquifer characteristics and soil conditions can significantly alter the groundwater chemical composition (Sarma & Singh, 2021). However, in addition to geogenic, anthropogenic factors also increasingly contribute towards its quality deterioration. In particular, increasing urbanization, agricultural intensification, and unregulated industrial and domestic waste disposal have emerged as significant anthropogenic sources of groundwater contamination. These human-induced pressures often interact with natural hydrogeochemical processes, enhancing the mobilization of potentially toxic constituents and resulting in complex groundwater quality challenges with serious implications for public health and environmental sustainability. If the recharge sources are contaminated through industrial and agricultural activities by the use of fertilizers, pesticides or industrial chemicals, then significant negative impacts on groundwater quality can be observed (He et al., 2022; Noori & Singh, 2024). Many studies across the world are reporting increased nitrate contamination (Abascal et al., 2022; Mahanta et al., 2022; Rezaei et al., 2017; Vetrimurugan & Elango, 2015), increased metal pollution and organic

contamination of groundwater (Dong et al., 2015; Zhao et al., 2019; Singh et al., 2017).This accelerating contamination of groundwater against the backdrop of expeditious growth in population, coupled with rapid economic development have directed the researchers to focus their research on both geogenic and human induced groundwater pollution.

1.3 The importance of Groundwater research

Since water quality can directly and indirectly impact the health of humans, plants, crops and other creatures, analysing the groundwater for different uses plays a pivotal part in water management and sustainable development. The spatial and temporal fluctuations of groundwater quality and its periodic assessments are of a critical concern worldwide. To address the concerns associated with groundwater pollution and scarcity, it is important to develop an elaborate understanding of its flow, draft, recharge and pollutant transport (Lapworth et al., 2022). This has been attempted by many researchers in past through local scale manual hydrological, aquifers and groundwater investigations. Hydrogeochemical characterization of groundwater systems has been extensively investigated in many regions worldwide (Promilton et al., 2025; Liu et al., 2022b). These studies provide detailed insights into the natural and anthropogenic processes influencing groundwater quality, and thereby improve understanding of local groundwater fluctuations and pollution dynamics. However, a broader-scale perspective that extends beyond local boundaries enables identification of regional drivers and causal mechanisms governing groundwater depletion and contamination (Dennehy et al., 2015). Therefore, the use of advance technologies such as geospatial and remote sensing tools; numerical and analytical models; and conjugation of geospatial tools with modelling softwares has been rapidly picking up pace in recent times. Both ground-based manual investigations and use of geospatial tools with or without groundwater models together are needed to completely comprehend groundwater, the invisible resource. Ground-based investigations are essential for defining realistic hydrogeological parameters and generating reliable input datasets required for the calibration and validation of geospatial and numerical models, thereby enabling these tools to more accurately represent natural groundwater

systems (Sahoo & Sahoo, 2019). Likewise, the numerical and spatial tools help to understand, analyse and predict the spatial and temporal variations of groundwater overdraft and pollution. Therefore, both of them are needed to develop the detailed understanding of dynamics of aquifer system, hydrogeology and groundwater flow, its distribution and pollution spread patterns of the area (Vetrimurugan et al., 2017). These tools overcome the issue of scale and provide a holistic and comprehensive picture of the entire region under consideration.

1.4 Groundwater analysis techniques

Many public administration bodies around the world are conducting regional groundwater assessments in order to essentially evaluate its availability and accessibility to their citizens and make sustainable management plans for future. Increasing number of researches are being conducted and periodically sponsored to monitor several hydrologic and hydrochemical variables, collecting both satellite and ground-based observation data to develop dynamically growing and efficient groundwater management plans (Akinwumiju & Olorunfemi, 2019). This has resulted in the inflow of the huge amount of data and this necessitates the wide use of advance softwares for modelling and analysis. Many techniques that have been suggested by researchers to better interpret water quality and model it, are discussed below.

The use of geographic information system (GIS) to prepare spatial distribution maps is a significant tool that helps in the preparation of interpolated maps of different quality parameters which have been taken at point locations. This technique has helped researchers in determining the values of parameters at unsampled location (Mirzaei & Sakizadeh, 2016). Likewise, water quality index (WQI) is a technique that has been considered reliable due to its adaptability and statistical simplicity (Sener et al., 2017). The calculated index provides a benchmark against which relative risk of using the water for a specific activity like irrigation or drinking can be determined. This method differentiates the area into categories for comparative evaluation and is not an index to calculate absolute water quality. Furthermore, multivariate statistical analysis such as principal component analysis (PCA) is also a widely used technique that explains

the maximum amount of data variability by reducing data dimensions and projecting its structure in a multivariate space (Wu et al., 2020). It becomes easier to inspect the data for hidden patterns and relationships without individually inspecting parameter to parameter relationship (Masood et al., 2022). The saturation index values can help us to understand if the subsurface mineral is in undersaturated, supersaturated or equilibrium condition in groundwater (Singh et al., 2017; Clark, 2015). Different lithogenic influences derived from various sedimentary, igneous or metamorphic sources can be analysed from bivariate plots of ionic concentrations, gibbs plot and piper plot (Sadeqi, 2023; Elumalai et al., 2023; Chitrakshi & Haritash, 2018; Thirumurugan et al., 2018). The analysis of groundwater using these methods can help government and people alike to decipher the present status of water quality to support policies and take management decisions.

One of the important end uses of groundwater is its use for irrigating crops in agricultural practices. Poor-quality groundwater can lead to soil degradation and reduced fertility. This can result in soil salinization which can hampers plant growth and reduces the long-term productivity of the land. Also, the high level of contamination or salinity can directly harm plants and impact their overall health. Therefore, when it comes to irrigation, groundwater should be analysed with respect to several factors such as total dissolved solids, major cations and anions. Researchers in past have identified three prevalent hazards associated with irrigation water quality worldwide, which include salinity, sodium and carbonate-bicarbonate hazard. These could be measured using specific ion toxicity or ratios such as SAR, %Na and PI (Li et al., 2013; Nikolaou et al., 2020). Additionally, understanding irrigation water quality is often complicated as it is triggered by multiple and combined effects of different quality parameters. Therefore, calculating an integrated index has been suggested as a better solution by previous studies (Ben Brahim et al., 2022, Aravinthasamy et al., 2020) especially because it can simplify the large and complex inter-related quality data to a single IWQI (irrigation water quality index) value. Therefore, calculating such an index is most useful for comparative purposes and helps the public to better understand the water quality for use in agriculture.

Also, recently several studies have addressed the developments in integration of artificial intelligence for the estimation of water quality via artificial neural networks. Modelling applications using artificial neural networks have found wide spread usage in not just engineering field but also in water quality analyses (Bhavya et al., 2023, Stylianoudaki et al., 2022, Sunayana et al., 2020) and estimation of water quality index (Aalipour et al., 2022, Yilma et al., 2018, Ismael et al., 2021). ANN models can determine the underlying relation between input and output parameters and optimize the network based on it. As a data-driven approach, ANNs are quite suitable for solution of complex problems. Moreover, they are capable of a good generalization capability (Maier & Dandy, 2000).

1.5 Need of the study

Groundwater is extensively used for irrigation in agriculture. This is however more extensive in state of Punjab because of government subsidies on electricity and irrigation equipments for farmers. Out of the 12 districts in Punjab that irrigate more than 50% of their farms through groundwater, Ludhiana shares the highest percentage of 95.6%, this implies that almost all of the agricultural farms in Ludhiana are irrigated through groundwater. The dominant cropping system here is rice-wheat. Statistics suggest that the productivity of rice and of wheat is highest in Ludhiana i.e., 4.37 ton ha^{-1} and 4.51 ton ha^{-1} respectively. This implies that the high load of fertilizers is used in the fields here, which results in nitrate contamination problem in this area. Previous studies carried out in this area have reported high value of NO_3^- in groundwater exceeding 45 mg/l in many parts of the district.

The 73% of the total municipal solid waste is being generated in the 5 mega cities of the State i.e Ludhiana, Jalandhar, Amritsar, Bathinda and Patiala. Also, famed for its history of hosiery, textiles and bicycles the indiscriminate disposal of industrial waste in the Ludhiana city of the district poses a potential threat to its groundwater. Hence, there is rampant disposal of waste in the city. Therefore, this situation necessitates a detailed study of the area's groundwater quality, aquifer properties, their response to recharge and discharge fluctuations, the quantitative release of

contaminants, and their flow and transport across the area. Thus, groundwater quality assessment and modeling will prove to be effective in carrying out such a study. The review of literature points out that comprehensive evaluation of the groundwater quality has not been done for Ludhiana district of Punjab. Also, though the groundwater flow model of the area has been made earlier, the model has not been used to further understand contaminant spread in the area.

1.6 Aims and Objectives of the research

For this study, the area under consideration is Ludhiana district in Punjab, India. Groundwater quality in Ludhiana district, Punjab, is facing a critical challenge due to rapid urbanization and industrialization. The region's heavy reliance on groundwater for irrigation and drinking water has led to overexploitation, causing both resource depletion and deterioration in the quality of shallow aquifers, prompting an increasing shift toward the use of deeper tube wells to access drinking water. While existing studies have touched on the topic of groundwater quality in Ludhiana, a comprehensive investigation is needed that incorporates multiple analytical approaches. Therefore, a study is proposed to assess the suitability of groundwater for both drinking and irrigation purposes, employing established methodologies like multivariate statistical analysis, water quality index calculations, assessments of sodium adsorption ratio, soluble sodium percentage, irrigation water quality index (IWQI) and the use of artificial neural networks to estimate IWQI. The spatial distribution of contaminants and index values will be determined using interpolation techniques. This research is crucial in empowering farmers to make informed decisions regarding irrigation practices and mitigate the negative impacts of poor-quality water. Furthermore, the study's findings can guide policymakers in the development of sustainable irrigation strategies and the reduction of environmental risks associated with the leaching of contaminants. By providing researchers with essential tools for predicting water quality and conducting spatial analysis, this study contributes to a more thorough understanding of the groundwater quality situation in the region, promoting responsible water resource management in line with Sustainable Development Goal 6. Moreover, the long-term behavior of groundwater in the study

region will be assessed using a groundwater modeling approach to understand the flow tendency of subsurface water, its fluctuation trend, and pollutant fate and transport. This is particularly important given the increasing contamination of groundwater in Punjab, attributed to the increase in agricultural, domestic and industrial waste.

Following objectives will be studied in this proposed research-

i) To evaluate groundwater quality and suggest its suitable use.
ii) To ascertain groundwater flow and contaminant spread through groundwater in the study area.
iii) To perform predictive analysis of potential evolution of contamination of concern for different future scenarios.

1.7 Organization of the thesis

The thesis has been organized in five chapters. A brief description of each chapter is given below.

Chapter 1: Introduction discusses the critical challenges faced by the world with respect to increasing groundwater scarcity and its deteriorating quality due to rapid urbanization and industrialization. It highlights the overexploitation of groundwater resources and the decline in the quality of shallow sources. The chapter also presents the research problem, objectives, scope and the significance of this study.

Chapter 2: Literature Review assesses key studies on groundwater quality and vulnerability conducted worldwide, with a focus on analytical techniques such as water quality indices and modelling approaches. It introduces concepts of groundwater vulnerability and then examines GIS-based geostatistical and overlay/index methods, outlining their principles, applications, and limitations. It also discusses numerical groundwater flow and solute transport models and the coupling of GIS with these models for spatially explicit, quantitative vulnerability mapping. Together, these sections synthesise existing knowledge and build the context for the present research.

Chapter 3: Materials and Method describes the study area, including the geographical and environmental context of Ludhiana district. It details the sampling strategies, data collection methods, and analytical techniques employed in the research, such as multivariate statistical analysis, water quality index calculations, sodium adsorption ratio, and irrigation water quality index evaluations. Additionally, this chapter explains the use of artificial neural networks for predictive analysis and interpolation techniques for mapping contaminant distribution. The groundwater modeling approach for assessing flow tendencies and pollutant transport is also elaborated here.

Chapter 4: Results and Discussion present the results of the analyses and discusses it in depth. It evaluates groundwater quality in terms of its suitability for drinking and irrigation purposes, based on findings from WQI, SAR, %Na, and IWQI calculations. The spatial distribution of contaminants and index values is analyzed, alongside groundwater flow and contaminant transport patterns. Predictive analysis of contaminant evolution under different scenarios is also explored, providing valuable insights into the region's water quality challenges.

Chapter 5: Conclusion, Future scope and Social impact summarizes the key findings of your research, reflecting on the objectives outlined in the introduction. Recommendations for stakeholders, including farmers, policymakers, and researchers, are provided to address groundwater quality issues effectively. Suggestions for future research directions, based on the limitations and findings of your study, are also included in this chapter. The contribution of the research to achieve Sustainable Development Goals is also emphasized here.

CHAPTER 2

LITERATURE REVIEW

2.1 Introduction

Globally, groundwater systems are experiencing significant stress due to increasing anthropgenic interventions, resulting in declining groundwater levels in aquifers, altered recharge regimes, and progressive deterioration of groundwater quality. Under these conditions, it is important to develop an elaborate understanding of its flow, draft, recharge and pollutant transport (Sahoo and Sahoo, 2019). This has been attempted by many researchers in past through local scale manual hydrological, aquifers and groundwater investigations. These physical investigations have provided the much needed, in depth analysis of the local groundwater fluctuations and pollution scenario but have failed to provide the true picture of the cause and effect of the problem that occurred beyond local scale and across boundaries (Dennehy et al., 2015). Therefore, use of advance technology such as geospatial and remote sensing tools; physical, numerical and analytical models; and conjugation of geospatial tools with modelling softwares has been rapidly picking up pace in recent history. These tools overcome the issue of scale and provide a holistic and comprehensive picture of the entire region under consideration. Also, these techniques can be time saving and cost effective when larger areas have to be analysed.

However, ground-based field investigations form the foundation for understanding groundwater, an inherently invisible resource, by providing direct and reliable insights into subsurface conditions and processes. The ground-based investigations help in defining the realistic parameters and providing input data for verifying and enabling geospatial and numerical tools to replicate the natural environment, as thus playing an important role in advancing these softwares (Sahoo and Sahoo, 2019). Likewise, the numerical and spatial tools help to understand, analyse and predict the spatial and temporal variations of groundwater overdraft and pollution. Therefore, both of them are needed to develop the detailed understanding of

dynamics of aquifer system, hydrogeology and groundwater flow, its distribution and pollution spread patterns of the area (Vetrimurugan et al., 2017).

Realising the need, many public administration bodies around the world are conducting regional groundwater assessments in order to essentially evaluate its availability and accessibility to their citizens and make sustainable management plans for future. Increasing number of researches are being conducted and periodically sponsored to monitor several hydrologic and hydrochemical variables, collecting both satellite and ground-based observation data to develop dynamically growing and efficient groundwater management plans (Akinwumiju & Olorunfemi, 2019). This has resulted in the inflow of the huge amount of data and necessitated the wide use of advance softwares for modelling and analysis. Groundwater quality assessment has increasingly moved from simple physicochemical characterization to integrated frameworks that combine hydrochemistry, geostatistics, health risk assessment and machine learning. This has enabled more robust diagnosis and prediction of contamination in diverse hydrogeological settings and address the concerns associated with groundwater pollution and scarcity.

2.2 Groundwater quality status and its health implications

Understanding groundwater chemistry and its evolution is fundamental for interpreting aquifer processes and assessing long-term sustainability. Numerous studies have employed classical hydrogeochemical approaches, including analysis of major ion chemistry, hydrochemical facies, ionic ratios, and geochemical modeling, to identify the natural and anthropogenic controls governing groundwater quality.Tools such as Piper and Gibbs diagrams, multivariate statistics, and PHREEQC-based saturation and inverse modeling have been widely used to elucidate water–rock interactions, mineral dissolution–precipitation processes, mixing mechanisms, and cation exchange reactions. Table 2.1 summarizes studies employing hydrogeochemical analysis, water quality indices, and multivariate statistical techniques for groundwater quality assessment in different hydrogeological environments.

Table 2.1: Summary of key groundwater quality assessment studies that highlight hydrogeochemical characterization and controlling processes

Study	Location	Methods & Tools	Key Findings
Gong et al. (2025)	Weining Plain, China	Water balance, end-member mixing analysis (EMMA), entropy-weighted water quality index	Yellow River water is the main recharge source; groundwater chemistry is largely geogenic; drinking suitability is generally limited.
Promilton et al. (2025)	Valliyur, Tamil Nadu, India	Major-ion hydrochemistry, Piper diagram, water quality indices, seasonal statistical analysis	Seasonal variation significantly affects groundwater quality, with post-monsoon improvement; hydrochemistry dominated by rock–water interaction and ion exchange.
Hamma et al. (2024)	Ain Sefra, Algeria	Multivariate statistics (PCA, HCA), water quality index (WQI), geochemical modeling	Four hydrochemical facies identified (Ca–Mg–HCO_3, Ca–Mg–Cl–SO_4, Ca–SO_4, Na–Cl); chemistry governed by water–rock interaction and mineral equilibrium; most samples suitable for drinking and irrigation with salinity limits.
Panchabhai and Mondal (2024)	Western India	Major-ion hydrochemistry, Piper and Gibbs diagrams, GIS analysis, WQI	Groundwater dominated by mixed Ca–HCO_3 and Ca–Mg–Cl facies; mainly influenced by rock–water interaction; many samples unsuitable for drinking in pre- and post-monsoon.
Dey et al. (2023)	Varuna River Basin, Uttar Pradesh, India	Major-ion hydrochemistry, ionic ratios, PHREEQC inverse modeling, WQI and health-risk assessment	Predominant Ca–Mg–HCO_3 facies; chemistry controlled by carbonate–silicate weathering, reverse ion exchange and flow-path evolution; mixing and reactions shape composition.
Marghade et al. (2020)	Yavatmal District, Maharashtra, India	Major-ion hydrochemistry, geochemical modeling (saturation indices, reaction simulations)	Elevated fluoride linked to rock–water interaction, ion exchange and fluorite equilibrium; geogenic processes dominate enrichment with health concerns.
Ansari et al. (2019)	Outer Himalaya, India	Multivariate statistics (PCA, HCA), ionic ratios, PHREEQC modeling	Spring water chemistry mainly controlled by silicate weathering and rock–water interaction, with secondary anthropogenic influence.

Groundwater suitability for drinking and irrigation has been widely assessed using composite water quality indices that integrate multiple physicochemical parameters into simplified and interpretable metrics. Early approaches primarily employed the Water Quality Index (WQI) to evaluate overall water quality status (Brown et al., 1970), followed by the development of modified and alternative indices such as the Groundwater Quality Index (GWQI) and RMS-WQI to improve sensitivity and parameter weighting (Adimalla & Taloor, 2020; Ghosh & Bera, 2023; Praween et al., 2025). More recent studies have extended index-based assessments by incorporating entropy-based weighting schemes (EWQI), multivariate statistical techniques, and geospatial analysis, enabling improved interpretation of spatial variability, identification of contamination hotspots, and enhanced groundwater resource management (Kumar & Augustine, 2022; Ukah et al., 2020).

Also, regional-scale assessments reveal that groundwater quality status and recharge mechanisms vary widely across agro-climatic settings, with many systems already showing significant constraints for safe drinking use. In the semi-arid Weining Plain of China, Gong et al. (2025) identified that groundwater recharge is predominantly sourced from irrigation infiltration and canal leakage, with over 80% of samples showing moderate to poor quality for drinking, highlighting the need for treatment. Similarly, Prasun & Singh (2025) evaluated groundwater in Aurangabad, Bihar, using advanced geostatistical methods and revealed significant spatial heterogeneity in physicochemical parameters, with about 8% of samples unsuitable for drinking without treatment. Hydrochemical analysis of the Chepe River in Nepal by Ranabhat et al. (2025) demonstrated water quality within drinking standards, with carbonate weathering as the main hydrochemical driver and irrigation suitability generally excellent. Table 2.2 presents a synthesis of studies that combine water quality indices with health risk assessment to identify vulnerable populations, seasonal risk variability, and emerging public health concerns linked to groundwater contamination.

Table 2.2: Summary of key groundwater quality assessment studies that highlight Water quality indices and human health risk assessment

Study (Author, Year)	Location	Methods & Tools	Key Findings
Farzana et al. (2025)	Peri-urban areas of Bangladesh	Physicochemical and heavy-metal analysis; WQI; US-EPA health risk assessment	WQI exhibited strong spatial variability; elevated Fe, Mn, and As resulted in significant non-carcinogenic and carcinogenic health risks in several locations.
Awasthi et al. (2025)	Nalagarh, NW Himalayas, India	Major ion hydrochemistry; WQI; GIS spatial analysis; health risk assessment for fluoride & arsenic	Most samples were unsuitable for drinking; fluoride and arsenic posed considerable health risks, particularly to children.
Maleky et al. (2025)	Jiroft city, Iran	Major ions; GWQI; ML algorithms (RF, SVM, ANN); USEPA health risk assessment	Machine-learning algorithms effectively classified groundwater quality; children exhibited the highest hazard quotients.
Nayak et al. (2023)	Bhubaneswar city, India	Major-ion analysis; WQI; multivariate statistics (PCA); USEPA health risk assessment (NO_3^-, F^-)	Nitrate and fluoride concentrations exceeded safe limits in urban pockets, posing significant non-carcinogenic health risks, especially to children
Gupta et al. (2023)	Narmada River basin, India	Hydrochemical characterization; WQI/EWQI; USEPA health risk assessment	Integrated WQI and health risk analysis identified groundwater degradation linked to agricultural and anthropogenic activities.
Saleem et al. (2016)	Greater Noida, India	Physicochemical analysis; weighted WQI	Majority of groundwater samples were suitable for drinking; WQI proved effective for rapid groundwater quality screening.
Brown et al. (1970)	Conceptual	Composite Water Quality Index formulation	Established the foundational framework of WQI, forming the basis for subsequent weighted and entropy-based indices.

Advancements in geospatial analysis and data-driven modeling have significantly enhanced groundwater quality assessment and prediction capabilities. GIS-based vulnerability models, such as modified DRASTIC and multi-criteria decision analysis (MCDA), are widely used to delineate contamination-prone zones by integrating hydrogeological, land-use, and anthropogenic factors. In parallel, machine learning (ML) techniques have demonstrated strong potential for predicting groundwater quality indices and contaminant concentrations with high accuracy, enabling non-linear representation of complex hydrogeochemical systems and supporting proactive groundwater management. Recent studies have increasingly integrated multivariate hydrogeochemical modeling with health risk assessment to better understand groundwater contamination drivers. Sidhu et al. (2024) investigated groundwater quality in Chandigarh and reported widespread pre- and post-monsoon contamination by nitrate and fluoride, primarily influenced by rock–water interaction and anthropogenic inputs. Similarly, Zhao et al. (2024) analyzed groundwater in the Yishu River basin and observed seasonal shifts in hydrochemical facies, with nitrate posing higher health risks during the wet season. In an arid setting, Hamma et al. (2024) applied geostatistical clustering and water quality indices in southwest Algeria, identifying salinity and reverse ion exchange as major controls on groundwater chemistry. Extending these approaches, Akakuru et al. (2023) integrated machine learning techniques, particularly artificial neural networks (ANN), with multiple linear regression (MLR) models to assess and predict groundwater quality around Obosi, southeastern Nigeria, demonstrating high predictive performance (R^2) compared to conventional pollution indices such as contamination factor (CF), pollution load index (PLI), and water quality index (WQI).Table 2.3 summarizes key studies that highlight the growing role of GIS and machine learning frameworks in groundwater vulnerability mapping, quality forecasting, and sustainable resource planning.

This review further aims at discussing different tools and methods that have been used to assess groundwater scarcity and pollution scenario around the world. It is divided into following parts – the use of GIS to assess groundwater vulnerability, use to numerical modelling and; the coupling of GIS and numerical models, as stated in Fig. 2.1.

Table 2.3: Summary of key groundwater quality assessment studies that highlight GIS based vulnerability assessment and machine learning prediction of groundwater quality

Study (Author, Year)	Location & Water Type	Methods & Tools	Key Findings
Uddin et al. (2024)	Coastal Bangladesh	RMS-WQI + XGBoost ML + GIS mapping + uncertainty analysis	XGBoost demonstrated excellent accuracy in predicting groundwater quality from RMS-WQI indicators, with low model uncertainty (<1 %).
Abu El-Magd et al. (2023)	Egypt (Ismailia region)	Support Vector Machine (SVM) integrated with WQI	SVM-WQI model produced higher accuracy in spatial groundwater quality classification than standalone methods.
Sarker et al. (2025)	Bangladesh (Juri Upazila)	Machine learning (XGBoost, Random Forest, etc.) + WQI prediction	XGBoost ML model best predicted WQI with R^2 ~0.97, demonstrating ML suitability for groundwater quality estimation.
Shanmuharajan et al. (2023)	Coimbatore region, Tamil Nadu, India	DRASTIC & modified DRASTIC models; GIS; validation with nitrate	Modified DRASTIC vulnerability mapping validated by nitrate concentration; anthropogenic/land-use impacts identified.
Iqbal et al. (2024)	Mymensingh Sadar, Bangladesh	GIS-DRASTIC vulnerability mapping; nitrate validation	DRASTIC vulnerability zones were spatially classified and validated against nitrate data; helps identify vulnerable aquifer zones.
Rezig et al., (2022)	El Asnam (Northern Algeria)	Vulnerability mapping using DRASTIC and Susceptibility Index	SI model valid for more than 50% of the study area and can be used by decisionmakers

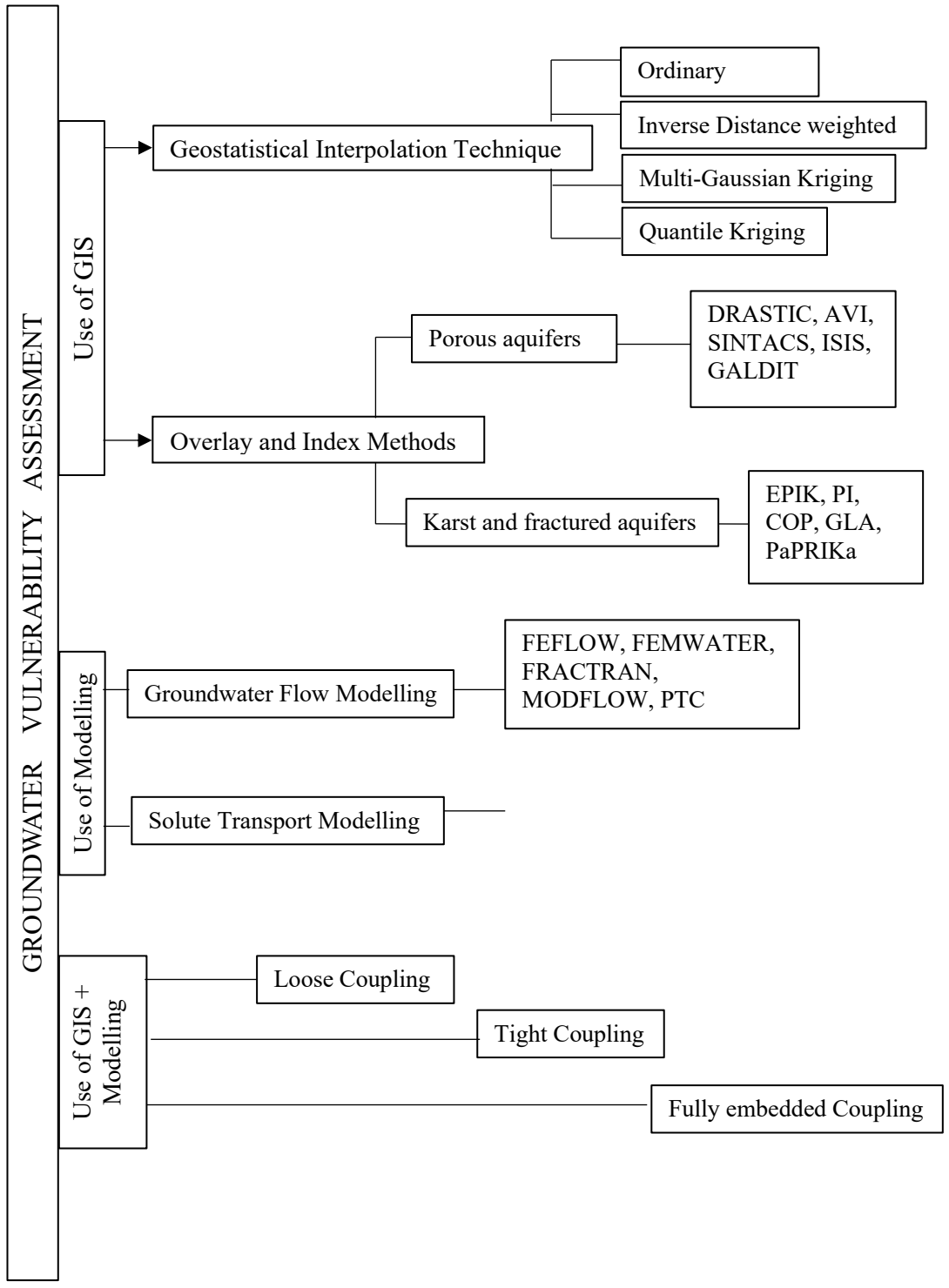

Fig. 2.1 Different methods of Groundwater Vulnerability Assessment using GIS and modelling

2.3 Use of GIS to assess Groundwater Vulnerability

Historically, Geostatistical methods were used widely to produce contour maps of groundwater heads and to determine the spatial distribution of pollutant spread in groundwater. These pollutant plume maps were prepared using different interpolation techniques such as ordinary kriging, cokriging and inverse distance weighted methods based on the type, amount and quality of available data. Results obtained from different interpolation techniques in different scenarios using different sizes and amount of sampling data were compared over the years and new variations of the ordinary interpolation techniques were suggested. Authors like Reed et al. (2004) suggested quantile kriging and multigaussian kriging method to be more robust and less biased in comparisons to other techniques and several other researchers suggested inclusion of additional information to interpolation data such as groundwater heads to improve the plume spread estimates (Burger & Schafmeister, 2000; Shlomi & Michalak, 2007). A study undertaken by Morio et al. (2010) used flow guided interpolation (FGI) method to adapt the information available at the initial stages of project. It coupled the flow data and existing sample data of the study area to add additional points in a standardized way throughout the concerned region, this significantly improved the estimates of the kriging interpolation. Therefore, the interpolation techniques and methods continue to be evolved so that they can be used to give adequate initial estimates of the subsurface contamination using limited historical and on-site data. These sites can then be prioritized on the basis of need for further detailed assessment and to carry out the remediation process.

Also, there has been widespread use of GIS based Indices to qualitatively measure the intrinsic aquifer vulnerability. The intrinsic aquifer vulnerability is determined by taking into account the intrinsic hydrogeological characteristics of the aquifer that do not change with time. This type of mapping does not take into account the dynamic factors such as the extent of polluting activities and the nature of the pollutant but is important to determine the contamination risk inherent in the aquifer system (Gogu & Dassargues, 2000a). At first, the characteristics of the aquifer are represented in the form of thematic maps which showcases the spatial distribution of

the different natural factors controlling aquifer properties. GIS software is then used to assign relative weightages to these layers according to their role in determining the vulnerability of aquifer to contaminant transport. These maps are then overlaid to produce vulnerability maps using the overlay and index operations of the GIS. The output map thus, is the representation of the spatially aggregation of weighted parameters according to the defined vulnerability index. The most frequently used GIS-based vulnerability indices include DRASTIC (Aller et al., 1987; Evans & Myers, 1990; Rundquist et al., 1991), GOD (Van Duijvenbooden & Van Waegeningh, 1987), AVI rating system (Van Stempvoort et al., 1993), and SINTACS (Gogu & Dassargues, 2000a), among others. However, these methods are used for porous-media aquifers and do not represent the vulnerability in karst and fractured aquifers. Some of the methods which are used to estimate vulnerability in karst and fractured aquifers are EPIK (Doerfliger et al., 1999), system approach-based method (Mádl-Szőnyi & Füle, 1998), PI (Goldscheider et al., 2000), COP (Vías et al., 2006), and Slovene approach (Ravbar & Goldscheider, 2007).

2.3.1. Vulnerability framework for Porous aquifers

2.3.1.1. Aquifer mapping using DRASTIC

DRASTIC is the most extensively used methods for vulnerability assessment. It originally includes the overlaying and indexing of seven thematic layers, (the name being an acronym) i.e., Depth to Water table (D), Net Recharge (R), Aquifer properties (A), Soil properties (S), Topography (Elevation) (T), Impact of Vadose Zone (I), and Hydraulic Conductivity (C) of the areas. The value of the DRASTIC index is determined by multiplying each parameter weight by its site rating and summing the total. The Eqn. (2.1) for the DRASTIC Index (DI) is:

$$DI = D_r.D_w + R_r.R_w + A_r.A_w + S_r.S_w + T_r.T_w + I_r.I_w + C_r.C_w \quad (2.1)$$

where D, R, A, S, T, I, C have been stated above, r is the rating for the study area, and w is the weight of each parameter.

The DRASTIC method was developed in 1987 by the combined alliance of USEPA (United States Environmental Protection Agency) and NWWA (National Water Well Association). The index aggregates the intrinsic hydrogeological features of the site to assess the probable contamination potential of the underground aquifer. Originally, it was developed for applications in porous aquifers. But it was extended to map the vulnerability of fractured aquifers as well. For this modification, an eighth parameter known as Fm (fractured media) was included in the index calculation. Fm took into consideration the three properties of distinct subsurface fractures i.e., length, fracture density and orientation and was successfully applied in the Gulf Islands of British Columbia, Canada (Denny et al., 2007).

DRASTIC has also been modified over the years by adding or eliminating factors for its index calculation to reproduce the vulnerability of aquifers to local conditions (Ahmed et al., 2015, Fritch et al., 2000; Babiker et al., 2005; Panagopoulos et al., 2006; Antonakos & Lambrakis, 2007; Guo et al., 2007; Liggett & Allen, 2011; Singh et al., 2015; Jenifer & Jha, 2018; Hernández-Espriú et al., 2014). Some of the variations of the DRASTIC method include the development of DRASTIC-P (Ahmed, 2009; Albuquerque et al., 2013; Douglas et al., 2018; Kazakis, 2013), DRASTIC- P LDLU (Jenifer & Jha, 2018), DRASTICA (Maqsoom et al., 2020), DRAMIC (Wang et al., 2007), DRASTIC (CD) (Secunda et al., 1998, Al-Adamat et al., 2003, Saidi et al., 2010, Boughriba et al., 2010, Shirazi et al., 2013), D-DRASTIC (Wang & Yang, 2008), DRASTIC-Fm (Denny et al., 2007), DRASTIC-N (Voutchkova et al., 2021). These variations removed the subjectivity associated with DRASTIC results because of the use of quantitative input layers (Vaezihir & Tabarmayeh, 2015) while also changing relative weights of the input layers to suit the study area. Such as the DRASTIC-P model, also known as Pesticide DRASTIC uses higher weights for slope and soil to represent the areas having strong agricultural activity (Douglas et al., 2018; Kazakis, 2013). Similarly, DRAMIC eliminates the use of soil media and topography for its index calculation to represent urban areas with flat topography and instead uses aquifer thickness (M) and contaminant impact (C) parameters (Wang et al., 2007). These modifications have also widened the scope of DRASTIC to estimate specific vulnerability associated with the aquifer system. The inclusion of specific vulnerability

assessment improved the estimates of aquifer susceptibility to contamination based on the degradation and transportation properties of specific pollutants as well as their relationship with the hydrogeological properties of the aquifer (Kazakis & Voudouris, 2015; Machiwal et al., 2018).

A study conducted by Vaezihir and Tabarmayeh (2015) developed both the intrinsic vulnerability and specific vulnerability maps for the Tabriz aquifer (Iran) and combined them to calculate the total vulnerability of their area. Intrinsic vulnerability was mapped using DRASTIC layers while specific vulnerability was mapped using DRAIA layers- Density of population, Recharge by rivers, Agriculture, Industry and Abstraction. The total vulnerability map obtained by this method showed good agreement with the on-site nitrate data. Table 2.4 summarises some modifications of DRASTIC used worldwide.

Few researchers have also modified the resultant scores obtained from the DRASTIC calculations. Vulnerability outputs have been coupled with water quality indices to improve susceptibility interpretation (Pusatli et al., 2009) and with pollution indices such as Nemerow's synthetic pollution index to better represent contamination risk (Wu et al., 2014). They have also been coupled with techniques such as information-analytic rough sets technique (Khan et al., 2014). These refinements have enhanced the capability of DRASTIC-based frameworks to characterize aquifer vulnerability under diverse hydrogeological and anthropogenic settings. By adapting parameter selection and recalibrating relative weights, modified indices demonstrate improved consistency with observed groundwater contamination patterns. The incorporation of pollutant-specific attributes has further increased the relevance of vulnerability assessments for contaminant-focused groundwater protection. Coupling vulnerability outputs with water quality indices and analytical approaches has strengthened the interpretative value of vulnerability maps. Such integrated methodologies provide a more comprehensive representation of contamination processes and transport within aquifer systems. Consequently, modified DRASTIC approaches have evolved into reliable tools for supporting groundwater protection strategies and sustainable aquifer management.

Table 2.4: List of Modified DRASTIC indices with formulas

No.	Modified DRASTIC Index (MDI)	Formula	Additional parameters considered	Study area	Unique Contribution	References
1.	KARSTIC	$MDI=K_w.K_r+A_w.A_r+R_w.R_r+S_w.S_r+T_w.T_r+I_w.I_r+C_w.C_r$	Karst development and fractures (K)	South Dakota, U.S.	Greater emphasis was given to karstic features for application in karst aquifers	Davis et al. (2002)
2.	Modified DRASTIC	$MDI=DI + 5M_r$	Lineament Influence (M)	Rio Artiguas basin, Central America	Better representation of the pollution potential of highly fractured areas was achieved	Mendoza and Barmen (2006)
3.	SI (Susceptibility Index)	$MDI= D_rD_w + R_rR_w + A_rA_w + T_rT_w + LU_rLU_w$	Land use pattern (LU)	Portugal	S, I and C were eliminated and the land use parameter was added to represent agricultural activities' impact (especially nitrates)	Ribeiro et al. (2017)
4.	DRASTIC-Fm	$MDI= DI+ Fm_r.Fm_w$	Discrete fracture network, orientation, length and fracture density	Southern Gulf Islands, British Columbia	Hydrogeologic environment of the Gulf Islands was adequately represented	Denny et al. (2007)
5.	DRASTIC-CI	$MDI=DI+L_r.L_w$	Excessive land use (L)	Sharon region, Israel	Effect of extensive land use resulting in alteration of the soil matrix was studied	Secunda et al. (1998)
6.	DRASTIC-LU	$MDI= DI + (LU_w.LU_r)$	Land use pattern (LU)	Central Ganga Plain, India	Impact of land use on water contamination was considered	Alam et al. (2014)

continued on next page

Table 2.4 (continued)

No.	Modified DRASTIC Index (MDI)	Formula	Additional parameters considered	Study area	Unique Contribution	References
6.	D-DRASTIC	$RI_i = DI_i/DI_{max}$ X $(H_i - H_{min})/(H_{max} - H_{min})$	Hazard values of concerned pollutant (H)	Upper Bann Catchment, Ireland	Hazard associated with the pollutant concentration was considered in pollution risk	Wang and Yang (2008)
7.	DRASTIC-N	MDI= DI+ $N_r.N_w$	Nitrate redox interface depth (N)	South western aquifers of Denmark	Nitrate-specific vulnerability was assessed by the geochemical information (redox interface depth)	Voutchkova et al. (2021)
8.	DRASTIC-P-LDLU	MDI= DI + $(LD_{w.}\ LD_r)$ + $(LU_{w.}\ LU_r)$	Lineament Density (LD), LandUse Landcover (LU)	Tiruchirappalli, Tamil Nadu, India	Inclusion of LD-LU highlighted the anthropogenic impact in an agricultural area	Jenifer and Jha (2018)
9.	DRAV	MDI= $D_w.D_r+R_w.R_r+A_w.A_r+V_w.V_r$	Lithology of the Vadose zone (V)	Tarim Basin, China	Effect of Lithology on seepage water in the vadose zone considered	Zhou et al. (2010)
10.	DRASTIC-A	MDI = DI+ $A_w.\ A_r$	Anthropogenic Impact (A)	Gilgit Baltistan, Pakistan	Anthropogenic impact was studied using urbanization index and land use map	Maqsoom et al. (2020)
11.	DRAMIC	MDI=$5D_r + 3R_r + 4A_r + 2M_r + 5I_r + 1C_r$	Aquifer thickness (M); impact of contaminant (C)	Wuhan City, China	Effect of contaminant's stability and ease of infiltration for urban area considered	Wang et al. (2007)

*DI is DRASTIC Index; whereas Subscripts r and w are the corresponding ratings and weights assigned to the parameter

2.3.1.2 Other Indices for Porous aquifers

GOD Scheme, AVI Rating system, SINTACS method, ISIS method and GALDIT method are some of the other indices which have been developed to measure vulnerability in porous aquifers. Though not as popular as DRASTIC, they have been widely used in different contexts (Mendoza & Barmen, 2006; Debernardi et al., 2008; Polemio et al., 2009; Kazakis & Voudouris, 2011).

DRASTIC has been considered to be a complex method that incorporates seven parameters to map aquifer vulnerability. Researchers have argued that its parameters tend to overlap and reduce its applicability on site. Some indices have therefore been developed with an aim to simplify the vulnerability assessment and increase their practical usage. The GOD_{index} is one such method that is simple and practical in its approach and uses just three parameters to map the vulnerability associated with the aquifer system (Foster, 1987). These parameters are- Groundwater occurence in confined, semi-confined or unconfined aquifer class (G); the type of aquifer's overlying formations (O) and the depth to water table (D). The model is also less data intensive. However, it has been known to perform badly in regions that have extended areas of small differences in vulnerability. Therefore, it is best suited for application on large regions with high vulnerability contrasts (Gogu & Dassargues, 2000a; Polemio et al., 2009; Ghazavi & Ebrahimi, 2015).

Likewise, the AVI Rating system, also known as the aquifer vulnerability index (Van Stempvoort et al., 1993) simplifies the process of vulnerability mapping by only considering the intrinsic susceptibility of the aquifer. The index is calculated by the addition of hydraulic resistances (i.e., obtained by dividing thickness of the aquifer's overlying layers with its hydraulic conductivity) of the layers. The value of the hydraulic resistance has a unit of time and can be indicative of the downward travel time taken by the pollutant to reach saturated surface. It has been stated that this parameter alone can indirectly account for the various parameters used in DRASTIC (excluding topography and aquifer media) and can represent the hindrance provided by unsaturated subsurface layers to vertical flow of contaminant. However, the details

of aquifer media can be incorporated if the lateral flow of the contaminant in an aquifer has to be considered.

Different hydrogeological systems present different scenarios of probable contamination based on their different intrinsic properties. Thus, different indices have been developed to map the vulnerability associated with these aquifers. In the later years after the development of DRASTIC, GALDIT index was one such index that was introduced by Chachadi and LoboFerreira (2001) specifically to address the challenges of mapping vulnerability of coastal aquifer system as it is highly prone to sea water intrusion (SWI). It uses a total of six parameters to calculate its index. Out of these six parameters, three parameters specifically take into account the properties of the coastal aquifer and play an important role in determining the extent of seawater intrusion, these are- Level of watertable above the sea level (L); Distance from the seashore (D); and the impact of already existing seawater intrusion in the coastal area (I). The remaining three parameters i.e., G, A, T that are needed for its calculation are- confinement of Groundwater (G) in different types of confined or unconfined aquifer system, aquifer hydraulic conductivity (A); and aquifer thickness (T). The index has been considered advantageous for requiring data that is simple and easily available (Panagopoulos et al. 2006). However, there is one drawback of this index i.e., it does not take into account the effect the groundwater pumping on SWI. Excessive pumping can draw salt water towards the well and can result in internal movement of salt water zone. Nevertheless, the index has been successfully applied to large complex coastal aquifer systems around the world.

The SINTACS method that was formulated by Civita (1990, 1993, 1994) and Civita and De Maio (1997) is another such method that was developed for vulnerability mappings of specific aquifer systems. It is basically an extension of DRASTIC method to improvise it and adapt it to the Mediterranean conditions, especially to the aquifer conditions of Italy. It uses weighted sum of seven layers to assess vulnerability, they are- S*oggiacenza* (depth to groundwater , depth to the water table), ***I****nfiltrazione* (recharge action , effective infiltration), ***N****onsaturo* (attenuation capacity of the unsaturated zone attenuation potential of the vadose zone)*, **T**ipologia della copertura*

(attenuation potential of the soil, type of the soil media), ***A****quifero* (hydrogeologic characteristics of the aquifer, characteristics of the saturated zone), ***C****onducibilita* (hydraulic conductivity) and ***S****uperficie topografica* (topographic slope). This method which can be used for medium to large scale mapping is more flexible in defining rates and weights of the input parameters as compared to DRASTIC (Ramos Leal et al., 2010, Majandang & Sarapirome, 2013).

Hence, as discussed above, there are wide number of indices that have been developed for the purpose of assessing the situation of the porous aquifer with respect to its vulnerability to the pollution and degradation. Some of these indices were either directly applied or slightly modified to become applicable to the karst aquifers. The ISIS method is one such method that was applied in both porous and karst aquifer systems (Civita & De Regibus 1995; Gogu & Dassargues, 2000a; Gogu et al., 2003). It is a hybrid method which was developed by comparing several aquifer studies and combining SINTACS, DRASTIC and GOD indices. This method was however criticised for considering too many input parameters and reducing its practical value. However, there are a particular set of indices that have been specifically developed for vulnerability mapping of karst aquifers system. The further sections of this paper dwell on vulnerability indices that were specifically formulated for the karst condition.

2.3.2 Indices for Karst aquifers

2.3.2.1 The COP method

Karstic aquifers are characterised by ever changing and heterogeneous hydrogeology. The rocks present in the system tends to dissolve in acidic water over time and lead to the formation of fractures, fissures, cracks, sink holes, swallow holes, pjoles and other such features in its surface and sub-surface strata. As a result, increased permeability of the system can accelerate the contaminant transport to water table via concentrated recharge processes. The contaminant can also travel across karst conduits over considerable distances (Goldscheider, 2005; Moreno-Gómez et al002E, 2018). Therefore, specialised overlay and weighted index methods have been

developed by the researchers all over the world to qualitatively analyse the vulnerability of karst aquifers (Doerfliger & Zwahlen;1995; Hötling et al., 1995; Goldscheider et al., 2000; Daly et al., 2002; Vias et al., 2006; Ravbar & Goldscheider, 2007).

In Europe, karst topography occupies significant portion i.e., upto 35 percent of its landmass. Therefore, the drinking water sourced from karst aquifers can contribute upto 50% or more of the total supply in some of its nations. In order to safeguard this resource from human contamination, the European government had commissioned a project to map the risk and vulnerability associated with these landforms from 1997 to 2003. The project, known as COST Action 620, was one of the most extensive studies conducted to devise frameworks for protecting karst aquifers (Zwahlen, 2004). The Framework was a guideline, it did not give formulae and detailed guidelines to quantify vulnerability. Consequently, the methodology was adapted by the different nations with or without modifications into many methods, specifically, to incorporate geological and legislative differences of nations (France, Spain, Slovenia, Switzerland, etc.).

The COP method is one of the several indices that were developed from the proposed guidelines given by the commission to map the intrinsic vulnerability of the aquifer. As suggested by the European approach, the method uses three factors for its index calculation i.e., Concentration of flow (C), Overlying layers (O), Precipitation regime (P). The O factor determines the degree of protection offered by the soil, subsoil, non-karst rock and unsaturated karst rock present above the aquifer. The presence and placement of these layers can significantly increase the residence time of flow by allowing for diffuse infiltration and giving scope for natural attenuation of the pollutant. However, both C and P factor assess the potential for alteration of the protection offered by O factor. The C factor takes into account the possibility of concentrated infiltration process that frequently happens in presence of karst landforms due to the accumulation of precipitation and surface runoff (Vrba & Zaporozec,1994; Kouli et al., 2008). Additionally, the P factor incorporate the consideration of both quantity and temporal variability of precipitation (Daly et al.,

2002; Vias et al., 2006). Thus, the incorporation of these factors makes this index flexible to address vulnerability in karst aquifers while taking into account heterogeneous conditions for pollutant transport to aquifer under various precipitation conditions.

The COP method has wide practical application across local, basin or regional scale. It was originally used across European nations (Spain and Turkey) to map aquifer system vulnerability. Amongst its various applications, it was found to be most effective in Spain where it produced better results in comparison to many other methods (SINTACS, AVI, EPIK, DRASTIC and PI) (Andreo et al., 2006; Vías et al., 2006). It has also been modified on the basis of local conditions and availability of data for its application in different parts of the world such as Mexico (Moreno-Gómez et al, 2018); Iran (Entezari et al., 2016); Arizona (Jones et al., 2019); Slovenia (Ravbar & Goldscheider, 2007), South Africa (Leyland et al., 2008) and Vietnam (Nguyet & Goldscheider, 2006). Its modification into Slovene approach has been discussed below.

2.3.2.2 The Slovene approach

Vulnerability mappings are generally done with the aim for resource or source protection. For resource protection, the aim is to protect the entire body of groundwater by considering the seepage of water through unsaturated zone to water table; whereas for source protection, a specific well or spring is targeted by considering flow in saturated zone (Daly et al., 2002). The COP method was extended to include source protection of Slovene karst aquifer systems by Ravbar and Goldscheider (2007). In addition to the C, O, P factors; the K factor (Karst saturated zone) was included in the Slovene approach to account for the lateral flow and contaminant transport processes within the saturated zone. The K factor includes the information for degree of karstification and the flow movement of groundwater towards the outlets by considering three sub factors- the first being the travel time, active status of the karst conduits and contribution of the aquifer to spring discharge (Andreo et al., 2009). The K-factor map is overlaid on the resource vulnerability map obtained by combining the

C, O and P factors (See Fig. 2.2). Also, the evaluation of the C factor in Slovene approach involves the demarcation of swallow hole recharge area and its hydrologic variability for contaminant infiltration (Ravbar & Goldscheider, 2007; Göppert & Goldscheider, 2008). The swallow holes are developed by expansion of the cracks present in karst rocks. This is because, the bedrock, usually limestone ($CaCO_3$), that occurs in karst system tends to dissolve or react with hydrogen ions (H^+) present in the ground water. The H^+ ions are majorly released from the dissociation of carbonic acid (H_2CO_3) present in the soil and infiltrated rain water (see Fig. 2.3). These swallow holes can play an important role in the transfer of pollutant to the groundwater i.e., the active hole will transfer it rapidly without considerable attenuation whereas the less active hole will release it slowly and indirectly (holes will become active and inactive based on groundwater levels). The swallow holes can also lead to the disappearance of the surface streams.

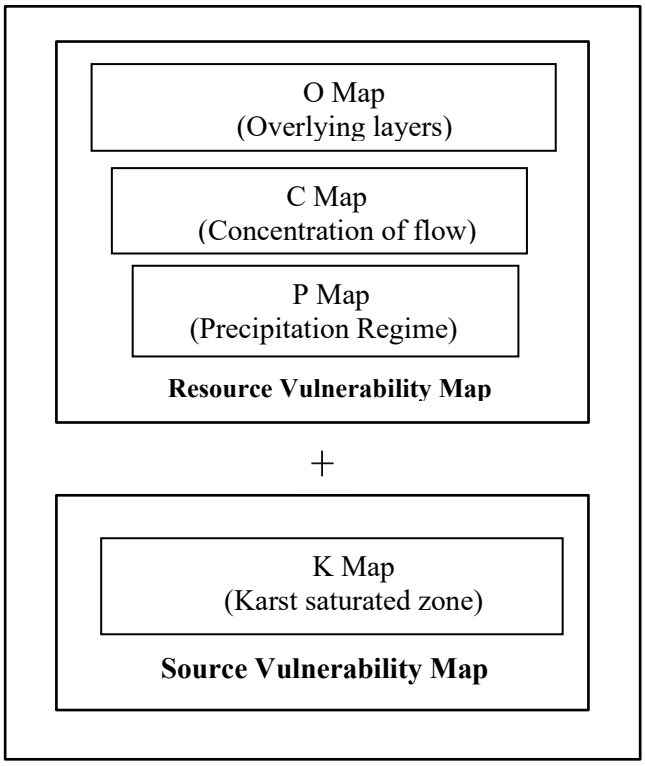

Fig. 2.2 The extension of COP method to include Source vulnerability map for Slovene approach (Sourced from Ravbar & Goldscheider, 2007)

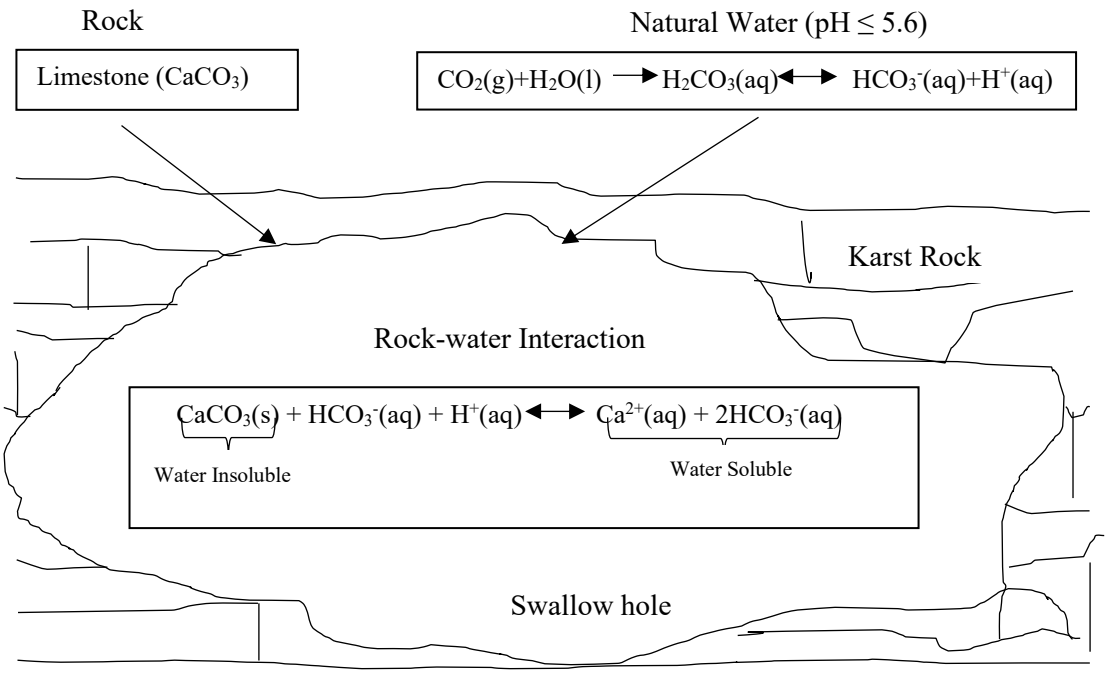

Fig. 2.3 The Formation of Swallow holes with gradual dissolution of $CaCO_3$

To incorporate the permanent and temporary flow activity of the swallow hole in the analysis, a temporal variability sub factor (tv) is to be considered for the calculation of C factor. The tv factor varies itself according to the recurrence period of swallow hole hydrological event. Therefore, the inclusion of additional information in Slovene approach has complemented and modified the applicability of the COP method. It has been stated to be a complete evolution of the European approach (Goldscheider et al., 2000; Zwahlen, 2004).

2.3.2.3 Other indices for Karst Aquifers

The EPIK method is one of the first indexes which was developed to map the vulnerability associated with karst (carbonate) aquifers (Doerfliger & Zwahlen, 1995; Doerfliger & Zwahlen, 1998; Doerfliger et al., 1999; Barrocu et al., 2007). The four parameters that are considered for mapping EPIK are- Epikarst (E), Protective cover (P), Infiltration conditions (I) and karst network (K). The consideration of the nature of Epikarst (E) as a standalone factor renders this method quite capable of mapping

risk associated with karst aquifer hydrogeology.

The presence of Epikarst in a karst system can significantly influence the aquifer recharge and contaminant transport. Epikarst is a subsurface zone immediately beneath the soil that is highly fissured and is generally surrounded by the low permeable rock (Mangin 1973, 1975). It can house small conduits draining into vertical pipes that join the karst underneath (See Fig. 2.4) and can have variable depth and connectivity. It can for example be well developed and connected or not connected to the karst network, or could be entirely absent (Doerfliger, 1996). Therefore, for mapping EPIK, the epikarst is classified into E1 (Highly developed), E2 (moderately developed) and E3 (small or absent) classes. EPIK method has been suitably applied to large as well as small aquifer systems (Barrocu et al., 2007; Gogu and Dassargues, 2000b; Hamdan et al., 2016). At the initial stages of development of Europeans' COST 620 approach, the EPIK method greatly influenced the discussions of the group as it was the sole method that was completely karst oriented at that time. However, due to the uncertainty related to the precise hydrological role of Epikarst and the difficulty in categorising it, the role of Epikarst was incorporated into the P factor (protective cover) for European's approach while the other factors were retained with slight modifications.

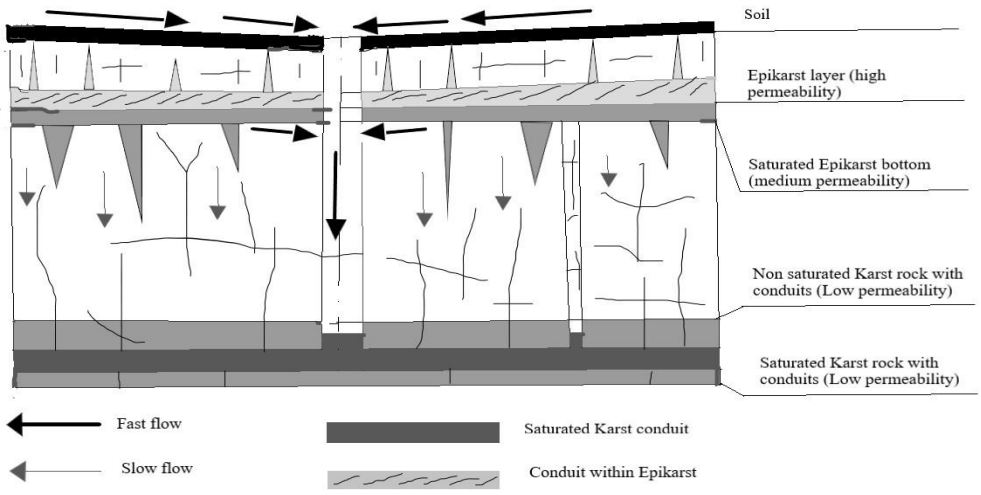

Fig. 2. 4 Water Recharge through the Epikarst zone (Sourced from Smart & Friedrich, 1986; Jeannin & Grasso, 1995; Doerfliger et al., 1999)

The European's Government COST 620 action consisted of three Working Groups (Zwahlen, 2004). While Group 1 worked on developing methodology for intrinsic vulnerability mapping and Group 2 worked on specific vulnerability, the 3rd Group worked on developing a framework for risk assessment. The PI index was developed during the initial stages of development of complete European Approach. It was the first method developed by Working group 1 at the Department of Applied Geology (AGK), University of Karlsruhe and was funded by the German Federal Institute for Geosciences and Natural Resources (BGR). The complete method was documented and published by Goldscheider et al. (2000). The parameters used in this method (as well as in European's approach) represents three steps to vulnerability – the first being the origin of contamination i.e, generally a land surface, the second is the pathway i.e., travel through the subsurface layers and the third is the uppermost boundary of target aquifer i.e., the water table. The PI index can thus be used for resource vulnerability mapping by considering the above origin-pathway-target model. It can however be extended to map source vulnerability by also considering the flow route of the contaminant in the saturated zone towards the spring or well. PI was developed at a very initial stage therefore, the factors it considers for its index calculation - protective cover(P) and Infiltration conditions (I); have different names then the ones suggested in the European approach. However, the method does not consider the factor of karst network development and precipitation regime individually for its calculations. Nevertheless, this method served as the basis of final development of the European's framework for mapping vulnerability associated with karst aquifers.

Apart from the previously discussed methods, other indices that have been developed to map karstic aquifer vulnerability over time are REKS (Malik & Svasta, 1999); RISKE (Pételet Giraud et al., 2000); RISKE 2 (Plagnes et al., 2005) and PRESK (Koutsi & Stournaras, 2011). Recently, a new method called PaPRIKa is has been developed in France to assist water agencies in defining protection zones using a national level strategy (Dörfliger & Plagnes, 2009; Kavouri et al., 2011). It has been derived from previous methods of EPIK, RISKE and RISKE2 (Doerfliger & Zwahlen 1998; Pételet- Giraud et al., 2000; Plagnes et al., 2005; Pranville et al., 2008). The Protection of aquifers (Pa) through this method is assessed using criteria such as-

protection of groundwater (P), Infiltration (I) and degree of kartisification (K). In addition, this method gives further consideration to the structural working of karst by considering the the type of the rock in the saturated zone of the aquifer (R). The method in its application takes into account the specific site differences present in karst hydrogeology of France. Therefore, it is essentially an adaptation of the European approach to the French Water Framework Directive (EU) legislation.

2.3.3 Limitations of GIS based overlay and index methods

As mentioned, there are many types of GIS based vulnerability assessment methods available. These methods are popular because they have fixed methodologies, are rapid in application and do not require intensive data. However, it has been suggested by many authors that the results obtained by these methods requires validation as there is a lack of numerical basis in their formulation. This has been established by some of the studies where the vulnerability maps obtained on numerical basis opposed the subjective results obtained by applying qualitative indices (Gogu et al., 2003; Frind et al., 2006). There are many methods that can be used by researchers to validate the results of GIS based overlay and index assessments, such as tracer tests (Jiang et al., 2015; Ravbar & Goldscheider, 2009), chemograph and hydrograph analysis, statistical analysis of field observation data (Kazakis et al., 2015; Vías et al., 2010; Almasri, 2008) and; analytical and numerical modelling. These validation methods should be selected to test the authenticity of the overlay and index methods while keeping in mind that the selected validation method is independent of the vulnerability assessment for that site (Zwahlen, 2004).

Also, there can be error propagation through the use of interpolation. This is one limitation associated with the use of both geostatistical interpolation as well as overlay and index methods. The inherent subjectivity with which the factors are weighted and rates assigned lead to more homogenized results, which are interpreted in the terms of low, high or moderate vulnerability. This depiction of results limits the discrimination of areas which would have otherwise displayed heterogeneous characteristics. Handling these inaccuracies is also difficult in these methods as there

is no quantification of uncertainty associated with this analysis (Gogu & Dassargues, 2000a).

Despite these limitations, these overlay methods are still widely used and have offered considerable help in taking management decisions especially in areas that lack sufficient data to carry out extensive quantitative analysis of the aquifer condition and pollutant spread. Many modifications have also been incorporated in these methods to remove the subjectivity associated with this overlay analysis. These methods have wide scope of being utilized as a preliminary analysis technique before taking a decision to conduct a complete quantitative study of the area using software-based models to give a clearer picture of the aquifer susceptibility.

2.4 Use of numerical modelling to manage Groundwater

The use of software-based models to represent the groundwater dynamics has picked up pace with the advent of powerful simulation tools and increase in accessibility of robust hardware system that can rapidly perform the calculations. Also, the ever changing status in terms of groundwater degradation needs constant planning which requires quantitative estimates of fluctuation and pollution. In such situations, groundwater models save considerable time in decision making if the conceptual understanding of the study area has previously been developed and data collected (Dennehy et al., 2015). These models provide the much needed quantitative estimate of the problem and its probable solution by replicating the situation as close to the reality as possible. Thus, they can act as a strong investigating and simulating tool. The predictive capacity of such modelling softwares can also be explored to find alternative solutions to the problem (Sahoo & Sahoo, 2019).

Groundwater modelling is a powerful management tool that helps in understanding the properties of groundwater aquifer as well as its response to recharge and discharge fluctuations. It also helps in quantifying release, flow and transport of various groundwater contaminants. This tool can serve multiple purposes as it organises the huge hydrological data, quantifies the existing situation by simulating

the present aquifer scenario in terms of both flow and transport processes; and predicts the future response of the system to probable scenarios (Dennehy et al., 2015; Saba et al., 2016). Many such models have been historically developed and used either individually or in conjugation with Remote sensing, GIS and other models to represent as close as possible the complexity of subsurface hydrogeology. Such models have always assisted in gaining deeper insights of the behaviour of the groundwater flow and transport, and have been widely used across world. Studies have been carried out to simulate different aquifer systems worldwide such as Coastal Plains of South Australia (Pavelic et al., 1997), Milk River Aquifer of Canada and USA (Petre et al., 2019), Chaudière-Appalaches region in Québec of Canada (Janos et al., 2018), High Plains aquifer in USA (Amaranto et al., 2019), Ordos catchment in China (Hou & Zhang, 2008), North Plain of China (Shao et al., 2009), etc. But the use of modeling tools for groundwater assessments has been slowly picking up pace in India. Studies have been carried out to simulate flow (Miglani et al., 2015; Kaur, 2013; Singh, 2005; Senthilkumar & Elango, 2004) and contaminant path tracking (Vetrimurugan et al., 2017; Saba et al., 2016; Gurunadha Rao & Gupta, 2000) across Indian regions.

2.4.1 Groundwater Flow models

Antecedent literature shows large application of modelling softwares to simulate local to regional groundwater basins for groundwater flow analysis (Michael & Voss, 2009; Harou et al., 2009; Izbicki et al., 2004; Howard & Maier, 2007; Bester et al., 2006; Chandio et al., 2012). Groundwater flow models use the values of groundwater heads to simulate the flow scenario of subsurface while taking various other parameters like hydraulic conductivity, transmissivity, aquifer properties, discharges and recharges into consideration. A schematic diagram showing the basis of groundwater flow modelling is represented in Fig. 2.5. The partial differential equation of the groundwater flow in three dimensions derived by using the Darcy's law that is used by the computational numerical models is-

$$\frac{\partial}{\partial x}\left[K_X.\frac{\partial H}{\partial x}\right]+\frac{\partial}{\partial y}\left[K_Y.\frac{\partial H}{\partial y}\right]+\frac{\partial}{\partial z}\left[K_Z.\frac{\partial H}{\partial z}\right]-Q=Ss.\frac{\partial H}{\partial t} \quad (2.2)$$

where H: hydraulic head (m); Kx, Ky, Kz: hydraulic conductivity of saturated zone (m s^{-1}); Q: flow rate per unit volume (s^{-1}); Ss: specific storage of porous material (m^{-1}); and t: time (s).

The study conducted by Toth (1963) is amongst the earliest known studies that was done in the direction of development of flow modelling. The work presented a theoretical analysis of the groundwater flow in a hypothetical small drainage basin. The possibility of three types of flow system in a basin- local, intermediate and regional, was discussed by the author. Further studies by the author elaborated on the investigation of the recharge and discharge areas to identify flow systems (Toth, 1970, 1971) and also presented an analysis of flow at a larger scale (Toth, 1972). The approach used by Toth (1963) was extended by Freeze and Witherspoon (1966) to obtain the flow patterns in general three dimensional, anisotropic and nonhomogeneous groundwater basin with any configuration of water table as opposed to two dimensional and homogeneous basin that were considered for two specific water table configurations earlier. Freeze and Witherspoon subsequently increased the complexity of the proposed model for its applications to different modelling situations with a motive to understand the impact of water table and geological formations on groundwater flow (Freeze & Witherspoon, 1967, 1968). A transient state model was also attempted by Freeze (1971) to simulate the groundwater flow in both the saturated and unsaturated zones of aquifers.

A number of studies were carried out on groundwater simulations during 1966-1976 (Tyson & Weber, 1964; Sauerwein, 1967; Pinder & Cooper, 1970; Shamir & Dagan,1971; De Ridder & Erez, 1977), but the use of groundwater flow models to simulate large regional scale aquifer system started with the USGS program- RASA (Regional Aquifer system analysis program) in 1978. During the implementation of this program many regional scale models were developed which included the Florida aquifer system, the California central valley aquifer system and the Great Basin aquifer system. The extensive study led to the publication of 1105 reports from 1978 to1996, which contributed significantly to creation of regional scale databases and conceptual models framework (Sun et al., 1997). Both steady state and transient state models were

developed for the study region by using historical data. Another such regional scale aquifer analysis was carried out in Netherland through the project 'National Analysis of Regional Groundwater Flow Systems' which was launched by the Dutch government in 1991. It mapped the geohydrological characteristics along with the abiotic and biotic data related to the aquifer system (Engelen & Jones, 1986; Engelen & Kloosterman, 1996).

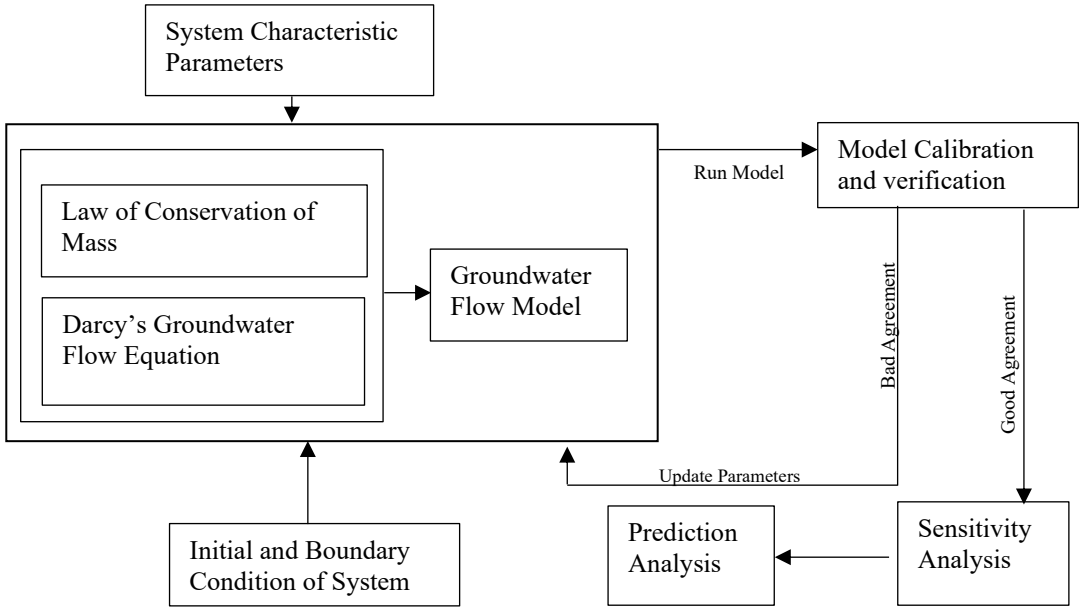

Fig. 2.5 Schematic Diagram showing steps for Groundwater Flow Modelling (Adapted from Saatsaz and Eslamian, 2020; Reilly et al., 1987)

Other than these extensive National programs, studies were also undertaken by researchers to develop models for groundwater surface water interaction in different parts of the world. Over the years, these studies expanded the scope of flow modelling and also contributed to the widening of the concepts and methodologies of flow models. The interactions between groundwater-wetland systems were studied by Siegel (1983), Woo and Winter (1993), Winter (1999), Gilvear et al. (1993) and Reeve et al. (2000) through steady state simulations. Whereas, studies undertaken by Restrepo et al. (1998) and Mansell et al. (2000) used transient-state simulations to represent the response of the groundwater–wetland system to changing natural and man-induced stresses. Apart from this, simulations of the flow in groundwater-canal

systems were undertaken in India by Sondhi et al. (1989) and Rao and Sarma (1993), the seepage losses through the canal and percolation losses through the ground were considered as the components of recharge in these studies.

2.4.1.1 Code and Support for models

The partial differential equation of the groundwater flow as derived from Darcy's law (Eqn. (2.2)) can be solved using different approaches- analytical and numerical solutions. An exact analytical solution is generally used to solve groundwater flow equations in isotropic and homogeneous media. However, aquifers are generally heterogeneous and anisotropic, and therefore, analytical solutions are impractical to be obtained in the case of complex flow problems. As such, recent research has proposed the superposition of numerous analytical fields to represent the aquifer complexity and natural environment. This ''analytic element method'' has extended the use of analytical solutions to realistic flow situations by overcoming its fundamental limitations. However, it is still a developing field and is slowly becoming popular. Therefore, the use of numerical finite difference (FD) and finite element (FE) methods of problem solving that give approximate solutions is more widespread. Earlier development of flow models had primarily used the FD method of approximations that uses the rectangular mesh technique. The FE method has also been used to mathematically represent irregular geometries of aquifer as it can be readily formulated on triangular and deformed rectangular meshes. Over the years, these solutions have been programmed using different coding languages for digital computers. They include PTC, CTRAN/W, INTERSAT/INTERTRANS, FEFLOW, FEMWATER, FRACTRAN, MODFLOW, HSSM, PREEQC, BIOSCEEN / BIOCLOR, TWODAN and PRINCE.

The most widely used code for groundwater simulations is the MODFLOW code. It was released in 1984 and subsequently improved through its 1988, 1996, 2000, 2005 and 2020 upgradation (Harbaugh et al., 2000; Harbaugh, 2005). This code is regarded as an industry standard due to its widespread usage and free availability. Its continued institutional support has led to its extensive testing. Originally, MODFLOW

was developed solely for groundwater-flow simulation. However, additional simulation capabilities are being regularly integrated to its structure through independent programming components known as 'Packages'. It can be coupled with any of these packages to simulate various conditions of the hydrogeological processes such as unsaturated-zone flow, solute transport and other complex aquifer-system interaction. The users of MODFLOW with no coding background can use softwares that provides a graphical user interface such as Model Muse, PMWIN, VIEWLOG, GMS (Groundwater modelling systems), Processing modflow, Groundwater Vista and Visual Modflow. These graphical user interfaces (GUIs) are needed to enable user interact with the code and input data and see the results.

Many organisations provide the support for research and development of groundwater modelling codes and software (Todd & Mays, 2005). The USGS (U.S. Geological Survey) provides access to multiple codes and softwares on its site, MODFLOW (along with add-on packages) is one of them. Similarly, U.S. EPA's CSMoS (Center for Subsurface Modelling Support) also provides direct support to groundwater models and provide public domain softwares. Other than these, the education and research in groundwater modelling is supported by the IGWMC (International Groundwater Modelling Center). It periodically organises short courses and workshops to spread the use of groundwater models.

2.4.2 Solute Transport models

With the development of Groundwater flow modelling that started in 1960's, the focus of researchers eventually shifted to simulating the groundwater quality situation. Based on strong evidence of experimental investigations, extensive studies that lead to the development of groundwater solute transport models were undertaken. Such studies led to the simulation of various pollutant travel paths and their distribution in the spatially varying geochemical systems. Many site specific solute models that incorporated the specific solute transport conditions were developed for 1D and 2D flow representation. Since there are different processes that dictate the transport of solute through the aquifer media, a universal model was difficult to be

built. As a result, the previously built models could be adopted only after validation of the actual site data. However, the developments in this field have led to the incorporation of increasing complexity of chemical processes and aquifer properties into a three-dimensional solute transport model. Such models are general in approach and are applicable to many sites.

The introduction of contaminants in the soil can happen through various sources (Patil & Chore, 2014). However, only the contaminants that percolate through the vadose zone and manage to reach the water-table will pollute the groundwater and continue to flow with it. In this process of percolation and transformation, the physical and chemical properties of the pollutant and aquifer media can significantly determine its passage concentration. Apart from such properties; there are a large number of physical, microbial and chemical processes that affect the solute transport in the subsurface (Reilly at al., 1987; Patil & Chore, 2014). Such physical and chemical processes that act on solute are- advection, dispersion, diffusion, retardation, redox reactions, biodegradation, hydrolysis and cation exchange (Saatsaz and Eslamian, 2020).

The essential movement of the pollutant through advection is caused by the groundwater flow and is governed by the Darcy's law (Reilly et al., 1987; Chawla & Singh, 2014). Therefore, the output variables from the flow models are needed for the development of solute transport model as major solute transport tends to be primarily dependent on the groundwater velocity. Other than advection, dispersion and diffusion are crucial physical processes that regulate solute flux (Saatsaz & Eslamian, 2020; Bobba, 2012). Dispersion results from the mixing of polluted and non-polluted groundwater whereas the diffusion is a molecular process where the ions tend to move from a region of higher solute concentration to lower concentration (Pandey et al., 2018; Demirel, 2014). Both of these processes are together referred to as hydrodynamic dispersion. Based on these processes, solute transport models that have been developed are typically either advection, advection-dispersion, or advection-dispersion-chemical reaction based (Bobba, 2012). A schematic diagram showing the basis of solute transport model is represented in Fig. 2.6.

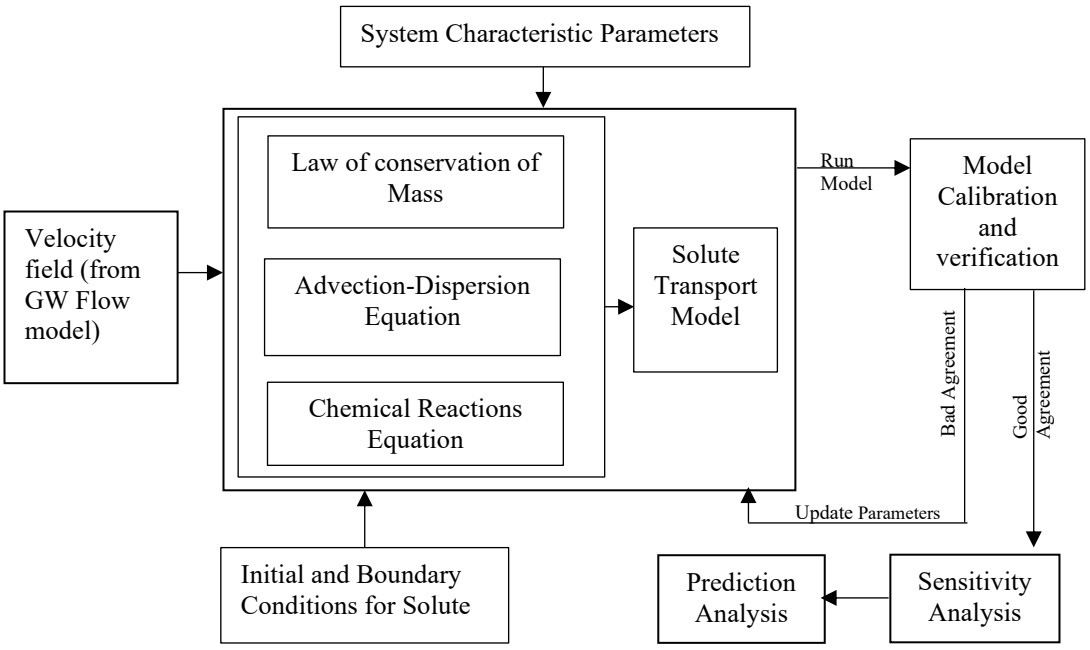

Fig. 2.6 Schematic diagram showing steps for Solute Transport Modelling (Adapted from Saatsaz & Eslamian, 2020; Reilly et al., 1987)

2.4.2.1 Solute Transport Equation and codes

Mathematical expression of the processes that determine the solute transport are based on the principle of conservation of mass which necessitates equality in net mass of the solute entering and leaving the system (Konikow et al., 1996). That is, during the particular time interval, the accumulation or loss of solute in an aquifer media and the outgoing solute flux should be in agreement with the initial solute concentration entering the system. Many researchers have developed a variety of equations that account for one or the other solute movement and transformation processes happening inside the system. The general three-dimensional equation used by Bear (1979), Goode and Konikow (1989) for the development of the MOC3D code is given as:

$$\frac{\partial(\varepsilon C)}{\partial t} + \frac{\partial(\rho_b \bar{C})}{\partial t} + \frac{\partial(\varepsilon C V_i)}{\partial x_i} - \frac{\partial}{\partial x_i}\left(\varepsilon D_{ij} \frac{\partial C}{\partial x_j}\right) - \sum C' W + \lambda(\varepsilon C + \rho_b \bar{C}) = 0 \qquad (2.3)$$

where ε is porosity, C is volumetric concentration (ML^{-3}), ρ_b is the bulk density of the aquifer material (ML^{-3}), $\bar{C}$ is the mass concentration of solute within the solid aquifer material (MM^{-1}),V is interstitial fluid velocity (LT^{-1}), D is a second-rank tensor of dispersion coefficients (L^2T^{-1}), W is a volumetric fluid sink (W<0) or fluid source (Wi>0) rate per unit volume of aquifer (T^{-1}), C' is the volumetric concentration in the sink/source fluid (ML^{-3}), and λ is the decay rate (T^{-1}).

One of the important assumptions that is considered for Eqn. (2.3) is the incompressibility of the fluid which is flowing through a porous medium. This assumption allows the changes in fluid storage to be represented by changes in porosity. Also, the processes that have been represented in this equation are advective transport, hydrodynamic dispersion, dilution and simple chemical reactions such as linear sorption, using retardation factor and decay terms (Konikow et al., 1996). In specific cases when solute transport modelling is done for sites contaminated with the organic liquid pollutants that are less soluble in water and tend to form a distinct fluid interface, i.e., the non-aqueous phase liquids (NAPLs), the calculations for total concentration of contaminant at the saturated zone is done by the addition of concentration of residual NAPLs (Leharne, 2019; Stoppiello et al., 2020).

Similar to the flow equation, solute transport equations can be solved with analytical, numerical (finite difference, finite element and finite volume) or a mixture of analytical and numerical techniques. For the purpose of the development of MOC3D code that has been integrated in MODFLOW, the equation was solved using finite difference method. This code has been developed in modular style using FORTRAN language. Over the years, many codes have been developed to solve different solute transport equations catering to different subsurface processes. Some of them are HYDRUS (2D/3D), FEHM (Finite Element Heat and Mass Transfer), MOC3D (Method of Characteristics in three dimensional), MOFAT (Multiphase Flow and Multicomponent Transport), NAPL Simulator, SUTRA, MODPATH (Particle tracking for MODFLOW), BIOPLUME (Biodegradation modelling), FEMSEEP (Finite element flow and transport), MT3DMS (Modular Transport, 3-Dimensional,

Multi-Species model), RT3D (Reactive Transport in Three Dimensions), SEAM3 and FEMWASTE are among the most widely used solute transport codes.

2.4.2.2 Measurement of Solute concentration at the Saturated zone

Groundwater solute transport models have been predominantly developed for the saturated zone of the subsurface i.e., the contaminants that manage to reach the water table are usually modelled. Therefore, researchers first need to estimate the input solute values at the saturated zone. This has been done by two methods- Firstly, by integrating different models (other than the solute transport model) that calculate the solute loadings that leach to saturated zone (El Khattabi et al., 2018; Almasri & Kaluarachchi, 2007; Zhang et al., 2019; Lyu et al., 2019) and secondly by using the observed solute values in groundwater directly (Jabeen et al., 2019; Colombo et al., 2019; Vetrimurugan et al., 2017). Many such solute transport studies that use the readings of solute input volume for the saturated zone either through direct field observations or by numerically calculating it through various other steps have been conducted across various countries using different codes and softwares (Table 2.5)

Nitrate is one of the major contaminants of concern across various regions of the world (Dar et al., 2012; Brindha & Elango, 2014) because nitrogen based fertilisers have been used intensively to promote crop growth in agriculture. However, such overuse has resulted in detection of elevated levels of nitrogen (in the form of nitrate) in groundwater, which is a matter of serious concern as high levels have been associated with serious health risk (Lee et al., 1992; Wolfe & Patz, 2002). Extensive studies have been conducted to determine the nitrate fate modeling in groundwater (Mercado, 1976; Carey & Lloyd, 1985; Malik, 2000; Shamrukh et al., 2001; Sankararamakrishnan et al., 2008; Dash et al. 2012). Such studies have mainly used soil transformation models to calculate the concentration of nitrate leaching to water table which has been then modelled for solute transport (Refsgaard et al., 1999; Lasserre et al., 1999; Birkinshaw & Ewen, 2000; Ledoux et al., 2007). The soil transformation models that were used were either developed for specific sites (Almasri & Kaluarachchi, 2004; Almasri & Kaluarachchi, 2007; El Khattabi et al., 2018) or

were adapted from previously developed models such as LEACHP (Wagenet & Huston, 1986), PRZM (Carsel et al., 1985), NLEAP (Shaffer et al., 1991) and GLEAMS (Leonard et al., 1987). El Khattabi et al., (2018) used the integration of Agriflux and VS2DT models for simulation of nitrate in root zone and unsaturated zone respectively. The AgriFlux modelled the phenomenon of nitrogen transformation in the soil (root zone) using the data for the climate, the type of crop and the quantity of fertilizer used. The calculated value of the nitrates that migrate through the root zone was used as an input for VS2DT model. Likewise, Almasri and Kaluarachchi, 2007 used an on-ground nitrogen loading model that used land use maps to calculate the input nitrogen load entering into the soil. These calculated input values were then used by soil nitrogen transformation model to account for different biochemical processes such as mineralization, nitrification, volatilization, denitrification, crop uptake and immobilization happening in the unsaturated zone and determine the amount of nitrate that manages to leach to the saturated zone.

For simulating the pollutant flow, the amount in the saturated zone can also be directly taken from the historically measured values. After selecting the input value of the solute for a specific year, the model is then calibrated for later years in accordance with the observed values. Such studies that have used observed concentrations of different contaminants for simulations include- Tritium (Gusyev et al., 2013; Gusyev et al., 2014), Nitrate and Chloride (Jhamnani & Singh, 2009; Vetrimurugan et al., 2017), Arsenic (Mukherjee & Fryar, 2008; Garg & Singh, 2016; Jabeen et al., 2019; Sathe & Mahanta, 2019); PCE (tetrachloroethylene) (Colombo et al., 2019).

The observed values of contaminant concentration in the rainfall and river water can also be used as an input of the solute transport model (Vetrimurugan et al., 2017; Gusyev et al., 2013; Gusyev et al., 2014). Vertimurugan et al. (2017) used the previously measured concentration of chloride and nitrate in groundwater, rainfall and river water at different study locations of Cauvery deltaic region as the input for solute transport. Similarly, studies by Gusyev et al. (2013) and Gusyev et al. (2014) used values of tritium in precipitation (calculated annually) as input and calibrated the model to match the observed values of tritium in baseflow.

Table 2.5: **List of studies that have used modelling to evaluate pollutant transport**

No.	Study area	Pollutants studied	Pollutant Concentration (at Saturated zone)	Code for flow simulation	Pre and Post processor	Code for solute transpost	Reference
1.	Sumas–Blaine aquifer, US	Nitrate	Onground nitrogen loading + Soil nitrogen transformation model	MODFLOW	Not mentioned	MT3D	Almasri and Kaluarachchi (2007)
2.	Catillon-sur-Sambre, France	Nitrate	Agriflux (root zone)+VS2DT (unsaturated zone)	MODFLOW	Visual MODFLOW	MT3D	El Khattabi et al. (2018)
3.	Research Center for Eco-Environmental Sciences, China	Electrical Conductivity, Nitrate	Hydrus 1D model	MODFLOW	Visual MODFLOW	MT3DMS	Lyu et al. (2019)
4.	Cauvery deltaic region, India	Chloride and Nitrate	GW Quality data 2007	MODFLOW	GMS	MT3DMS	Vetrimurugan et al. (2017)
6.	Sites at middle and lower reaches of Yangtze River, China	Organic Pollutants	Monitoring well data	MODFLOW	GMS	MT3DMS	Gao et al. (2020)
7.	Multan District, Pakistan	Arsenic	Monitoring well data	MODFLOW	Visual MODFLOW	MT3D	Jabeen et al. (2019)
	Chengdu Plain, Southwest China	Nitrate	Export coefficient model calculated diffuse nitrogen loss from agricultural land	MODFLOW	Visual MODFLOW	MT3DMS	Zhang et al. (2019)

By calibrating numerical models against long-term monitoring data from groundwater, rainfall, and surface water sources, researchers have been able to realistically reproduce contaminant migration and persistence under varying hydrological conditions. The successful application of such approaches across a range of contaminants—including nutrients, tracers, heavy metals, and chlorinated solvents—highlights their robustness and adaptability. Over the years, these modelling efforts have established the critical role of numerical simulations in assessing contaminant behavior, predicting future contamination scenarios, and supporting the formulation of scientifically sound groundwater management and water-resource protection strategies.

2.5 Integrating GIS and numerical modelling

GIS is one of the most widely used support tool with the groundwater modelling softwares. The inherent tools of GIS can easily adapt the geometrical and alphanumeric data needed to define models, while keeping its spatial and temporal variability intact. It is because of its data handling advantage that numerous GIS applications have been used extensively with various modelling softwares since 1980s (Kolm, 1996; Sengupta et al., 1996; Diepenbroek et al., 2002; Chenini & Ben Mammou, 2010; Kresic & Mikszewski, 2012; Ashraf & Ahmad, 2012; Tait et al., 2004; Velasco et al., 2014; Merwade et al., 2008; Samper et al., 2007; Strassberg et al. 2010; Saitoh et al. 2011). The coaction of GIS with modelling softwares creates a synergistic effect, the GIS not only supports the data management process but also eases out the operation of complex modelling steps, it thus creates a strong support for modelling operations from the start till the end.

The development of numerical model for a subsurface system is generally preceded by the development of conceptual model for the study area. The conceptual model uses the available information of the area to define the processes of the groundwater system. The information in the conceptual model has to be successfully transported to the numerical setup i.e., the allotment of input values has to take place in the numerical model for the simulation to be run. The GIS software plays a major

role at this step i.e., in pre-processing the initial available spatio-temporal information and then transferring this information efficiently to mesh networks of numerical models. Thus, the integration of GIS with the modelling tools is helpful in accurately assigning the initial values to the numerical grid. Also, since the spatio-temporal variability of the input and output data can be easily handled using a GIS software, it helps in visualisation of the final results. Arc Hydro groundwater tool is also one such tool that is very efficient in mesh generation and can distribute the data from conceptual models to the numerical models efficiently (Strassberg et al., 2010). Also, other USGS tools that can be used to create meshes in ArcGIS which can be exported to numerical models have been described by Silver (2014). Also, at the national level, IWFM (Integrated Water Flow Model) is one such GIS based interface that was developed by California's Government to visualize the stratigraphy, finite element grid and the initial conditions of the system.

GIS can be integrated with groundwater models through loose coupling, full coupling (or embedded coupling) and tight coupling strategies (Maidment, 1993; Abel et al., 1994; Kopp, 1996; Deckmyn et al., 1997; Goodchild et al., 1992; Sui & Maggio, 1999; Brimicombe, 2009) (See Fig. 2.7). Loose coupling is performed when both GIS software and the numerical model works as separate entities and data has to be saved in the readable files format that can be interchanged between them. Here, the GIS software is being majorly used for the pre- and post-processing of the data. As making changes will be easier in such an independent coupled system, therefore, this coupling is advantageous in a scenario where the pre and post processing steps has to be redefined for every model application.

In the embedded coupling strategy, either the numerical model is embedded inside a GIS environment and developed using a GIS programming language or the GIS software is programmed inside the numerical model, thus making it one unit. However, the downside of this coupling is that it requires intensive programming efforts and the resultant products do not always offer the same level of expert analysis as the independent commercial softwares (Sui & Maggio, 1999). Softwares such as Argus ONE and GMS makes use of the embedded coupling strategy (Pinder, 2002).

In the tight coupling strategy, both the softwares interact with each other through a predefined route of data exchange (Bhatt et al., 2014). This exchange is generally automatic through the generation of ASCII files (Steyaert & Goodchild, 1994; Martin et al., 2005). Also, in this coupling, the GIS and modelling software share the same geodatabase. This coupling has been argued to offer the advantages of both loose coupling and embedded coupling as both GIS and numerical model can develop independently with the advantage of a shared access to the data and model parameters through some specific tools (Bhatt et al., 2014).

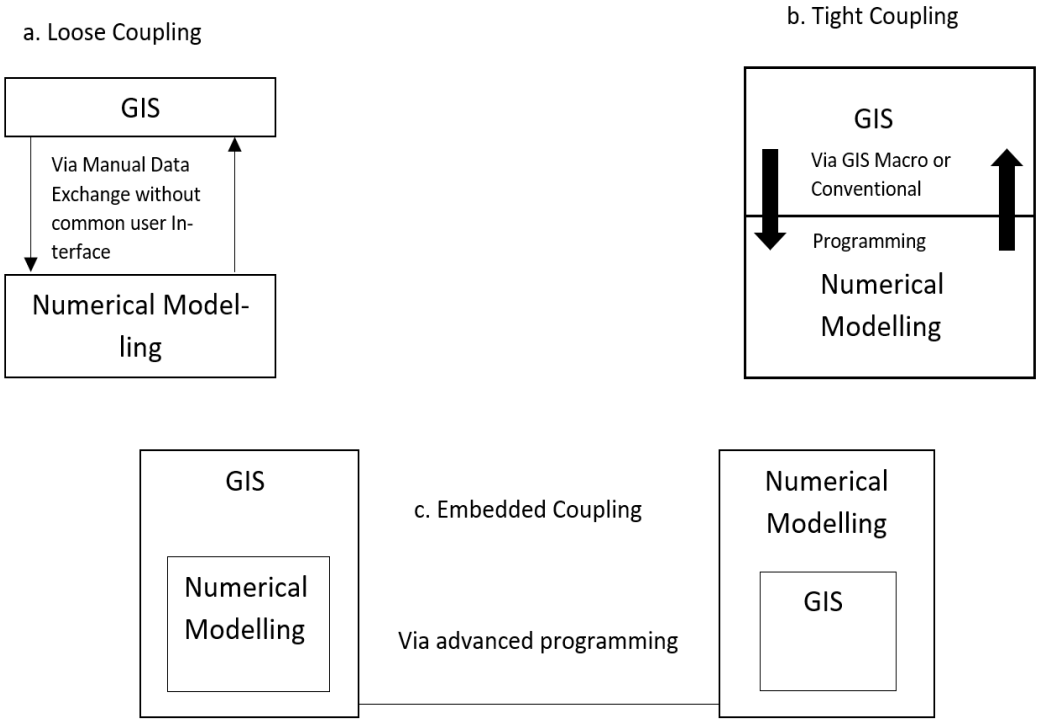

Fig. 2.7 Loose, Tight and Embedded coupling of GIS and Numerical Modelling (Sui and Maggio,1999)

Many studies have been carried out in the past that have integrated GIS and modelling softwares at various levels using different coupling strategies. Such GIS and modelling interfaces that were developed over past includes- Water Erosion Prediction Project (WEPP) + Geographic Resources Analysis Support System (GRASS) (Engel et al., 1993); Hydrologic Data Development System (HDDS) + ARC/INFO (Smith,

1997); Hydrologic Engineering Center (HEC) + ARC/INFO (Hellweger & Maidment, 1999); and Better Assessment Science Integrating Point and Nonpoint Sources (BASINS) + Soil and Water Analysis Tool (SWAT) (Lahlou et al., 1998; Di Luzio et al., 2002), etc. Also, various extensions to commercial GIS softwares were developed over the years, to enhance its capabilities to groundwater modelling. Such efforts include the development of Watershed Modeling System (WMS) (Nelson, 1997), ArcGIS-SWAT (Olivera et al., 2006) and Map WindowSWAT (MWSWAT) (Leon, 2009). The integration between GIS and numerical model can be achieved by coupling the two softwares at various levels based on data requirements and specific research objectives. The process is advantageous so much so that it considerably reduces the human errors associated with the data input process and save a lot of time in data handling and it also helps in representing the complexity associated with the real environment in the softwares.

2.6 Conclusion

Groundwater occurrence, its degradation and depletion is a complicated process that needs to be thoroughly analysed before taking management decisions. This review has discussed different methods that have been devised to perform this analysis with an aim to enhance the scientific and conceptual understanding of the available techniques. These methods should be applied after considering the data and software availability constraints while ensuring that the objectives of the targeted research are being met. Methods such as interpolation and overlay index analysis are performed in the absence of adequate quantitative information about the groundwater system usually for preliminary investigation of the areas that can pose grave concerns. However, they cannot be used to represent the complex groundwater processes and predict the future contaminant scenarios, a requirement which is fulfilled by the use of numerical models. Nevertheless, these numerical models are software based and require huge amount of spatio-temporal data with an easy accessibility of powerful computers to perform the simulations. In fact, none of these methods is free from uncertainties. Besides, our understanding of the environmental processes is limited which makes it even more difficult to adequately analyse the subsurface system. The

assignment of ranks and weights in overlay and index methods, the use of underlying assumptions associated with the equations and the handling of huge spatio-temporal data in numerical methods make these methods vulnerable to errors. Under existing circumstances, conjunction of different techniques can be done with an aim to optimizing the software performance. This will help in overcoming the shortcomings of the existing methods. The integration of GIS and numerical model is thus looked upon as being advantageous in this regard as it offers better data management options and also helps in visual representation of the model input and output.

However, handling integrated models will require additional expertise, the lack of which can cause a lot of human errors at input, output and analysis stage. It should also be realised that the hybrid models will need advance computing power and additional data. Therefore, the development of research in this direction will also need development of codes for formal integration of heterogeneous spatial and temporal data while resolving its resolution and quality related conflicts.

Nevertheless, providing more data or using more sophisticated models may not necessarily lead to a successful assessment of a groundwater vulnerability. With the growing number of available choices, it would be of paramount for future researchers to aim for a efficient application of assessment methods by primarily addressing the uncertainties inherent in the technique. Understanding this at the initial data input stage will further stop the error propagation in the analysis. Thus, these methods if employed with adequate understanding will enhance the present understanding of the groundwater system and help the decision makers to make informed choices for the future.

CHAPTER 3

METHODOLOGY

3.1 Study area

Ludhiana district falls in the Malwa region of the Punjab state and spans an area of 3767 km^2. It is one of the biggest and the most populous district of the Punjab state (Singh et al., 2019a). It is bounded by latitudes 30°34′06″N and 31°01′44″N and longitudes 75°21′30″E and 76°20′01″E on the four sides. It falls in survey of India toposheet nos. 44M /12, 16; 44N /5, 6, 9, 10, 13, 14 and 53B/1, 2, 5, 6. The district experiences tropical climatic conditions, characterized by hot summers, mild winters, and a short monsoon season, which significantly influences groundwater recharge and agricultural practices. Hot summers begin from early March and continue till the end of June. South west monsoon brings the major portion of rainfall of the area during the months of July to September, while remaining rainfall is brought about by western disturbances in winter months. There is a gradual shift from summer to winter season through a transition phase between mid-September to mid-November which is followed by winters till mid-March.

Administratively, the district is a neighbour to the districts of Jalandhar & Shahid Bhagat Singh Nagar in the north, Rupnagar & Fatehgarh Sahib in the east, Sangrur & Barnala in the south and south west respectively, and Moga & Ferozepur in the west (Directorate of census operations, 2011). In Ludhiana district, there are total 7 Sub-Divisions/Tehsils, 07 Sub-Tehsil and 13 Blocks. Also, there are a total 916 Villages in the district (District administration Ludhiana, 2021). Total population of the district as per the 2011 census is 3498739 (Directorate of census operations, 2011). The population density for the district is 928 persons, per square km. According to the Central ground water board's (CGWB) report, the annual groundwater extraction for irrigation, industrial and domestic uses in the district is 279969.95 Ham, 7104.15 Ham and 14938.81 Ham, respectively (CGWB, 2021). Almost all of the agricultural fields in the area are irrigated through groundwater (as high as 95.6%).

The river Satluj forms the northern boundary of the district, separating it from Jalandhar. The Satluj river enters Ludhiana district approximately 32 km east of Samrala Tehsil, flowing westward along the district's northern boundary for about 96 km. It leaves slightly towards north of the Jagraon tehsil and maintains direction of flow from east to west. The catchment area of the river Satluj has numerous drains amongst which notable water body that flows through the district is the Budha nallah which runs parallel to Satluj, on its south and ultimately joins it at Gorsian Kadar Baksh in the north-west. The nallah has been reported to pick up effluents and sewage through its passage across Ludhiana city and affect groundwater quality.

3.1.1 Land Use Land Cover of Ludhiana district

Fig. 3.1 shows the geographical location and land use/ land cover (LULC) map of the study area. The LULC map of the area has been taken from Bhuvan, ISRO geoportal. The database that is available on the portal has been prepared using terrain corrected data of the Resourcesat-2 from LISS-III sensor of 3 seasons pertaining to 2015-16 and LULC Vector of 2011-12. As can be seen, agriculture is the dominant land use in the district, covering 83.96% (3159 sq. km.), followed by built-up areas at 13% (489 sq. km.). Forests, water bodies, and wastelands account for small fractions, with 0.64%, 1.6%, and 0.8% of the total land area, respectively. Wheat and paddy along with potato are the predominant crops in the district, but a slow beginning of crop diversification has started happening. Rotation of cereal crops with legumes and oilseeds will reduce the exploitation of groundwater as farmers dependency on water intensive crops such as rice will decrease.

The dominance of agricultural land use indicates a high dependency of the region on groundwater resources for irrigation purposes. Extensive cultivation of water-intensive crops, particularly paddy, has resulted in significant stress on the groundwater regime, manifested through declining water table trends in several blocks of the district. Land use practices therefore play a critical role in governing recharge–withdrawal dynamics and influencing groundwater availability. A shift towards less

water-intensive crops and improved irrigation practices is essential for ensuring long-term groundwater sustainability in the study area.

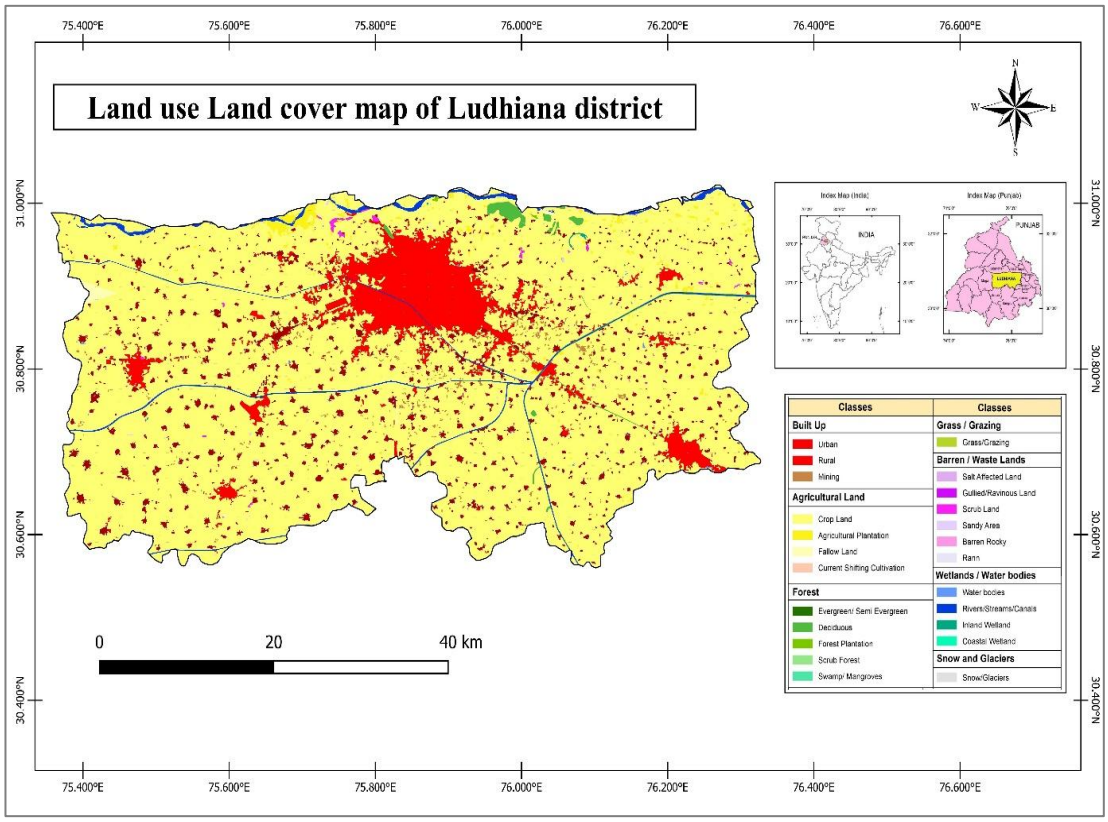

Fig. 3.1 Land use Land cover map of the Ludhiana district of Punjab, India (Source: Bhuvan Geoportal (National Remote Sensing Centre [NRSC], 2014)

3.1.2 Geology and Aquifer characteristics

Geologically, the district is covered with a thick pile of fluvial sediments which are further classified into the older alluvium and the newer alluvium group (see Fig. 3.2). The older alluvium sediments are composed of polycyclic sequence of brown to grey sand, silt and clay that date back to late pleistocene age (Singh & Punj, 1999). These sediments are also bedded with kankar and random distributions of pebble and grit. The newer alluvium group dates back to more recent holocene age. These sediments can also be further classified into the terrace alluvium that has been deposited in the flood plains of Satluj river and the recent channel alluvium that has been deposited by the active channel of the river. Both of these deposits consist of fine,

medium and coarse grained micaceous sand, silt and clay. The district is also covered with aeolian sediments called the Bhatinda formation. It comprises of fine micaceous sand and silt that range in colour from yellow to brown with occasional nodules of kankar. Thus, Ludhiana district is divisible into four geomorphic surfaces viz., the older alluvial plain, the older flood plain, the active flood plain and the aeolian plain.

The aquifer system of the area consists of 5 prominent sand aquifers separated by thick clay beds down to 400 m depth (CGWB, 2013, 2017). The first, second, third, fourth and fifth aquifers occur between 10-30 m, 50-120 m, 150-175 m, 200-250 m and 300-400 m depth, respectively. The storativity of the system ranges between 4.3×10^{-4} to 6.98×10^{-4}; and transmissivity lie between 628-1120 m^2 /day. Also, the altitude of the area varies from 221 meters in the west to 273 meters in the east with land sloping from north east to south west (Kaur, 2013). The general groundwater flow direction follows the natural slope (CGWB, 2021).

The average normal recharge from rainfall and other sources for the district, using the GEC-15 methodology has been calculated as 57008 ham and 158430 ham, respectively, for the year 2017 (Ground Water Resource Estimation Committee, 2017). However, only 90 percent of this total recharge i.e., 193894 ham, has been taken as the net annual ground water availability for the area (the remaining 10 percent is the estimated natural discharge). Similarly, the existing total groundwater extraction for all the purposes has been calculated as 354707 ham, with stage of groundwater development of the district at 183% (Sidhu et al., 2020).

The multi-aquifer system, coupled with thick intervening clay layers, governs the vertical movement and storage characteristics of groundwater in the region. Despite moderate to high transmissivity, the low storativity indicates limited replenishment capacity of the aquifers under intensive pumping conditions. The substantial gap between net annual groundwater availability and existing extraction reflects severe overexploitation of the resource. Consequently, the district falls under the over-exploited category, highlighting the urgent need for sustainable groundwater management and recharge augmentation measures.

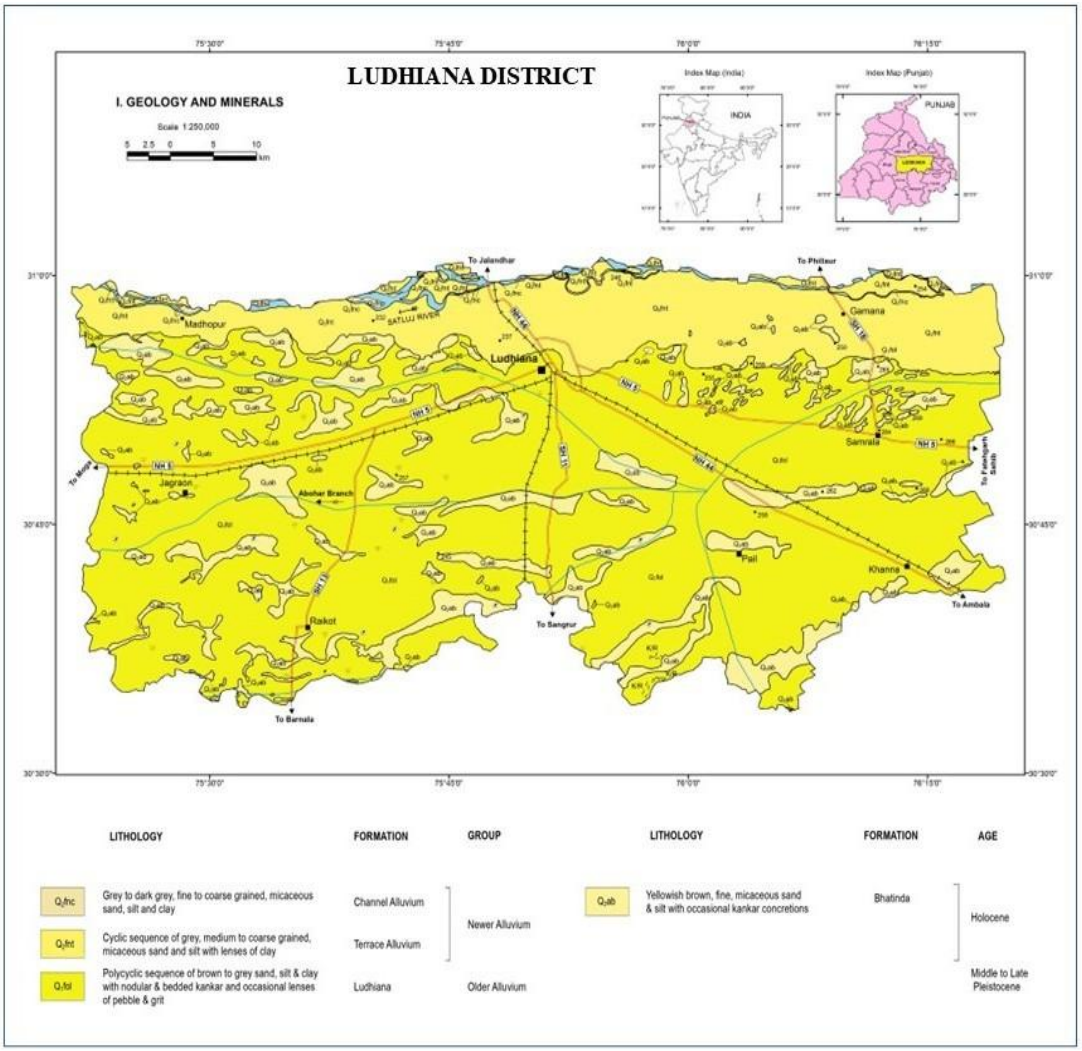

Fig. 3.2 District resource map of Ludhiana for Geology (Source: Geological survey of India)

3.2. Materials and method

The methodology adopted in this study can be divided into the following parts: sample collection and laboratory analysis, geochemical analysis, multivariate statistical analysis, spatial interpolation, assessment of drinking and irrigation water quality indices, and development of a groundwater flow model for the study area. Each component was designed to provide a systematic understanding of groundwater quality, its spatial variability and the controlling hydrochemical processes.

3.2.1 Sampling and Laboratory testing

Sampling for the study was done by collecting groundwater samples from hand pumps, tube wells and bore wells from one hundred and fifty-two (152) locations spread across Ludhiana district in Punjab (see Fig. 3.3). The coordinates of every location were noted using GPS (Global positioning system) and other details related to the source, depth and end usage were collected. The samples were collected and analysed following standard procedures outlined by APHA (American Public Health Association [APHA], 2017) in sterilized plastic bottles of 1 litre capacity. The collected samples were preserved in airtight ice boxes and taken to the laboratory to perform physicochemical analysis of water.

Fig. 3 3 Sample collection spread across Ludhiana district in Punjab

After the samples were taken to the laboratory to perform physicochemical analysis (see Fig.3.4), Total dissolved solids (TDS), pH and electrical conductivity (EC) was measured using "LABMAN LMMP-30" water quality metre. The LABMAN LMMP-30 is a multi-parameter water quality meter used in laboratory and field settings for environmental monitoring and is known for its accuracy, portability, and ability to store and transfer data for further analysis. Titrations were performed to

measure total hardness (TH), total alkalinity (TA), calcium (Ca^{2+}) and chloride (Cl^{-}) concentrations. Titration is an analytical technique in which a solution of known concentration (titrant) is slowly added to a solution of unknown concentration till a visible colour change indicates the completion of reaction. These values were further used to calculate the concentration of magnesium (Mg^{2+}), bicarbonate (HCO_3^{-}) and carbonate ions (CO_3^{2-}) in the samples. Double beam spectrometer (UV 3092) was used to measure nitrate (NO_3^{-}), sulphate (SO_4^{2-}), silica (SiO_2) and phosphate (PO_4^{3-}). Also, systronics flame photometer, which works by introducing sample into flame and measures the intensity of emitted light, was used to quantify sodium (Na^{+}) and potassium (K^{+}) concentrations. Fluoride (F^{-}) was measured using 'Orion Star A324 portable digital multi-parameter'. All the parameters were measured using analytical grade and double distilled water by following the standard procedures as laid down in APHA (APHA, 2017).

Fig. 3.4 Water quality testing and analysis in Laboratory at Delhi Technological University

3.2.2 Analytical accuracy of the readings

The analytical accuracy of the obtained sample readings was measured by calculating its charge balance error (CBE) from the following equation (Eqn. 3.1).

$$\text{CBE} = \frac{(\Sigma \text{ Cations} - \Sigma \text{ Anions})}{(\Sigma \text{ Cations} + \Sigma \text{ Anions})} \times 100 \quad (3.1)$$

For the purpose of calculations, the total cation concentration and the total anionic concentration were determined after converting the readings in milliequivalent per litre. The evaluated percentage charge balance error is within ± 5% as suggested by Domenico and Schwartz (1990).

3.2.3 Geochemistry analysis

3.2.3.1 Hydrochemical facies

The Piper (1944) plot has been used by numerous researchers to determine the water type of collected samples and account for its hydrochemical facies (Kanagaraj et al., 2018; Li et al., 2013; Mostaza-Colado et al. 2018; Snousy et al. 2022) using three cations i.e., Ca^{2+} and Mg^{2+} (alkaline earth metals), and Na^{+} (alkali earth metal); and three anion constituents i.e., HCO_3^{-} (weak acid), and SO_4^{2-} and Cl^{-} (strong acid). The diagram has two base triangles with left triangle representing cation concentrations and right triangle representing anion concentrations. Between the two triangles, there is a diamond graph where the point for the sample is marked in one of its 6 chemical facies at the intersection of the lines projecting from anion and cation triangle. The plot was generated using Aquachem 10.

3.2.3.2 Ionic ratios

Weathering of carbonates, silicates and evaporites can lead to increase in Ca^{2+} and Mg^{2+} ions in groundwater whereas Na^{+} and K^{+} generally leach out from only evaporites and silicates. In case of anions, SO_4^{2-} and Cl^{-} in water could be the result of halite, evaporite or sulfate minerals dissolution; and HCO_3^{-} is a dominant anion in both silicate and carbonate weathering. To identify different subsurface weathering processes of study area, ionic ratios as suggested by Hounslow (1995) were calculated. Also, to further understand the results, gibbs plot (Gibbs, 1970) and other bivariate plots were generated (Chitrakshi & Haritash, 2018; Rajmohan & Elango, 2004;

Thirumurugan et al., 2018). Different graphs to determine geochemistry of the study area were prepared by using MS-Excel 2022 and Aquachem 10.

3.2.3.3 Saturation Index

The Rock mineral and groundwater reactions that happen in aquifer system are kinetically impeded and move slowly towards equilibrium. The saturation state of such minerals with respect to groundwater is calculated based on log of the ratio of Ion activity product (*IAP*) and Solubility product (K_{sp}) (Clark, 2015), and is known as saturation index (SI) (see Eqn. 3.2).

$$\text{SI} = \log \frac{IAP}{K_{sp}} \tag{3.2}$$

The calculated value of SI can provide an assessment of the degree of saturation of any mineral for a given solution. Theoretically, the values of SI > 0 implies that mineral is in supersaturated condition and can precipitate; the value of SI = 0 indicates that the rock-water interaction has reached an equilibrium status and the values of SI < 0 implies that mineral is in undersaturated state and will dissolve in the water if present. However, for practical purposes the values of saturation index between -0.2 to 0.2 can be considered for equilibrium phase (Merkel et al., 2005). For the present study, the SIs for the complete set of samples has been calculated using aqueous species modelling by PHREEQC Interactive 3.7.3 software.

3.2.4 Multivariate Statistical Analysis

3.2.4.1 Principal Component Analysis

PCA is an important multivariate statistical analysis procedure that reduces data's dimensions and projects its structure to explain the maximum amount of data variability (Watkins, 2021). It is calculated by multiplying the parameters with their eigen vectors (weightings) in the direction of the component. Though, the number of components is equal to the input data variables, only the few initial components that

account for maximum variance are analysed. Thus, it becomes easier to inspect the majority of the data for hidden patterns and relationships without individually inspecting parameter to parameter relationship (Reimann et al., 2002). The PCA for the data has been performed using JMP Pro 16.2. The robust method of conducting PCA and correlation analysis was adopted to minimize the impact of outliers on the data after its log transformation.

3.2.4.2 Hierarchical Cluster Analysis

Clustering analysis is a technique that groups together observations that have similar characteristics across a 'n' dimensional space (where 'n' is the number of parameters) and tend to form clusters. Identifying these clusters can help us in understanding the spatial similarity between the samples that is based on an agglomerative combination of the parameters. For the present study, JMP Pro 16.2 was used to perform a two-way clustering analysis on the dataset, to understand the Q mode and R mode groupings of the data. Hierarchical clusters have been formed using ward linkages method (Masood et al., 2022).

3.2.5 Spatial Analysis using Geographic Information System

3.2.5.1 IDW interpolation

Inverse Distance Weighted (IDW) is an algorithm that is run by the software to create a geodatabase of interpolated values. It is a deterministic method of calculation where the calculated value represents weighted average (calculated as inverse of distance) of the nearby observation points (Seyedmohammadi et al., 2016). The algorithm assigns more weightage to the nearby points and determines the interpolated value by assigning them high impact.

The Interpolation function of Inverse distance weighting is as follows (Mirzaei & Sakizadeh, 2016) -

$$Z(x) = \frac{\sum_{i=1}^{n} w_i z_i}{\sum_{i=1}^{n} w_i} \quad (3.3)$$

where, $$w_i = d_i^{-u} \quad (3.4)$$

Z(x) is the output interpolated value, z_i is the parameter value at the sampling point, w_i is the weight assigned to point i, n is the total number of points considered for interpolation, d_i is the distance between point i and the output point, and u is the weighting power with a negative sign that influences the weight based on inverse distance. For this research, the maps have been prepared using IDW interpolation technique using spatial analyst tool in QGIS 3.10.9 software.

3.2.6 Analysis for drinking water quality

3.2.6.1 Water Quality Index

The quality of water is defined by a range of variables that quantify its physical, chemical and biological properties. The aggregation of these properties based on arithmetic, geometric, harmonic or logarithmic principles presents a cumulative site-specific value to assess its water quality (Uddin et al., 2021). The calculation of WQI is one such method where quantifiable data is modified into an ordinal and qualitative value through weighted or unweighted aggregation.

In this study weighted arithmetic WQI has been calculated by taking into consideration 10 parameters- pH, TDS, TH, TA, Ca^{2+}, Mg^{2+}, Cl^-, F^-, SO_4^{2-} and NO_3^-. The values of these parameters have been compared with the acceptable limits specified by Bureau of Indian Standards (2012). Following equations were used to arrive at the index value-

$$\text{WQI} = \frac{\sum_{i=1}^{n} W_i Q_i}{\sum_{i=1}^{n} W_i} \quad (3.5)$$

where, Q_i is the quality rating for i^{th} parameter; W_i is the weight of i^{th} parameter.

The Quality ratings of the parameters has been calculated by using the below given formula-

$$Q_i = 100* [(V_o-V_i)/ (S_n-V_i)] \quad (3.6)$$

where V_o is the measured value of i^{th} parameter at a particular sampling location, V_i is the ideal value of i^{th} parameter in pure water, and S_n is the acceptable limit of the i^{th} parameter according to Bureau of Indian Standards (2012).

For all the parameters, the ideal values (V_i) have been taken as zero for pure water except, pH, where the ideal value has been taken as 7.0, while the acceptable limit has been taken as 8.5 (for impure water) (Ram et al., 2021). Q_i will lie between 0 to 100 if the tested parameter is within the specified limit and will lie above 100 if the parameter value is above the prescribed standards.

Apart from the Quality ratings, the weights (W_i) that have been assigned to the various water quality parameters have been calculated from the equation that projects an inverse relationship between the weights and the specified acceptable limits for selected parameters. The equation is-

$$W_i = \frac{K}{S_n} \quad (3.7)$$

where, W_i is the calculated weight for the i^{th} parameter and K is the proportionality constant.

For this study, the value of K has been calculated as 1.12 by using the below mentioned equation-

$$K = \frac{1}{\sum(\frac{1}{S_n})} \quad (3.8)$$

The WQI value, thus arrived at, has been further classified into five classes (Yadav et al., 2010) and a WQI map using a series of colours such as red (very poor), orange (poor), yellow (average), green (good) and blue (excellent) has been prepared using QGIS 3.10.9.

3.2.7 Analysis for Irrigation water quality

3.2.7.1 Hazard analysis

There are different categories of possible hazards that were assessed in this research to understand the quality of irrigation water. Salinity hazard for the area was categorized by using EC (µS/cm) values whereas sodium hazard was assessed by calculating the soluble sodium percentage (SSP) and sodium absorption ratio (SAR). Also, a USSL diagram was made to classify the irrigation water with respect to both salinity and sodium hazard combined. The carbonate-bicarbonate hazard was assessed by calculating the Permeability Index (PI), which provides an indicator of the water's potential for soil permeability issues. The overall irrigation water quality index (IWQI) was calculated according to the formulas proposed by Meireles et al. (2010) which integrate various water quality parameters. The indices calculation and plot generation were done using MS Excel 2022 and Aquachem 10 softwares.

3.2.7.2 Irrigation water quality index

Irrigation practices can lead to issues such as salinity, sodicity, and waterlogging in the soil. Assessing the quality of irrigation water and its potential impact on soil and crop yield is a complex task, influenced by various water quality parameters (Minhas et al., 2019, Batarseh et al., 2021). Such parameters are employed to assess the potential precipitation of salts and the development of salinity and sodicity due to irrigation, thus categorizing water suitability for irrigation. This study aims to calculate an irrigation water quality index that can take into account these parameters and aggregate them to give a single value that can indicate the interplay between salinity, soil sodicity, and toxicity risk (Singh et al., 2019b, Yıldız & Karakuş, 2020). This index will help in assessing and mitigating potential problems that may

arise in irrigated soils and affect plant growth.

The individual characteristics of water resources can be consolidated together to arrive at an index, the value of which can be used to interpret the water quality in simplified term. The choice of variables that are selected to be included for index calculations can be subjective as they can be based on opinions of experts or can be selected using a statistical technique. For this paper, the parameters that contribute to the maximum variability in irrigation water quality as suggested by Meireles et al. (2010) were selected to arrive at irrigation water quality index.

To establish the index, a sub-index known as q_i was calculated. It was a quality measured value which was calculated for every parameter separately using the criteria proposed by Ayers and Westcot (1985). The laboratory results of ionic concentrations were input in Eqn.3.9 as follows:

$$q_i = q_{imax} - [((x_i - x_{lower}) * q_{iamp}) / x_{amp}] \quad (3.9)$$

where x_i is the observed value of the parameter, x_{lower} is the corresponding value of the lower limit of the class to which the parameter belongs, x_{amp} is the class amplitude. The different parameter classes are mentioned in Table 3.1. Similarly, classes for q_i corresponding to the x_i values are also mentioned in the Table 3.1. Here, q_{imax} is the max value of the q_i class, and q_{iamp} is the q_i class amplitude.

The highest value of the parameter was used as a upper limit to calculate x_{amp} for the last category of class for the parameter. Also, the parameter weights (w_i) that were used to calculate the IWQI were taken as per the suggestions of Meireles et al. (2010) (Table 3.2). The final equation (Eqn. 3.10) that was used for IWQI is-

$$IWQI = \sum_{i=1}^{n} q_i w_i \quad (3.10)$$

IWQI value thus obtained will be a dimensionless number ranging from 0 to

100. Categorisation of this value has been proposed to define restrictions on water use, following the classifications suggested by Meireles et al. (2010) to account for the risk of salinity problems, soil water infiltration reduction as well as toxicity to plants. These categories are: No restriction; for IWQI values that lie between 85-100; Low restriction (70-85); Moderate restriction (55-70); High restriction (40-55) and Severe restriction (0-40).

Table 3.1: Parameter limiting values for quality measurement (q_i) calculations

q_i	EC (µS/cm)	SAR $(meq/l)^{1/2}$	Na^+ (meq/l)	Cl^- (meq/l)	HCO_3^- (meq/l)
85-100	200 – 750	2 – 3	2 – 3	1 – 4	1 – 1.5
60-85	750 – 1500	3 – 6	3 – 6	4 – 7	1.5 – 4.5
35-60	1500 – 3000	6 – 12	6 – 9	7 – 10	4.5 – 8.5
0-35	<200 and ≥ 3000	<2 and ≥12	<2 and ≥9	<1 and ≥ 10	<1 and ≥ 8.5

Table 3.2 Weights (W_i) taken for IWQI calculation

Parameters	W_i
Electrical Conductivity (EC)	0.211
Sodium (Na^+)	0.204
Bicarbonate (HCO_3^-)	0.202
Chloride (Cl^-)	0.194
Sodium Absorption Ratio (SAR)	0.189
Total	1

3.2.7.3 Visualization of Irrigation water quality using spatial interpolation

Spatial variability of the individual indices, along with the overall irrigation water quality index was visualized through GIS-based interpolation maps. These maps were prepared using Inverse distance weighted (IDW) technique in QGIS software (version 3.10.9). IDW is an algorithm that creates a geodatabase of interpolated values using a deterministic method of calculation where the calculated value represents the weighted average (calculated as the inverse of distance) of the nearby observation points (Seyedmohammadi et al., 2016). It works on the principle that closer values have more significant impact than the far values on the predicted output, which aligns

with the principle of spatial autocorrelation. This technique was chosen over other methods because this technique produces smooth surfaces which helps in visualizing spatial changes in data.

3.2.7.4 Artificial neural network based model to predict IWQI

For the modelling part, the model was created using artificial neural networks (ANN). It is the predictive modelling tool that is based on the concept of experiential learning. The neural network iteratively learns and develops itself by comparing the predicted values with the targeted values (Kouadri et al., 2022, Sarma & Singh, 2022). They are widely used because of their statistical flexibility as the model is built without hypothesizing advance relationships between variables. Also, they can approximate both linear and non-linear relationships between input and output variables (Mallik at al., 2022; Rustam et al., 2022; Taşan, 2023). The information in the neural network flow in a feed forward architecture from the input layer to the output layer. The variables in the input layer are assigned synaptic weights and an activation function, the result of which produces a hidden layer (Ahmed et al., 2019). The final output layer is response to the activation functions assigned to the hidden layer. The activation functions and the number of hidden layers can be user defined. Based on user discretion, the model can be made with more than one hidden layer as this can in some cases lead to more efficient approximation by using the smaller number of neurons in the network.

Feed forward architecture based networks can also have a back propagation of errors, where the error from the output layer is propagated backwards to the hidden layer and input layer. This allows the system to update its assigned synaptic weights to the inputs so that a better result could be obtained.

For the present study, the ANN analysis was implemented using IBM's SPSS neural network module using multi-layer perceptron based feed forward architecture. In this architecture, the input nodes in the neural network propagate the values to nodes in the hidden layers, which can be represented using the Eqn. 3.11:

$$y = f\left(\sum_j w_j\, x_j + b\right) \tag{3.11}$$

where x is the input value, w is the weight assigned to the input value through the network, b is the associated bias and f is the transfer function.

The model was run after specifying the software to rescale the input data using standardized option. The other specifications included selecting the batch process for training the network, specifying creation of two hidden layers and using sigmoid activation function. The sigmoid activation function has the following form (Eqn. 3.12):

$$y(c) = 1/(1 + e^{-c}) \tag{3.12}$$

This function takes input in any range of real numbers and transforms them to the range (0,1). Also, it can capture non-linear relationships between inputs and outputs, which helps in improving the model's accuracy. The neural network model for this study was constructed using a sigmoid activation function. It included one input layer with five nodes, two hidden layers (Layer H1 with three nodes, Layer H2 with two nodes), and a single output node. The model used gradient descent algorithm for back propagation of errors. The model was thus created through the four stages- initial weights assignment, feed forward output generation, back propagation of errors and upgradation of weights and biases.

The model's accuracy was evaluated using the Root Mean Square Error (RMSE) as calculated by Eqn. 3.13:

$$RMSE = \sqrt{\sum_{k=1}^{n} \frac{(y_k - \hat{y_k})^2}{n}} \tag{3.13}$$

where y_k is the observed k^{th} value, $\hat{y_k}$ is the predicted k^{th} value and n is number of observations.

3.2.7.5 Predictive Analysis of Future Groundwater Quality Scenarios

Groundwater is a vital resource for agricultural production in Ludhiana district, Punjab. However, over the past few decades, its quality has come under increasing pressure. The key drivers of this deterioration include intensive irrigation practices, excessive groundwater extraction, and contamination from industrial effluents. To understand how these stressors might influence irrigation water quality in the future, an Irrigation Water Quality Index (IWQI) based predictive framework was applied to three hypothetical scenarios. These forward-looking scenarios represent different combinations of management strategies, climate conditions, and levels of human intervention, each leading to distinct changes in groundwater chemistry. By projecting IWQI trends across these scenarios, the framework identifies optimal strategies to safeguard irrigation water quality for sustained agricultural productivity in the region.

The three scenarios studied were:

- Scenario 1 – Higher Abstraction and Reduced Recharge. This reflects a situation in which groundwater extraction intensifies, while recharge from rainfall and surface sources declines. Such conditions could occur during prolonged droughts or as a result of poor water management practices.

- Scenario 2 – Increased Contamination Pressure. Here, both agricultural and industrial contamination increase, accompanied by moderately high abstraction. This is an intensified pollution-pressure scenario where chemical parameters worsen considerably.

- Scenario 3 – Improved Management and Partial Quality Recovery. This scenario assumes that selected management interventions, such as improved irrigation scheduling, artificial groundwater recharge projects, regulated groundwater abstraction, and improved treatment of domestic and industrial effluents, are gradually implemented in the study area. These measures are expected to reduce the direct input of contaminants, improve aquifer

replenishment, and slow down the deterioration of groundwater quality. As a result, partial recovery in water quality may occur over time, although complete restoration may not be achieved immediately due to the delayed response of the aquifer system and the continued influence of existing contamination.

3.2.8 Groundwater flow and contaminant transport model of the study area

The first step in groundwater modeling process is to develop a conceptual model of the region using the information related to aquifer lithology (structural contours, bore logs, and aquifer properties), groundwater levels, groundwater draft, climatic data and water inflow network. These datasets help in spatial discretization and grid design of the study area. The three-dimensional movement of ground water through the heterogeneous and anisotropic aquifer is given by the following partial differential equation.

$$\frac{\partial}{\partial x}\left(K_{xx}\frac{\partial h}{\partial x}\right)+\frac{\partial}{\partial y}\left(K_{yy}\frac{\partial h}{\partial y}\right)+\frac{\partial}{\partial z}\left(K_{zz}\frac{\partial h}{\partial z}\right)\pm w=S_s\frac{\partial h}{\partial t} \quad (3.14)$$

where,

K_{xx}, K_{yy} and K_{zz} = hydraulic conductivity along the x, y and z coordinate axes (m/day);

h = hydraulic head (m);

w = volumetric flux per unit volume and represents sources and/or sinks of water (m^3/day);

Ss = specific storage of the porous material (m^{-1}); and

t = time (days).

There are number of numerical techniques to solve this equation. Prominent among them are finite difference and finite element methods. In the present study, the US Geological Survey's MODFLOW model served as the modeling framework. MODFLOW is a modular, three-dimensional finite-difference groundwater flow model. Groundwater flow within the aquifer is simulated using a block-centered finite-

difference approach.

The various steps that were performed to form the flow model of the study area are outlined below. The process started with the development of conceptual model that identified the system's composition. Thereafter, selection of the three-dimensional numerical modelling code and its associated graphical user interface, identification of the contaminant and the mechanisms for its transport, interpretation of the local results, calibration and validation of the model were carried out (Vetrimurugan et al., 2017; Pinder, 2002). The discreet steps can be outlined as-

1. Development of the conceptual model - A thorough study of geology, water level fluctuation and borehole lithologs was conducted to understand the distribution of aquifers and to develop a conceptual model that can adequately represent the aquifer.

2. Setting up of boundary conditions-The setting up of boundary conditions draws limit on the model and separates it from the rest of the world. The boundaries can be constant head or variable head boundaries based on the properties of hydrogeological features that are designated as such boundaries. Well defined and distinct features that have a definite water level are desirable for such a designation.

3. Discretization of the model into grids- After development of conceptual model and setting up of boundary condition, the map was projected in the map module and then imported into the software to create finite difference grid with a constant cell size. The creation of grid divided the entire area of concern into discretized cells and vertically into layers while assigning the depth to layers.

4. Deciding upon the values of initial groundwater head- The groundwater head values that are used as initial inputs were finalized after studying the long-term hydrograph and water table fluctuation data of the area.

5. Data collection for various input parameters- There are number of input parameters that were needed to be put in a model to make it run. Data of aquifer parameters such as hydraulic conductivity, transmissivity, specific yield/ storativity, groundwater withdrawal, recharge and evapotranspiration rates are derived majorly using pumping tests, land use patterns, soil types and rainfall. The input solute concentration was also needed to study the flow path of pollutant.

6. Model calibration and validation- The model calibration was carried out to minimize the difference between the simulated and observed groundwater head. The input parameters that were less well known were varied over a wider range than the well-known values. Calibrated model was validated against present situation so that it can be used for prediction.

After setting up the model i.e. performing its calibration and validation, it can be used to forecast future conditions of the aquifer system with respect to various changes that will happen over time to the discharge, recharge rates, pollutant input, climate and subsurface earth. Such a predictive capacity of a model can help to device sustainable strategies for groundwater management.

3.2.8.1 MODFLOW model setup and simulation approach

A regional groundwater-flow model of Ludhiana district was developed using MODFLOW-2005 through a Python/FloPy-based modelling workflow. The model was developed in two stages: an initial steady-state simulation representing baseline groundwater conditions and a subsequent transient simulation representing interannual changes in groundwater levels.

Although the aquifer system of Ludhiana district comprises unconfined, semi-confined and confined aquifer units, the system was represented as an equivalent single-layer unconfined aquifer for regional-scale simulation. This simplification was adopted because the long-term groundwater-level observations used for calibration

and validation are mainly associated with shallow observation wells representing the upper aquifer system, whereas consistent spatial and temporal observations from deeper confined aquifers are limited. Accordingly, the model is intended to represent regional groundwater-head behaviour in the upper aquifer system rather than detailed vertical flow between individual aquifer units.

The model domain was discretized into 106 rows and 191 columns with a uniform cell size of approximately 488.5 m x 488.5 m. The top elevation of each cell was derived from the Digital Elevation Model (DEM). The bottom elevation was assigned as 200 m below the ground-surface elevation, thereby representing an equivalent single-layer aquifer thickness of 200 m. Cells outside the delineated flow domain were assigned as inactive cells and therefore acted as no-flow cells. Their purpose is to exclude areas outside the defined groundwater-flow domain from numerical simulation. However, inactive cells were not used to represent the Sutlej river. River-intersecting cells within the active model domain were retained as active cells and were assigned River Package boundary conditions. Groundwater exchange with the Sutlej River occurs through active river cells rather than through inactive outside-domain cells.

The steady-state model does not represent a chronological simulation period because it solves for an equilibrium groundwater-flow condition. In the present study, the steady-state model represents baseline conditions corresponding to the annual-average groundwater levels observed during calendar year 2013. Recharge, pumping and boundary stresses applied in the steady-state model therefore represent baseline average conditions. The calibrated steady-state hydraulic-head distribution was subsequently used as the initial head condition for the transient model.

The transient simulation was conducted for the period from 1 January 2014 to 31 December 2023. It consisted of ten annual stress periods corresponding to calendar years 2014 through 2023. Each annual stress period was subdivided into 12 computational time steps. These time steps allow gradual simulation of groundwater-head response to recharge, abstraction and aquifer storage during each year. They do

not represent monthly calibration periods because the available observed groundwater levels and applied stress datasets were evaluated at the annual-average scale. The mean simulated hydraulic head over each annual stress period was therefore compared with the corresponding annual-average observed groundwater head.

3.2.8.2 Model calibration and validation

Model calibration was undertaken by comparing simulated hydraulic heads with observed groundwater heads and adjusting selected model parameters within hydrogeologically reasonable ranges. Calibration was conducted in a staged manner using manual trial-and-error adjustment, PEST++-based parameter evaluation and bounded automatic refinement through repeated MODFLOW simulations. The steady-state model was calibrated against annual-average groundwater heads representing calendar year 2013. The purpose of steady-state calibration was to establish a representative baseline groundwater-head distribution for the study area and to provide initial hydraulic heads for transient simulation. The transient model used the calibrated steady-state head distribution as its initial condition. Principal steady-state adjustable parameters included hydraulic conductivity zoning, General head boundary scaling, Sutlej river boundary parameters, constrained recharge and pumping-distribution parameters and localized stress adjustments representing unresolved spatial stress variability. Transient calibration was carried out using annual-average observed groundwater heads for seven calendar years, from 2014 to 2020. During transient calibration, the steady-state spatial conceptual model, including hydraulic conductivity distribution, river boundary, GHB configuration and spatial stress structure, was retained. Transient parameter adjustment focused on specific yield and bounded annual multipliers applied to recharge and groundwater abstraction for calibration years only. Specific storage was kept fixed at 1×10^{-5}.

Independent validation was conducted for calendar years 2021, 2022 and 2023. During validation, no aquifer parameter, boundary parameter, recharge multiplier or groundwater-abstraction multiplier was estimated using validation-year observed groundwater heads. Recharge and draft stresses for the validation years were applied

from the prescribed annual stress series without fitted validation-year correction multipliers; that is, their annual correction multipliers were maintained at unity. Simulated annual-average heads were then compared with observed annual-average groundwater heads to evaluate predictive performance. Model performance was evaluated using following residual-based statistical indicators:

Mean error (ME)

$$\mathrm{ME} = \frac{1}{n}\sum_{i=1}^{n}(h_s - h_o) \tag{3.15}$$

where, Mean Error (ME) is the mean of difference between the simulated head (h_s) and the observed head (h_o), it is also reported as bias.

Mean absolute error (MAE)

$$\mathrm{MAE} = \frac{1}{n}\sum_{i=1}^{n}|h_s - h_o| \tag{3.16}$$

where, Mean Absolute Error (MAE) is the mean of the absolute value of the differences in the simulated head (h_s) and the observed head (h_o).

Root mean square error (RMSE)

$$\mathrm{RMSE} = \sqrt{\frac{1}{n}\sum_{i=1}^{n}(h_s - h_o)_i^2} \tag{3.17}$$

where, RMSE is root mean square error; h_s is simulated value, h_o is observed value; and n is number of pairs of observed and simulated values.

Normalized root mean squared error (NRMSE)

$$\mathrm{NRMSE} = \frac{\mathrm{RMSE}}{(h_o)_{max} - (h_o)_{min}} \times 100 \tag{3.18}$$

where, NRMSE (%) is calculated by dividing the root mean square error (RMSE) by the range of observed hydraulic-head values, defined as the difference between the maximum and minimum observed heads, and multiplying the resulting ratio by 100.

3.2.8.3. Analysis of contaminant spread using groundwater flow parameters and modelling

The analysis was carried out to determine whether the distribution of the measured nitrate values for the year 2020 was controlled by regional groundwater flow processes or by localized anthropogenic influences. Both statistical correlation and spatial autocorrelation techniques were employed to interpret the contamination pattern. To evaluate whether nitrate concentrations exhibit spatial clustering at the district scale Global Spatial Autocorrelation Analysis (Moran's I) was computed for the dataset (n = 152 sampling locations). This index helps in quantitatively assessing whether contamination exist as hotspots or form one large continuous contaminated zone. Also, the distribution analysis of measured nitrate concentration in groundwater for the year 2020 was done by evaluating its relationship with the hydraulic head's distribution across the district. Groundwater flow direction was established using observed hydraulic head data, and nitrate concentrations were spatially compared against both simulated and observed head surfaces. Correlation analysis was performed to evaluate statistical relationships between nitrate concentration and hydraulic parameters.

Further, the measured dataset of nitrate was used to evaluate the decadal-scale evolution of its concentrations under prevailing hydrogeological conditions and to assess the persistence and spatial evolution of contamination hotspots using predictive modelling. A groundwater contaminant transport model was developed by integrating MODFLOW flow simulations with the MT3DMS transport package to predict contaminant distribution over time. Hydraulic parameters that were used are porosity = 0.12, longitudinal dispersivity = 20 m, transverse ratios = 0.1 (horizontal) and 0.01 (vertical). A standard finite difference advection scheme was used and the modelling was carried out for a scenario that assumed zero additional nitrate loading with no reaction taking place (IREACT = 0). Initial concentrations were defined from site investigation data. Output concentrations were stored in '.ucn' files and converted to '.csv' for detailed spatial and temporal analysis.

CHAPTER 4

RESULTS AND DISCUSSION

4.1 Physicochemical characterisation of groundwater

This study has analysed the groundwater samples for 18 parameters, whose statistical summary has been presented in Table 4.1. The table also shows the percentage of samples that comply with the permissible limits set by the India's IS 10500: 2012 drinking water specifications (Bureau of Indian Standards [BIS], 2012).

Table 4.1 Summarisation of analysed parameters for range, mean and percent suitability against the prescribed standards

S.No	Parameters	Range(min-max)	Mean±SD	BIS Standards	Suitability (%)
1	pH	6.34-7.91	7.27±0.26	6.5-8.5	100
2	EC (uS/cm)	252-1544	721.34±250.88	NM*	
3	Salinity (ppt)	0.05-0.74	0.30±0.14	NM	
4	TDS (ppm)	127.50-772	361.83±125.67	500	84.87
5	TH (mg/l)	95-515	282.76±82.35	200	15.13
6	TA (mg/l)	250-1610	764.14±227.93	200	0
7	CO_3^{2-} (mg/l)	1-144	35.04±25.03	NM	
8	HCO_3^- (mg/l)	280.60-1964.20	861.95±269.24	NM	
9	Cl^- (mg/l)	12-264	55.39±35.60	250	99.34
10	SO_4^{2-} (mg/l)	3.75-231.85	32.98±26.37	200	99.34
11	NO_3^- (mg/l)	0.01-118	8.51±15.53	45	96.7
12	PO_4^{3-}(mg/l)	0-0.34	0.07±0.10	NM	
13	F^- (mg/l)	0.19-3.40	0.66±0.38	1	93.42
14	SiO_2(mg/l)	11.80-142.94	61.50±16.01	NM	
15	Na^+ (mg/l)	6.29-668.9	80.60±105.25	NM	
16	K^+ (mg/l)	2.96-70.2	10.44±7.12	NM	
17	Ca^{2+} (mg/l)	16.032-142.284	58.18±21.38	75	82.24
18	Mg^{2+} (mg/l)	7.2-73.2	33.02±12.73	30	35.53

*NM is not mentioned

4.1.1 Major Ions

The concentrations of Na^+, Ca^{2+}, $Mg^{2+}$and K^+ in the water samples varies in the ranges of 6.3-668.9, 16.0-142.3, 7.2-73.2, 3.0-70.2 mg/l, respectively. Out of the total volume of cations accounted for in the area, Na^+ alone contributes 44.2% (in mg/l), followed by Ca^{2+} that contributes 31.9%, Mg^{2+} that contributes 18.1% and K^+ that accounts for 5.7%. The decreasing order of their dominance (in mg/l) is $Na^+ > Ca^{2+} > Mg^{2+} > K^+$. The presence of sodium in combination with Cl^- at high concentrations can impart a strong salty taste to the groundwater (Misstear et al., 2022). However, chloride is present in much less quantity in the area and so the groundwater does not taste salty. Also, the concentration of K^+ is generally low in water under natural conditions (Xu et al., 2023).

With respect to anions, concentrations of HCO_3^- in sampled groundwater varied considerably, with values ranging from 280.6-1964.2 mg/l and a mean of 862.0 mg/l. The concentrations of Cl^-, CO_3^{2-} and SO_4^{2-} ranged from 12.0-264.0, 0.1-144.0 and 3.8-231.9 mg/l, respectively. The dominant anion in the groundwater of Ludhiana district is HCO_3^- which is usually derived from rock weathering (Gao et al., 2022) alone contributes upto 86.7% (in mg/l) of the total anionic budget followed by Cl^-, CO_3^{2-} and SO_4^{2-} with 5.6%, 3.5% and 3.3% contribution, respectively. The remaining three anions i.e., NO_3^-, F^- and PO_4^{3-} contribute to less than 1% of anionic weight. The decreasing order of their dominance (in mg/l) is $HCO_3^- > Cl^- > CO_3^{2-} > SO_4^{2-} > NO_3^- > F^- > PO_4^{3-}$.

4.1.2 Total Dissolved Solids and Electrical Conductivity

For this study, the value of TDS ranges between 127.5 to 772 mg/l with the mean at 361.83 mg/l. The acceptable limit of TDS as per BIS standards is 500 mg/l. About 15.13 % of samples in the study area lie above this acceptable limit with relatively high values at Barhampur pind, Dholanwal pind, Halwara Highway, Jargari pind, Dhandari Kalan, Hans Kalan and Sarinh pind. Water with a TDS concentration below 1000 mg/l is categorized as fresh (Misstear et al., 2022; Todd & Mays, 2005).

All the samples belong to the freshwater category as per the aforementioned classification.

The electrical conductivity (EC) values in the study region exhibits variations between 252 to 1544 µS/cm with an average value of 721.34 µS/cm. High levels of EC in groundwater represents its ionic strength that could result from surface infiltration of compounds that dissolve to produce ions and then undergo cation exchanges. For this study, 18.42 % of samples fall in low conductivity class (EC<500 µS/cm); 66.45% in medium conductivity class I (EC: 500–1000 µS/cm), and 15.13% in medium conductivity class II (EC: 1000–3000 µS/cm). None of the samples fall in high conductivity class (EC>3000 µS/cm) (Xu et al., 2023; Sawyer et al., 1994).

4.1.3 Total Hardness and Total Alkalinity

The range of minimum and maximum value of hardness in the samples is 95mg/l and 515mg/l respectively, with mean of 282.76 mg/l. As per the classification proposed by Sawyer et al. (1994), the samples have been grouped into soft, moderately hard, hard and very hard categories. While none of the samples fall in soft category, only 5.9% of the samples are moderately hard, and the majority of them i.e., 57.9% and 36.2% of the samples fall into hard and very hard categories (see Table 4.2). Also, 84.87% of the samples lie above the acceptable limit of 200 mg/l as specified by BIS, 2012.

Table 4.2: Categorisation of samples for water hardness

Range	Inference	No. of samples	Suitability %
<50	Soft	0	0
50-150	Moderately hard	9	5.9
150-300	Hard	88	57.9
>300	very hard	55	36.2

The pH of the subsurface water can directly affect the dissolution of other chemical parameters. The average value of the pH of the samples is 7.27, which

signifies the alkaline nature of groundwater. Also, for total alkalinity, 100% of the samples lie above the acceptable limit of 200 mg/l as per the specifications of BIS, 2012. The range of minimum and maximum values for total alkalinity is 250mg/l to 1610mg/l, with an average of 764.14mg/l.

4.2 Spatial Distribution Mapping

Many studies have established that the use of interpolation in GIS acts as a significant aid in preparation of spatial distribution maps (Gong et al., 2014; Ram et al., 2021; Vaiphei et al., 2020; Singh & Noori, 2022). The preparation of such maps of different groundwater parameters is very important as the sampling sites represent point data which needs to be interpolated to help us in presuming and determining the values of parameters at an unsampled location. The interpolated maps of groundwater quality parameters such as TH, TA, EC, TDS, pH, Na^{+}, Ca^{2+}, Mg^{2+}, K^{+}, SiO_2, HCO_3^{-}, Cl^{-}, CO_3^{2-}, SO_4^{2-}, NO_3^{-}, F^{-} and PO_4^{3-} can be seen in Fig. 4.1.

The distribution of pH does not show much variation across the district as most of the values lie between 7 and 8. The variation in fluoride distribution is also minimal with only few pockets showing value greater than 1 and 1.5. Similarly, in case of nitrate only few pockets with bright red and dark purple colours show a higher range of values. As can be seen from map, most of the area in the case of sulphate have been interpolated to have values below 40 mg/l and only one sample from Churpur pind exceeds the acceptable limit of 200 mg/l (BIS, 2012). The area of the district also shows less toxicity with respect to phosphate as the all values lie below 0.3 mg/l.

The spatial distribution of sodium indicates that most of the district has concentrations below 100 mg/l; however, a few localized pockets show values exceeding 200 mg/l. Relatively higher sodium concentrations are observed around Dhandari Kalan and Barhampur Pind. Similarly, in the case of calcium, the maximum area of the district falls below the acceptable limit of 75 mg/l, with only a few isolated pockets showing concentrations above this limit. These localized high-value zones may reflect the influence of groundwater–rock interaction, or anthropogenic inputs.

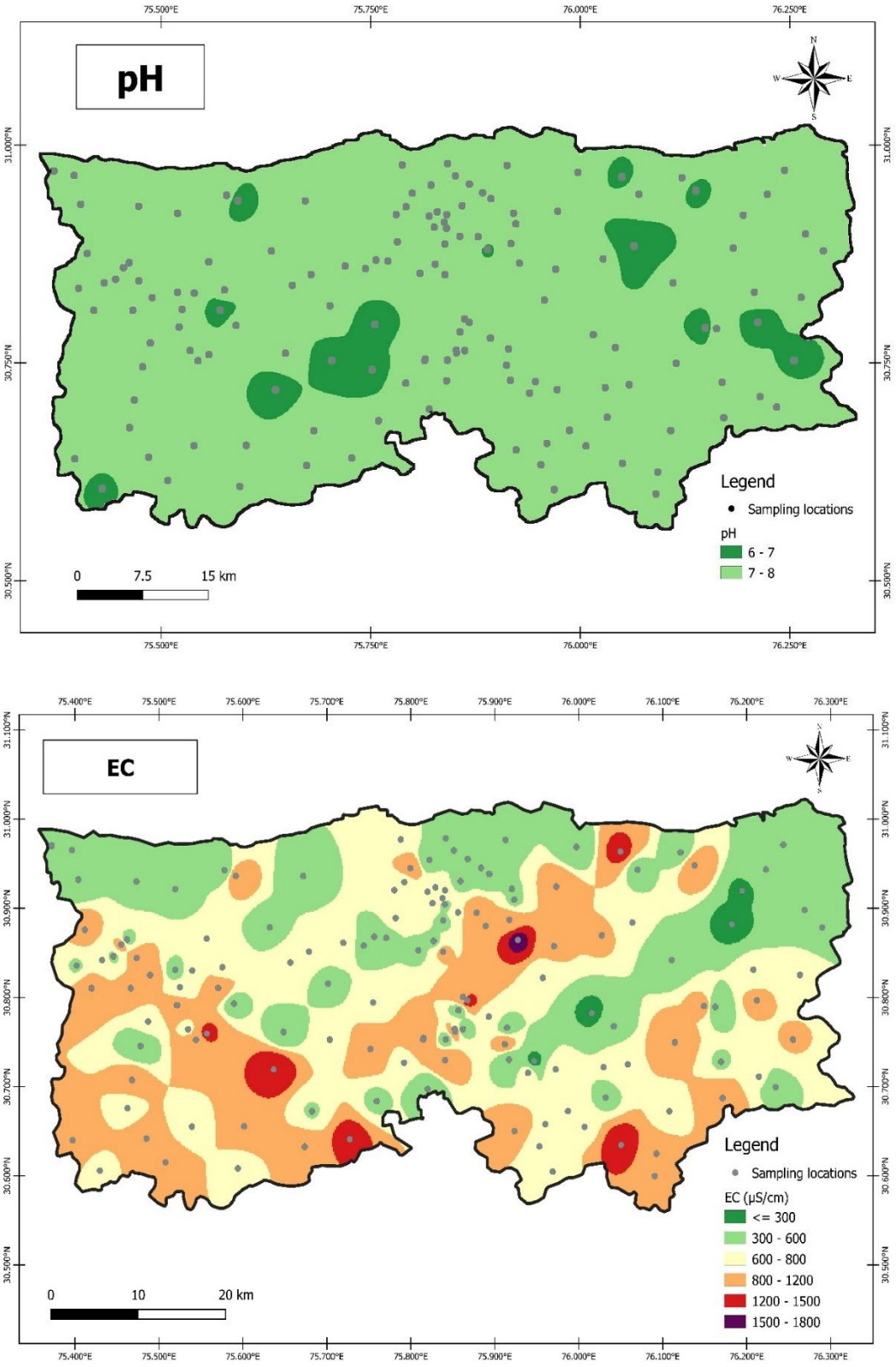

Fig. 4. 1 Spatial distribution maps of pH, EC, TDS, TA, TH and major anions and cations across Ludhiana district

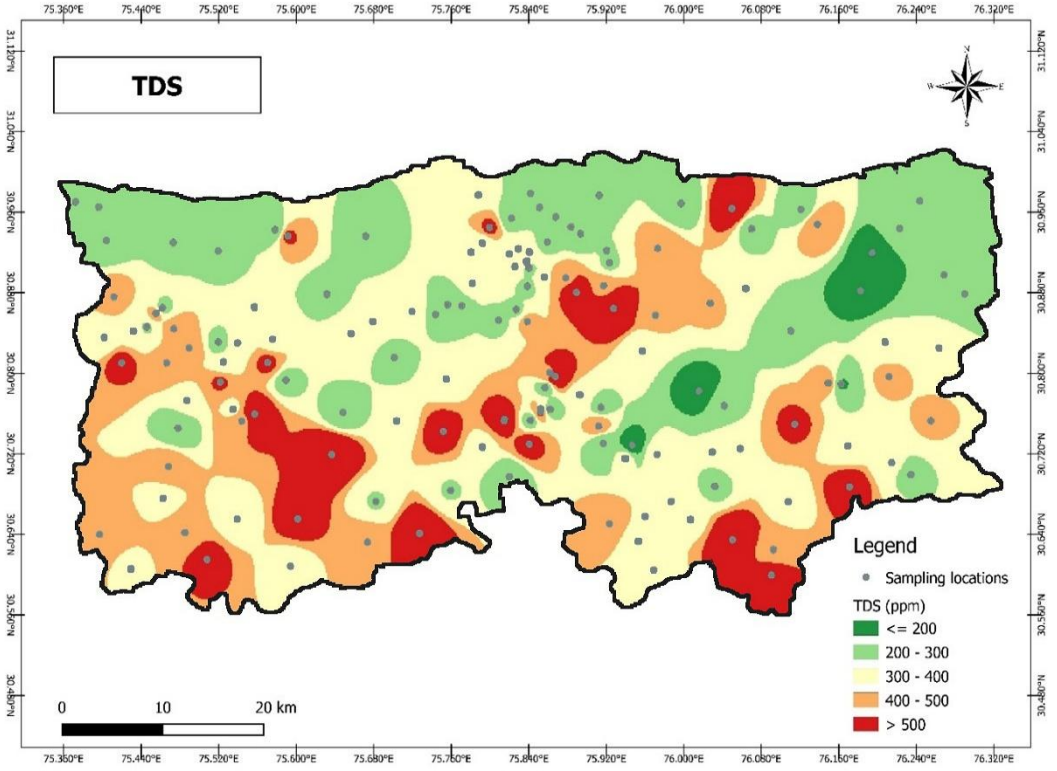

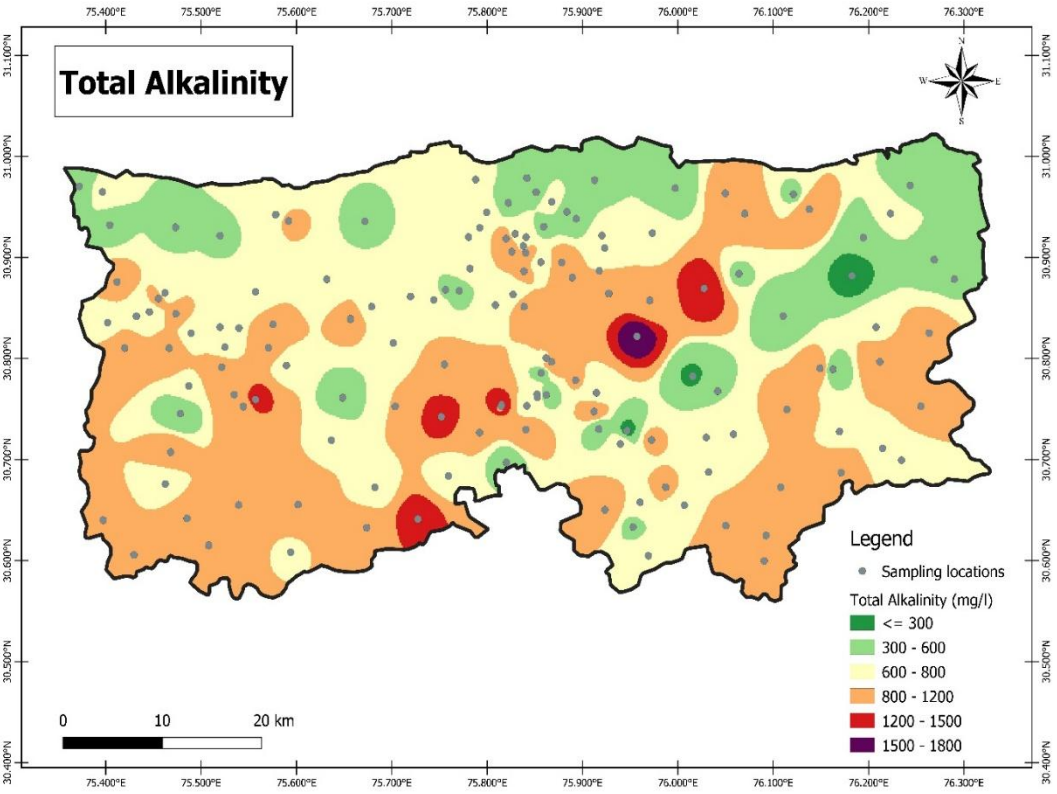

Fig.4.1 (Continued)

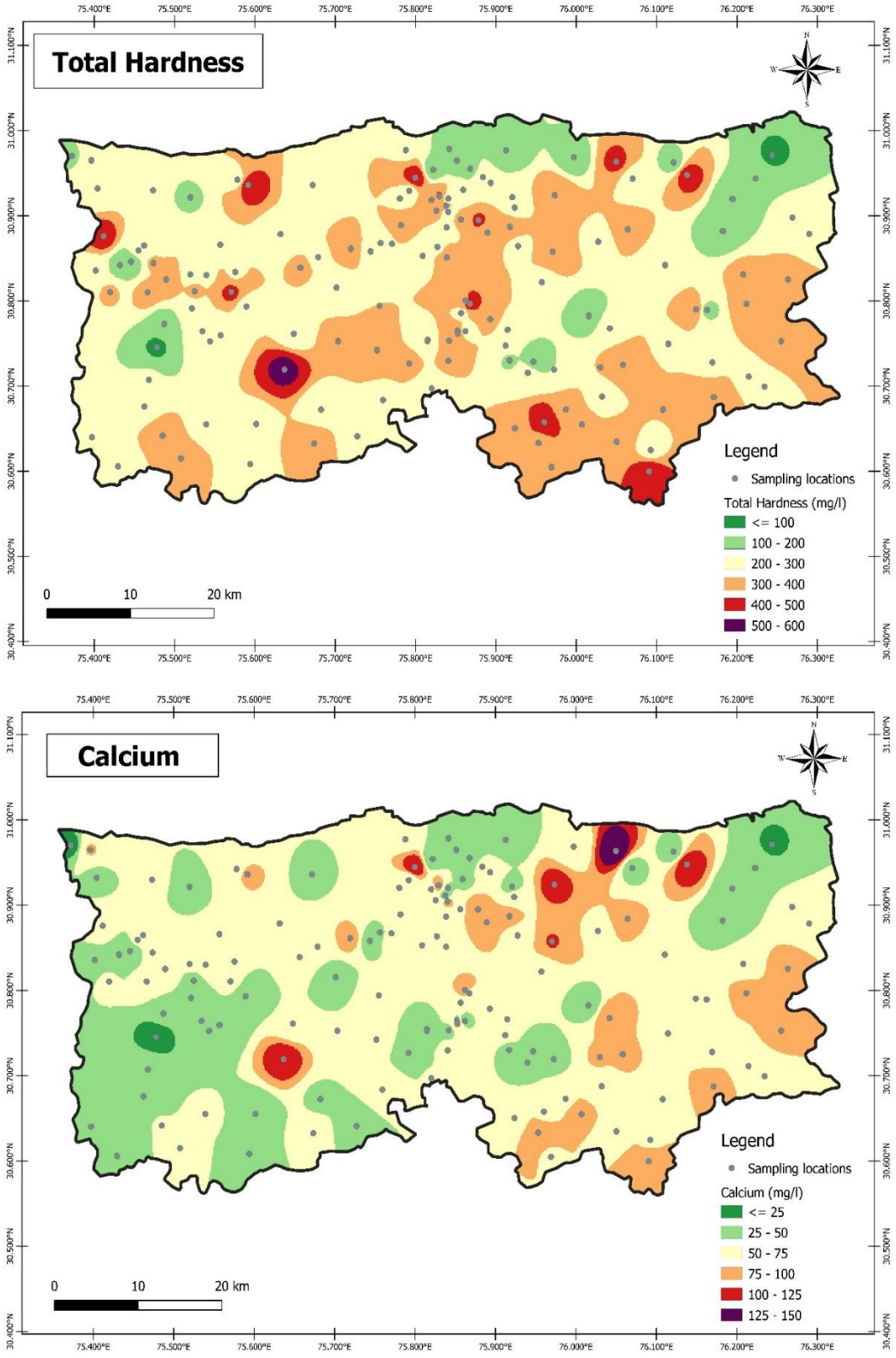

Fig.4.1 (Continued)

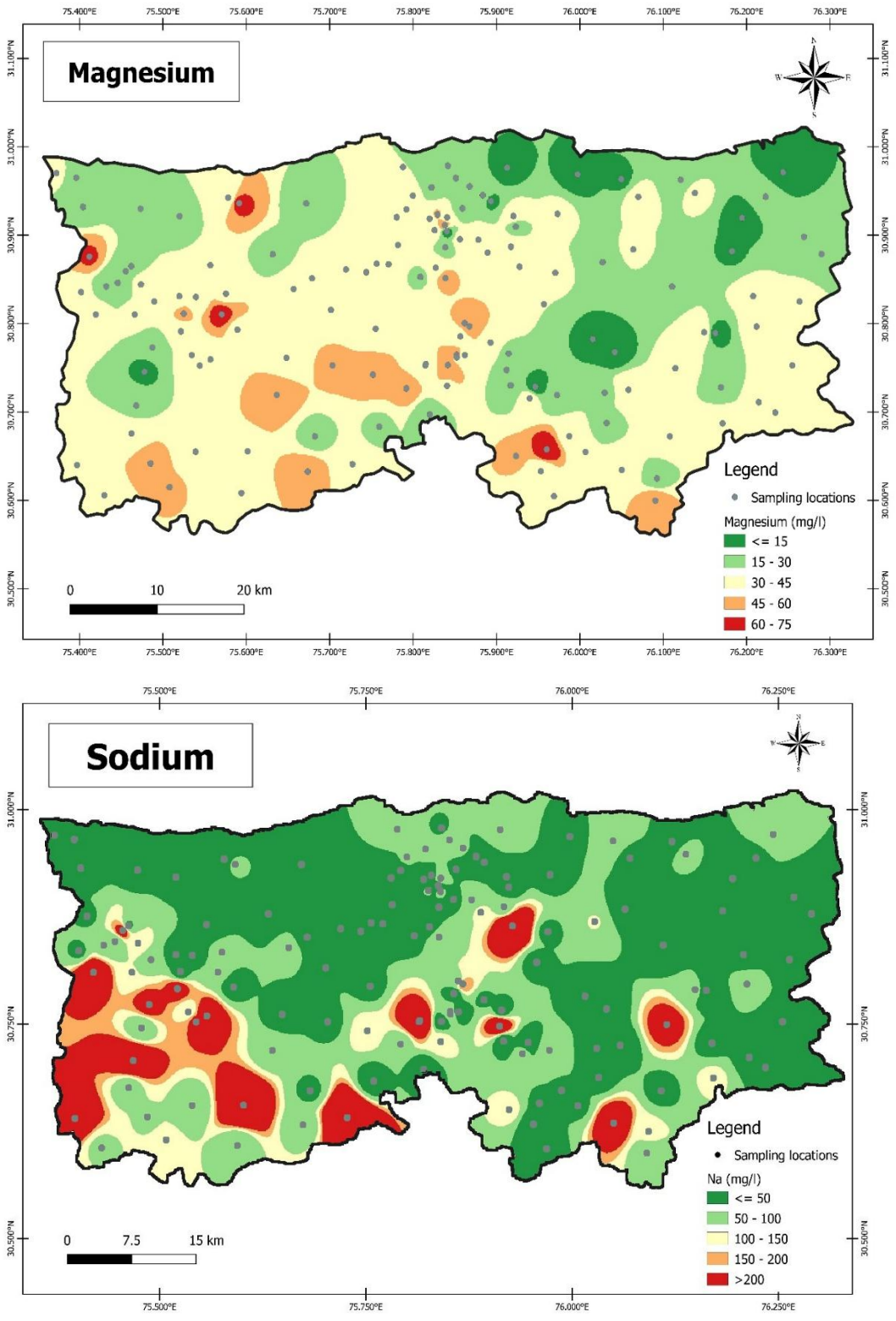

Fig.4.1 (Continued)

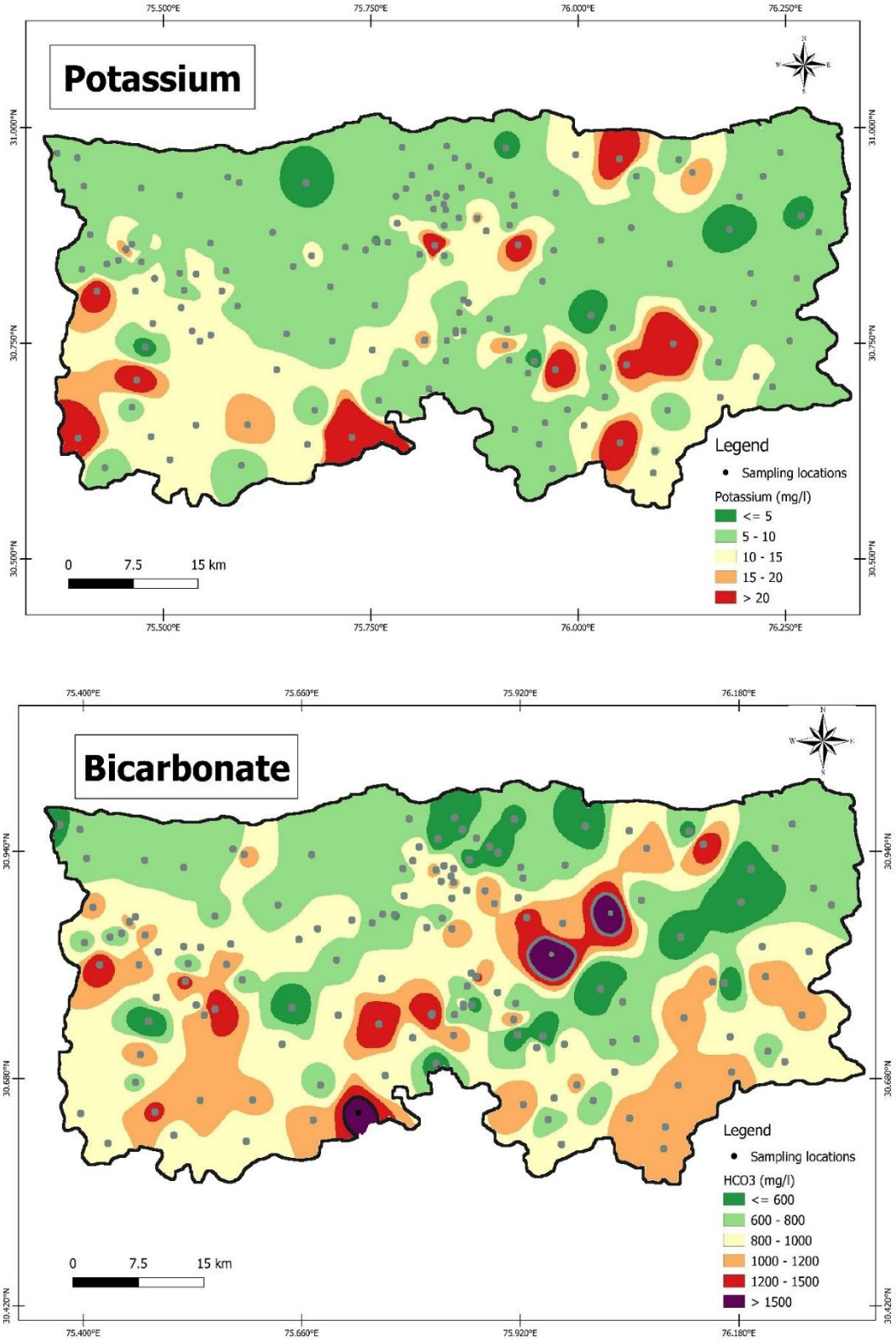

Fig.4.1 (Continued)

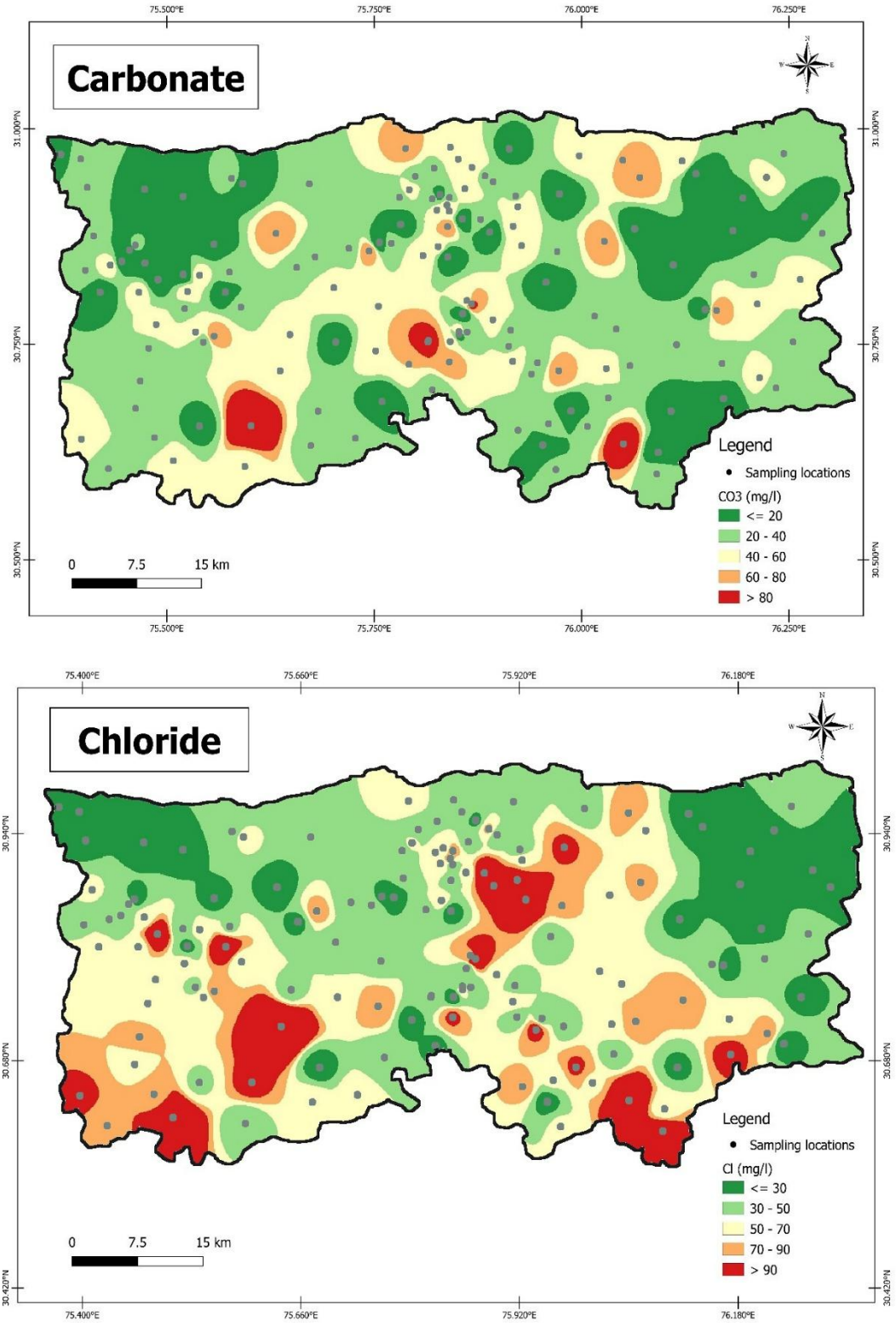

Fig.4.1 (Continued)

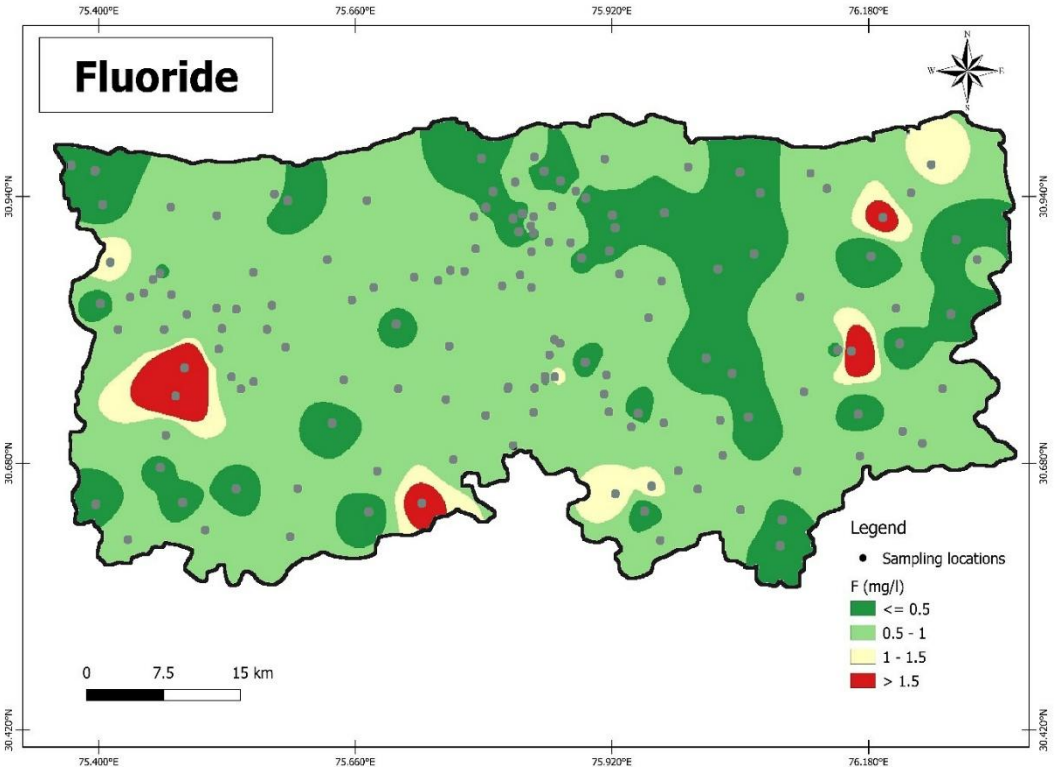

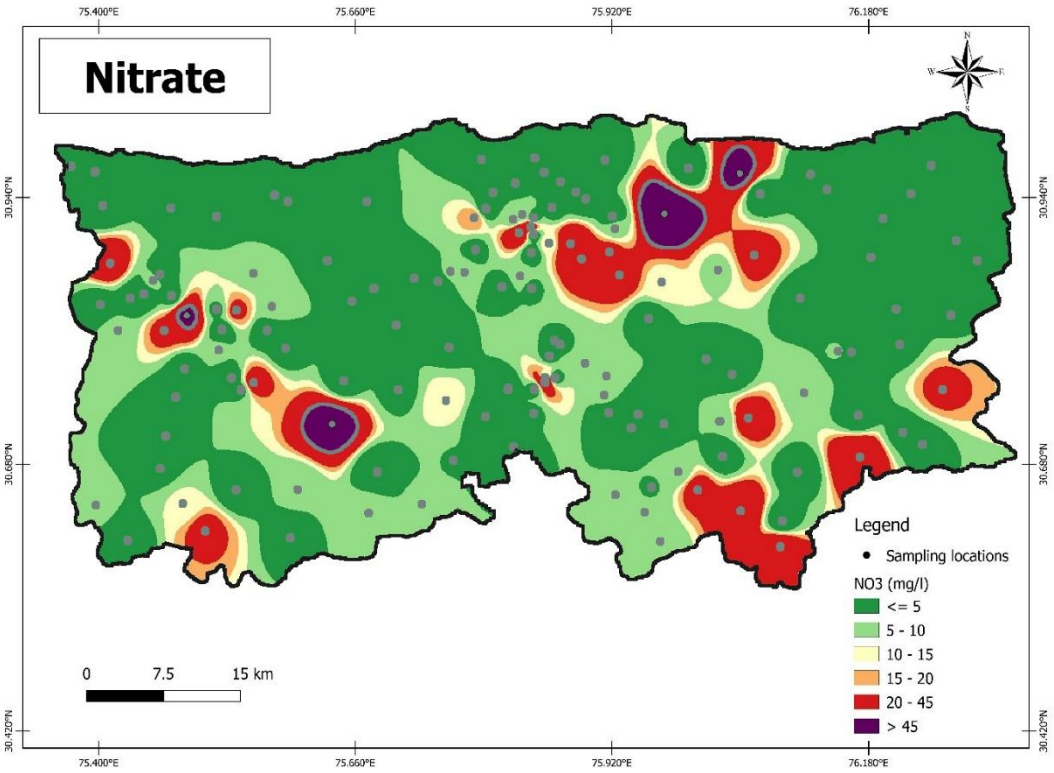

Fig.4.1 (Continued)

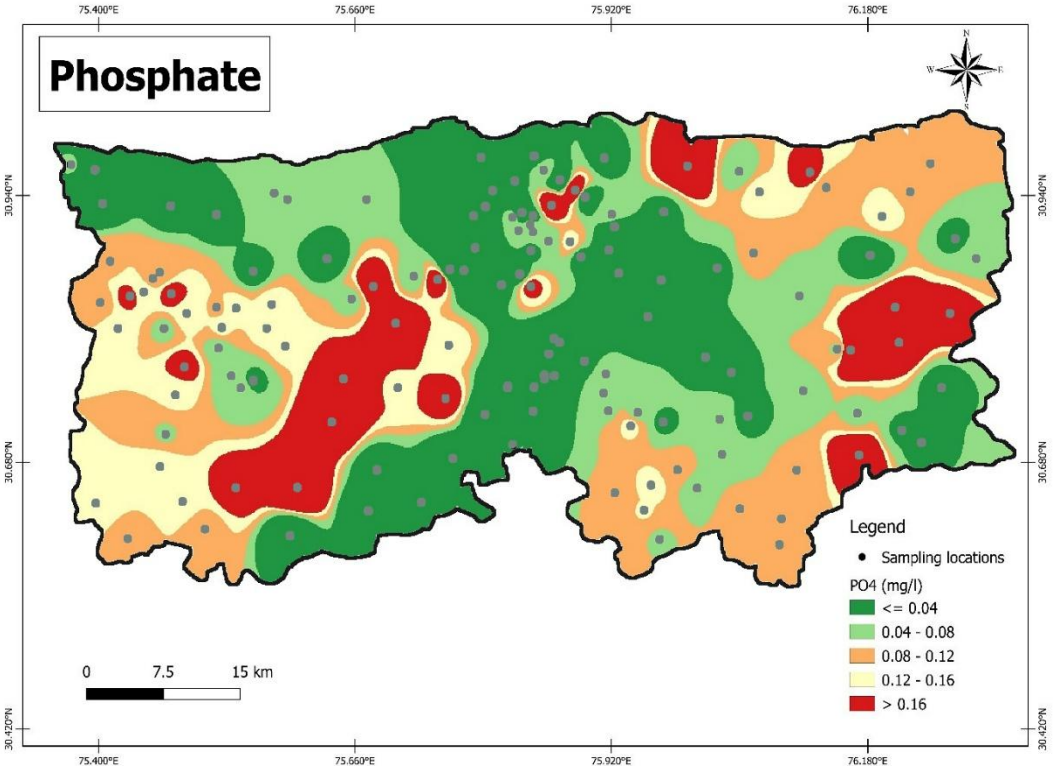

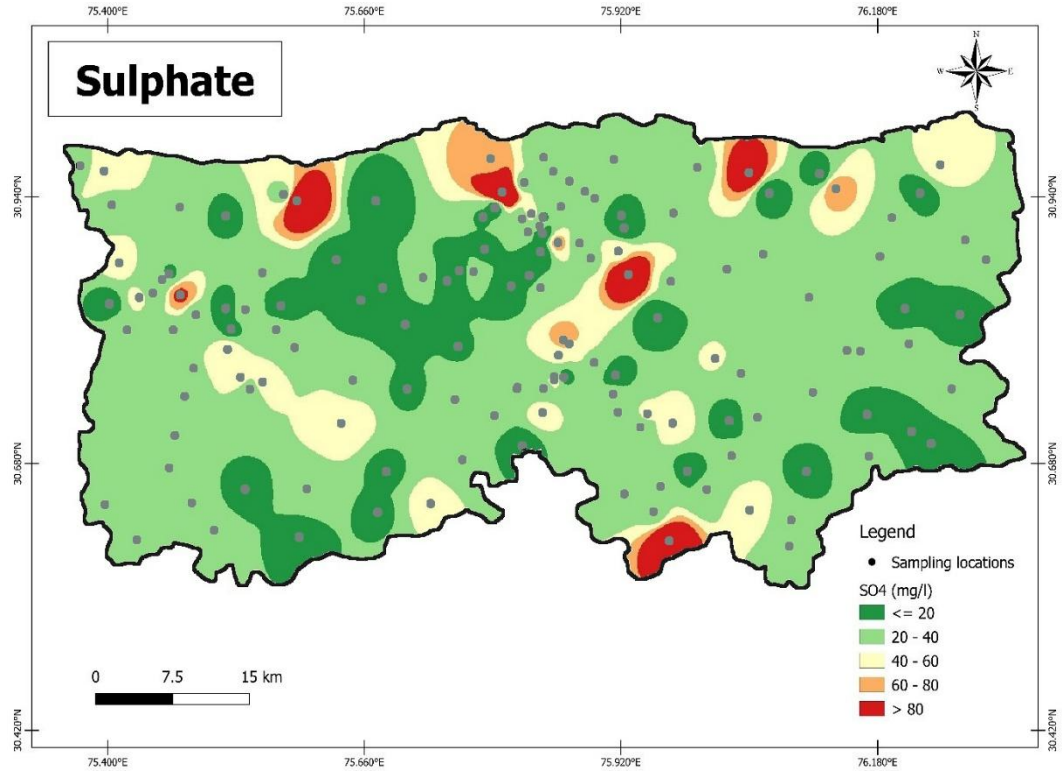

Fig.4.1 (Continued)

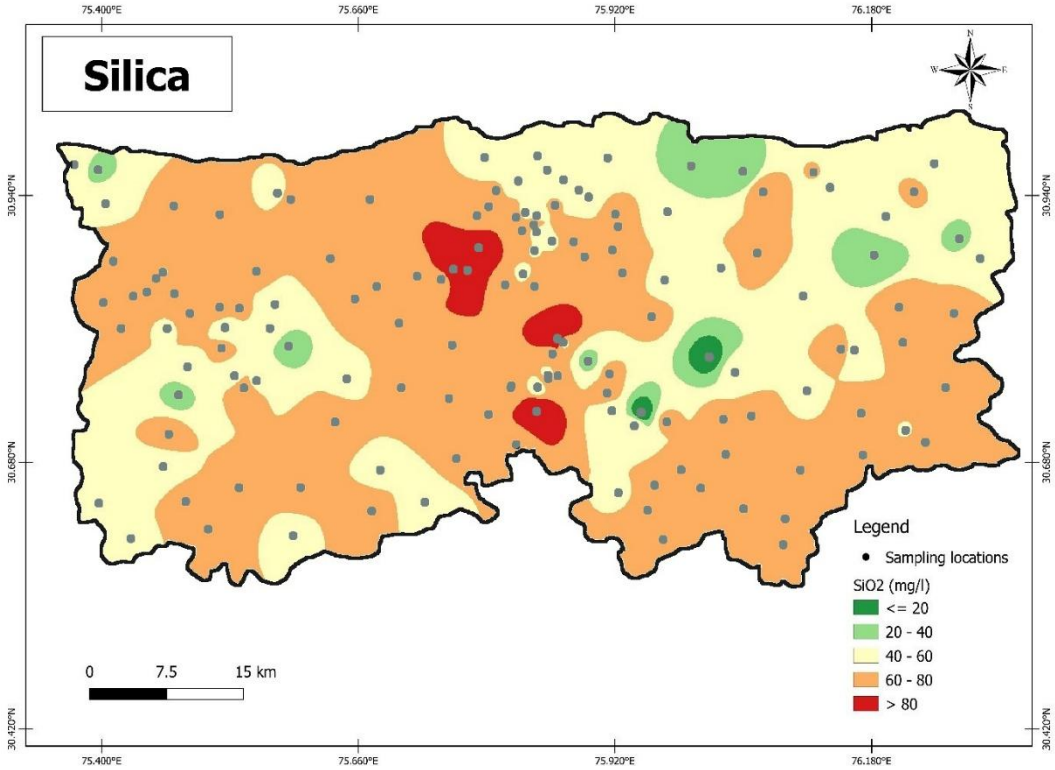

Fig.4.1 (Continued)

There is no specified BIS limit for silica but the relative high value has been seen in a very small pocket near Alamgir pind. Comparatively, better spatial variation can be seen in the case of Mg^{2+} as more than 50 percent of the area lie above the acceptable limit of 30 mg/l. Also, TDS, EC, TH and TA values show high variation across the district between the range of 127.5-772.0 mg/l, 252.0-1544.0 µS/cm, 95.0-515.0 mg/l, 250.0-1610.0 mg/l.

4.3 Characterisation of Geochemistry of the area

4.3.1 Hydrochemical facies

To determine the chemical characteristics of the groundwater of the study area, the samples were plotted on a Piper graph (see Fig. 4.2). As can be seen from the cationic triangle, majority of the water samples i.e., 105 samples (69.1%) fall in the category B which implies that they belong to no dominant category. 24 samples

(15.8%) fall in $Na^+ + K^+$ category, 20 samples (13.2%) in Ca^{2+} category and 3 samples (2.0%) in Mg^{2+} category. In the anionic triangle, all the samples fall in $HCO_3^- + CO_3^{2-}$ type. In the diamond graph, most of the samples i.e., 123 samples (80.9%) fall in category 5 i.e., the area of secondary alkalinity where alkaline earth (Ca^{2+} and Mg^{2+}) balances weak acids such as HCO_3^- and CO_3^{2-}.

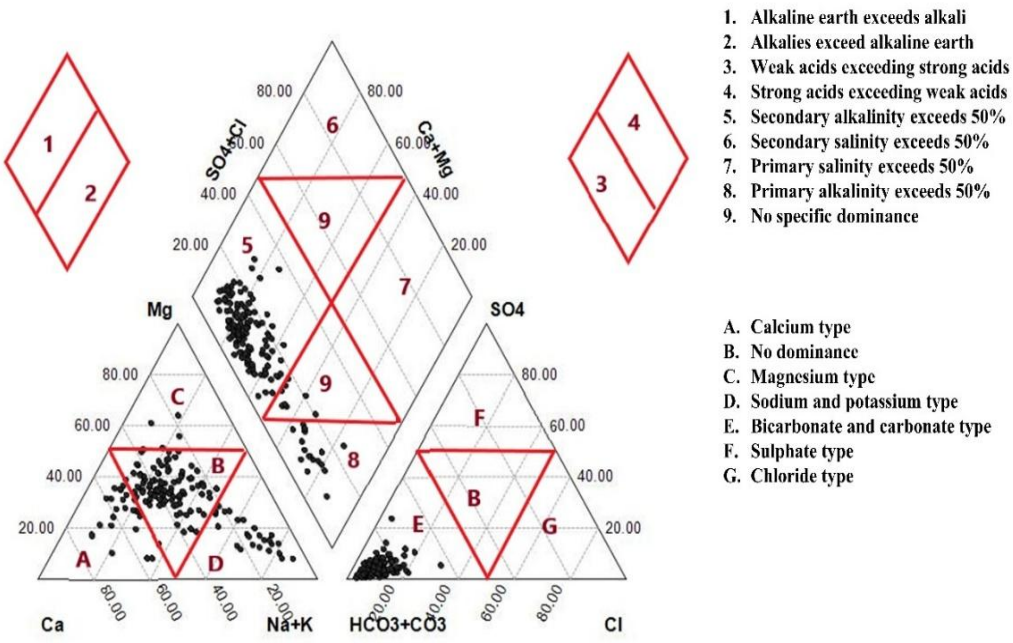

Fig. 4.2 Piper diagram of the collected samples

Also, 10 (4.6%) samples lie in mixed category with no particular cationic or anionic dominance, and 19 samples (12.5%) lie in category 8 which is the area of primary alkalinity i.e., alkali metals like Na^+ and K^+ balances weak acid like HCO_3^- (bicarbonate) and CO_3^{2-} (carbonate).

4.3.2 Rock Weathering Process

A study conducted by Gibbs (1970) showed that precipitation, weathering, or evaporation-crystallization are the primary processes that affect the water chemistry

of a region. This analysis has been accepted world-wide and cited by various authors (Chitrakshi & Haritash, 2022; Mostaza-Colado et al., 2018; Tay et al., 2014). Gibbs diagram i.e., a scatter plot of TDS vs cation ratio (Na^+/ Na^++ Ca^{2+}), and a scatter plot of TDS vs anion ratio (Cl^- / Cl^- + HCO_3^-) was, thus, plotted (See Fig.4.3) to understand the dominant process affecting the groundwater chemistry of the study area. The plot shows that rock and water interaction is the major geogenic process affecting the geochemistry of the study area.

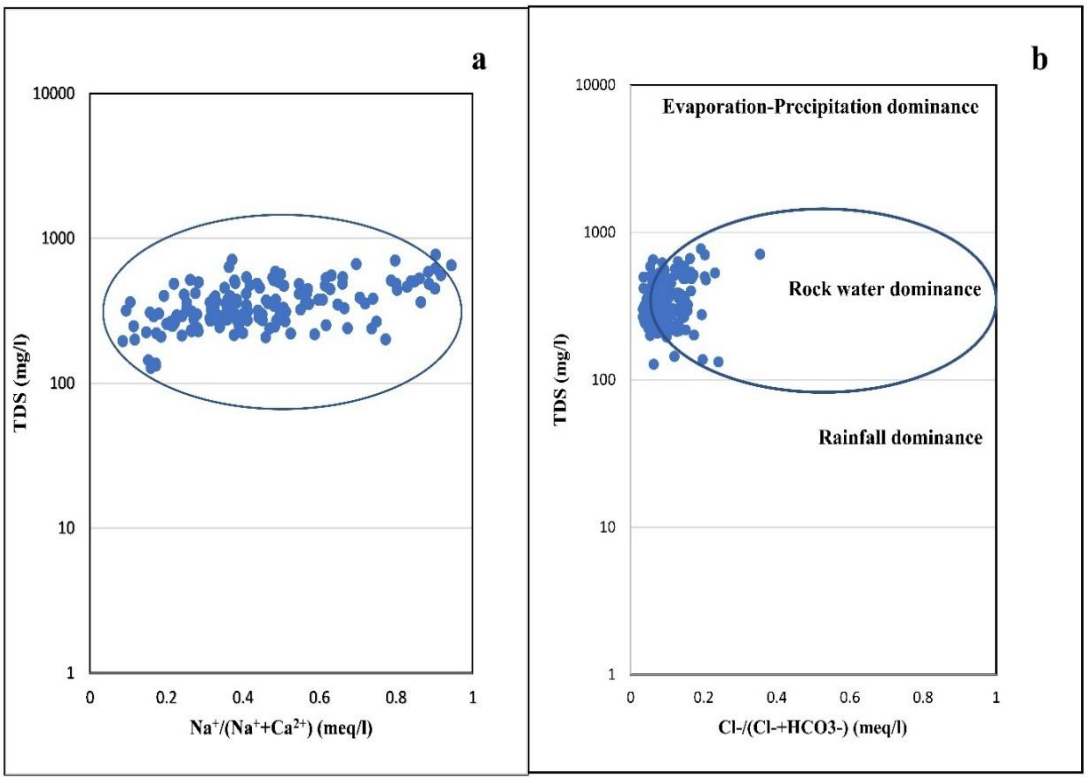

Fig. 4.3 Gibbs Diagram for mechanisms controlling groundwater chemistry in the study area. a) TDS vs Na^+/(Na^++Ca^{2+}), b) TDS vs Cl^-/(Cl^-+ HCO_3^-)

To identify different geogenic subsurface weathering processes taking place in the study area, different ionic ratios as suggested by Hounslow (1995) were calculated. The summary of the results has been depicted in Table 4.3. The bivariate plot of Cl^- Vs Na^+ indicates that majority of the samples fall below the equiline (1:1) i.e., $Na^+ > Cl^-$, which implies that halite dissolution is not the source of sodium in groundwater, and it has been derived from other minerals such as albite-plagioclase, or from ion

exchange (see Fig.4.4a) (Rajmohan & Elango, 2004). Further, comparing the samples for the concentration of sulphate and calcium reveal that $Ca^{2+} > SO_4^{2-}$ for almost all the samples (see Fig.4.4b). It can be deduced that the source of calcium is not gypsum as in that case calcium and sulphate concentrations would have been equal. Therefore, for the present study the source of calcium could be calcite, dolomite or silicate weathering. Also, the ratio of HCO_3^-/ Sum of anions >0.8 indicate that major source of minerals in groundwater is silicate or carbonate weathering.

The ratio of HCO_3^-/SiO_2 can indicate carbonate from silicate weathering as the concentration of bicarbonate ion will be less than or equal to silica if albite (plagioclase) is weathered as it releases considerable amounts of silica in comparison to other silicates (Hounslow, 1995). The analysis shows that 87 out of 152 samples have the value of HCO_3^-/SiO_2 ratio >10 indicating carbonate weathering for 57.23 % of samples, 4 samples have the value <5 indicating silicate weathering whereas 61 samples have the values between 5 and 10 indicating contribution from either silicate or carbonate weathering processes. Out of the 87 samples that indicate carbonate weathering, 39 samples have $Mg^{2+}/Ca^{2+}+Mg^{2+}$ >0.5, which confirm dolomite dissolution or calcite precipitation, and 48 samples have value less than 0.5 indicating limestone-dolomite weathering. Out of 4 samples that have the value <5, 3 samples have $Mg^{2+}/Ca^{2+}+Mg^{2+}$ value less than 0.5, which indicates granitic weathering and 1 sample with value greater than 0.5 indicates ferromagnesian mineral weathering.

For the 61 samples that have values between 5 and 10, the source of weathering is ambiguous. However, TDS values can be used to indicate weathering category for these samples as its values is generally 500 and above for carbonate rocks. Out of 61 samples, 56 samples have TDS below 500 that suggest the occurrence of silicate weathering processes. Also 21 samples out of these have magnesium content greater than calcium which indicates in the direction of weathering of ferromagnesian minerals in the area.

The ratio of $Na^+ + K^+ - Cl^-/Na^+ + K^+ - Cl^- + Ca^{2+}$ can help to understand the possibility of plagioclase weathering for the study area (Hounslow, 1995). The value

of this ratio for 69 samples out of 152 lies in between 0.2 and 0.8 which confirms the possibility of plagioclase weathering. However, 83 samples have the value less than 0.2 and greater than 0.8 which implies that plagioclase weathering is unlikely in these areas. Further, the value of $SiO_2/Na^+ + K^+ - Cl^-$ for 24 samples lie in between 1 and 2 implying albite weathering. Also, for 41 samples the value of ratio is more than 2 indicating the weathering by ferromagnesian minerals.

Table 4.3: Summary of different ionic ratios for source rock deduction

Ratio	Value	Reference	Result, no. of samples (%)
HCO_3^-/SiO_2	>10	Carbonate weathering	87 (57.23%)
	>5 and <10	Ambiguous	61 (40.13%)
	<5	Silicate weathering	4(2.6%)
$(Na^+ + K^+ - Cl^-)/(Na^+ + K^+ - Cl^- + Ca^{2+})$	>0.2 and <0.8	Plagioclase weathering possible	69 (45.4%)
	<0.2 and >0.8	Plagioclase weathering unlikely	83 (54.6%)
$SiO_2/ Na^+ + K^+ - Cl^-$	<1	Cation Exchange	87 (57.2%)
	>1 and<2	Albite weathering	24 (15.8%)
	>2	Ferromagnesian minerals	41 (27%)

4.3.3 Ion Exchange Process

The dissolution of carbonate minerals like calcite and dolomite introduces Ca^{2+}, Mg^{2+} and HCO_3^- ions into groundwater. The ratio of Ca^{2+} and Mg^{2+} ions to HCO_3^- generally lies in between 1:1 and 1:2 for a simple dissolution process (Zhang et al., 1995). For the present study, most of the samples for $Ca^{2+} + Mg^{2+}$ Vs HCO_3^-

graph plot below 1:2 equiline (see Fig. 4.4d) whereas for Ca^{2+} Vs HCO_3^- graph, all the samples plot below 1:2 equiline (see Fig. 4.4c). This suggests that HCO_3^- is relatively abundant in water and the levels of Ca^{2+} and Mg^{2+} ions is being influenced by other factors. According to Drever (1997) and Hounslow (1995), molar ratios of Ca^{2+}/ HCO_3^- and Ca^{2+}+ Mg^{2+}/ HCO_3^- that are less than 0.5, indicate exchange of calcium and magnesium in water by sodium through the process of cation exchange, or it is also possible that HCO_3^- enrichment has majorly occurred from silicate weathering. But since carbonate weathering is a significant process that is affecting the geochemistry of the study area; therefore, it can be concluded that cation exchange is taking place in the area.

The weathering of carbonate minerals will likely increase the groundwater Ca^{2+} and Mg^{2+} content which will induce the precipitation of calcite and dolomite. This process will in turn remove Ca^{2+} and Mg^{2+} from groundwater while releasing considerable amount of CO_2 (see Eqn. 4.1 and 4.2)

$$Ca^{2+} + 2HCO_3^- \rightleftharpoons CaCO_3 \downarrow + CO_2 \uparrow + H_2O \quad (4.1)$$

$$Mg^{2+} + 2\ HCO_3^- + CaCO_3 \rightleftharpoons CaMg(CO_3)_2 \downarrow + CO_2 \uparrow + H_2O \quad (4.2)$$

Thus, the dissolution of this CO_2 into the water will result in the dissolution of Na^+ and K^+ from silicate minerals or evaporites. As can be seen from the bivariate plot of Ca^{2+} and Na^+, the value of Ca^{2+} decreases with an increase in Na^+ (see Fig. 4.4e) (Thirumurugan et al., 2018).

The $SiO_2/(Na^+ + K^+ - Cl^-)$ ratio for 87 samples out of 152 (57.23 %) samples is <1, also suggesting cation exchange taking place in the study area (Hounslow, 1995; Tay et al., 2014). Another graph that can be plotted for this purpose is a bivariate plot between Na^++ K^+ (corrected for Cl^-) and Ca^{2+}+ Mg^{2+} (corrected for HCO_3^-+ SO_4^{2-}) (see Fig. 4.4f) (Jankowski et al.,1998). It has been suggested by Jankowski et al. (1998) that the water undergoing active ion exchange should plot in this graph with a slope of -1 whereas if the slope of the plot is zero than the area should not be affected by cation exchange. For the present study, the plot shows a negative slope away from zero i.e.,

it shows a slope of -0.56, which indicates cation exchange processes taking place and affecting the groundwater geochemistry of the area (Kumar, 2014).

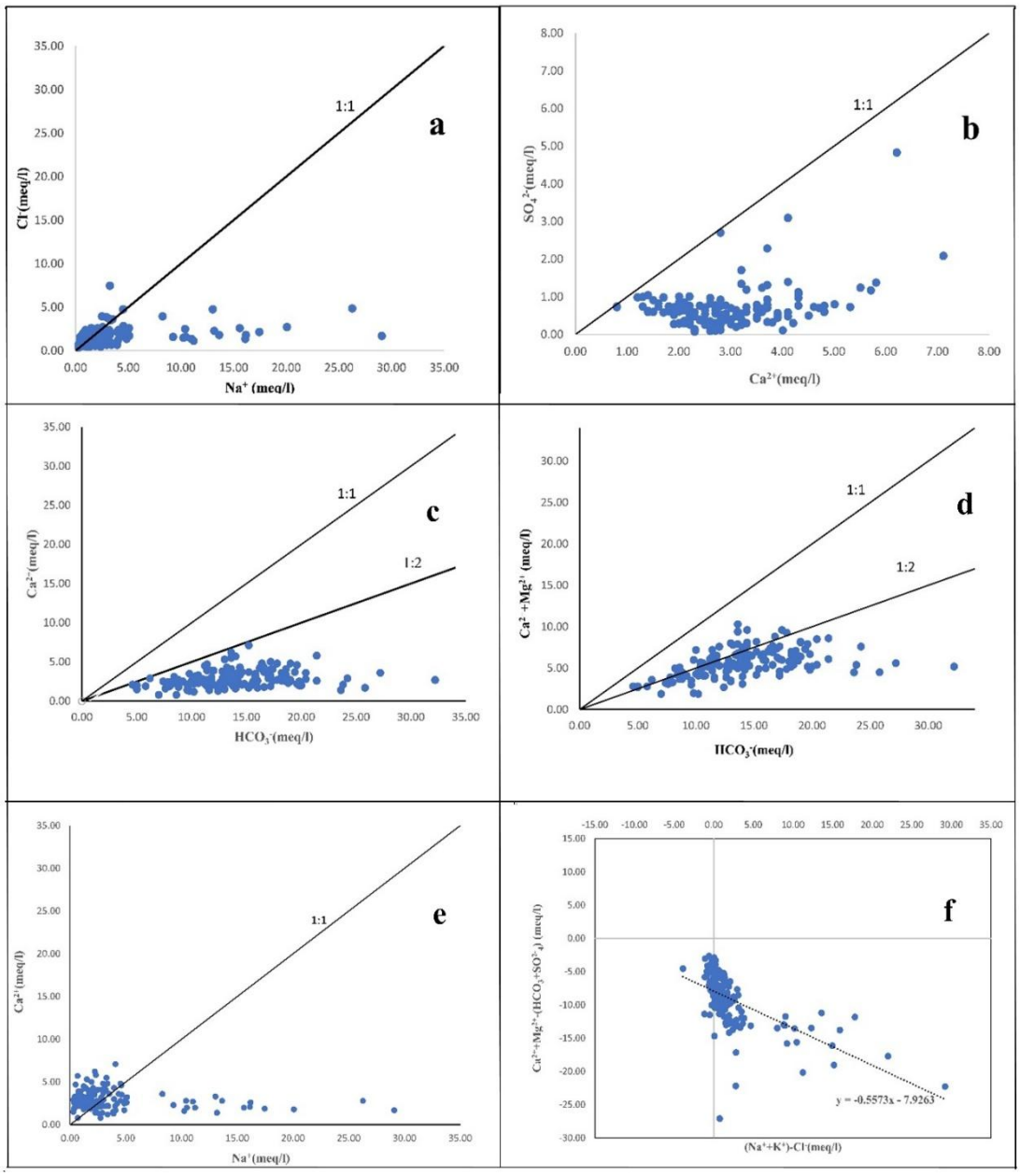

Fig. 4.4 Bivariate plot of a) Cl^- vs Na^+ b) SO_4^{2-} vs Ca^{2+} c) Ca^{2+} vs HCO_3^- d) (Ca^{2+}+ Mg^{2+}) vs HCO_3^- e) Ca^{2+} vs Na^+ f) (Ca^{2+}+Mg^{2+}) -(HCO_3^- + SO_4^{2-}) vs (Na^++ K^+)- Cl^-

The verification of ion exchange process happening in the study area can be done by studying the chloro-alkaline indices (CAI-I and CAI-II) that have been

proposed by Schoeller (1965) and subsequently used by many studies (Li et al., 2013; Marghade et al., 2012). Negative values of CAI-I and CAI-II indicate the occurrence of ion exchange process where Ca^{2+} and Mg^{2+} ions of groundwater are getting exchanged with Na^{+} or K^{+} in the aquifer materials, whereas positive values of CAI-I and CAI-II indicate the occurrence of a reverse ion exchange. These indices are calculated using the following formulas (Eqn. 4.3 and 4.4), where all ions are expressed in meq/l.

$$\text{CAI I} = \frac{Cl^{-} - (Na^{+} + K^{+})}{Cl^{-}} \tag{4.3}$$

$$\text{CAI II} = \frac{Cl^{-} - (Na^{+} + K^{+})}{SO_4^{2-} + HCO_3^{-} + CO_3^{2-} + NO_3^{-}} \tag{4.4}$$

For the study area, 29 samples out of 152 have positive values of CAI-I and CAI-II indicating the possibility of reverse ion exchange but however, remaining samples have negative values of CAI-I and CAI-II, giving strong evidence of ion exchange process (see Fig. 4.5) occurring in the study area.

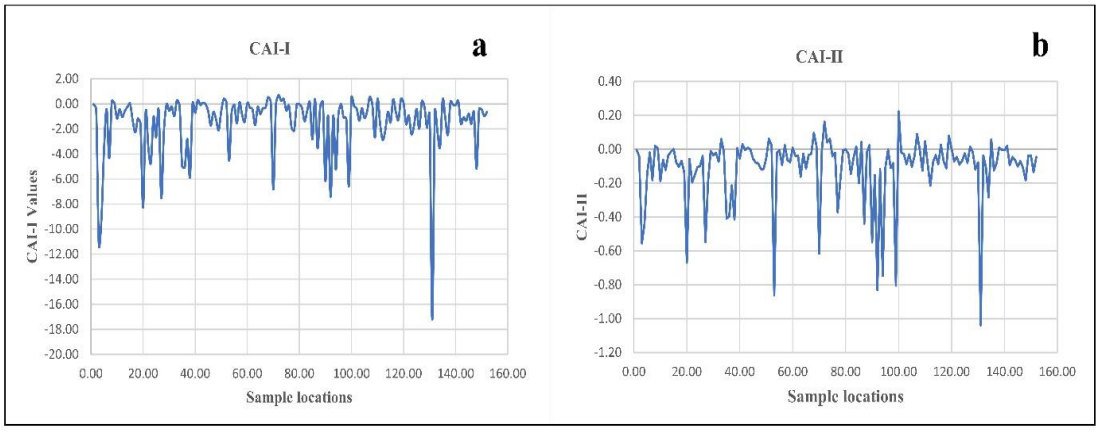

Fig. 4.5 Ion Exchange process in groundwater based on a) Chloro-alkaline Index I and b) Chloro-alkaline Index II

The general equations depicting ion exchange (Li et al., 2013) are mentioned below-

$$Ca^{2+}+2NaX \rightleftharpoons 2Na^{+}+CaX_2 \quad (4.5)$$

$$Mg^{2+}+2NaX \rightleftharpoons 2Na^{+}+MgX_2 \quad (4.6)$$

$$Ca^{2+}+2KX \rightleftharpoons 2K^{+}+CaX_2 \quad (4.7)$$

$$Mg^{2+}+2KX \rightleftharpoons 2K^{+}+MgX_2 \quad (4.8)$$

4.3.4 Saturation Index

The analysis of the SI values for major minerals such as anhydrite, aragonite, calcite, dolomite, gypsum, halite, hydroxyapatite and sylvite can be seen in Fig. 4.6 and Table 4.4. SI values for halite, fluorite, sylvite, and hydroxyapatite range from -8.66 to −5.61, -2.63 to −0.49, -8.51 to -6.54 and −7.22 to 10.08, respectively. Accordingly, the average SI values for these minerals are -7.22, -1.73, -7.51, and 5.06. The influence of phosphate minerals such as hydroxyapatite ($Ca_{10}(PO_4)_6(OH)_2$) to groundwater chemistry has been predicted in 122 locations, out of which majority of the samples i.e., 95 samples lie above 0.2 (77.9%) and the remaining 27 samples below -0.2 (22.13%). All of the samples exhibit negative SI values for halide minerals such as halite (NaCl), fluorite (CaF_2) and sylvite (KCl).

A similar trend is witnessed for evaporite minerals such as Gypsum ($CaSO_4.2H_2O$) and anhydrite ($CaSO_4$), as all the calculated values of SIs for them is below -0.2, i.e., no location has exhibited equilibrium or a supersaturated condition. Both Gypsum and Anhydrite are composed of calcium sulphate, where gypsum is the dihydrate form and anhydrite is its anhydrous form (Hardie, 1978). These minerals can occur individually or together; however, gypsum can be mostly found near the surface and anhydrite in deep aquifers because of the dehydration effects (Sadeqi, 2023). The range of values for gypsum and anhydrite are -3.27 to -1.21 and -3.58 to -1.51; with an average of -2.43 and -2.73, respectively.

Most of the samples show positive saturation index values when it comes to carbonate minerals such as calcite, aragonite and dolomite. For aragonite, 131 samples (86.2%) have values greater than 0.2, and only 4 samples have value less than -0.2. Also, the values of 17 samples lie between 0.2 and -0.2. Similarly, for calcite, 143

samples (94.1%) have values greater than 0.2, and only 3 samples have values less than -0.2; whereas 6 samples have also been found to lie between 0.2 and -0.2. For dolomite, 146 samples (96.1%) have been analysed to have values greater than 0.2, whereas only 3 samples have value less than -0.2 and 3 samples have value in between 0.2 and -0.2. The range of values for calcite, aragonite and dolomite are -0.45 to 2, -0.6 to 1.86 and -1.46 to 3.69; with an average of 1.32, 1.17 and 2.35, respectively.

Therefore, it can be concluded that groundwater is undersaturated with respect to halite, sylvite, fluorite, gypsum and anhydrite. This means that groundwater is deficient in Na^{+}, Cl^{-} and SO_4^{2-} and their subsequent increase is possible by dissolution through weathering processes (Elumalai et al., 2023; Kumar, 2014). Also, the groundwater is supersaturated with respect to calcite, aragonite, dolomite and hydroxyapatite at majority of locations which implies that these minerals have significant influence on the groundwater chemistry of the study area and that there is no further scope of $Ca^{2+}$and Mg^{2+} dissolution.

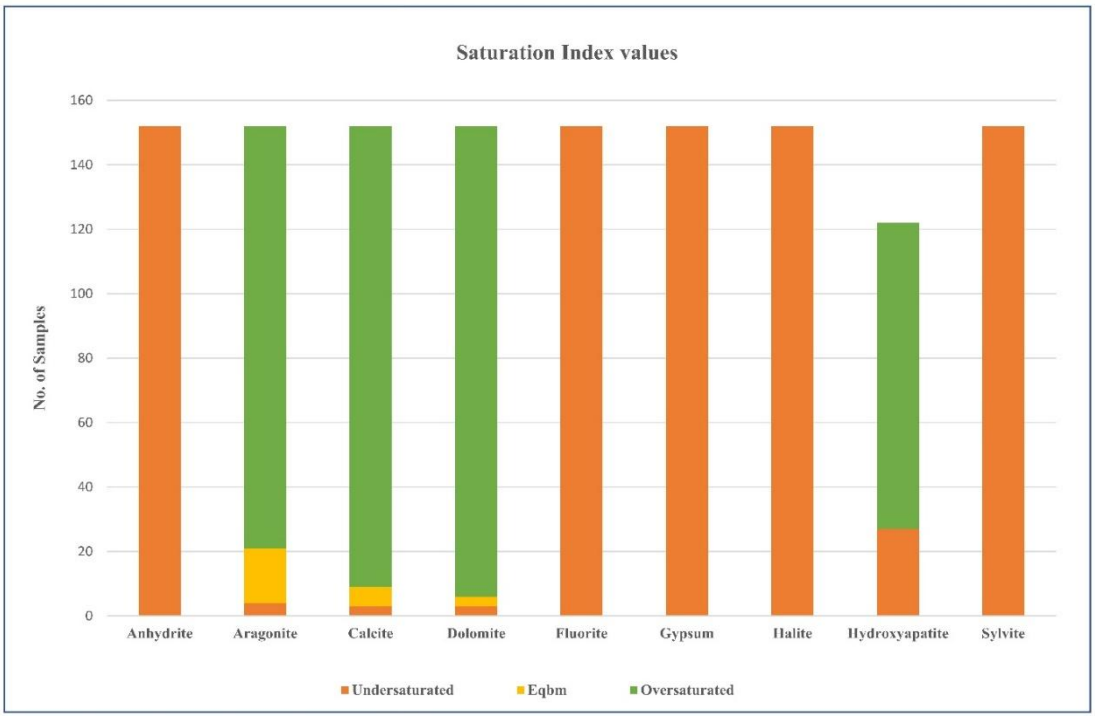

Fig. 4.6 Graph depicting undersaturated, equilibrium and oversaturated conditions of samples for various minerals

These minerals are infact prone to precipitation and subsequent crystallization (Zhou et al., 2020; Amiri et al., 2016). However, many factors such as temperature, pH and residence time can affect the kinetics and nucleation of reactions that may impede the process of precipitation of minerals even at supersaturated conditions.

Table 4.4: Summary of saturation indices values of groundwater samples for various minerals

SI Value	Anhydrite	Aragonite	Calcite	Dolomite	Fluorite
Max	-1.51	1.86	2	3.69	-0.49
Min	-3.58	-0.60	-0.45	-1.46	-2.63
Avg	-2.73	1.17	1.32	2.35	-1.74
<0.2	100%	2.6%	1.9%	1.9%	100%
-0.2 to 0.2	-	11.2%	3.9%	1.9%	-
>0.2	-	86.2%	94.1%	96.1%	-

SI Value	Gypsum	Halite	Hydroxy-apatite*	Sylvite
Max	-1.21	-5.61	10.08	-6.54
Min	-3.27	-8.66	-7.22	-8.51
Avg	-2.43	-7.22	5.06	-7.51
<0.2	100%	100%	22.1%	100%
-0.2 to 0.2	-	-	-	-
>0.2	-	-	77.9%	-

*found for 122 samples

4.4 Multivariate Statistical analysis

4.4.1 Principal component and Correlation analysis

For the current study, JMP Pro 16.2 was used to perform the multivariate analysis. The data had to be treated before being used as the input. For nitrates, carbonates and phosphates; a small number of samples (less than 25%) had value below detection limit. To be included in the statistical tests, these values were replaced with the arbitrarily chosen value between zero and one half of the lowest value measured. Also, methods like PCA are based on correlation and covariance matrix that can be affected by non- normally distributed data (Reimann et al., 2008) i.e., these

statistical tests are based on the assumption that the input data is drawn from a normal or a lognormal distribution. Therefore, an attempt was made to understand if the present data follows a normal distribution. In the original data, none of the parameters except total hardness showed normal distribution. Data was, thus, transformed using box-cox and log transformation (both ln and log10) to test the normality condition. It was found that only 50% of parameters could follow a normal distribution after these conversions.

Ancillary researches have established that in majority of the cases, a geochemical or environmental data never approaches a normal or a log normal distribution (Darwish, 2011; Reimann & Filzmoser, 2000; Reimann et al., 2002). This is because data is highly spatial dependent and is skewed because of presence of outliers. It has, therefore, been suggested that statistical techniques such as non-parametric and robust methods that do not make assumptions about the data distribution can be applied to such environmental data, preferably after log transformation. The robust method down weights the outlier values and give a better estimate of the variance. Hence, following the advice, the log (ln) transformed data was subjected to PCA that was based on a robust method for calculating the correlations (Reimann & Filzmoser, 2000).

The correlations matrix (Table 4.5) depicts linear relationships between variables pairwise. It lists down correlations coefficients that tell us about the strength of this relationship (Li et al., 2013). The advantage of the robust method is that all the variables are considered at the same time in a multivariate state providing us with true multivariate correlation analysis. As seen from the table 6, EC-salinity (0.99), EC-TDS (0.99), TA- HCO_3^- (0.98) share very high correlation with each other which is due to their dependency on each other. EC is highly correlated with TA (0.82), TH (0.64), Na^+(0.77), K^+(0.69), Mg^{2+}(0.62), HCO_3^- (0.82), Cl^- (0.70), NO_3^- (0.57) and moderately correlated with Ca^{2+}(0.40), SO_4^{2-} (0.43) and SiO_2(0.32). The moderate to strong correlations between EC and major ions depicts the role of these ions in the mineralization of water sample.

Table 4.5: Correlation matrix for measured hydrochemical parameters

	pH	EC	Salinity	TDS	TA	TH	Na^+	K^+	Ca^{2+}	Mg^{2+}	CO_3^{2-}	HCO_3^-	Cl^-	NO_3^-	SO_4^{2-}	F^-	SiO_2	PO_4^{3-}
pH	1.00																	
EC	-0.32	1.00																
Salinity	-0.34	0.99	1.00															
TDS	-0.33	0.99	0.99	1.00														
TA	-0.27	0.82	0.83	0.82	1.00													
TH	-0.48	0.64	0.65	0.64	0.51	1.00												
Na^+	-0.01	0.77	0.76	0.77	0.72	0.09	1.00											
K^+	-0.13	0.69	0.68	0.69	0.65	0.25	0.73	1.00										
Ca^{2+}	-0.38	0.40	0.41	0.40	0.23	0.80	-0.14	0.13	1.00									
Mg^{2+}	-0.40	0.62	0.64	0.62	0.58	0.82	0.26	0.28	0.32	1.00								
CO_3^{2-}	0.32	0.01	0.01	0.01	0.17	-0.15	0.20	0.13	-0.27	0.02	1.00							
HCO_3^-	-0.36	0.82	0.83	0.82	0.98	0.56	0.68	0.62	0.29	0.60	-0.02	1.00						
Cl^-	-0.17	0.70	0.68	0.70	0.49	0.43	0.53	0.51	0.29	0.41	0.13	0.47	1.00					
NO_3^-	-0.37	0.57	0.57	0.57	0.38	0.60	0.22	0.31	0.49	0.49	-0.18	0.43	0.50	1.00				
SO_4^{2-}	-0.15	0.43	0.41	0.43	0.13	0.18	0.34	0.22	0.18	0.11	-0.07	0.15	0.28	0.14	1.00			
F^-	0.12	0.03	0.03	0.03	0.03	-0.19	0.20	0.12	-0.30	-0.01	0.05	0.02	-0.02	0.08	0.01	1.00		
SiO_2	-0.20	0.32	0.34	0.32	0.31	0.36	0.13	0.13	0.27	0.37	-0.09	0.33	0.10	0.24	-0.12	0.11	1.00	
PO_4^{3-}	-0.27	0.02	0.02	0.02	0.08	-0.02	0.07	0.09	-0.04	0.02	-0.05	0.10	0.12	0.04	-0.09	0.02	-0.11	1.00

Total alkalinity has strong positive correlations with HCO_3^- (0.99) and Cl^- (0.5) as these anions contribute to its properties. TA also shares positive correlation with TH (0.51), Na^+(0.72), K^+(0.65) and Mg^{2+}(0.58), which can be explained by the reaction of metallic ions with anions contributing to alkalinity. Total hardness (TH) has high positive correlation with Ca^{2+}(0.80) and Mg^{2+} (0.82) which are the two major ions that are known to contribute to water hardness. Na^+ and K^+ have high correlation (0.73) with each other, and both of them share high correlation with HCO_3^- i.e., 0.68 and 0.62 respectively. Mg^{2+} also has high correlation with HCO_3^- (0.60). This indicates the occurrence of silicate and carbonate weathering that tend to release these ions in groundwater. Cl^- and NO_3^- also have high correlation of 0.50, indicating their occurrence in water through anthropogenic pollution.

After looking at the robust correlation estimate, 2 groups (EC-TDS- Salinity and TA-HCO_3^-) with very high correlation (>0.9) were identified. Such parameter can result in the problem of multicollinearity of the data during PCA as they are essentially measuring the same thing (Loewen & Gonulal, 2015). Therefore, one parameter from both the groups was retained i.e., EC and HCO_3^- and the remaining three parameters were removed from analysis. Also, to measure the suitability of data for conducting PCA, KMO and Bartlett test was conducted. Bartlett method tests the strength of correlation among variables by testing the null hypothesis that the correlation matrix is an identity matrix. For the present study, p value is 0.000 at 153 degrees of freedom at $\chi 2 = 4270.6$, thus implying that parameters are correlated and acceptable for PCA (Snousy et al., 2022). KMO test is conducted to measure the data for sampling adequacy (MSA) which produces a value between 0 to 1, with values above 0.5 considered acceptable. The overall KMO value has come out to be 0.781, which is considered good but the individual value of CO_3^{2-} is 0.196 and of PO_4^{3-} is 0.36 which is less than 0.5, these two variables are therefore dropped from further PCA analysis (see Fig. 4.7).

PCA was now carried out with the remaining parameters. A decision on the number of Principal components (PCs) to retain was taken after considering the eigen value criterion, where components with eigen value greater than 1 are considered

significant (Loewen & Gonulal, 2015). So, accordingly it was decided that four components will be retained. The PCs obtained in this step were subjected to varimax rotation (orthogonal strategy) as rotation tends to produce a more differentiated and interpretable solution by spreading the loadings according to their high and low intensity.

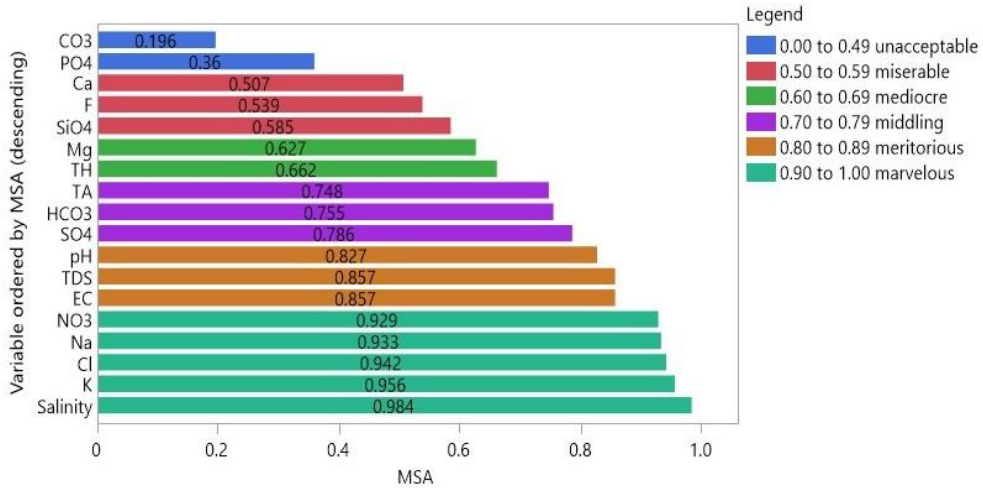

Fig. 4.7 The overall and individual measure of sampling adequacy for different parameters

The extracted four PCs explain a cumulative variance of 75.4% out of the total variance. For each component, variables loading above 0.45 influence the underlying component in a significant way (Comrey and Lee, 2021). PC1 explains 29.1% of the total variance i.e., the maximum amount of variance accounted for by PCs (see Table 4.6). It has strong loadings from EC (0.82), Na^+ (0.95), K^+ (0.81), HCO_3^- (0.71), Cl^- (0.68) and SO_4^{2-} (0.45). These loadings point in the direction of water mineralization by these ions as they significantly tend to influence EC values of the samples. PC2 explains 28.3% of total variance, and has high loadings from TH (0.93), Ca^{2+} (0.81), Mg^{2+} (0.70), HCO_3^- (0.47), SiO_2(0.46), EC (0.50), NO_3^- (0.65) and a strong negative loading from pH (-0.62). This component depicts the geogenic influence of the rock weathering through carbonate and silicate mineral dissolution on the groundwater. It also depicts the human induced pollution of water through agricultural activities. PC3

explains 10.2% of total variance. It has high loadings from F^- (0.51), SiO_2(0.65) and a strong negative loading from SO_4^{2-} (-0.47). Strong positive loadings of fluoride and silica point in the direction of dissolution of fluorosilicates and negative loadings of sulphate indicate a different source other than mineral dissolution. Also, PC4 explains 7.8% of total variance, with high loadings from SO_4^{2-} (0.50), NO_3^- (0.45) and F^- (0.61). In this case, strong positive loadings from NO_3^-, SO_4^{2-} and F^- point in the direction of anthropogenic sources of pollution which may have been contributed through activities such as fertiliser application, brick making and steel production.

Table 4.6: Rotated component matrix representing four extracted principal components (PCs) for the study area

Variables	PC1	PC2	PC3	PC4
pH	-0.07	**-0.62**	0.09	0.07
EC	**0.82**	**0.50**	-0.23	0.14
TH	0.23	**0.93**	-0.04	-0.20
Na^+	**0.95**	-0.07	0.06	0.10
K^+	**0.81**	0.11	0.09	0.05
Ca^{2+}	-0.01	**0.81**	-0.31	-0.21
Mg^{2+}	0.37	**0.70**	0.12	0.06
HCO_3^-	**0.71**	**0.47**	0.20	-0.03
Cl^-	**0.68**	0.32	-0.33	0.01
NO_3^-	0.35	**0.65**	0.29	**0.45**
SO_4^{2-}	**0.45**	0.07	**-0.47**	**0.50**
F^-	0.22	-0.24	**0.51**	**0.61**
SiO_2	0.11	**0.46**	**0.65**	0.24
Eigen value	**3.78**	**3.68**	**1.32**	**1.01**
CV (%)	**29.1**	**57.4**	**67.6**	**75.4**

4.4.2 Hierarchical Cluster Analysis

The resultant dendrogram (tree of clusters) is shown in Fig. 4.8. The classification has grouped together 152 samples into 4 clusters in both Q and R mode. The Q mode clustering dendrogram depicts 4 different colour groupings to depict 4 clusters of the sampling sites. In Q mode, 68 samples (out of 152) are grouped in

cluster 1 and represent low ionic strength. In Cluster 2, 14 out of 19 samples have been collected from areas that lie nearby northern boundary of the district from where Satluj river flows.

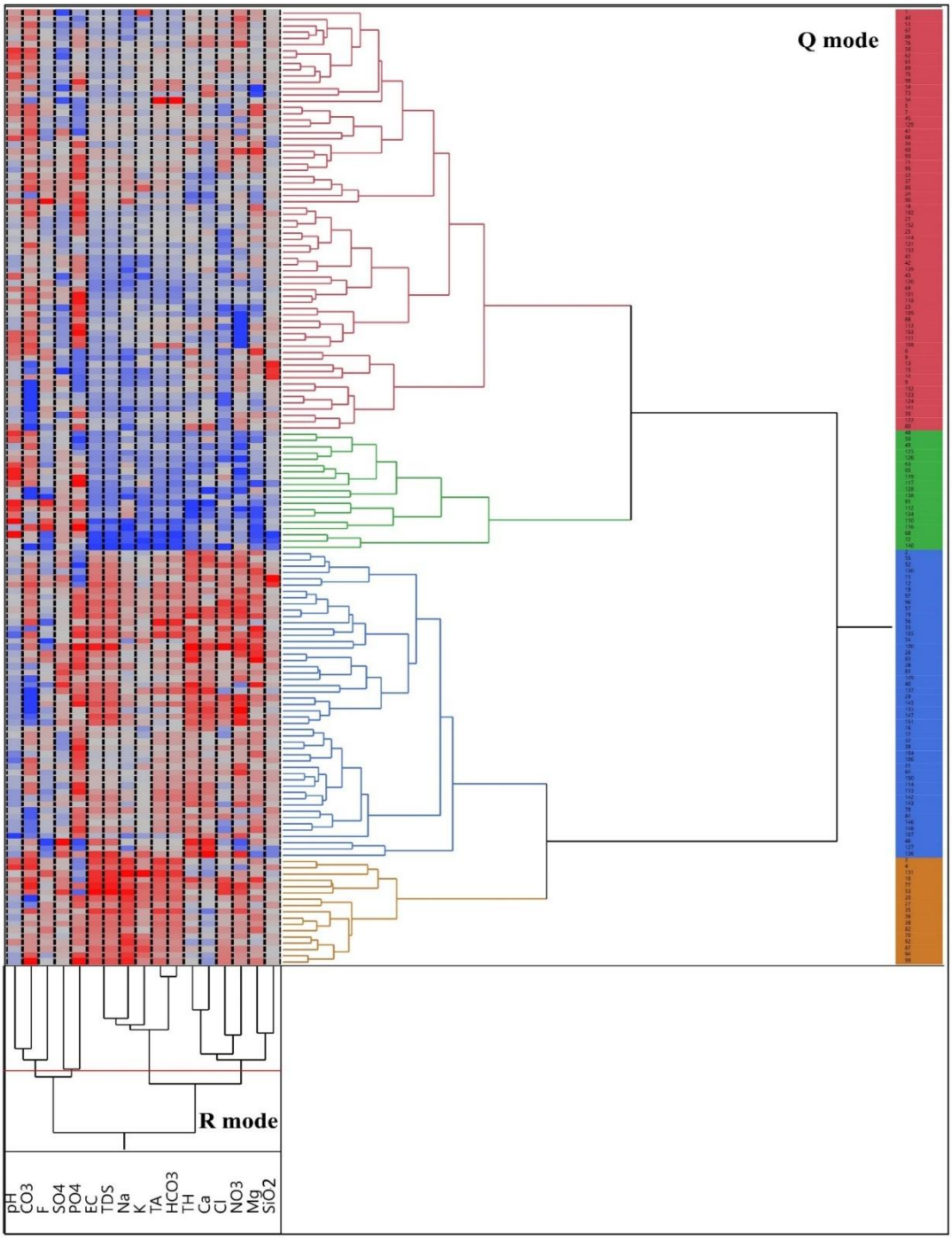

Fig. 4.8 Dendrogram depicting two-way clustering process for both Q mode and R mode

The samples in this cluster belong to shallow aquifer and are relatively clean. In cluster 3, 68 sites represent moderately mineralized groundwater, whereas, 17 sites in cluster 4 represent high mineralization.

The red line in the R mode cluster analysis cuts the top 4 clusters that show statistical significance. Reading from left to right, cluster 1 constitutes pH, CO_3^{2-} and F^- together that indicates towards dissolution of fluorite in groundwater, which can further influence calcite and dolomite precipitation, and carbonate ions activity in water. Cluster 2 has SO_4^{2-} and PO_4^{3-} as its elements and depict contamination from detergents and fertilisers. EC, TDS, Na^+, K^+, TA and HCO_3^- constitute cluster 3 that depicts the interrelationship of these elements with each other as Na^+, K^+ and HCO_3^- are the major ions contributing towards EC and TDS. Cluster 4 has contribution from TH, Ca^{2+}, Cl^-, NO_3^-, Mg^{2+} and SiO_2 that signifies the contribution of calcium towards hardness of water while also signifying anthropogenic pollution from Cl^- and NO_3^-. Also, Mg^{2+} and SiO_2 form a subpair in this cluster and shows that rock weathering processes consisting of aluminosilicate minerals are contributing to groundwater chemistry.

4.5 Characterisation of Ground water quality for drinking based on WQI

As indicated from the water quality index-based analysis, majority of the samples i.e., 57.9% of samples fall under good water quality (ranging between 26 to 50) in the study area, while only 2.6% of the sites have excellent water quality (in the range of 0 to 25). This is also clearly depicted by the WQI map, the good water quality is largely widespread across the district and is not confined to a particular region. It can also be seen that 32.9% of samples account for poor water (51-75) quality, majorly in the central part in Pakhowal, Dehlon, Doraha and Ludhiana I block of the district; and small pockets in north east in Macchiwara block; and western parts of Jagraon block of district. Also, there is progressive descent of groundwater quality from poor to unsuitable in the north eastern part in Macchiwara block, mid-east in Samrala block, and mid-western parts in Jagraon block of the district. Almost 4% of the sites represent very poor, whereas, 2.6% of the sites represent unsuitable drinking water quality in the

district. Overall, the quality of groundwater belongs to the good category in majority of the study area and is suitable for drinking as well as domestic uses (see Fig. 4.9 and Table 4.7).

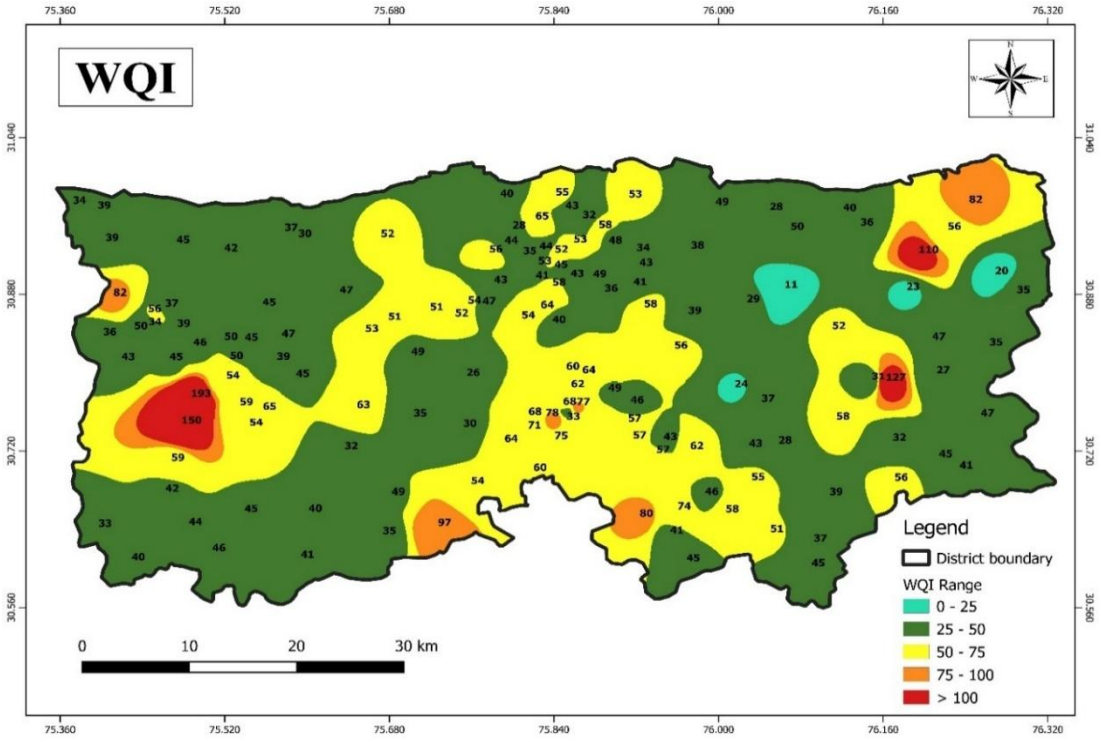

Fig. 4.9 Spatial distribution of water quality index values according to different categories across Ludhiana district

Similar results related to the poor water quality in the central parts of district has been reported by Padhi et al. (2017), Kumar et al. (2021) and CGWB (2021). The quality of groundwater in the area is dependent upon both geogenic and anthropogenic factors. This region has huge area under agricultural activity and small scale industrial units, which may have rendered the groundwater unsuitable in few pockets. The poor water in and around Ludhiana I, Dehlon, Doraha, Pakhowal and Jagraon blocks could be attributed to industrial units manufacturing agriculture based products, marbles, bricks, machine parts and bicycles. Also, there is an open drain known as 'Budha nala' flowing around Ludhiana I and Machhiwara blocks that drains domestic sewage and

effluents from dyeing clusters, which contribute to the poor groundwater quality in the area.

Table 4.7: Percent suitability of groundwater samples against water quality index categories

Range	Inference	No. of samples	Suitability %
0-25	Excellent	4	2.6
25-50	Good	88	57.9
50-75	Poor	50	32.9
75-100	Very poor	6	4
>100	Unsuitable	4	2.6

The evaluation of WQI has determined the suitability of groundwater in study area for drinking purpose and highlighted those areas which would need remedial treatment before its use. It is recommended that areas identified with unsuitable or marginally suitable water quality should be monitored on micro level to regulate the pollution activities from industrial units, agricultural processes and sewage discharges. As recommended by CGWB (2014), data from various research and development organisation of the area should be collated to plan, prevent and control the further degradation of water quality. Also, conjunctive use of groundwater and surface water can be encouraged to overcome increasing deterioration of the source. It is required that water quality management plan is adopted and effectively implemented by various stakeholders in a collective manner.

4.6 Classification of irrigation water

The quality of water that is used for irrigation can help in reducing the occurrence of deteriorating soil quality and crop yield (Chitrakshi & Haritash, 2018; Minhas et al., 2019). It is one of the critical factors that help in maintaining soil fertility. Thus, understanding of water quality is crucial to maintain agriculture land's performance over the years. There are different categories of possible hazards that are used by scientists to understand the quality of irrigation water.

4.6.1 Salinity hazard

Water salinity, as measured by electrical conductivity (EC), is a crucial factor affecting crop productivity. High EC levels in irrigation water can have a significant impact on plants by creating a physiological drought condition (Zaman et al., 2018; Sarma & Singh, 2023; Ben Brahim et al., 2022). This condition arises because the high salt concentration in the soil solution increases the osmotic pressure, making it difficult for plant roots to absorb water from the soil. Even if the soil appears to be adequately moist, the presence of excess salts hampers the plant's ability to take up water (US Salinity Laboratory staff [USSL staff], 1954; Hem, 1985). As a result, the plant experiences a water deficit, leading to wilting. This happens because the water lost through transpiration from the plant's shoots cannot be replenished due to the high osmotic potential of the soil-water.

Table 4.8: Categorization of irrigation water for Salinity hazard

EC (µS/cm)	Hazard Class	Category	No. of samples (% of total)
< 250	Low	C1	0 (0 %)
250 – 750	Medium	C2	95 (62.5%)
750 – 2250	High	C3	57 (37.5%)
≥ 2250	Very high	C4	0 (0 %)

In the study area, as can be seen in Table 4.8 (also see Fig. 4.11), most of the groundwater samples lie between 250 to 750 µS/cm i.e., in the 'medium' salinity hazard category i.e., 62.5% of the samples out of 152 lies in this category. The remaining samples i.e., 56 of total, fall in the third category which associates 'high' salinity hazard to these sites. But none of the samples fall the 'very high' category. Therefore, based on the above categorization not much of salinity hazard can be associated to the study area.

4.6.2 Sodium hazard

The growth of plants is primarily limited by the salinity level of irrigation water. However, when water with an imbalanced sodium content is used, it can further

decrease crop yield, particularly in certain soil texture conditions (Zaman et al., 2018). Elevated sodium levels in irrigation water compared to calcium and magnesium content can result in diminished water infiltration, a condition referred to as "sodicity" (USSL staff, 1954; Hem, 1985). This phenomenon occurs when soil accumulates an excess of sodium, causing soil clays to expand and scatter, leading to surface crusting and blockage of pores. These detrimental effects on soil structure impede water penetration and have the potential to enhance runoff. Consequently, the downward movement of water through the soil is restricted, potentially depriving actively growing plant roots of adequate water supply, despite surface water pooling following irrigation (Bauder et al., 2011). Therefore, the suitability of groundwater for agricultural purposes with respect to sodium hazard can be determined by assessing the following indices-

4.6.2.1 Soluble sodium percentage

High sodium levels in soil-water not only reduces the soil permeability, it can also be potentially toxic to plants as excessive sodium uptake will disrupt their physiological processes. The quantification of sodium concentration in water is thus essential to avoid the reduction in permeability and the plant toxicity by characterizing the irrigation water (USSL staff, 1954). Soluble sodium percentage (SSP or % Na) is one of the indices that helps us to determine the potential of water to contribute to sodium hazard (Zaman et al., 2018). It is calculated using the following Eqn. 4.9 (all the ionic concentrations are in milliequivalent per litre)-

$$\% Na = \left(\frac{Na^{+}+K^{+}}{Ca^{2+}+Mg^{2+}+Na^{+}+K^{+}}\right) \times 100 \quad (4.9)$$

The classification of soluble sodium percentage falls into five categories- unsuitable, doubtful, permissible, good, and excellent. As indicated in the Table 4.9 (also see Fig. 4.11), most of the samples i.e., 52.6% fall in the ‘good’ category whereas only 3 samples fall in unsuitable category. The remaining samples, i.e., 34 (22.4%) and 20 (13.2%) fall in ‘excellent’ and ‘permissible’ categories respectively.

This index calculates the soluble sodium ions present in the irrigation water that will react with the soil i.e., the tendency of the water to enter into a cation exchange reaction in soil.

Table 4.9: Classification of groundwater according to the %Na values

% Na Range	Classification of range	No. of samples	% of samples
< 20	Excellent	34	22.4
20-40	Good	80	52.6
40-60	Permissible	20	13.2
60-80	Doubtful	15	9.9
> 80	Unsuitable	3	1.9

However, out of the mixture of monovalent and divalent ions, the divalent ions are preferentially adsorbed on soils. If the % Na is not considerably higher (>50), the possibility of extensive displacement of Ca^{2+} and Mg^{2+} by Na^{+} is less. Therefore, Sodium adsorption ratio (SAR) that better relates to the adsorption of sodium by the soil by taking into account the mass law equilibrium of different cationic species, is more widely used than the % Na ratio.

4.6.2.2 Sodium adsorption ratio (SAR)

Sodium adsorption ratio was formulated based on the research work of Gapon (1933), Mattson and Wiklander (1940), Davis (1945) and Schofield (1947). They suggested that the ratio of the soluble monovalent cation with the square root of the molar concentration of the soluble divalent cation can give better estimate of the adsorbed cation on the exchange complex of the soil. Therefore, when the soil and irrigation water will eventually move towards equilibrium, the values of SAR can be used to very closely predict the exchangeable sodium cations available on the soil (Wilcox, 1955). Therefore, SAR is a more useful index to measure the sodium hazard of the irrigation water. It is calculated using Eqn. 4.10:

$$SAR = \frac{Na^{+}}{\sqrt{\frac{Ca^{2+}+Mg^{2+}}{2}}} \quad (4.10)$$

The classification of SAR falls into four categories- S1 (low sodium water), S2 (medium sodium water), S3 (high sodium water) and S4 (very high sodium water). Groundwater with a SAR value less than 10 can be used to irrigate any type of soil as the chances of soil adsorbing high Na^{+} ions are little. The sodicity class 'S2' presents sodicity hazard in fine textures soils, whereas 'S3' level of hazard can produce high levels of exchangeable sodium in most soils. The water that falls in 'S4' category should not be generally used in irrigation. As indicated in the Table 4.10 (also see Fig. 4.11), most of the samples i.e., 97.4% fall in the 'S1- Low sodium' category. Whereas, only 3 samples fall in 'S2- Medium sodium' category and only 1 sample falls in 'S3- High sodium' category.

Table 4.10: Classification of groundwater according to the sodicity class based on the SAR values

SAR	Sodicity class	Sodicity hazard	No. of samples (% of total)
< 10	S1	Low	148 (97.4%)
10 – 18	S2	Medium	3 (1.9%)
18 – 26	S3	High	1 (0.7%)
> 26	S4	Very High	0 (0%)

The exchange of cations in soil-water complex will eventually move towards equilibrium. The rate at which this equilibrium condition occurs is directly impacted by the EC of the water. Also, the potential of the irrigation waters with the same sodium content to cause swelling and dispersion in soils varies with respect to its salinity content. Therefore, assessing the potential soil infiltration and permeability problems resulting from the application of irrigation water with high sodicity cannot be adequately done based solely on SAR. A more accurate classification of irrigation water is presented by the USSL diagram (USSL staff, 1954; Zaman et al., 2018) as it is based on both the electrical conductivity (EC) and SAR values of the water (See Fig.

4.10). The sodicity classes in the USSL diagram are represented with negatively sloped lines. This is because, even if two water samples have similar SAR they may not have the same sodicity class. Rather, based on historical evaluations the sample with high EC value will tend to have a high sodium hazard. The USSL diagram shows that majority of the samples fall in S1C2, S1C3 and S2C3 classes, indicating low to medium sodium hazard and medium to high salinity hazard in the study region.

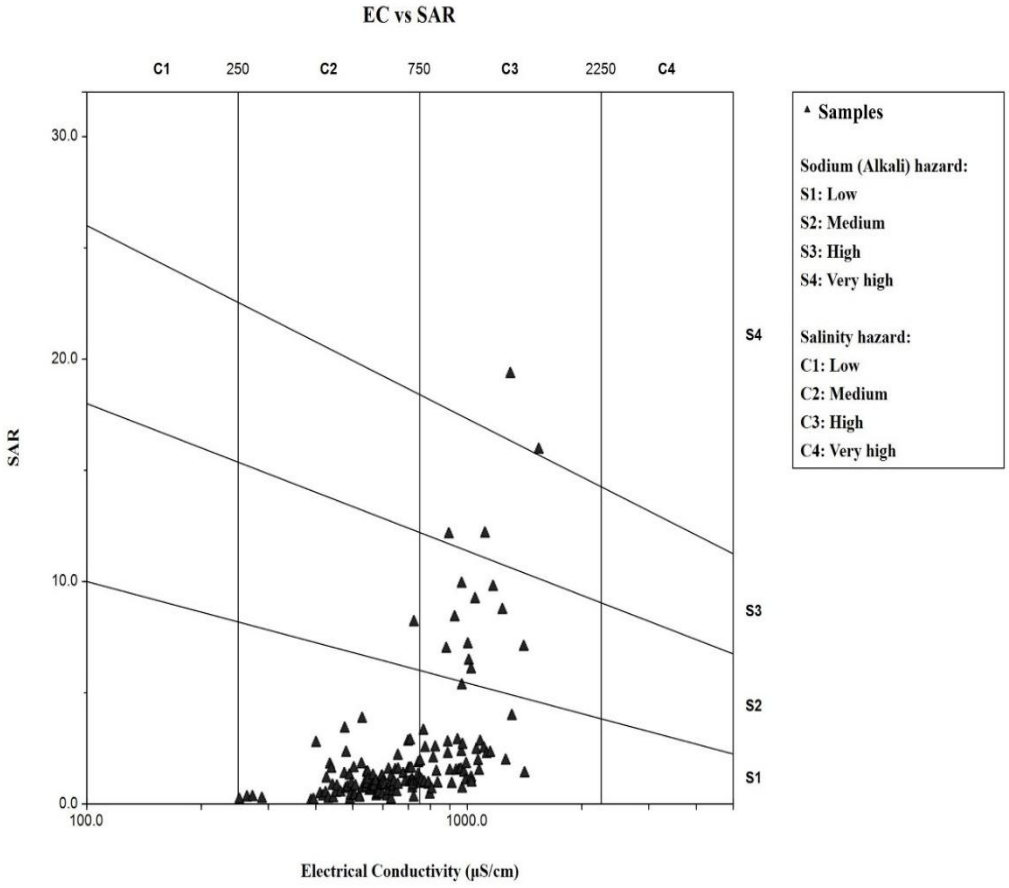

Fig. 4.10: Groundwater suitability for irrigation according to USSL classification

4.6.3 Carbonate-Bicarbonate hazard

In addition to the above indices that evaluate the sodium hazard of water by comparing Na^+ concentrations with other cations, the presence of anions such as bicarbonates and carbonates in irrigation water can also impact the soil permeability. The interaction of bicarbonates and carbonates with Ca^{2+} and Mg^{2+} leads to the

formation and precipitation of $CaCO_3$ and $MgCO_3$. This removes Ca^{2+} and Mg^{2+} from water and increases the relative proportion of sodium. Therefore, appreciable concentrations of carbonate and bicarbonate ions in the irrigation water can further increase the soil's sodicity and its associated potential sodium hazard (Murtaza et al., 2021; Aggarwal et al., 2021).

Over the years, separate indices such as residual sodium carbonate (RSC) and modifications of the ratios that calculate sodium hazard such as adjusted SAR, has been proposed by researchers to quantify the carbonate-bicarbonate effect on aggravating soil's sodicity (Eaton, 1950, Wilcox et al., 1954). However, essentially these ion interactions create the soil permeability problems which can be measured by the permeability index (PI).

The Permeability Index (PI) which was originally introduced by Doneen in 1964 examines the soil's capacity to facilitate downward water percolation which is influenced by the presence of Na^+, Mg^{2+}, Ca^{2+}, and HCO_3^- in the soil. The following Eqn. 4.11 is used to measure the PI-

$$PI = \left(\frac{Na^+ + \sqrt{HCO_3^-}}{Ca^{2+} + Mg^{2+} + Na^+}\right) \times 100 \quad (4.11)$$

Table 4.11: Classification of groundwater according to permeability index (PI)

PI Class	Range	No. of samples	% of samples
Class I	PI > 75%	77	51%
Class II	25% < PI < 75%	75	49%
Class III	PI < 25%	0	0%

This index categorizes water into three distinct classes: Class I (PI > 75%), Class II (25% < PI < 75%), and Class III (PI < 25%) (See Table 4.11 and Fig. 4.11). Out of 152 samples, 77 samples fall into Class 1 and 75 samples fall in Class II which

is characterized by their superior permeability. None of the samples fall in class III.

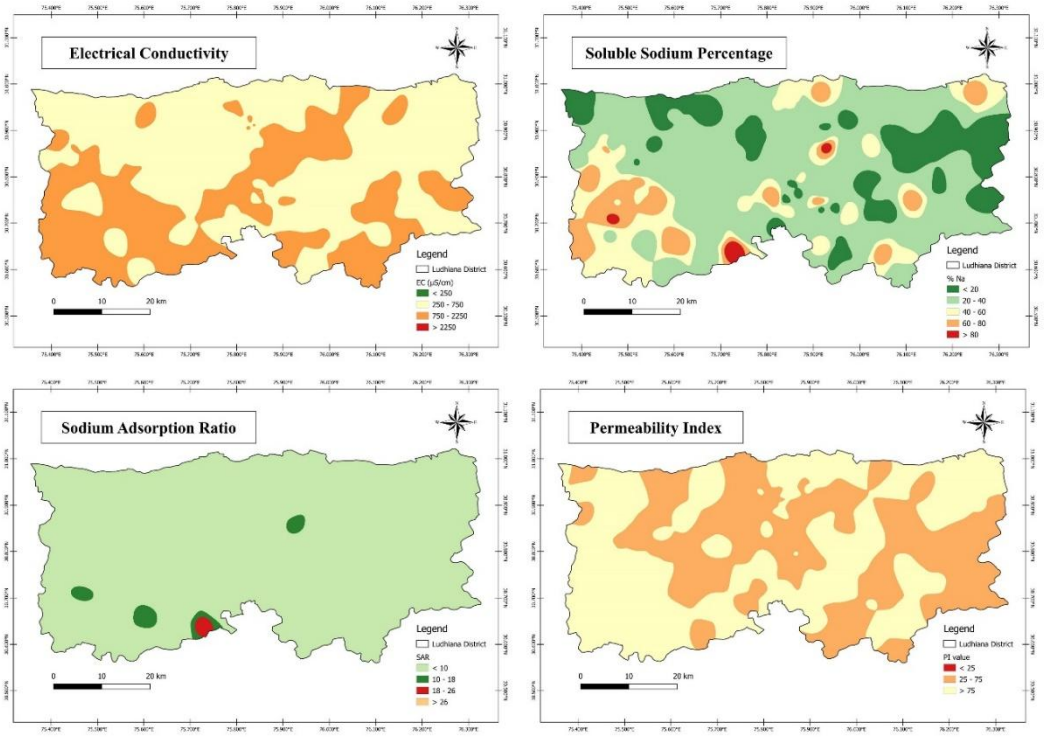

Fig. 4.11: Spatial interpolation maps of EC, SSP (%Na), SAR and PI across Ludhiana district

4.7 Irrigation water quality index

Based on the analysis of samples for IWQI, more than half of the samples fall into categories of 'Severe' and 'High' restriction combined (see Fig 4.12 and Table 4.12). Out of the total 152 samples, 33 samples i.e., 21.7 % of the samples fall in the 'Severe restriction' category whereas 57 samples i.e., 37.5% fall into the category of 'high restriction'. The sites with severe groundwater use restriction are depicted in dark red colour in the map, these sites can be seen to be located in eastern part of Samrala and Khanna block; in some parts of central and northern Ludhiana II and Macchiwara block, in southern and western parts of Pakhowal and Sidhwan Bet block. Groundwater from these sites should be avoided to be used for irrigation under normal conditions. It is only under special cases that this water can be used to irrigate for

plants with high salt tolerance. The sites with 'High' restrictions are depicted in orange colour in the map. These sites can be seen to be spread across the entire district as this category covers the maximum area of the map. The groundwater in these areas may be used for irrigation in soils with high permeability and should be used for watering of plants with moderate to high tolerance to salts with special salinity control practices.

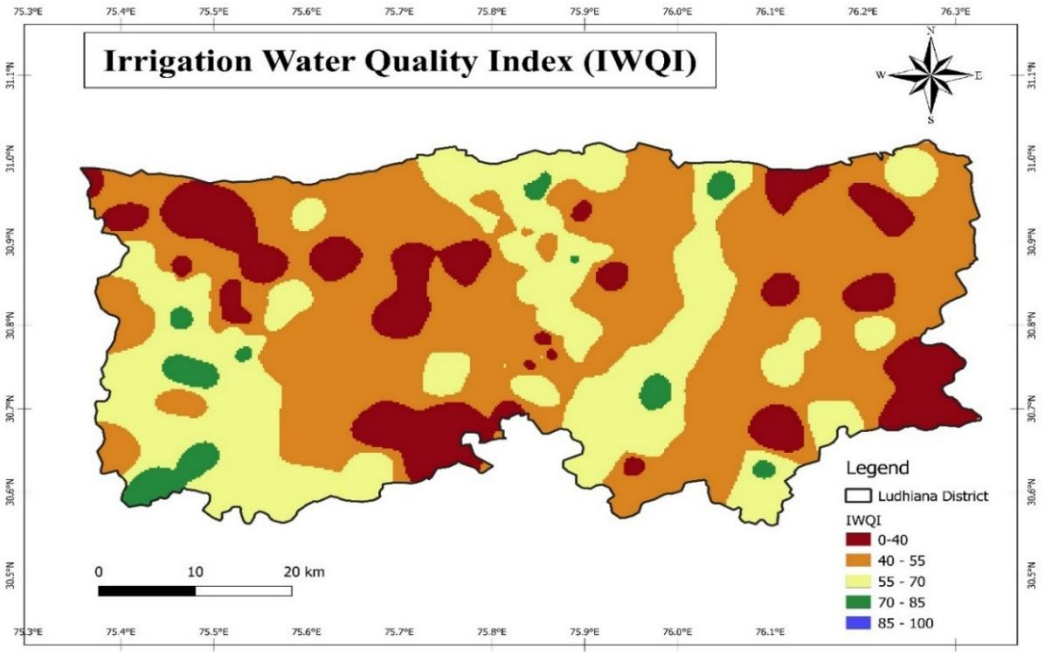

Fig. 4.12: Spatial distribution of irrigation water quality index value according to the different categories across Ludhiana district

Also, 33.6% of samples i.e., 51 samples out of 152 fall in 'Moderate' restriction category. This region is depicted by yellow colour in the map. As can be seen from the map, the areas with groundwater that falls in moderate restriction are focused on west and central parts of the district in Jagraon, Sudhar, Ludhiana I, Ludhiana II and Dehlon blocks of the district. The groundwater in these areas may be used in soils with moderate to high permeability values in which plants with moderate tolerance to salts may be grown. There are only 11 sites the index of which falls in 'Low' restriction category. These are located at Sherpur kalan, Bardeke, Turmuri, Ghaloti, Akhara, Hathur and Dholanwal village sites. The groundwater in these locations can be used

for soils with light texture and moderate permeability. Also, none of the calculated values fall in the 'No restriction' category.

Table 4.12: Percentage of samples conforming to the different IWQI categories

IWQI Value	Category of restriction	No. of samples	Percentage (%) of samples
0-40	Severe	33	21.7
40-55	High	57	37.5
55-70	Moderate	51	33.6
70-85	Low	11	7.2
85-100	No	0	0

4.8 Artificial neural network

A total of 152 groundwater samples collected from different locations across Ludhiana district were used for the development of the ANN model. The input parameters selected for modeling were EC, SAR, Cl^-, HCO_3^-, and Na^+, while the output parameter was the Irrigation Water Quality Index (IWQI). The neural network was developed in two phases: training and testing (validation). As suggested by researchers in past, to prevent the possibility of overfitting and improve model generalization, 90 % of the samples (135 samples) were used to train the neural network and the remaining 17 samples was used for the testing and validation (Leong et al., 2018, 2020). During the training phase, the proposed network was trained to capture the underlying relationship between the chosen inputs and outputs. The network was then tested with a test data set, which was not used for training. The network was considered suitable for further predictions only after its performance was validated by testing its ability to accurately predict the required output, i.e., IWQI values.

After specifying the conditions for the network algorithm in IBM SPSS, as described in methodology section, the model was run ten times. The summary of the estimated root mean square error (RMSE) for each run is presented in Table 4.13. The structure of the neural network (NN(ii)) that has the least RMSE values for both training (0.09) and testing (0.07) is shown in the Fig. 4.13. As suggested by the

previous studies the performance of the model is considered good if the RMSE value is less (Ahmed et al., 2019; Mallik et al., 2022; Rustam et al., 2022, Taşan, 2023). The RMSE value of 0.09 or 0.07 means that, on average, the model's predictions deviate from the actual values by 0.09 or 0.07 units. This suggests that the model's predictions are relatively close to the actual values, indicating a good level of accuracy. As can be seen in the Table 8, RMSE values for training and testing data for each of the ten neural networks is relatively small, with an average of 0.11(training) and 0.10(testing). Therefore, it can be concluded that the proposed model fits accurately to the given data. The neural network that has been formed can replicate the complex environmental relationships between these inputs, which will ensure that when it is applied to a dataset that is noisy and incomplete (which is often the situation in practical scenarios), the calculations of IWQI will remain reliable. The validated model can be employed to predict IWQI values for the region by using input data generated from plausible future scenarios. Also, ANN models, if integrated well with the system, will offer an advantage of scalability by generating quick and accurate predictions in real time applications.

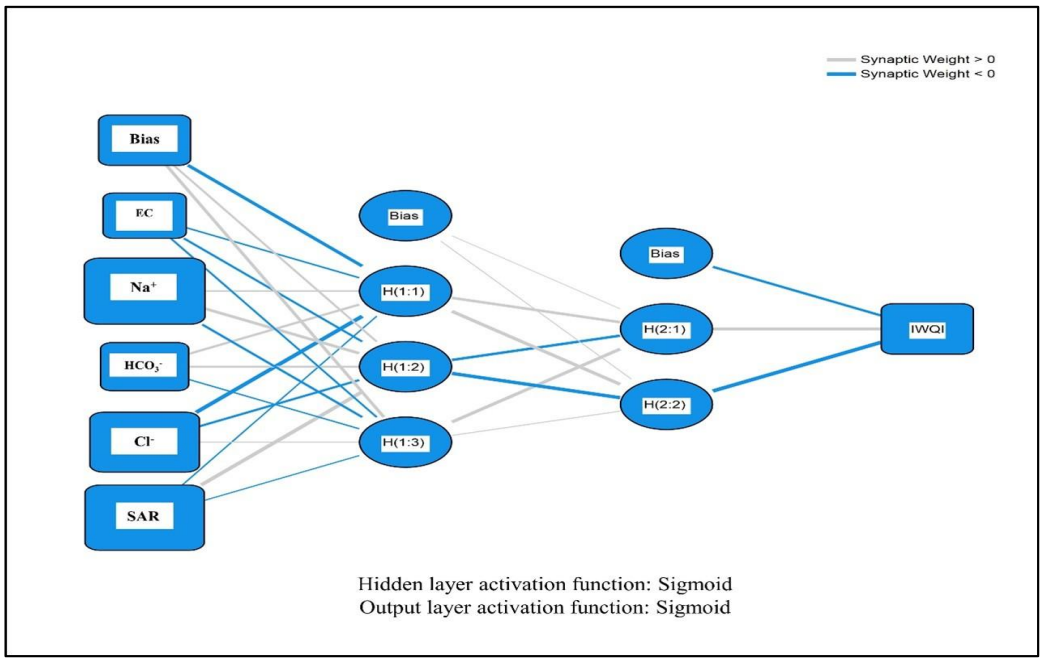

Fig. 4.13: The diagram of artificial neural network (NN (ii)) showing input, hidden and output layers

Table 4.13: RMSE values for training and testing data for different neural networks

N. Network (NN)	Training (Sample size 135)		Testing (Sample size 17)	
	SSE *	RMSE*	SSE	RMSE
NN (i)	2.24	0.13	0.18	0.10
NN (ii)	0.98	0.09	0.09	0.07
NN (iii)	1.80	0.12	0.17	0.10
NN (iv)	1.57	0.11	0.16	0.10
NN (v)	1.67	0.11	0.14	0.09
NN (vi)	1.66	0.11	0.15	0.09
NN (vii)	1.56	0.11	0.15	0.09
NN (viii)	1.83	0.12	0.17	0.10
NN (ix)	1.88	0.12	0.17	0.10
NN (x)	1.79	0.12	0.18	0.10
Mean	1.70	0.11	0.16	0.10
St. Dev.	0.30	0.01	0.03	0.01

*SSE: Sum of square error, RMSE: Root mean square error

Sensitivity analysis was conducted to assess the impact of input variables on the model. For this purpose, the relative significance of each input variable in every neural network was determined by analyzing the weights assigned to them by the network. The average importance of the inputs across ten neural networks was then calculated and converted into normalized importance (Table 4.14) by dividing each average value by the maximum average importance and expressing it as a percentage. This normalization facilitates a direct comparison among input variables by placing them on a common scale. The result provides insight into the dominant controlling parameters influencing model performance and help identify the most influential variables. Such an analysis enhances the interpretability and reliability of the developed neural network model.

The result shows that the Cl^- is the most important input variable that has the most predictive power, followed by SAR that has a normalized importance of 59.7 %. This is followed by Na^+ (58.5%), HCO_3^- (53.1%) and EC (27.2%).

Table 4.14: Impact of various input parameters on model prediction

Neural Network (NN)	EC	Na^+	HCO_3^-	Cl^-	SAR
NN (i)	0.217	0.198	0.172	0.302	0.110
NN (ii)	0.096	0.282	0.121	0.227	0.274
NN (iii)	0.070	0.168	0.151	0.405	0.206
NN (iv)	0.041	0.211	0.188	0.336	0.224
NN (v)	0.142	0.181	0.147	0.335	0.195
NN (vi)	0.134	0.184	0.213	0.288	0.181
NN (vii)	0.050	0.208	0.174	0.316	0.253
NN (viii)	0.043	0.186	0.162	0.418	0.192
NN (ix)	0.072	0.156	0.214	0.393	0.166
NN (x)	0.047	0.190	0.234	0.332	0.198
Average importance	0.091	0.196	0.178	0.335	0.200
Normalized importance (%)	27.20%	58.50%	53.10%	100%	59.70%

4.9 Comparative Scenario Analysis Based on IWQI Classifications

The Table 4.15 presents the distribution of water samples across five IWQI-based restriction categories, ranging from Severe Restriction to No Restriction, for the current baseline conditions and for each future scenario. Fig. 4.14 compares the distribution of water samples across IWQI restriction categories under baseline and future scenarios, illustrating the shifts in groundwater quality projections for Ludhiana district.

- **Scenario 1 – Higher Abstraction and Reduced Recharge.** The proportion of samples in the Severe Restriction category decreases from 21.71% to 15.13%, possibly due to a shift of IWQI values from severe to high restriction category as high Restriction sees a notable increase (37.5% → 45.39%), highlighting that higher abstraction rates push a larger share of samples into higher salinity or hazard categories. Moderate restriction levels remain relatively stable, but low-quality extremes may slightly diminish.

- **Scenario 2 – Increased Contamination Pressure.** Severe Restriction jumps significantly to 29.61%, indicating a marked deterioration of water quality in many areas. High restriction remains the largest category (39.47%), and moderate restriction drops sharply to just 23.68%, showing that many moderately restricted classes worsen into higher restriction classes. Low restriction conditions remain unchanged at 7.24%, showing no expansion of areas with high groundwater quality.

- **Scenario 3 – Improved Management and Partial Quality Recovery.** This scenario assumes that selected management interventions are gradually implemented in the study area. As a result, it is seen that partial recovery in water quality occur over time. Moderate Restriction becomes the largest category (44.08%), indicating that improved management can shift more areas into a mid-range, less hazardous quality class. Severe restriction cases drop to 13.16%, the lowest among all scenarios. High and low restriction proportions balance out with better recharge and conservative extraction measures.

Table 4.15: IWQI category distribution for baseline and scenarios

IWQI Category	Original (Count / %)	Scenario 1 (Count / %)	Scenario 2 (Count / %)	Scenario 3 (Count / %)
Severe Restriction	33 (21.71%)	23 (15.13%)	45 (29.61%)	20 (13.16%)
High Restriction	57 (37.50%)	69 (45.39%)	60 (39.47%)	52 (34.21%)
Moderate Restriction	51 (33.55%)	53 (34.87%)	36 (23.68%)	67 (44.08%)
Low Restriction	11 (7.24%)	7 (4.61%)	11 (7.24%)	13 (8.55%)
No Restriction	0 (0.00%)	0 (0.00%)	0 (0.00%)	0 (0.00%)

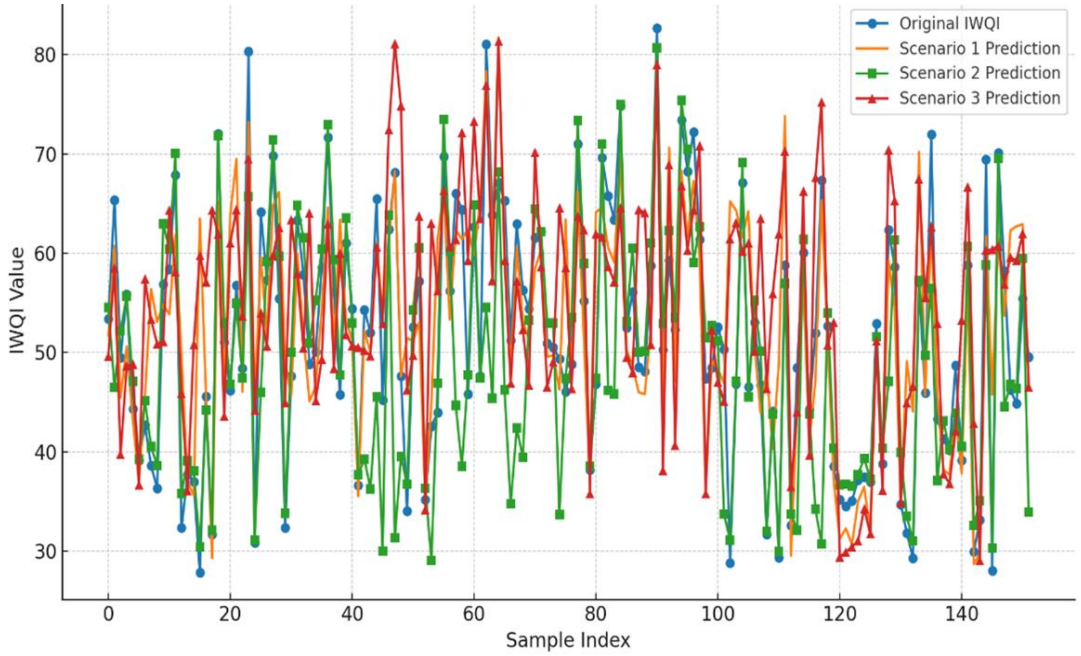

Fig. 4.14 Comparison of original IWQI vs Scenario Predictions

4.10 Policy Implications

Groundwater withdrawal stress, contamination pressure, and management interventions are visually summarized in Fig. 4.15, demonstrating key shifts in IWQI restriction categories across scenarios. Scenario 1 demonstrates that higher abstraction stress moves a substantial fraction of groundwater sources into high restriction categories, even if the most extreme cases reduce in number. This indicates the need for strict groundwater withdrawal regulation. Scenario 2 highlights that without pollution mitigation, water quality can degrade rapidly, pushing a high percentage of sources into severe restriction classes. Scenario 3 shows that effective policy instruments such as rainwater harvesting, micro-irrigation techniques, proper industrial effluent treatment, and crop diversification can lead to substantial recovery in groundwater quality. Therefore, the analysis suggests that continuous IWQI monitoring will allow farmers and authorities to respond early before water moves into high hazard zones. Also, the differing outcomes among scenarios underline the importance of tailoring interventions to local hydrological, climatic, and land use conditions.

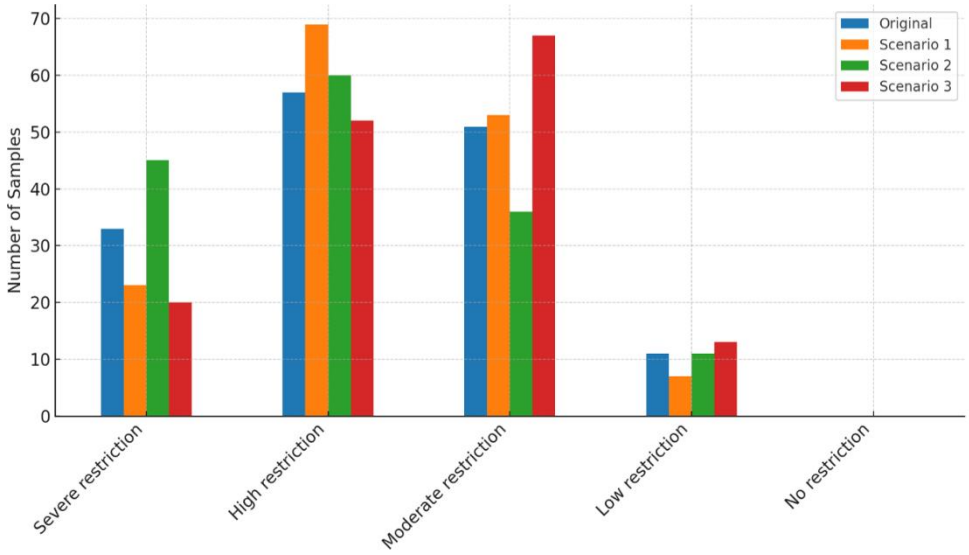

Fig. 4.15 Comparison of IWQI categories under baseline and future scenarios

4.11 Characterization of Groundwater Flow

A single-layer regional groundwater-flow model was developed for Ludhiana district using MODFLOW to represent groundwater conditions in the upper aquifer system, as illustrated in the conceptual model shown in Fig. 4.16. Although the regional aquifer system includes unconfined, semi-confined and confined units, it was conceptualized as an equivalent single-layer unconfined aquifer because the long-term groundwater-level observations available for model evaluation predominantly represented the shallow aquifer system. The model top elevation was derived from the Digital Elevation Model (DEM), and the aquifer bottom was assigned at 200 m below ground-surface elevation.

The modelling framework comprised steady-state and transient simulations. The steady-state model represented baseline groundwater-flow conditions corresponding to the annual-average groundwater levels observed during calendar year 2013. Its calibrated hydraulic-head distribution was subsequently used as the initial condition for transient simulation. The transient simulation was conducted for the period from 1 January 2014 to 31 December 2023, represented by ten annual stress periods. Each annual stress period was subdivided into 12 computational time steps to

represent gradual groundwater-head response within the year; however, these subdivisions were not treated as monthly calibration periods. Transient calibration was performed using annual-average observed groundwater levels for calendar years 2014 to 2020, while calendar years 2021 to 2023 were reserved for independent validation without further parameter adjustment. Fig. 4.17 presents the three-dimensional representation of the model top elevation, calibrated groundwater-head surface (2013) and bottom elevation of the Ludhiana groundwater-flow model.

The Sutlej River, an important hydraulic feature along the northern part of Ludhiana district, was represented using the MODFLOW River Package (RIV). River-aquifer interaction was simulated using river stage, riverbed bottom elevation and riverbed conductance, enabling groundwater recharge from the river or groundwater discharge to the river depending on the simulated hydraulic gradient. General Head Boundary (GHB) conditions were applied along appropriate non-river external boundary cells to represent regional groundwater inflow and outflow, while river cells were excluded from overlapping GHB assignment.

Recharge values were spatially represented using twelve block-based zones corresponding to the administrative blocks of Ludhiana district. Each model cell was assigned to the nearest block reference location to generate a continuous recharge zonation across the numerical domain. Annual block-wise recharge quantities were converted to recharge flux values in m/day using the represented block area and the number of days in a year, and were applied through the MODFLOW Recharge Package (RCH). This framework allowed regional variations in net groundwater recharge among the blocks to be represented in the model.

Groundwater abstraction was simulated through the MODFLOW Well Package (WEL). Block-wise annual groundwater draft estimates provided the base abstraction input and were converted from hectare-metre per year to equivalent daily pumping volumes in m^3/day. Hydraulic conductivity was represented using eight spatial zones derived from available exploratory-well and pumping-test information, with zonal distributions extended across the model domain using a nearest-neighbour

approach. In the transient model, specific yield was treated as an adjustable aquifer storage parameter, whereas specific storage was retained at a fixed value.

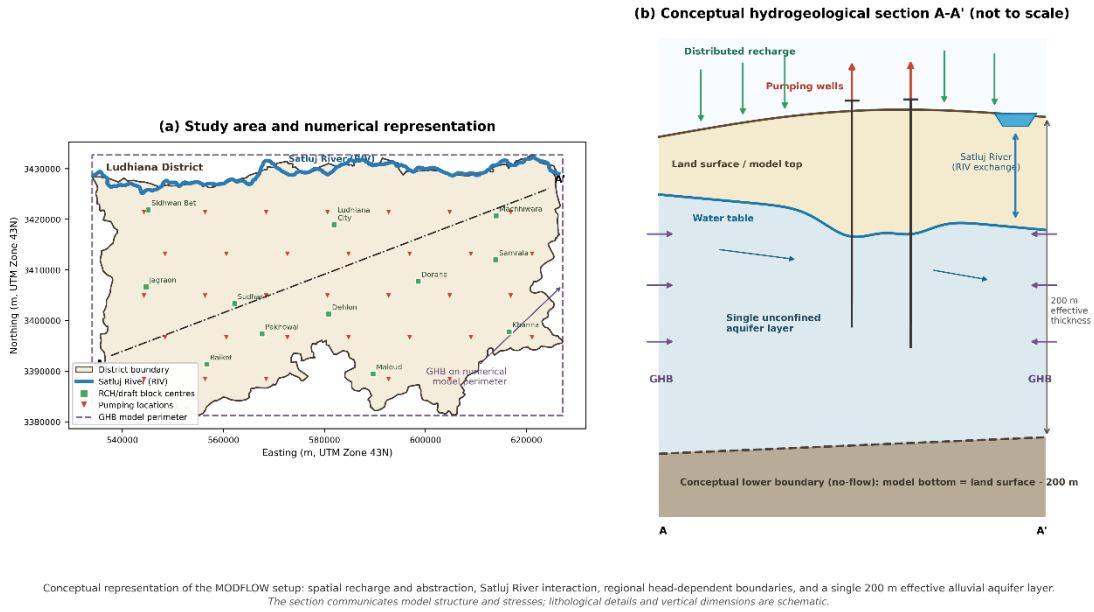

Conceptual representation of the MODFLOW setup: spatial recharge and abstraction, Satluj River interaction, regional head-dependent boundaries, and a single 200 m effective alluvial aquifer layer.
The section communicates model structure and stresses; lithological details and vertical dimensions are schematic.

Fig. 4.16 Conceptual model of groundwater flow for Ludhiana district of Punjab, India

Model calibration was carried out by adjusting selected parameters within hydrogeologically reasonable limits to improve agreement between observed and simulated groundwater heads. For the steady-state model, the principal adjustable parameters included the spatially distributed hydraulic conductivity values, Sutlej river boundary parameters and General head boundary parameters. For the transient model, specific yield was additionally evaluated to represent the storage response of the unconfined aquifer, whereas specific storage was retained at a fixed value and was not calibrated. Recharge and groundwater abstraction were treated as secondary, constrained stress parameters rather than freely adjustable calibration variables. The base recharge and draft inputs were derived from the block-wise estimates available in the CGWB Dynamic Ground Water Resource Assessment data which is calculated using GEC framework. Because net recharge and abstraction are subject to spatial uncertainty, particularly in the intensively irrigated and paddy-dominated agricultural

setting of Ludhiana district, bounded recharge modifiers and pumping-distribution adjustments were subsequently evaluated within the block-based framework but within scientifically realistic ranges. Pumping was represented primarily through the block-wise abstraction distribution, supplemented by a smaller spatially distributed component based on 26 geocoded tubewell/village locations. Localized stress adjustments were used only to represent unresolved uncertainty in net local stresses or hydrogeological variability.

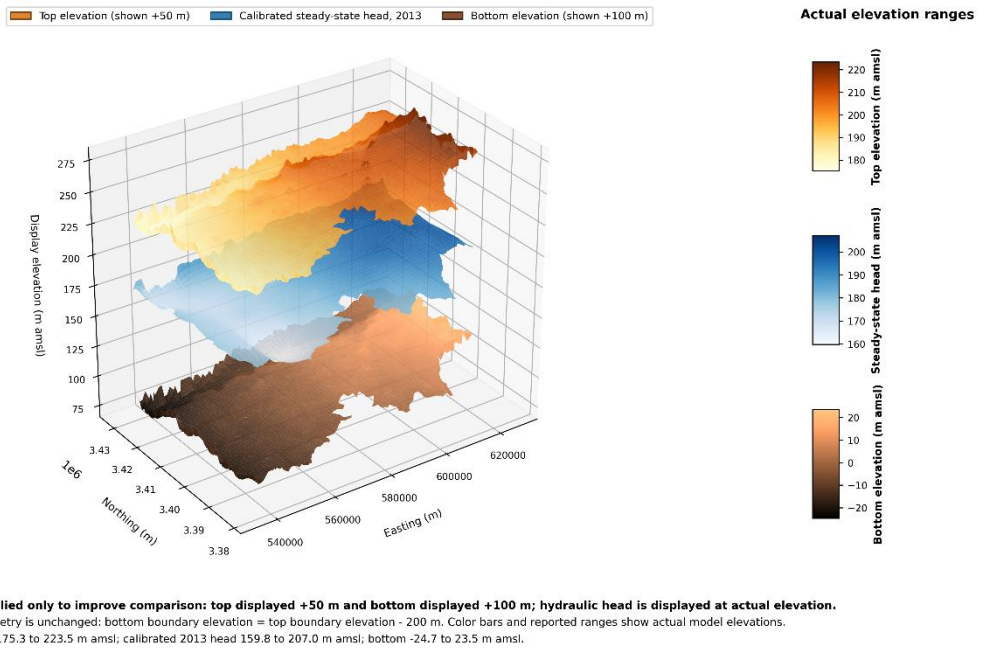

Visual offset applied only to improve comparison: top displayed +50 m and bottom displayed +100 m; hydraulic head is displayed at actual elevation.
Actual model geometry is unchanged: bottom boundary elevation = top boundary elevation - 200 m. Color bars and reported ranges show actual model elevations.
Actual ranges: top 175.3 to 223.5 m amsl; calibrated 2013 head 159.8 to 207.0 m amsl; bottom -24.7 to 23.5 m amsl.

Fig. 4.17 Three-Dimensional view of the top elevation, calibrated steady state water level (2013) and bottom elevation of the Groundwater flow model of Ludhiana district (Vertically offset for visualization only).

Following calibration, the steady-state model, reproduced the baseline groundwater heads with an RMSE of 1.471 m, MAE of 1.245 m, mean error of -0.031 m, NRMSE of 3.028% and coefficient of determination R^2 of 0.985 (See Fig. 4.18). Transient calibration was performed for seven calendar years, from 2014 to 2020, using 54 retained observation wells and a total of 378 annual head comparisons. Specific yield was evaluated as the principal transient aquifer-storage parameter, whereas specific storage was retained at a fixed value. Bounded annual recharge and

groundwater-abstraction multipliers were evaluated for the calibration years to represent uncertainty in annual stress magnitude, while the calibrated spatial aquifer and boundary-condition framework from the steady-state model was retained. Automatic parameter evaluation involved repeated MODFLOW simulations in which the differences between observed heads (h_o) and simulated heads (h_s) were quantified through the sum of squared residuals and associated statistical indicators, particularly RMSE, MAE and mean error.

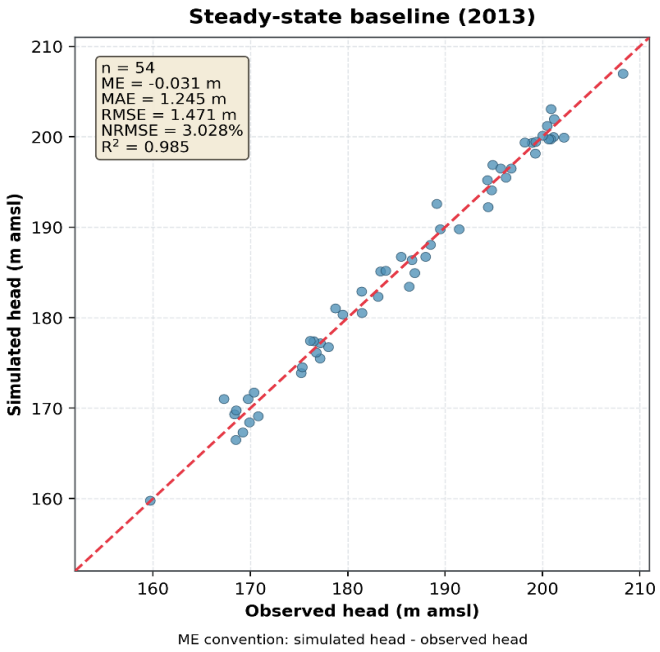

Fig. 4.18 Plot between observed vs simulated hydraulic heads (2013)

Over the calibration period, the model produced an overall RMSE of 2.214 m, MAE of 1.723 m, mean error of 0.303 m, NRMSE of 4.324% and R^2 of 0.968. Annual calibration RMSE values ranged from 1.636 m in 2014 to 2.532 m in 2018, while mean error ranged from -0.172 m to 0.596 m. The generally small mean-error values indicate limited systematic bias in simulated groundwater heads, while the high R^2 values, ranging from 0.959 to 0.982 during calibration years, indicate that the model adequately reproduced the regional spatial variation in observed groundwater heads (See Table 4.16 and Fig. 4.19).

Table 4.16 Statistical performance of the groundwater-flow model during the calibration period

Calibration Period	Mean Error, ME (m)	Mean Absolute Error, MAE (m)	Root Mean Square Error, RMSE (m)	NRMSE (%)	Coefficient of Determination, R^2
2014	-0.172	1.357	1.636	3.357	0.982
2015	0.429	1.501	2.037	4.109	0.971
2016	0.540	1.775	2.288	4.736	0.967
2017	0.083	1.600	2.093	4.297	0.971
2018	0.596	1.999	2.532	5.287	0.959
2019	0.328	1.875	2.374	4.828	0.964
2020	0.316	1.955	2.411	4.709	0.964
Overall calibration period	0.303	1.723	2.214	4.324	0.968

During the independent validation period, the model achieved an overall RMSE of 3.072 m, MAE of 2.488 m, mean error of -0.252 m, NRMSE of 5.617% and R^2 of 0.950. Annual validation RMSE values ranged from 2.577 m in 2021 to 3.643 m in 2023 (See Table 4.17 and Fig. 4.19). The relatively small overall mean error and high coefficient of determination indicate that the model retained reasonable predictive capability outside the calibration period. Although the validation RMSE increased compared with the calibration period, the model continued to reproduce the regional groundwater-head pattern satisfactorily. The increase in error during the later validation years may be attributed to uncertainty in annual recharge and abstraction stresses, local pumping distribution, recharge variability, and aquifer response, which is expected in a regional single-layer representation of a complex irrigated aquifer system.

Overall, the calibration and validation results indicate that the developed model provides a reasonable regional representation of groundwater-flow conditions and interannual groundwater-head behaviour in Ludhiana district (See Fig. 4.20). The steady-state model established an appropriate initial groundwater-head condition, while the transient model reproduced multi-year changes with acceptable bias and

strong correspondence between observed and simulated heads (See Fig. 4.21). The validation results further show that the calibrated parameter set remained stable when applied to years that were not used during calibration, supporting the reliability of the model for independent simulation. Minor deviations between observed and simulated heads are expected because local pumping intensity, return flow, recharge variability and small-scale aquifer heterogeneity cannot be fully resolved in a regional single-layer model. As the model uses annual-average groundwater observations and annual stress periods, its predictive application is most appropriate for regional interannual assessment rather than detailed seasonal or monthly groundwater-level simulation.

Table 4.17 Statistical performance of the groundwater-flow model during the validation period

Validation Period	Mean Error, ME (m)	Mean Absolute Error, MAE (m)	Root Mean Square Error, RMSE (m)	NRMSE (%)	Coefficient of Determination, R^2
2021	-0.587	2.096	2.577	5.186	0.960
2022	-0.317	2.355	2.898	5.705	0.955
2023	0.147	3.014	3.643	6.783	0.936
Overall validation period	-0.252	2.488	3.072	5.617	0.950

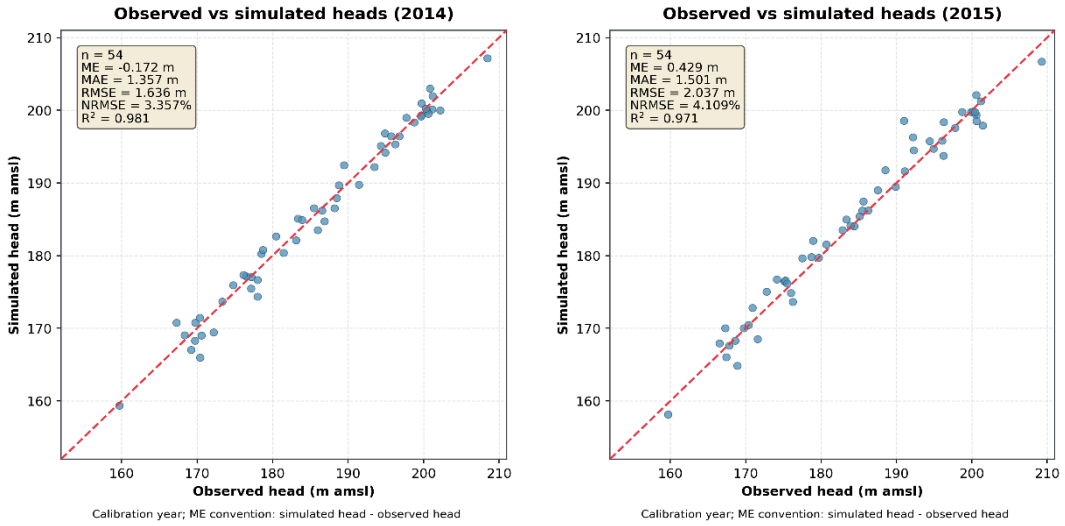

Fig. 4.19 Plots between observed vs simulated hydraulic heads for 2014-2023

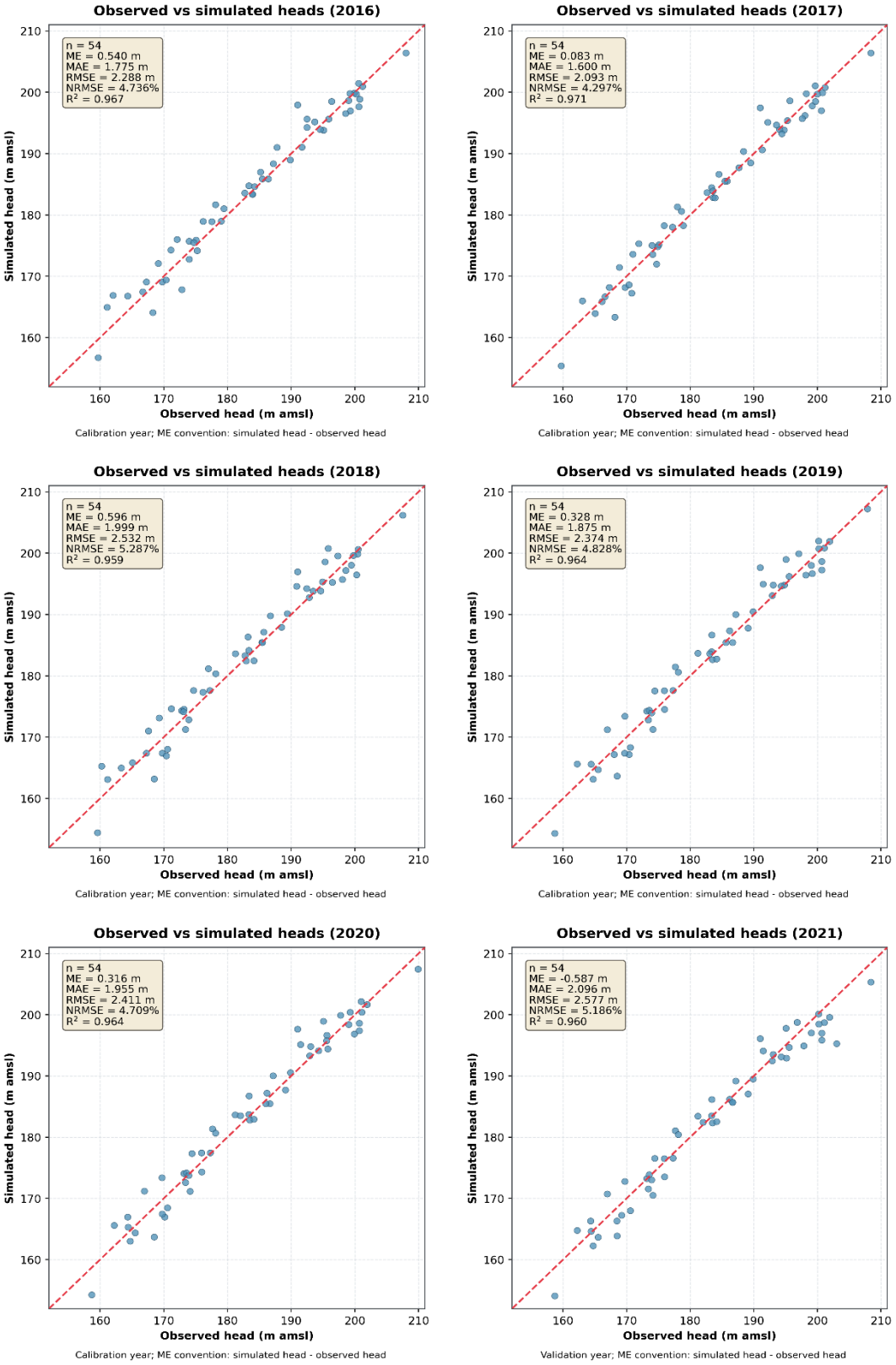

Fig 4.19 (Continued)

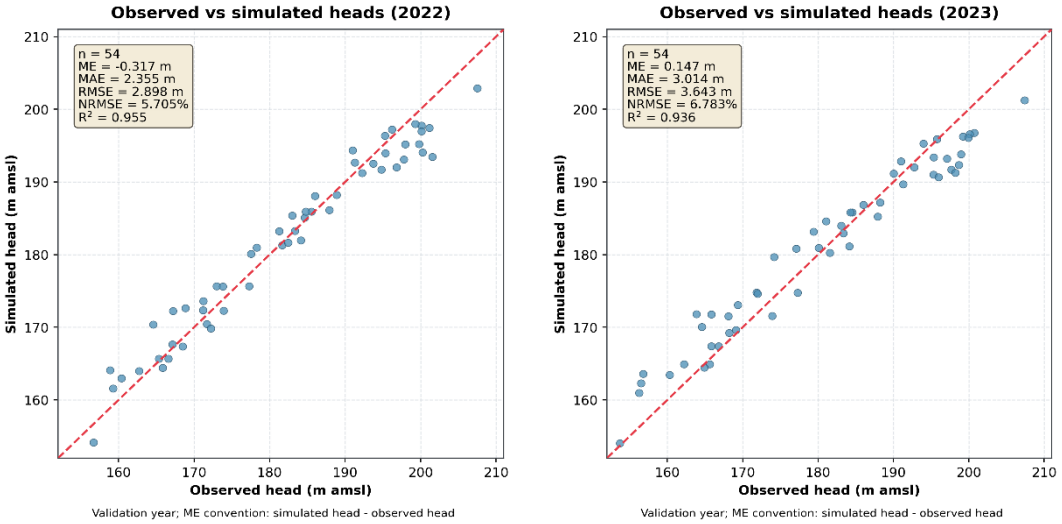

Fig 4.19 (Continued)

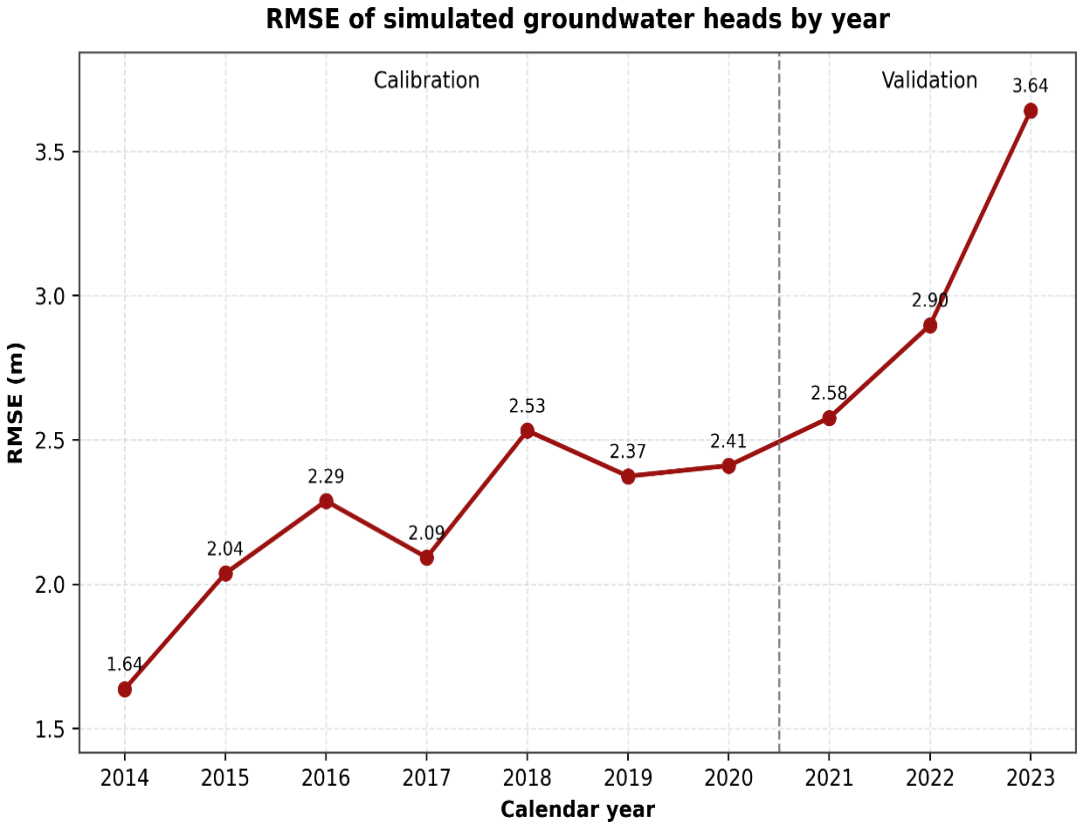

Fig. 4.20 Root mean square error (RMSE) of the simulated hydraulic heads

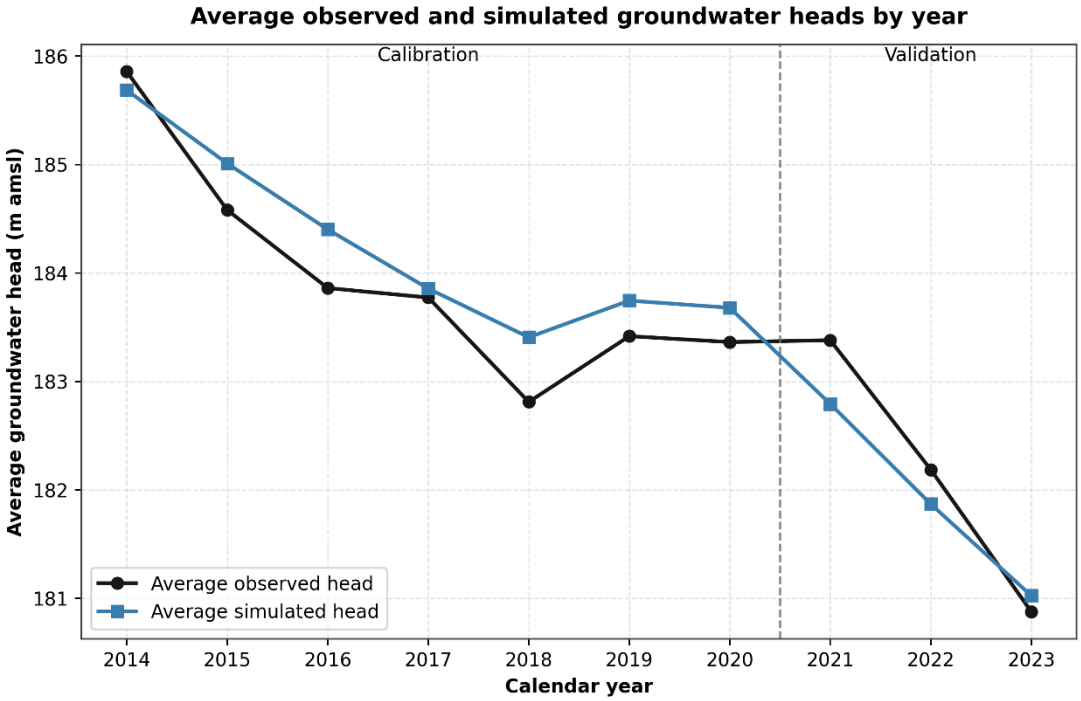

Fig. 4.21 Time series of the average observed and simulated hydraulic heads

4.12 Analysis of contaminant spread in groundwater

The simulated groundwater heads for the year 2020 were used to understand the distribution of measured nitrate concentration which was used for the quality mapping of the study area in this research. Groundwater flow direction was established using observed and simulated hydraulic head data, and nitrate concentrations were spatially compared against both simulated and observed head surfaces. The analysis showed that the highest hydraulic head was observed at the location (616700 E, 3397204 N), while the lowest hydraulic head was observed at (575657 E, 3418787 N), indicating that the general groundwater flow direction is towards the west, with an approximate flow angle of 152°.

4.12.1 Spatial distribution of nitrate over Observed Hydraulic Head Surface

The spatial relationship between nitrate concentration and observed hydraulic heads was examined by overlaying nitrate sampling locations on the interpolated observed hydraulic head surface for 2020 (Fig. 4.22).

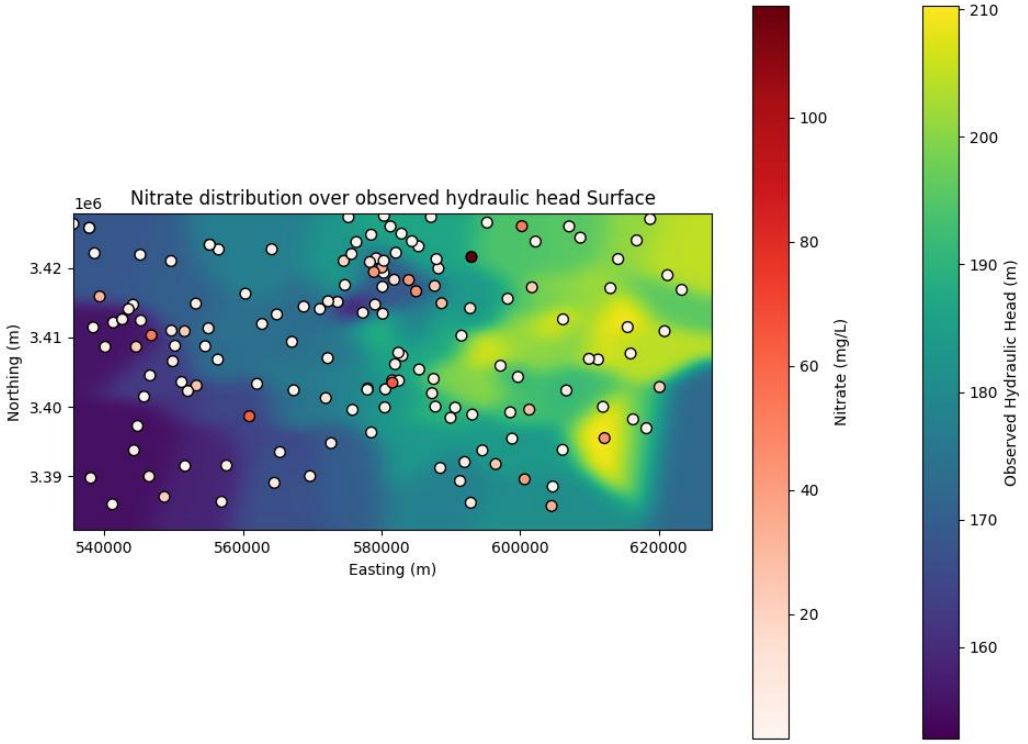

Fig. 4.22 Nitrate distribution over observed hydraulic head surface (2020)

When nitrate concentrations are plotted over this observed head surface, several important spatial patterns emerge. A noticeable clustering of nitrate sampling points occurs in the central part of the district. Within this zone, moderate to elevated nitrate concentrations are observed across a range of hydraulic head values. This indicates that contamination here may be controlled more by land-use intensity than by hydraulic position alone. Relatively higher nitrate concentrations are observed in parts of the southeastern sector, which correspond to comparatively higher hydraulic heads. Since groundwater flows from high head to low head regions, these southeastern high-head zones likely represent recharge-dominant areas. Elevated nitrate in such areas suggests that contamination may be entering the aquifer system locally through vertical percolation rather than being transported from distant upgradient sources.

However, to quantitatively assess whether nitrate contamination exhibits spatial clustering at the district scale, Global Spatial Autocorrelation Analysis (Moran's I) was computed. The analysis yielded: Moran's I = 0.056; Z-score = 1.45

and p-value = 0.083. The positive Moran's I value indicates a slight tendency toward clustering but the p-value exceeds the 0.05 significance threshold, indicating that the observed spatial pattern is not statistically significant at the 95% confidence level. The analysis suggest that contamination is controlled by localized processes rather than a single dominant district-wide driver. In other words, nitrate hotspots exist, but they do not form one large continuous contaminated zone. This outcome is supported by the analysis of the measured nitrate values, which reveal that majority of samples fall within the low concentration range (<10 mg/l), while a limited number of locations exhibit substantially elevated concentrations, extending beyond 50 mg/L and reaching extreme values above 100 mg/l. This skewed behaviour suggests that nitrate contamination is not regionally uniform but instead spatially localized. The dominance of low-to-moderate values indicates that large portions of the aquifer remain relatively less impacted, whereas high concentrations appear confined to discrete zones. Such statistical structure is characteristic of anthropogenic contaminants influenced by localized sources such as agricultural return flow, fertilizer application, septic leakage, or irrigation recharge zones.

4.12.2 Relationship of nitrate with groundwater flow parameters

Correlation analysis was performed to evaluate statistical relationships between nitrate concentration and hydraulic parameters. For nitrate vs simulated hydraulic head, correlation coefficient came out to be r = 0.118. This indicates a very weak positive relationship. Nitrate concentration does not significantly increase or decrease with modelled head values. For nitrate vs simulated hydraulic gradient, correlation coefficient came out to be r = 0.076. This extremely weak relationship suggests nitrate concentration is not directly controlled by areas of high hydraulic gradient or flow intensity. For nitrate vs observed hydraulic head, correlation coefficient was r = –0.095. This weak negative correlation indicates slightly higher nitrate concentrations in areas of relatively lower observed heads, but the relationship is statistically insignificant. Thus, the results demonstrate localized clustering patterns independent of the regional groundwater flow. The spatial characteristics indicate that nitrate contamination is more likely influenced by localized recharge infiltration,

agricultural fertilizer application, irrigation return flow, shallow groundwater abstraction and spatial variability in soil and vadose zone characteristics. The nitrate occurrence is likely controlled by vertical recharge processes rather than lateral groundwater transport at the regional scale. This implies that contamination sources are spatially distributed rather than originating from a single upstream source.

Since the district is characterized by intensive agricultural activity that typically involve high nitrogen fertilizer application rates, flood irrigation practices and multiple crop cycles per year; therefore, the excess nitrogen which is not taken up by the crops may accumulate in the soil profile and leach into groundwater during irrigation or monsoon recharge events. The distribution of nitrate concentration which is thus observed in the measured data, is consistent with spatial variability in fertilizer application rates, cropping intensity and irrigation practices. The nitrate distribution in the study area represents a recharge-controlled, source-distributed system, rather than a single plume-type advective contamination system.

4.12.3 Predictive nitrate transport

Although the 2020 nitrate distribution shows weak correlation with regional hydraulic gradients, this does not preclude future transport under the prevailing groundwater-flow regime. The measured concentrations reflect conditions influenced by spatially variable, localized anthropogenic inputs. Assuming no additional external nitrate loading after 2020, the nitrate mass already present in the aquifer may nevertheless be redistributed over time by advection and hydrodynamic dispersion. Therefore, to evaluate long-term groundwater-quality sustainability, it is necessary to assess the potential migration and persistence of nitrate under the current hydraulic conditions.

Accordingly, a conservative base predictive scenario was simulated by coupling the calibrated transient MODFLOW flow field with an MT3D-USGS transport model. In this coupled framework, MODFLOW provides the groundwater flow velocities and storage terms, while MT3D-USGS computes solute concentration

evolution through advection and dispersion using the MODFLOW–MT3D flow-transport linkage (FTL) file. In the base scenario, kinetic reactions were disabled (IREACT = 0), meaning no first-order decay/denitrification was simulated, and the recharge concentration was specified as 0 mg/l in the source–sink mixing (SSM) configuration. This setup represents a "no new nitrate input" assumption after 2020 and isolates the effect of hydrodynamic redistribution (flushing and dilution/spreading) of the legacy nitrate distribution. The initial nitrate field (2020) was derived from measured nitrate concentrations from groundwater samples and interpolated to the model grid to define starting concentrations. Transport parameters adopted in the simulation included an effective porosity of 0.12, longitudinal dispersivity of 20 m, and transverse dispersivity ratios of 0.1 (horizontal) and 0.01 (vertical). Advection was simulated using the standard finite-difference formulation available in MT3D-USGS.

The measured values that were used as initial concentration exhibited substantial spatial variability, with concentrations ranging from 0.01 to 118.00 mg/l (mean 8.64 mg/l; median 3.10 mg/l), and approximately 3.3% of samples exceeding the drinking-water threshold of 45 mg/l. Model results indicate a progressive decline in mean nitrate over the simulation period, from 8.86 mg/l in Year 1 to 6.51 mg/l in Year 10, which is approximately a 27% reduction (See Fig. 4.23). The spatial footprint of high nitrate also decreases: the proportion of model area exceeding 45 mg/l reduces from ~1.70% to ~0.88%, although localized hotspots persist (See Fig. 4.25). Peak concentrations decline as well; the maximum observed concentration at model start was 118 mg/l, while the maximum simulated concentration after 10 years was approximately 69.95 mg/l. Under the assumptions used in this model, any simulated reduction in mean concentration or hotspot intensity is attributable to advective flushing and dispersive mixing rather than biochemical attenuation.

Spatially, concentrations remain right-skewed, with most grid cells (and monitoring locations) in the low-concentration range (0–10 mg/l) but with distinct hotspot zones near inferred source areas. Consistent with this behaviour, the number of locations exceeding higher thresholds (e.g., ≥25 and ≥50 mg/l) decreases more

strongly than the number exceeding a lower threshold (e.g., ≥10 mg/l), indicating that the model preferentially attenuates extreme concentrations through mixing and flushing while low-level contamination persists for longer (Fig. 4.24).

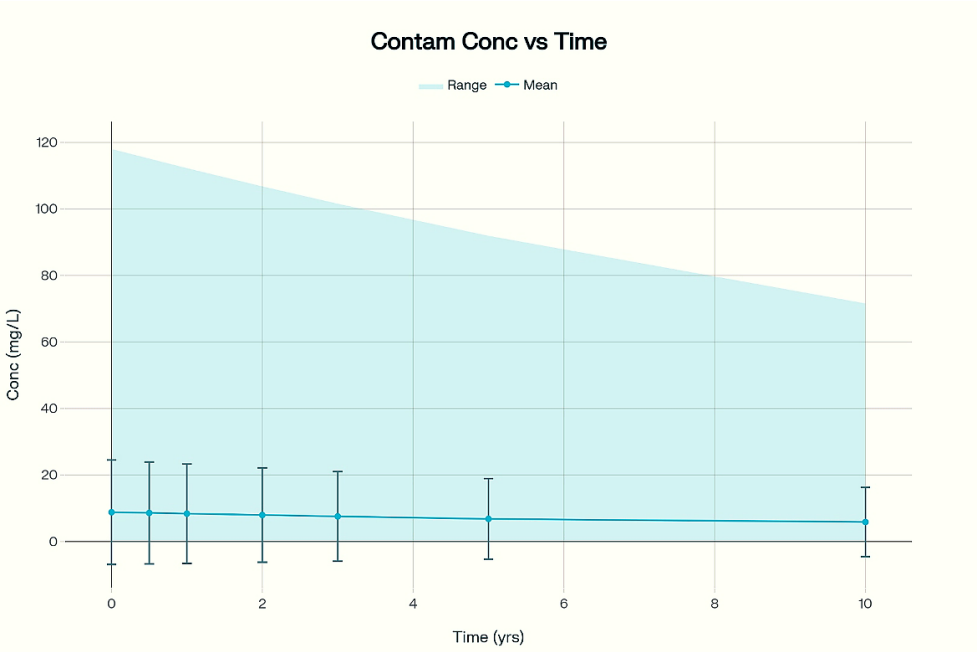

Fig. 4.23 Temporal decline in contaminant concentration range and mean over 10 years.

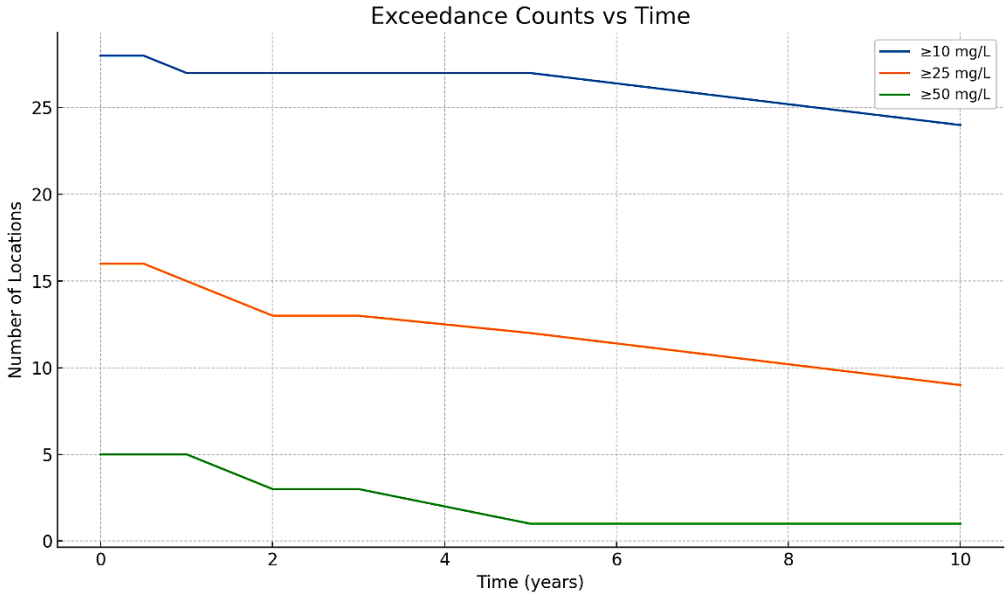

Fig. 4.24 Temporal decline in monitoring sites surpassing key contaminant concentration limits

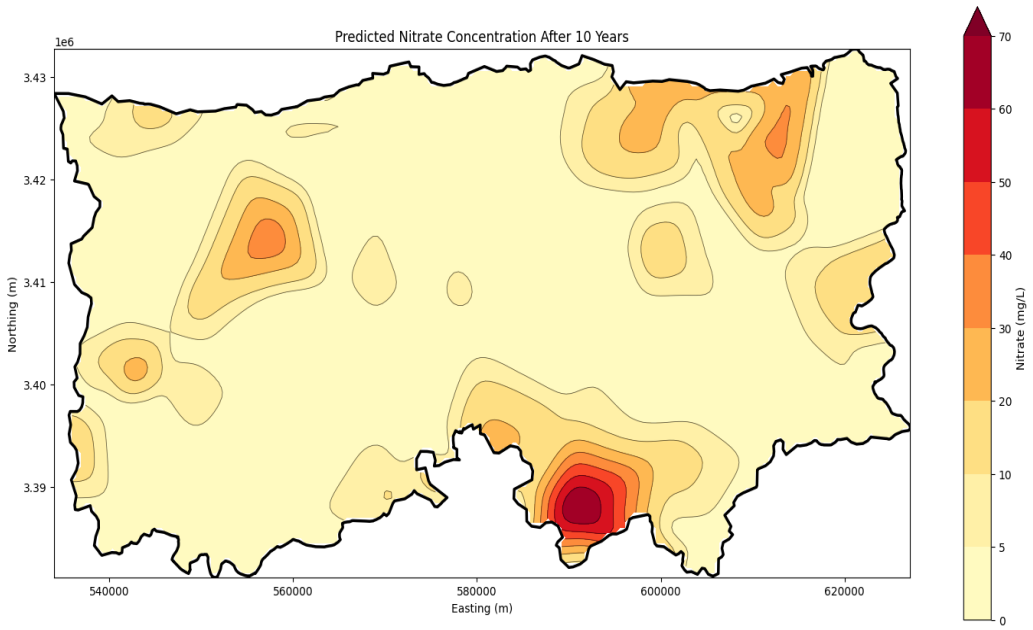

Fig. 4.25 Spatial distribution of predicted nitrate values after 10 years

These outcomes suggest that monitored natural attenuation may be viable in portions of the aquifer where concentrations are declining at acceptable rates; however, persistent high-concentration source zones may still require targeted management or remediation to achieve regulatory objectives within practical timeframes. The developed modeling framework further enables predictive evaluation of alternative remediation strategies and land-use scenarios, providing a basis for adaptive groundwater-quality management and long-term sustainability.

CHAPTER 5

CONCLUSION, FUTURE SCOPE AND SOCIAL IMPACT

5.1 Conclusion

The groundwater in the study area i.e., Ludhiana district, has significant influences from geogenic and anthropogenic sources and exhibit high spatial variability of measured parameters across the district. Groundwater is also used to irrigate almost all of its agricultural fields (as high as 95.6%). The present research is the comprehensive study that has been undertaken to analyse the groundwater quality for its potability and its use as irrigation water. The following conclusions can be summarized from it:

1. The sequence of comparative abundance for ions (in meq/l) as revealed from the laboratory tests for the district is Na^+ (37.1%)> Ca^{2+} (30.8%)> Mg^{2+} (29.1%)> K^+(2.8%) for cations and HCO_3^- (80%)> Cl^- (8.9%)> CO_3^{2-}(6.5%)> SO_4^{2-} (3.9%) > NO_3^-, F^-, PO_4^{3-}(<1%) for anions. The piper diagram has analysed that majority of the samples i.e., 80.9%, fall in the category of secondary alkalinity (where Ca^{2+} and Mg^{2+} balances HCO_3^- and CO_3^{2-}).

2. The geogenic influence of the groundwater has been confirmed from gibbs diagram that shows that rock and water interaction is the dominant process affecting the groundwater of the area. Also, based on the analysis of different ionic ratios, carbonate weathering and silicate weathering are both significantly affecting the groundwater chemistry of the area, with a slight dominance of carbonate weathering. Ion exchange process is taking place in the aquifer as confirmed from CAI index values.

3. In terms of saturation index, the groundwater is undersaturated with respect to halite, fluorite, gypsum, anhydrite and sylvite, whereas, it is supersaturated for calcite, dolomite, hydroxyapatite and aragonite minerals.

4. The spread of groundwater in terms of quality across the district can be understood by drinking water quality index which suggests that 2.6% and 57.9% of the samples fall under excellent and good quality category, whereas, 32.9%, 4% and 2.6% of the samples exhibit poor, very poor and unsuitable drinking water conditions.

5. The multivariate statistical analysis of the data has been conducted using principal component analysis (PCA) and hierarchical cluster analysis (HCA). For PCA, the extracted four components explain a cumulative variance of 75.4%; and for HCA, two-way clustering has been adopted to generate hierarchical cluster of water samples in both R and Q mode. Both the analysis divides the components and clusters based on different categories of water mineralization developed on the basis of different geogenic and anthropogenic activities undergoing in the study area.

6. The suitability of groundwater for irrigation quality was assessed by classifying the groundwater for salinity, sodium and carbonate-bicarbonate hazard using EC (µS/cm), %Na, SAR and PI values. In terms of EC, 62.5% of the samples out of 152, fall between 250 to 750 (µS/cm) i.e., in the 'medium' category. The remaining 57 samples fall in the category of 'high' salinity hazard. For %Na values, 114 sample fall in excellent to good category, whereas, for SAR analysis,148 samples fall in low sodicity category. Also, all the samples fall in class I and II for PI value.

7. The values of EC, SAR, Na^+, Cl^-, and HCO_3^- were used as an input to measure irrigation water quality index (IWQI) of the groundwater. The categories of restrictions based on calculated IWQI was defined as: No restriction (between 85-100), Low restriction (70-85), Moderate restriction (55-70), High restriction (40-55) and Severe restriction (0-40). Based on this analysis, 21.7 % of the samples fall in the 'severe restriction' category whereas 57 samples i.e., 37.5% fall into the category of 'high restriction'. The remaining samples fall in moderate to low restriction.

8. An optimized model was created with artificial neural network to estimate IWQI using multilayer perceptron feed forward mechanism in IBM SPSS software. The calculated RMSE value of the proposed model is 0.09 and 0.07 for training and testing data. This implies that the proposed model fits accurately and can be used for future IWQI prediction.

9. The weak statistical association between nitrate concentration and hydraulic parameters indicated that regional groundwater flow is not the primary mechanism governing nitrate occurrence within the study area. Although observed hydraulic head contours for 2020 demonstrated a clear westward regional gradient, nitrate concentrations do not exhibit a coherent downgradient plume aligned with this direction. Instead, concentrations are spatially heterogeneous, which suggests that nitrate contamination is controlled predominantly by localized recharge processes and anthropogenic inputs rather than by regional advective transport.

10. A conservative predictive nitrate-transport scenario was simulated by coupling the calibrated transient MODFLOW flow field with an MT3D-USGS transport model, using the observed 2020 nitrate distribution as the initial condition and representing transport through advection and hydrodynamic dispersion. Reactions were disabled (IREACT = 0) and increase of nitrate concentration through future recharge was set to zero in the SSM configuration. Under these assumptions, model results indicate a progressive decline in mean nitrate from 8.86 mg/l (Year 1) to 6.51 mg/l (Year 10; ~27% reduction), a reduction in the high-nitrate footprint (>45 mg/l) from ~1.70% to ~0.88% with persistent localized hotspots, and a decrease in peak concentrations (maximum simulated ~69.95 mg/l after 10 years).

5.2 Recommendations

Groundwater quality in Ludhiana district is currently under stress from both geogenic processes and anthropogenic activities, particularly industrial effluents and

intensive agriculture. Hydrogeochemical evaluation shows that the dominant hydrochemical facies is secondary alkalinity, governed mainly by rock–water interactions with significant contributions from carbonate and silicate weathering. While a majority of the samples fall within "good" to "poor" categories for drinking purposes, there are localized pockets of "very poor" or "unsuitable" water linked to specific pollution sources.

The measured attributes suggest that, at present, groundwater is not heavily polluted except at a few locations and therefore does not pose a major safety threat. However, growing anthropogenic pressures in the form of industrial expansion and agriculture, coupled with increasing dependence on groundwater and diminishing water levels, may aggravate the situation in the future. To safeguard water quality, future work should include in-depth study of water-consumption patterns and changing water-supply regimes alongside continued hydrochemical analysis.

From the irrigation perspective, salinity and sodium hazards are generally moderate, but the integrated Irrigation Water Quality Index (IWQI) indicates that nearly 60% of the samples fall under high to severe restriction categories for irrigation use, suggesting long-term risks to soil health and crop productivity. Groundwater in most locations can still be used for irrigation, but water from sites classified in the severe-restriction IWQI category should be avoided for normal irrigation conditions. Scenario-based IWQI prediction further highlights both the vulnerability of Ludhiana's groundwater and the scope for improvement through proactive management; without intervention, over-extraction and ongoing contamination are likely to push more sources into high or severe restriction classes, whereas the partial recovery observed in Scenario 3 demonstrates the real potential for improvement if appropriate management strategies are implemented in time.

Overall, these findings underscore an urgent need for targeted pollution control, regulated groundwater extraction, and the adoption of sustainable irrigation practices. Such a study is important for farmers, enabling them to make informed choices about groundwater quality, counteract the negative effects of poor-quality

water, and adjust irrigation practices accordingly. The analysis can also support policymakers in designing measures to mitigate environmental risks associated with leaching of contaminants into soils and nearby water bodies, thereby helping to reverse negative trends and secure the region's groundwater resources for the future.

5.3 Impact of the study

The assessment of groundwater quality in Ludhiana district provides essential scientific insights for sustainable water resource management, benefiting both the environment and society. The following sections outline the key environmental, social, and economic impacts that this research can deliver.

5.3.1 Environmental impacts

The hydrogeochemical characterization and mapping of drinking water quality zones help identify areas where groundwater quality is poor or unsuitable, thereby enabling targeted aquifer protection and reducing long-term contamination risks to soil and nearby surface water bodies. By distinguishing geogenic controls, such as rock–water interaction, carbonate weathering, and silicate weathering, from anthropogenic inputs, including industrial effluents and intensive agricultural activities, the study provides a scientific basis for pollution control and source-specific management. This can help prevent further degradation of groundwater systems.

The assessment of mineral saturation states, including undersaturation with respect to halite and gypsum and supersaturation with respect to calcite and dolomite, provides insight into possible scaling, clogging, and geochemical evolution within the aquifer. Such information is important for maintaining long-term aquifer health and planning groundwater-related infrastructure. In addition, the detailed classification of irrigation water hazards, including salinity, sodicity, and carbonate–bicarbonate hazards, along with IWQI-based restriction categories, helps identify locations where continued groundwater use may lead to soil salinization or sodification. This can support timely management actions to preserve soil fertility and maintain agricultural

productivity. Furthermore, scenario-based IWQI prediction using artificial neural networks demonstrates that future groundwater quality is sensitive to management choices, emphasizing the environmental benefits of timely interventions such as reducing pollutant loading, optimizing fertilizer use, and controlling groundwater abstraction.

5.3.2 Social and Economic impacts

By quantifying areas where groundwater is safe, marginal, or unsuitable for drinking, this study supports safer domestic water sourcing and helps identify priority locations where alternative water supplies or treatment measures may be required. This is particularly important for rural and peri-urban communities that depend heavily on groundwater, as it can help reduce potential health risks. The classification of irrigation water restrictions, ranging from “no restriction” to “severe restriction,” also provides farmers with practical information for adapting cropping patterns, irrigation schedules, and soil amendment practices. Such guidance can contribute to stabilizing crop yields and farm income in a region where agriculture is highly dependent on groundwater resources.

The ANN-based predictive framework developed for IWQI further offers a useful decision-support tool for local agencies and extension services. It can support proactive planning rather than reactive crisis management, thereby helping to reduce economic losses associated with crop failure, salinity-induced land degradation, and related infrastructure damage. In addition, the mapping of stressed zones and pollution hotspots can guide regulatory actions, such as controlling industrial discharge, monitoring agrochemical use, and strengthening groundwater surveillance. These measures can also promote participatory groundwater governance and improve trust between communities, farmers, and authorities. In the long term, protecting groundwater quality and preventing soil salinization will help preserve the agricultural base of Ludhiana, support rural livelihoods and food security, and reduce the vulnerability of small and marginal farmers to climate-related and market-related shocks.

5.3.3 Contribution to sustainable development goals

This study which has been conducted in Ludhiana district aligns with multiple United Nations Sustainable Development Goals (SDGs) by providing scientific evidence for sustainable water management, agricultural resilience, and environmental protection as illustrated in Fig. 5.1. The irrigation suitability assessment (EC, SAR, %Na, PI, and IWQI) identifies safe irrigation zones while flagging high-risk areas, supporting sustainable agricultural practices that maintain soil health and crop productivity essential for food security (SDG 2: Zero Hunger). Simultaneously, drinking water quality index evaluation maps zones from excellent to unsuitable quality, enabling safer drinking water access and reducing health risks from contaminated groundwater sources (SDG 3: Good Health and Well-being).

Fig. 5.1 Highlighted United Nation's Sustainable Development Goals (SDGs) aligning with the present study

Hydrogeochemical analysis of facies, ion ratios, and mineral saturation establishes a robust foundation for pollution source identification, integrated water quality monitoring, and regulated abstraction to protect vulnerable aquifers, ensuring sustainable groundwater quantity and quality (SDG 6: Clean Water and Sanitation). In industrializing Ludhiana district, the study guides urban and peri-urban groundwater

management, helping planners integrate aquifer protection into land-use decisions while promoting efficient water and fertilizer use, crop diversification, and reduced agrochemical loading through irrigation restriction zoning (SDG 11: Sustainable Cities and Communities; SDG 12: Responsible Consumption and Production).

Finally, by recommending avoidance of severely restricted groundwater for irrigation, the research prevents soil salinization and sodification, preserving soil ecosystem services and combating land degradation essential for long-term agricultural sustainability (SDG 15: Life on Land).

5.4 Future scope of the study and its limitations

The present study was based on groundwater sampling conducted over one year to evaluate the spatial distribution and hydrogeochemical characteristics of groundwater quality in Ludhiana district. Since groundwater quality is influenced by seasonal variations such as rainfall recharge, irrigation return flow, groundwater abstraction, and pumping intensity, future studies should include multi-season sampling, particularly during pre-monsoon and post-monsoon periods, to better capture temporal fluctuations in groundwater quality. Repeated monitoring at regular intervals would help in understanding seasonal trends, contaminant transport, and the long-term impact of anthropogenic and natural processes on groundwater chemistry.

Also, establishing long-term monitoring networks in high-risk zones would enable temporal trend analysis to validate IWQI predictions and assess management effectiveness. Coupled hydro-chemical and socio-economic studies of water use patterns and farmer economics can support location-specific adaptation strategies. The integration of climate projections with hydrogeochemical models would help assess the impact of changing recharge conditions. Field testing of remediation techniques such as managed aquifer recharge, along with enhancement of the ANN-IWQI model for real-time decision support through mobile-based platforms, can provide a comprehensive framework for supporting groundwater management policies and long-term water security in Punjab.

References

Aalipour, M., Štastný, B., Horký, F., & Amiri, B. J. (2022). Scaling an Artificial Neural Network-Based Water Quality Index Model from Small to Large Catchments. *Water (Switzerland)*, *14*(6). https://doi.org/10.3390/w14060920

Abascal, E., Gómez-Coma, L., Ortiz, I., & Ortiz, A. (2022). Global diagnosis of nitrate pollution in groundwater and review of removal technologies. *Science of the Total Environment*, *810*, 152233. https://doi.org/10.1016/j.scitotenv.2021.152233

Abel, D. J., Kilby, P. J., & Davis, J. R. (1994). The systems integration problem. *International Journal of Geographical Information Systems*, *8*(1), 1–12. https://doi.org/10.1080/02693799408901984

Abu El-Magd, S. A., Ismael, I. S., El-Sabri, M. A. S., Abdo, M. S., & Farhat, H. I. (2023). Integrated machine learning–based model and WQI for groundwater quality assessment: ML, geospatial, and hydro-index approaches. *Environmental Science and Pollution Research*, *30*(18), 53862-53875. https://doi.org/10.1007/s11356-023-25938-1

Adimalla, N., & Taloor, A. K. (2020). Hydrogeochemical investigation of groundwater quality in the hard rock terrain of South India using Geographic Information System (GIS) and groundwater quality index (GWQI) techniques. *Groundwater for Sustainable Development*, *10*, 100288. https://doi.org/10.1016/j.gsd.2019.100288

Aggarwal, A., Soni, J., Sharma, K., Sapra, M., Chitrakshi, Karaca, O., & Haritash, A. K. (2021). Hydrogeochemical Assessment of Groundwater for Drinking and Agricultural Use: A Case Study of Rural Areas of Alwar, Rajasthan. *Environmental Management*, *67*(3), 513–521. https://doi.org/10.1007/s00267-020-01361-x

Ahmed, A. A. (2009). Using Generic and Pesticide DRASTIC GIS-based models for vulnerability assessment of the Quaternary aquifer at Sohag, Egypt. *Hydrogeology Journal*, *17*(5), 1203–1217. https://doi.org/10.1007/s10040-009-0433-3

Ahmed, A. N., Othman, F. B., Afan, H. A., Ibrahim, R. K., Fai, C. M., Hossain, M. S., Ehteram, M., & Elshafie, A. (2019). Machine learning methods for better water quality prediction. *Journal of Hydrology*, *578*, 124084. https://doi.org/10.1016/j.jhydrol.2019.124084

Ahmed, I., Nazzal, Y., Zaidi, F. K., Al-Arifi, N. S. N., Ghrefat, H., & Naeem, M. (2015). Hydrogeological vulnerability and pollution risk mapping of the Saq and overlying aquifers using the DRASTIC model and GIS techniques, NW Saudi Arabia. *Environmental Earth Sciences*, *74*(2), 1303–1318. https://doi.org/10.1007/s12665-015-4120-5

Akakuru, O. C., Akaolisa, C. C. Z., Aigbadon, G. O., Eyankware, M. O., Opara, A. I., Obasi, P. N., Ofoh, I. J., Njoku, A. O., & Akudinobi, B. E. B. (2023). Integrating machine learning and multi-linear regression modeling approaches in groundwater quality assessment around Obosi, SE Nigeria. *Environment, Development and Sustainability*,

25(12), 14567–14606. https://doi.org/10.1007/s10668-022-02679-8

Akinwumiju, A. S., & Olorunfemi, M. O. (2019). Development of a conceptual groundwater model for a complex basement aquifer system: The case OF OSUN drainage basin in southwestern Nigeria. *Journal of African Earth Sciences*, *159*. https://doi.org/10.1016/j.jafrearsci.2019.103574

Al-Adamat, R. A. N., Foster, I. D. L., & Baban, S. M. J. (2003). Groundwater vulnerability and risk mapping for the Basaltic aquifer of the Azraq basin of Jordan using GIS, Remote sensing and DRASTIC. *Applied Geography*, *23*(4), 303–324. https://doi.org/10.1016/j.apgeog.2003.08.007

Alam, F., Umar, R., Ahmed, S., & Dar, F. A. (2014). A new model (DRASTIC-LU) for evaluating groundwater vulnerability in parts of central Ganga Plain, India. *Arabian Journal of Geosciences*, *7*(3), 927–937. https://doi.org/10.1007/s12517-012-0796-y

Albuquerque, M. T. D., Sanz, G., Oliveira, S. F., Martínez-Alegría, R., & Antunes, I. M. H. R. (2013). Spatio-Temporal Groundwater Vulnerability Assessment - A Coupled Remote Sensing and GIS Approach for Historical Land Cover econstruction. *Water Resources Management*, *27*(13), 4509–4526. https://doi.org/10.1007/s11269-013-0422-0

Aller, L., Bennett, T., Lehr, J. H., Petty, R. J., & Hackett, G. (1987). *DRASTIC: A standardized method for evaluating ground water pollution potential using hydrogeologic settings* (EPA/600/2-87/035). U.S. Environmental Protection Agency.

Almasri, M. N. (2008). Assessment of intrinsic vulnerability to contamination for Gaza coastal aquifer, Palestine. *Journal of Environmental Management*, *88*(4), 577–593. https://doi.org/10.1016/j.jenvman.2007.01.022

Almasri, M. N., & Kaluarachchi, J. J. (2004). Assessment and management of long-term nitrate pollution of ground water in agriculture-dominated watersheds. *Journal of Hydrology*, *295*(1–4), 225–245. https://doi.org/10.1016/j.jhydrol.2004.03.013

Almasri, M. N., & Kaluarachchi, J. J. (2007). Modeling nitrate contamination of groundwater in agricultural watersheds. *Journal of Hydrology*, *343*(3–4), 211–229. https://doi.org/10.1016/j.jhydrol.2007.06.016

Amaranto, A., Munoz-Arriola, F., Solomatine, D. P., & Corzo, G. (2019). A Spatially Enhanced Data-Driven Multimodel to Improve Semiseasonal Groundwater Forecasts in the High Plains Aquifer, USA. *Water Resources Research*, *55*(7), 5941–5961. https://doi.org/10.1029/2018WR024301

American Public Health Association. (2017). *Standard Methods for examination of water and wastewater (23rd ed.)*. American Public Health Association, American Water Works Association, Water Environment Federation, Washington, DC.

Amiri, V., Nakhaei, M., Lak, R., & Kholghi, M. (2016). Investigating the salinization and freshening processes of coastal groundwater resources in Urmia aquifer, NW Iran. *Environmental Monitoring and Assessment*, *188*(4), 233. https://doi.org/10.1007/s10661-016-5231-5

Andreo, B., Goldscheider, N., Vadillo, I., Vías, J. M., Neukum, C., Sinreich, M., Jimenez P., Brechenmacher J., Carrasco F., Hotzl H., Perles M.J., & Zwahlen, F. (2006). Karst groundwater protection: First application of a Pan-European Approach to vulnerability, hazard and risk mapping in the Sierra de Líbar (Southern Spain). *Science of the Total Environment*, *357*(1–3), 54–73. https://doi.org/10.1016/j.scitotenv.2005.05.019

Andreo, B., Ravbar, N., & Vías, J. M. (2009). Source vulnerability mapping in carbonate (karst) aquifers by extension of the COP method: Application to pilot sites. *Hydrogeology Journal*, *17*(3), 749–758. https://doi.org/10.1007/s10040-008-0391-1

Ansari, Md. A., Deodhar, A., & Kumar, U. S. (2019). Modeling of geochemical processes and multivariate statistical analysis for hydrochemical assessment of spring water of the Outer Himalaya, India. *Environmental Earth Sciences*, *78*(24), 665. https://doi.org/10.1007/s12665-019-8682-5

Antonakos, A. K., & Lambrakis, N. J. (2007). Development and testing of three hybrid methods for the assessment of aquifer vulnerability to nitrates, based on the drastic model, an example from NE Korinthia, Greece. *Journal of Hydrology*, *333*(2–4), 288–304. https://doi.org/10.1016/j.jhydrol.2006.08.014

Aravinthasamy, P., Karunanidhi, D., Subba Rao, N., Subramani, T., & Srinivasamoorthy, K. (2020). Irrigation risk assessment of groundwater in a non-perennial river basin of South India: implication from irrigation water quality index (IWQI) and geographical information system (GIS) approaches. *Arabian Journal of Geosciences*, *13*(21). https://doi.org/10.1007/s12517-020-06103-1

Ashraf, A., & Ahmad, Z. (2012). Integration of groundwater flow modeling and GIS. In *Water resources management and modeling*. InTech. https://doi.org/10.5772/34257

Awasthi, A., Rana, S., Thakur, A., Thakur, S. K., & Jaswal, D. (2025). *Groundwater quality and health risk assessment in the Baddi–Barotiwala–Nalagarh industrial belt of the northwestern Himalayas*. *Scientific Reports, 16*(1), 3388. https://doi.org/10.1038/s41598-025-33393-w

Ayers, R. S., & Westcot, D. W. (1985). *Water quality for agriculture* (FAO Irrigation and Drainage Paper No. 29). Food and Agriculture Organization of the United Nations.

Babiker, I. S., Mohamed, M. A. A., Hiyama, T., & Kato, K. (2005). A GIS-based DRASTIC model for assessing aquifer vulnerability in Kakamigahara Heights, Gifu Prefecture, central Japan. *Science of the Total Environment*, *345*(1–3), 127–140. https://doi.org/10.1016/j.scitotenv.2004.11.005

Barrocu, G., Muzzu, M., & Uras, G. (2007). Hydrogeology and vulnerability map (Epik method) of the "Supramonte" karstic system, north-central Sardinia. *Environmental Geology*, *51*(5), 701-706. https://doi.org/10.1007/s00254-006-0382-2

Batarseh, M., Imreizeeq, E., Tilev, S., Al Alaween, M., Suleiman, W., Al Remeithi, A. M., Al Tamimi, M. K., & Al Alawneh, M. (2021). Assessment of groundwater quality for

irrigation in the arid regions using irrigation water quality index (IWQI) and GIS-Zoning maps: Case study from Abu Dhabi Emirate, UAE. *Groundwater for Sustainable Development*, *14*. https://doi.org/10.1016/j.gsd.2021.100611

Bauder, T. A., Waskom, R. M., Sutherland, P. L., Davis, J. G., Follett, R. H., & Soltanpour, P. N. (2011). *Irrigation water quality criteria* (Service in Action No. 0.506). Colorado State University Extension.

Bear, J. (1979). *Hydraulics of groundwater*. McGraw-Hill.

Ben Brahim, F., Msaddki, H., & Bouri, S. (2022). Groundwater Quality Index Mapping for Irrigation Purposes in the El Hezma-El Hmila Aquifer (Medenine, Tunisia). *Clean - Soil, Air, Water*, *50*(9). https://doi.org/10.1002/clen.202100203

Bester, M. L., Frind, E. O., Molson, J. W., & Rudolph, D. L. (2006). Numerical investigation of road salt impact on an urban wellfield. *Ground Water*, *44*(2), 165–175. https://doi.org/10.1111/j.1745-6584.2005.00126.x

Bhatt, G., Kumar, M., & Duffy, C. J. (2014). A tightly coupled GIS and distributed hydrologic modeling framework. *Environmental Modelling and Software*, *62*, 70–84. https://doi.org/10.1016/j.envsoft.2014.08.003

Bhavya, R., Sivaraj, K., & Elango, L. (2023). Ant Colony Based Artificial Neural Network for Predicting Spatial and Temporal Variation in Groundwater Quality. *Water (Switzerland)*, *15*(12). https://doi.org/10.3390/w15122222

Birkinshaw, S. J., & Ewen, J. (2000). Nitrogen transformation component for SHETRAN catchment nitrate transport modelling. *Journal of Hydrology*, *230*(1–2), 1–17. https://doi.org/10.1016/S0022-1694(00)00174-8

Bobba, A. G. (2012). Ground Water-Surface Water Interface (GWSWI) Modeling: Recent Advances and Future Challenges. *Water Resources Management*. Kluwer Academic Publishers. https://doi.org/10.1007/s11269-012-0134-x

Boughriba, M., Barkaoui, A. E., Zarhloule, Y., Lahmer, Z., El Houadi, B., & Verdoya, M. ‘(2010). Groundwater vulnerability and risk mapping of the Angad transboundary aquifer using DRASTIC index method in GIS environment. *Arabian Journal of Geosciences*, *3*(2), 207–220. https://doi.org/10.1007/s12517-009-0072-y

Brimicombe, A. (2009). *GIS, Environmental Modeling and Engineering*. CRC Press. https://doi.org/10.1201/9781439808726

Brindha, K., & Elango, L. (2014). Soil and groundwater quality with reference to nitrate in a semiarid agricultural region. *Arabian Journal of Geosciences*, *7*(11), 4683–4695. https://doi.org/10.1007/s12517-013-1100-5

Brown, R. M., McClelland, N. I., Deininger, R. A., & Tozer, R. G. (1970). *A water quality index—Do we dare? Water & Sewage Works, 117*(10), 339–343.

Bureau of Indian Standards. (2012). *IS 10500:2012 drinking water specification*. Government

of India.

Burger, H., & Schafmeister, M.T. (2000). Gerichtete Interpolation zur verbesserten Darstellung strömungsabhängiger Grundwasserbeschaffenheitsmerkmale. [Directed interpolation for improved representation of flow-dependent groundwater properties]. [In German.] *Grundwasser*, *5*(2), 79–85. https://doi.org/10.1007/s767-000-8350-9

Carey, M. A., & Lloyd, J. W. (1985). Modelling non-point sources of nitrate pollution of groundwater in the Great Ouse Chalk, U.K. *Journal of Hydrology*, *78*(1–2), 83–106. https://doi.org/10.1016/0022-1694(85)90155-6

Carsel, R. F., Mulkey, L. A., Lorber, M. N., & Baskin, L. B. (1985). The Pesticide Root Zone Model (PRZM): A procedure for evaluating pesticide leaching threats to groundwater. *Ecological Modelling*, *30*(1–2), 49–69. https://doi.org/10.1016/0304-3800(85)90036-5

Central Ground Water Board. (2013). *Ground water information booklet: Ludhiana district, Punjab*. Ministry of Water Resources, Government of India.

Central Ground Water Board. (2014). *Water quality issues and challenges in Punjab*. Ministry of Water Resources, Government of India.

Central Ground Water Board. (2017). *Aquifer mapping and management plan: Ludhiana district, Punjab*. Ministry of Water Resources, River Development and Ganga Rejuvenation, Government of India.

Central Ground Water Board. (2018). *Ground water quality in shallow aquifers of India*. Ministry of Water Resources, River Development and Ganga Rejuvenation, Government of India.

Central Ground Water Board. (2021). *Ground water year book: Punjab and Chandigarh 2020–2021*. Ministry of Jal Shakti, Government of India.

Chachadi, A. G., & Lobo-Ferreira, J. P. (2001). *Sea water intrusion vulnerability mapping of aquifers using GALDIT method*. In *Proceedings of the Workshop on Modelling in Hydrogeology* (pp. 143–156). Anna University.

Chandio, A. S., Lee, T. S., & Mirjat, M. S. (2012). The extent of waterlogging in the lower Indus Basin (Pakistan)-A modeling study of groundwater levels. *Journal of Hydrology*, *426–427*, 103–111. https://doi.org/10.1016/j.jhydrol.2012.01.017

Chawla, A., & Singh, S. K. (2014). Modelling of contaminant transport from landfills. *International Journal of Engineering Science and Innovative Technology*, *3*(5), 222-227.

Chenini, I., & Ben Mammou, A. (2010). Groundwater recharge study in arid region: An approach using GIS techniques and numerical modelling. *Computers and Geosciences*, *36*(6), 801–817. https://doi.org/10.1016/j.cageo.2009.06.014

Chitrakshi, & Haritash, A. K. (2018). Hydrogeochemical characterization and suitability appraisal of groundwater around stone quarries in Mahendragarh, India.

Environmental Earth Sciences, *77*(6), 252. https://doi.org/10.1007/s12665-018-7431-5

Chitrakshi, & Haritash, A. K. (2022). *Appraisal of hydrochemistry and suitability assessment for water in an agriculture-dominated aquatic ecosystem of Rajasthan, India*. *Rendiconti Lincei. Scienze Fisiche e Naturali, 33*, 851–866. https://doi.org/10.1007/s12210-022-01107-3

Civita, M. (1990). *Legenda unificata per le carte della vulnerabilità dei corpi idrici sotterranei* (Studi sulla vulnerabilità degli acquiferi, 1). Pitagora Editrice.

Civita, M. (1994). *La carta della vulnerabilità degli acquiferi all'inquinamento: Teoria e pratica* (Studi sulla vulnerabilità degli acquiferi). Pitagora Editrice.

Civita, M., & De Maio, M. (1997). *SINTACS: Un sistema parametrico per la valutazione e la cartografia della vulnerabilità degli acquiferi all'inquinamento. Metodologia e automatizzazione*. Pitagora Editrice.

Civita, M., & De Regibus, C. (1995). *Sperimentazione di alcune metodologie per la valutazione della vulnerabilità degli acquiferi*. *Quaderni di Geologia Applicata, 3*, 63–71.

Civita, M. (1993). Groundwater vulnerability maps: a review. In *Proc., IX symposium on pesticide chemistry- Mobility and degradation of xenobiotics*, 587–631, Piacenza.

Clark, I. (2015). *Groundwater geochemistry and isotopes*. CRC Press. https://doi.org/10.1201/b18347

Colombo, L., Alberti, L., Mazzon, P., & Formentin, G. (2019). Transient flow and transport modelling of an historical CHC source in North-West Milano. *Water (Switzerland)*, *11*(9). https://doi.org/10.3390/w11091745

Comrey, A. L., & Lee, H. B. (2021). Interpretation and Application of Factor Analytic Results. In *A First Course in Factor Analysis* (pp. 252–274). Psychology Press. https://doi.org/10.4324/9781315827506-16

Daly, D., Dassargues, A., Drew, D., Dunne, S., Goldscheider, N., Neale, S., Popescu I., & Zwahlen, F. (2002). Main concepts of the "European approach" to karst-groundwater-vulnerability assessment and mapping. *Hydrogeology Journal*, *10*(2), 340–345. https://doi.org/10.1007/s10040-001-0185-1

Dar, I. A., Sankar, K., Shah, T. S., and Dar, M. A. (2012). Assessment of nitrate contamination of Lidder catchment Kashmir, India. *Arabian Journal of Geosciences*, *5*(2), 233–243. https://doi.org/10.1007/s12517-010-0171-9

Darwish, M. A. G. (2011). Geochemical reconnaissance survey and environmental assessment for stream sediments of Wadi Um Gier, Southeastern Desert, Egypt. *Environmental Earth Sciences*, *62*(3), 657–672. https://doi.org/10.1007/s12665-010-0555-x

Dash, C.J., Sarangi, A. & Singh, D.K. (2012). Spatial and Temporal Variation of Nitrate-N in Groundwater at IARI Farm. *Indian Society of Agricultural Engineers*, 49, p.50.

Davis, A. D., Long, A. J., & Wireman, M. (2002). KARSTIC: A sensitivity method for carbonate aquifers in karst terrain. *Environmental Geology*, *42*(1), 65–72. https://doi.org/10.1007/s00254-002-0531-1

Davis, L. E. (1945). Simple kinetic theory of ionic exchange for ions of unequal charge. *Journal of Physical Chemistry*, *49*(5), 473–479. https://doi.org/10.1021/j150443a009

De Ridder, N. A., & Erez, A. (1977). *Optimum use of water resources* (No. 21). International Institute for Land Reclamation and Improvement.

Debernardi, L., De Luca, D. A., & Lasagna, M. (2008). Correlation between nitrate concentration in groundwater and parameters affecting aquifer intrinsic vulnerability. *Environmental Geology*, *55*(3), 539–558. https://doi.org/10.1007/s00254-007-1006-1

Deckmyn, J., Paniconi, C., Giacomelli, A., & Kleinfeldt, S. (1997). A modular approach to integrated environmental modeling systems incorporating GIS and visualization functionality. In *Proc., International Workshop on New Developments in Geographic Information Systems,* 85-95. Ann Arbor, MI, ERIM International.

Demirel, Y. (2014). *Nonequilibrium thermodynamics: Transport and rate processes in physical, chemical and biological systems*. Third Edition. Elsevier B.V. https://doi.org/10.1016/C2012-0-00459-0

Dennehy, K. F., Reilly, T. E., & Cunningham, W. L. (2015). Groundwater availability in the United States: the value of quantitative regional assessments. *Hydrogeology Journal*, *23*(8), 1629–1632. https://doi.org/10.1007/s10040-015-1307-5

Denny, S. C., Allen, D. M., & Journeay, J. M. (2007). DRASTIC-Fm: A modified vulnerability mapping method for structurally controlled aquifers in the southern Gulf Islands, British Columbia, Canada. *Hydrogeology Journal*, *15*(3), 483–493. https://doi.org/10.1007/s10040-006-0102-8

Dey, S., Raju, N. J., Gossel, W., & Mall, R. K. (2023). Hydrogeochemical characterization and geochemical modeling for the evaluation of groundwater quality and health risk assessment in the Varuna River basin, India. *Environmental Geochemistry and Health*, *45*(7), 4679–4702. https://doi.org/10.1007/s10653-023-01521-y

Dhillon, M. S., Kaur, S., & Aggarwal, R. (2019). *Delineation of critical regions for mitigation of carbon emissions due to groundwater pumping in central Punjab*. *Groundwater for Sustainable Development, 8*, 302–308. https://doi.org/10.1016/j.gsd.2019.02.004

Di Luzio, M., Srinivasan, R., Arnold, J. G., & Neitsch, S. L. (2002). *ArcView interface for SWAT2000: user's guide.* TWRI Report No. TR-193, Texas Water Resources Institute, Texas.

Diepenbroek, M., Grobe, H., Reinke, M., Schindler, U., Schlitzer, R., Sieger, R., & Wefer, G. (2002). PANGAEA - an information system for environmental sciences. *Computers and Geosciences*, *28*(10), 1201–1210. https://doi.org/10.1016/S0098-3004(02)00039-0

Directorate of census operations. (2011). *District census handbook Ludhiana: Village and town directory (Part XII-A, Series 04)*. Government of Punjab.

District administration Ludhiana. (2021). *District environment plan Ludhiana*. Government of Punjab.

Doerfliger, N. (1996). Advances in karst groundwater protection strategy using artificial tracer tests analysis and multi-attribute vulnerability mapping (EPIK method). (PhD thesis), Faculty of Sciences, Neuchâtel University.

Doerfliger, N., & Zwahlen, F. (1995). EPIK: a new method for outlining of protection areas in karst environment. In: Günay G, Johnson I (eds) *Proc., 5th International symposium and field seminar on karst waters and environmental impacts*. 117–123. Antalya, Sep 1995, Balkema, Rotterdam.

Doerfliger, N., & Zwahlen, F. (1998). *Practical Guide, Groundwater Vulnerability Mapping in Karstic Regions (EPIK): Applications to Groundwater Protection Zones*. Swiss Agency for the Environment, Forests and Landscape SAEFL. Bern, Switzerland.

Doerfliger, N., Jeannin, P. Y., & Zwahlen, F. (1999). Water vulnerability assessment in karst environments: A new method of defining protection areas using a multi-attribute approach and GIS tools (EPIK method). *Environmental Geology*, *39*(2), 165–176. https://doi.org/10.1007/s002540050446

Domenico, P. A., Schwartz, F. W. (1990). *Physical and chemical hydrogeology*. Wiley, New York.

Doneen, L. D. (1964). Notes on water quality in agriculture. *Water science and engineering, 4001.* Department of Water Sciences and Engineering, University of California.

Dong, W., Lin, X., Du, S., Zhang, Y., & Cui, L. (2015). Risk assessment of organic contamination in shallow groundwater around a leaching landfill site in Kaifeng, China. *Environmental Earth Sciences*, *74*(3), 2749–2756. https://doi.org/10.1007/s12665-015-4669-z

Dörfliger, N., & Plagnes, V. (2009). Cartographie de la vulnérabilité des aquifères karstiques guide méthodologique de la méthode PaPRIKa. [Mapping the vulnerability of karst aquifers. Guidelines of the method PAPRIKa]. Rapport BRGM RP-57527-FR, BRGM, Orleans, France.

Douglas, S. H., Dixon, B., & Griffin, D. (2018). Assessing the abilities of intrinsic and specific vulnerability models to indicate groundwater vulnerability to groups of similar pesticides: a comparative study. *Physical Geography*, *39*(6), 487–505. https://doi.org/10.1080/02723646.2017.1406300

Drever, J.I. (1997). *The Geochemistry of Natural Water: Surface and Groundwater Environments* (3rd ed.). Prentice Hall.

Duan, R., Li, P., Wang, L., He, X., & Zhang, L. (2022). Hydrochemical characteristics, hydrochemical processes and recharge sources of the geothermal systems in Lanzhou City, northwestern China. *Urban Climate*, *43*, 101152.

https://doi.org/10.1016/j.uclim.2022.101152

Eaton, F. M. (1950). Significance of carbonates in irrigation waters. *Soil Science,* 69, 123-133.

El Khattabi, J., Louche, B., Darwishe, H., Chaaban, F., & Carlier, E. (2018). Impact of Fertilizer Application and Agricultural Crops on the Quality of Groundwater in the Alluvial Aquifer, Northern France. *Water, Air, and Soil Pollution*, *229*(4). https://doi.org/10.1007/s11270-018-3767-4

Elumalai, V., Rajmohan, N., Sithole, B., Li, P., Uthandi, S., & Tol, J.V. (2023). Geochemical evolution and the processes controlling groundwater chemistry using ionic ratios, geochemical modelling and chemometric analysis in uMhlathuze catchment, KwaZulu-Natal, South Africa. *Chemosphere, 312*(1), 137179. https://doi.org/10.1016/j.chemosphere.2022.137179

Engel, B. A., Srinivasan, R., & Rewerts, C. (1993). A spatial decision support system for modeling and managing agricultural non-point-source pollution. In *M. F. Goodchild, B. O. Parks, & L. T. Steyaert (Eds.), Environmental modeling with GIS* (pp. 231–237). Oxford University Press.

Engelen, G. B., & Jones, G. P. (1986). *Developments in the Analysis of Groundwater Flow Systems*. https://doi.org/10.1016/s0140-1963(18)31013-9

Engelen, G.B., & Kloosterman, F.H. (1996). *Hydrological system analysis: methods and application*. Kluwer Academic Publishers.

Entezari, M., Yamani, M., & Jafari Aghdam, M. (2016). Evaluation of intrinsic vulnerability, hazard and risk mapping for karst aquifers, Khorein aquifer, Kermanshah province: a case study. *Environmental Earth Sciences*, *75*(5), 1–10. https://doi.org/10.1007/s12665-016-5258-5

Evans, B. M., & Myers, W. L. (1990). A GIS-based approach to evaluating regional groundwater pollution potential with DRASTIC. *Journal of Soil and Water Conservation*, *45*(2), 242-245.

Farzana, F., Roy, T. K., Hossain, S. A., Mazrin, M., Islam, M. S., Mahiddin, N. A., & Idris, A. M. (2025). *Assessment of groundwater quality and potential health risks related to heavy metals in a peri-urban area of a developing country*. *Scientific Reports, 15*, 27970. https://doi.org/10.1038/s41598-025-13651-7

Food and Agriculture Organization of the United Nations (FAO). (2003). *Review of world water resources by country* (Water Reports No. 23). FAO.

Foster, S. (1987). Fundamental concepts in aquifer vulnerability, pollution risk and protection strategy. In *Vulnerability of soil and groundwater to pollutants* (Vol. 38, pp. 69–86).

Freeze, R.A., (1971). Three-dimensional, transient, saturated-unsaturated flow in a groundwater basin. *Water Resources Research, 7*(2), 347-366.

Freeze, R.A., & Witherspoon, P.A. (1966). Theoretical analysis of regional groundwater flow: 1. Analytical and numerical solutions to the mathematical model. *Water Resources Research, 2*(4), 641-656.

Freeze, R.A., & Witherspoon, P.A. (1967). Theoretical analysis of regional groundwater flow: 2. Effect of water table configuration and subsurface permeability variation. *Water Resources Research, 3*(2), 623-634.

Freeze, R.A., & Witherspoon, P. A. (1968). Theoretical analysis of regional groundwater flow: 3. Quantitative interpretations. *Water Resources Research, 4*(3), 581-590.

Frind, E. O., Molson, J. W., & Rudolph, D. L. (2006). Well vulnerability: A quantitative approach for source water protection. *Ground Water*. https://doi.org/10.1111/j.1745-6584.2006.00230.x

Fritch, T. G., McKnight, C. L., Yelderman, J. C., & Arnold, J. G. (2000). An aquifer vulnerability assessment of the paluxy aquifer, central Texas, USA, using GIS and a modified DRASTIC approach. *Environmental Management*, *25*(3), 337–345. https://doi.org/10.1007/s002679910026

Gao, C., Guo, X., Shao, S., & Wu, J. (2020). Using MODFLOW/MT3DMS and electrical resistivity tomography to characterize organic pollutant migration in clay soil layer with a shallow water table. *Environmental Technology (United Kingdom)*, *24* (28), 4490-4499. https://doi.org/10.1080/09593330.2020.1767699

Gao, Y., Chen, J., Qian, H., Wang, H., Ren, W., & Qu, W. (2022). *Hydrogeochemical characteristics and processes of groundwater in an over 2260 year irrigation district: A comparison between irrigated and non-irrigated areas*. *Journal of Hydrology, 606*, 127437. https://doi.org/10.1016/j.jhydrol.2022.127437

Gapon, E. N. (1933). On the theory of exchange adsorption in soils. *Journal of General Chemistry. USSR*, *3*(3), 144-163.

Garg, S., & Singh, S. K. (2016). Modeling of arsenic transport in groundwater using MODFLOW: A case study. *International Journal of Geomatics and Geosciences, 7*(1), 56-81.

Ghazavi, R., & Ebrahimi, Z. (2015). Assessing groundwater vulnerability to contamination in an arid environment using DRASTIC and GOD models. *International Journal of Environmental Science and Technology*, *12*(9), 2909–2918. https://doi.org/10.1007/s13762-015-0813-2

Ghosh, A., & Bera, B. (2023). Hydrogeochemical assessment of groundwater quality for drinking and irrigation applying groundwater quality index (GWQI) and irrigation water quality index (IWQI). *Groundwater for Sustainable Development*, *22*. https://doi.org/10.1016/j.gsd.2023.100958

Gibbs, R. J. (1970). Mechanisms controlling world water chemistry. *Science*, *170*(3962), 1088–1090. https://doi.org/10.1126/science.170.3962.1088

Gilvear, D. J., Andrews, R., Tellam, J. H., Lloyd, J. W., & Lerner, D. N. (1993). Quantification of the water balance and hydrogeological processes in the vicinity of a small groundwater-fed wetland, East Anglia, UK. *Journal of Hydrology*, *144*(1–4), 311–334. https://doi.org/10.1016/0022-1694(93)90178-C

Gogu, R. C., & Dassargues, A. (2000a). Current trends and future challenges in groundwater vulnerability assessment using overlay and index methods. *Environmental Geology*, *39*(6), 549–559. https://doi.org/10.1007/s002540050466

Gogu, R. C., & Dassargues, A. (2000b). Sensitivity analysis for the EPIK method of vulnerability assessment in a small karstic aquifer, southern Belgium. *Hydrogeology Journal*, *8*(3), 337–345. https://doi.org/10.1007/s100400050019

Gogu, R. C., Hallet, V., & Dassargues, A. (2003). Comparison of aquifer vulnerability assessment techniques. Application to the Néblon river basin (Belgium). *Environmental Geology*, *44*(8), 881–892. https://doi.org/10.1007/s00254-003-0842-x

Goldscheider, N. (2005). Karst groundwater vulnerability mapping: Application of a new method in the Swabian Alb, Germany. *Hydrogeology Journal*, *13*(4), 555–564. https://doi.org/10.1007/s10040-003-0291-3

Goldscheider, N., Klute, M., Sturm, S., & Hötzl, H. (2000). *The PI method – a GIS-based approach to mapping groundwater vulnerability with special consideration of karst aquifers*. *Zeitschrift für Angewandte Geologie, 46*(3), 157–166.

Gong, G., Mattevada, S., & O'Bryant, S. E. (2014). Comparison of the accuracy of kriging and IDW interpolations in estimating groundwater arsenic concentrations in Texas. *Environmental Research*, *130*, 59–69. https://doi.org/10.1016/j.envres.2013.12.005

Gong, M., Li, P., & Kong, J. (2025). Estimation of Groundwater Recharge and Assessment of Groundwater Quality in the Weining Plain, China. *Water*, *17*(5), 704. https://doi.org/10.3390/w17050704

Goodchild, M., Haining, R., & Wise, S. (1992). Integrating GIS and spatial data analysis: Problems and possibilities. *International Journal of Geographical Information Systems*, *6*(5), 407–423. https://doi.org/10.1080/02693799208901923

Goode, D. J., & Konikow, L. F. (1989). *Modification of a method-of-characteristics solute-transport model to incorporate decay and equilibrium-controlled sorption or ion exchange* (U.S. Geological Survey Water-Resources Investigations Report 89-4030). U.S. Geological Survey. https://doi.org/10.3133/wri894030

Göppert, N., & Goldscheider, N. (2008). Solute and colloid transport in karst conduits under low- and high-flow conditions. *Ground Water*, *46*(1), 61–68. https://doi.org/10.1111/j.1745-6584.2007.00373.x

Ground Water Resource Estimation Committee. (2017). *Report of the Ground Water Resource Estimation Committee: GEC 2015*. Ministry of Water Resources, River Development & Ganga Rejuvenation, Government of India.

Guo, Q., Wang, Y., Gao, X., & Ma, T. (2007). A new model (DRARCH) for assessing groundwater vulnerability to arsenic contamination at basin scale: A case study in Taiyuan basin, northern China. *Environmental Geology*, *52*(5), 923–932. https://doi.org/10.1007/s00254-006-0534-4

Gupta, D., Chaudhary, S., Singh, A., Shukla, R., & Mishra, V. K. (2023). Hydrochemical assessment of groundwater quality in the Narmada River Basin (Central India). *Water Supply*, *23*(2), 459–481. https://doi.org/10.2166/ws.2022.409

Gurunadha Rao, V. V. S., & Gupta, S. K. (2000). Mass transport modelling to assess contamination of a water supply well in Sabarmati river bed aquifer, Ahmedabad City, India. *Environmental Geology*, *39*(8), 893–900. https://doi.org/10.1007/s002549900037

Gusyev, M. A., Abrams, D., Toews, M. W., Morgenstern, U., & Stewart, M. K. (2014). A comparison of particle-tracking and solute transport methods for simulation of tritium concentrations and groundwater transit times in river water. *Hydrology and Earth System Sciences*, *18*(8), 3109–3119. https://doi.org/10.5194/hess-18-3109-2014

Gusyev, M. A., Toews, M., Morgenstern, U., Stewart, M., White, P., Daughney, C., & Hadfield, J. (2013). Calibration of a transient transport model to tritium data in streams and simulation of groundwater ages in the western Lake Taupo catchment, New Zealand. *Hydrology and Earth System Sciences*, *17*(3), 1217–1227. https://doi.org/10.5194/hess-17-1217-2013

Hamdan, I., Margane, A., Ptak, T., Wiegand, B., & Sauter, M. (2016). Groundwater vulnerability assessment for the karst aquifer of Tanour and Rasoun springs catchment area (NW-Jordan) using COP and EPIK intrinsic method. *Environmental Earth Sciences*, *75*(23). https://doi.org/10.1007/s12665-016-6281-2

Hamma, B., Alodah, A., Bouaicha, F., Bekkouche, M. F., Barkat, A., & Hussein, E. E. (2024). Hydrochemical assessment of groundwater using multivariate statistical methods and water quality indices (WQIs). *Applied Water Science*, *14*(2), 33. https://doi.org/10.1007/s13201-023-02084-0

Harbaugh, A.W., (2005). *MODFLOW-2005, the U.S. Geological Survey's Modular Ground Water Flow Model-The Groundwater Flow Process. Techniques and Methods.* 6-A16. U.S. Geological Survey, Reston,Virginia.

Harbaugh, A.W., Banta, E.R., Hill, M.C., & McDonald, M.G. (2000). *The U.S. Geological Survey's Modular Ground Water Flow Model- User Guide to Modularization Concepts and the Ground Water Flow Process.* U.S. Geological Survey. Open-File Report 00-92.

Hardie, L.A. (1978). Anhydrite and gypsum. In G.V. Middleton, M.J. Church, M. Coniglio & F.J. Longstaffe (Eds.), *Encyclopedia of Sediments and Sedimentary Rocks.* Springer. https://doi.org/10.1007/978-1-4020-3609-5_7

Haritash, A. K., Mathur, K., Singh, P., & Singh, S. K. (2017). Hydrochemical characterization and suitability assessment of groundwater in Baga–Calangute stretch of Goa, India. *Environmental Earth Sciences*, *76*(9). https://doi.org/10.1007/s12665-017-6679-5

Harou, J. J., Pulido-Velazquez, M., Rosenberg, D. E., Medellín-Azuara, J., Lund, J. R., & Howitt, R. E. (2009). Hydro-economic models: Concepts, design, applications, and future prospects. *Journal of Hydrology*. https://doi.org/10.1016/j.jhydrol.2009.06.037

He, S., Li, P., Su, F., Wang, D., & Ren, X. (2022). Identification and apportionment of shallow groundwater nitrate pollution in Weining Plain, northwest China, using hydrochemical indices, nitrate stable isotopes, and the new Bayesian stable isotope mixing model (MixSIAR). *Environmental Pollution*, *298*, 118852. https://doi.org/10.1016/j.envpol.2022.118852

Hellweger, F. L., & Maidment, D. R. (1999). *Definition and connection of hydrologic elements using geographic data*. *Journal of Hydrologic Engineering, 4*(1), 10–18. https://doi.org/10.1061/(ASCE)1084-0699(1999)4:1(10)

Hem, J. D. (1985). Study and interpretation of the chemical characteristics of natural water. *US Geological Survey Water-Supply Paper*, *2254*.

Hernández-Espriú, A., Reyna-Gutiérrez, J. A., Sánchez-León, E., Cabral-Cano, E., Carrera-Hernández, J., Martínez-Santos, P.,and Colombo, D. (2014). The DRASTIC-Sg model: An extension to the DRASTIC approach for mapping groundwater vulnerability in aquifers subject to differential land subsidence, with application to Mexico City. *Hydrogeology Journal*, *22*(6), 1469–1485. https://doi.org/10.1007/s10040-014-1130-4

Hötling, B., Haertlé, T., Hohberger, K.H., Nachtigall, K.H., Villinger, E., Weinzierl, W. & Wrobel, J.P. (1995). Konzept zur Ermittlung der Schutzfunktion der Grundwasserueberdeckung. [Concept for the Determination of the Protective Effectiveness of the Cover above the Groundwater against Pollution]. [In German] *Geologisches Jahrbuch*, 63, 5-24.

Hou, G.C., & Zhang, M.S., (2008). *Exploration and Study of Groundwater in the Ordos Basin*. Geological Publishing House, Beijing.

Hounslow, A. W. (1995). *Water quality data: Analysis and interpretation*. CRC Press. https://doi.org/10.1201/9780203734117

Howard, K. W. F., & Maier, H. (2007). Road de-icing salt as a potential constraint on urban growth in the Greater Toronto Area, Canada. *Journal of Contaminant Hydrology*, *91*(1–2), 146–170. https://doi.org/10.1016/j.jconhyd.2006.10.005

Iqbal, M. A., Salam, M. A., Nur-E-Alam, M., Rubaida, N. J., Rahman, H., & Uddin, M. F. (2024). Monitoring groundwater vulnerability for sustainable water resource management: A DRASTIC-based comparative assessment in a newly township area of Bangladesh. *Groundwater for Sustainable Development*, *27*. https://doi.org/10.1016/j.gsd.2024.101373

Ismael, M., Mokhtar, A., Farooq, M., & Lü, X. (2021). Assessing drinking water quality based on physical, chemical and microbial parameters in the Red Sea State, Sudan using a combination of water quality index and artificial neural network model. *Groundwater for Sustainable Development*, *14*. https://doi.org/10.1016/j.gsd.2021.100612

Izbicki, J. A., Stamos, C. L., Nishikawa, T., & Martin, P. (2004). Comparison of ground-water flow model particle-tracking results and isotopic data in the Mojave River ground-water basin, southern California, USA. *Journal of Hydrology*, *292*(1–4), 30–47. https://doi.org/10.1016/j.jhydrol.2003.12.034

Jabeen, M., Ahmad, Z., & Ashraf, A. (2019). Monitoring regional groundwater flow and contaminant transport in Southern Punjab, Pakistan, using numerical modeling approach. *Arabian Journal of Geosciences*, *12*(18). https://doi.org/10.1007/s12517-019-4766-5

Jankowski, J., Acworth, R.I., & Shekarforoush, S. (1998). Reverse ion exchange in deeply weathered porphyritic dacite fractured aquifer system, Yass, New South Wales, Australia. In G.B. Arehart & J.R. Hulston (Eds.), *9th International Symposium on Water–Rock Interaction* (pp 243–246). A. A. Balkema, Rotterdam.

Janos, D., Molson, J., & Lefebvre, R. (2018). Regional groundwater flow dynamics and residence times in Chaudière-Appalaches, Québec, Canada: Insights from numerical simulations. *Canadian Water Resources Journal*, *43*(2), 214–239. https://doi.org/10.1080/07011784.2018.1437370

Jasechko, S., Perrone, D., Befus, K. M., Bayani Cardenas, M., Ferguson, G., Gleeson, T., Luijendijk, E., McDonnell, J., Taylor, R. G., Wada, Y., & Kirchner, J. W. (2017). Global aquifers dominated by fossil groundwaters but wells vulnerable to modern contamination. *Nature Geoscience,* *10*(6), 425–429. https://doi.org/10.1038/ngeo2943

Jeannin P.Y., & Grasso A.D. (1995). Recharge respective des volumes de roche peu perméable et des conduits karstiques, role de l'épikarst. *Bull Hydrogéol*, *14*, 95–111.

Jenifer, M. A., & Jha, M. K. (2018). Comparative evaluation of GIS-based models for mapping aquifer vulnerability in hard-rock terrains. *Environmental Earth Sciences*, *77*(19). https://doi.org/10.1007/s12665-018-7821-8

Jha, B. M., & Sinha, S. K. (2010). Towards better management of ground water resources in India. *Water and Energy International*, *67*(1), 2–18.

Jhamnani, B., & Singh, S. K. (2009). Chloride transport from landfills. *Journal of Institution of Public Health Engineers of India*, *2*.

Jiang, G., Guo, F., Polk, J. S., Kang, Z., & Wu, J. (2015). Delineating vulnerability of karst aquifers using hydrochemical tracers in Southwestern China. *Environmental Earth Sciences*, *74*(2), 1015–1027. https://doi.org/10.1007/s12665-014-3862-9

Jones, N. A., Hansen, J., Springer, A. E., Valle, C., & Tobin, B. W. (2019). Modeling intrinsic vulnerability of complex karst aquifers: modifying the COP method to account for sinkhole density and fault location. *Hydrogeology Journal*, *27*(8), 2857–2868. https://doi.org/10.1007/s10040-019-02056-2

Kanagaraj, G., Elango, L., Sridhar, S. G. D., & Gowrisankar, G. (2018). Hydrogeochemical processes and influence of seawater intrusion in coastal aquifers south of Chennai, Tamil Nadu, India. *Environmental Science and Pollution Research*, *25*(9), 8989–9011. https://doi.org/10.1007/s11356-017-0910-5

Kaur, S. (2013). *Modelling the impact of climate change on groundwater resources in central Punjab* [Doctoral dissertation, Punjab Agricultural University]. Krishikosh.

https://krishikosh.egranth.ac.in/handle/1/5810015826

Kavouri, K., Plagnes, V., Tremoulet, J., Dörfliger, N., Rejiba, F., & Marchet, P. (2011). PaPRIKa: A method for estimating karst resource and source vulnerability-application to the Ouysse karst system (southwest France). *Hydrogeology Journal*, *19*(2), 339–353. https://doi.org/10.1007/s10040-010-0688-8

Kazakis, N., (2013). Groundwater Pollution Risk Assessment in Anthemountas Basin. PhD Thesis, Department of Geology, Aristotle University of Thessaloniki (in Greek).

Kazakis, N., & Voudouris, K. (2011). Comparison of three applied methods of groundwater vulnerability mapping: A case study from the Florina basin, Northern Greece. In *Advances in the Research of Aquatic Environment* (pp. 359–367). Springer Berlin Heidelberg. https://doi.org/10.1007/978-3-642-24076-8_42

Kazakis, N., & Voudouris, K. S. (2015). Groundwater vulnerability and pollution risk assessment of porous aquifers to nitrate: Modifying the DRASTIC method using quantitative parameters. *Journal of Hydrology*, *525*, 13–25. https://doi.org/10.1016/j.jhydrol.2015.03.035

Kazakis, N., Oikonomidis, D., & Voudouris, K. S. (2015). Groundwater vulnerability and pollution risk assessment with disparate models in karstic, porous, and fissured rock aquifers using remote sensing techniques and GIS in Anthemountas basin, Greece. *Environmental Earth Sciences*, *74*(7), 6199–6209. https://doi.org/10.1007/s12665-015-4641-y

Khan, A., Khan, H. H., Umar, R., & Khan, M. H. (2014). An integrated approach for aquifer vulnerability mapping using GIS and rough sets: study from an alluvial aquifer in North India. *Hydrogeology Journal*, *22*(7), 1561–1572. https://doi.org/10.1007/s10040-014-1147-8

Kolm, K. E. (1996). Conceptualization and characterization of ground-water systems using Geographic Information Systems. In *Remote Sensing and GIS for Site Characterization: Applications and Standards*. ASTM International.

Konikow, L. F., Goode, D. J., & Hornberger, G. Z. (1996). *A three-dimensional method-of-characteristics solute-transport model (MOC3D)* (U.S. Geological Survey Water-Resources Investigations Report 96–4267). U.S. Geological Survey.

Kopp, S. M. (1996). *Linking GIS and hydrological models: Where we have been, where we are going?*. IAHS-AISH Publication, (235), 133–139.

Kouadri, S., Pande, C. B., Panneerselvam, B., Moharir, K. N., & Elbeltagi, A. (2022). Prediction of irrigation groundwater quality parameters using ANN, LSTM, and MLR models. *Environmental Science and Pollution Research*, *29*(14), 21067–21091. https://doi.org/10.1007/s11356-021-17084-3

Kouli, M., Lydakis-Simantiris, N., & Soupios, P. (2008). GIS-Based Aquifer Modeling and Planning Using Integrated Geoenvironmental and Chemical Approaches. In L. F. Konig & J. L. Weiss (Eds.). *Groundwater: Modeling, Management and Contamination, 125*, 86–99. Nova Science Publishers Inc (Verlag).

Koutsi, R., & Stournaras, G. (2011). Groundwater vulnerability assessment in the Loussi polje area, N Peloponessus: the PRESK method. In *Advances in the Research of Aquatic Environment,* 335–342. Springer Berlin Heidelberg. https://doi.org/10.1007/978-3-642-24076-8_39

Kresic, N., & Mikszewski, A. (2012). *Hydrogeological conceptual site models: data analysis and visualization*. CRC Press.

Kumar, P. J. S. (2014). Evolution of groundwater chemistry in and around Vaniyambadi Industrial Area: Differentiating the natural and anthropogenic sources of contamination. *Geochemistry*, *74*(4), 641–651. https://doi.org/10.1016/j.chemer.2014.02.002

Kumar, R., Mittal, S., Sahoo, P. K., & Sahoo, S. K. (2021). Source apportionment, chemometric pattern recognition and health risk assessment of groundwater from southwestern Punjab, India. *Environmental Geochemistry and Health*, *43*(2), 733–755. https://doi.org/10.1007/s10653-020-00518-1

Kumar, P. J. S., & Augustine, C. M. (2022). Entropy-weighted water quality index (EWQI) modeling of groundwater quality and spatial mapping in Uppar Odai Sub-Basin, South India. *Modeling Earth Systems and Environment*, *8*(1), 911–924. https://doi.org/10.1007/s40808-021-01132-5

Lahlou, M., Shoemaker, L., Choudhury, S., Elmer, R., & Hu, A. (1998). *Better assessment science integrating point and nonpoint sources (BASINS), version 2.0: User's manual* (EPA-823-B-98-006). U.S. Environmental Protection Agency, Office of Water.

Lapworth, D. J., Boving, T. B., Kreamer, D. K., Kebede, S., & Smedley, P. L. (2022). Groundwater quality: Global threats, opportunities and realising the potential of groundwater. *Science of the Total Environment*. Elsevier B.V. https://doi.org/10.1016/j.scitotenv.2021.152471

Lasserre, F., Razack, M., & Banton, O. (1999). A GIS-linked model for the assessment of nitrate contamination in groundwater. *Journal of Hydrology*, *224*(3–4), 81–90. https://doi.org/10.1016/S0022-1694(99)00130-4

Ledoux, E., Gomez, E., Monget, J.M., Viavattene, C., Viennot, P., Ducharne, A., Benoit, M., Mignolet, C., Schott, C., & Mary, B. (2007). Agriculture and groundwater nitrate contamination in the Seine basin. The STICS-MODCOU modelling chain. *Science of the Total Environment*, *375*(1–3), 33–47. https://doi.org/10.1016/j.scitotenv.2006.12.002

Lee, Y. W., Dahab, M. F., & Bogardi, I. (1992). Nitrate Risk Management under Uncertainty. *Journal of Water Resources Planning and Management*, *118*(2), 151–165. https://doi.org/10.1061/(asce)0733-9496(1992)118:2(151)

Leharne, S. (2019). Transfer phenomena and interactions of non-aqueous phase liquids in soil and groundwater. In *ChemTexts*, *5*(1). https://doi.org/10.1007/s40828-019-0079-2

Leon, L. F. (2009). MapWindow interface for SWAT (MWSWAT). In: *Soil and Water*

Assessment Tool (SWAT) Global Application. WASWAC Special Publ, 4.

Leonard, R. A., Knisel, W. G., & Still, D. A. (1987). GLEAMS: Groundwater loading effects of agricultural management systems. *Transactions of the American Society of Agricultural Engineers*, *30*(5), 1403–1418. https://doi.org/10.13031/2013.30578

Leong, L. Y., Hew, T. S., Ooi, K. B., & Wei, J. (2020). Predicting mobile wallet resistance: A two-staged structural equation modeling-artificial neural network approach. *International Journal of Information Management*, *51*. https://doi.org/10.1016/j.ijinfomgt.2019.102047

Leong, L. Y., Jaafar, N. I., & Ainin, S. (2018). Understanding facebook commerce (f-commerce) actual purchase from an artificial neural network perspective. *Journal of Electronic Commerce Research*, *19*(1), 75–103.

Leyland, R. C., Witthüser, K. T., & Van Rooy, J. L. (2008). *Vulnerability mapping in karst terrains, exemplified in the wider Cradle of Humankind World Heritage Site* (Research Report No. KV 208/08). South African Water Research Commission.

Li, P., Wu, J., & Qian, H. (2013). Assessment of groundwater quality for irrigation purposes and identification of hydrogeochemical evolution mechanisms in Pengyang County, China. *Environmental Earth Sciences*, *69*(7), 2211–2225. https://doi.org/10.1007/s12665-012-2049-5

Liggett, J. E., & Allen, D. M. (2011). Evaluating the sensitivity of DRASTIC using different data sources, interpretations and mapping approaches. *Environmental Earth Sciences*, *62*(8), 1577–1595. https://doi.org/10.1007/s12665-010-0642-z

Liu, L., Wu, J., He, S., & Wang, L. (2022a). Occurrence and distribution of groundwater fluoride and manganese in the Weining Plain (China) and their probabilistic health risk quantification. *Exposure and Health*, *14*(2), 263-279. https://doi.org/10.1007/s12403-021-00434-4

Liu, C., Hou, Q., Chen, Y., & Huang, G. (2022b). Hydrogeochemical Characteristics and Groundwater Quality in a Coastal Urbanized Area, South China: Impact of Land Use. *Water (Switzerland)*, *14*(24). https://doi.org/10.3390/w14244131

Loewen, S., & Gonulal, T. (2015). Exploratory factor analysis and principal components analysis. In *Advancing Quantitative Methods in Second Language Research* (182–212). Taylor and Francis. https://doi.org/10.4324/9781315870908-9

Lyu, S., Chen, W., Wen, X., & Chang, A. C. (2019). Integration of HYDRUS-1D and MODFLOW for evaluating the dynamics of salts and nitrogen in groundwater under long-term reclaimed water irrigation. *Irrigation Science*, *37*(1), 35–47. https://doi.org/10.1007/s00271-018-0600-1

Machiwal, D., Jha, M. K., Singh, V. P., & Mohan, C. (2018). Assessment and mapping of groundwater vulnerability to pollution: Current status and challenges. *Earth-Science Reviews*. Elsevier B.V. https://doi.org/10.1016/j.earscirev.2018.08.009

Mádl-Szőnyi, J., & Füle, L. (1998). Groundwater vulnerability assessment of the SW Trans-

Danubian Central range, Hungary. *Environmental Geology*, *35*(1), 9–18. https://doi.org/10.1007/s002540050287

Mahanta, A. R., Rawat, K. S., Singh, S. K., Sanjeevi, S., & Mishra, A. K. (2022). Evaluation of long-term nitrate and electrical conductivity in groundwater system of Peninsula, India. *Applied Water Science*, *12*(2), 17. https://doi.org/10.1007/s13201-021-01568-1

Maidment, D.R., (1993). *GIS and hydrological modeling*. In: Goodchild, M.F., Parks, B., Steyaert, L. (Eds.), Environmental Modeling with GIS. Oxford University Press, New York, pp. 147-167.

Maier, H. R., & Dandy, G. C. (2000). Neural networks for the prediction and forecasting of water resources variables: A review of modelling issues and applications. *Environmental Modelling and Software*, *15*(1), 101–124. https://doi.org/10.1016/S1364-8152(99)00007-9

Majandang, J., & Sarapirome, S. (2013). Groundwater vulnerability assessment and sensitivity analysis in Nong Rua, Khon Kaen, Thailand, using a GIS-based SINTACS model. *Environmental Earth Sciences*, *68*(7), 2025–2039. https://doi.org/10.1007/s12665-012-1890-x

Maleky, S., Faraji, M., Hashemi, M., & Esfandyari, A. (2025). Investigation of groundwater quality indices and health risk assessment of water resources of Jiroft city, Iran, by machine learning algorithms. *Applied Water Science*,*15*(1). https://doi.org/10.1007/s13201-024-02330-z

Malik, P., & Svasta, J. (1999). REKS: an alternative method of Karst groundwater vulnerability estimation. In Proc., Hydrogeology and Land Use Management- XXIX Congress of the International Association of Hydrogeologists, Bratislava, Slovakia, 79–85.

Malik, R. P. S. (2000). Agriculture and water quality in India towards sustainable management. *Water quality management and control of water pollution*, 73-85.

Mallik, S., Chakraborty, A., Mishra, U., & Paul, N. (2022). Prediction of irrigation water suitability using geospatial computing approach: a case study of Agartala city, India. *Environmental Science and Pollution Research. 30*(55): 116522-116537.https://doi.org/10.1007/s11356-022-21232-8

Mangin, A. (1973). Sur la dynamique des transferts en aquifere karstique. In *Proceedings of the Sixth International Congress of Speleology, Olomouc* (Vol. 4, pp. 157-162).

Mangin, A. (1975). *Contribution à l'étude hydrodynamique des aquifères karstiques*. Doctoral dissertation, Université de Dijon.

Mansell, R. S., Bloom, S. A., & Sun, G. (2000). A model for wetland hydrology: Description and validation. *Soil Science*, *165*(5), 384–397. https://doi.org/10.1097/00010694-200005000-00002

Maqsoom, A., Aslam, B., Khalil, U., Ghorbanzadeh, O., Ashraf, H., Tufail, R. F., Farooq D., & Blaschke, T. (2020). A GIS-based DRASTIC Model and an Adjusted DRASTIC

Model (DRASTICA) for Groundwater Susceptibility Assessment along the China–Pakistan Economic Corridor (CPEC) Route. *ISPRS International Journal of Geo-Information*, *9*(5). https://doi.org/10.3390/ijgi9050332

Marghade, D., Malpe, D. B., & Zade, A. B. (2012). Major ion chemistry of shallow groundwater of a fast growing city of Central India. *Environmental Monitoring and Assessment*, *184*(4), 2405–2418. https://doi.org/10.1007/s10661-011-2126-3

Marghade, D., Malpe, D. B., Subba Rao, N., & Sunitha, B. (2020). Geochemical assessment of fluoride enriched groundwater and health implications from a part of Yavtmal District, India. *Human and Ecological Risk Assessment: An International Journal*, *26*(3), 673–694. https://doi.org/10.1080/10807039.2018.1528862

Martin, P. H., LeBoeuf, E. J., Dobbins, J. P., Daniel, E. B., & Abkowitz, M. D. (2005, December). Interfacing GIS with water resource models: A state-of-the-art review. *Journal of the American Water Resources Association*. https://doi.org/10.1111/j.1752-1688.2005.tb03813.x

Masood, A., Aslam, M., Pham, Q. B., Khan, W., & Masood, S. (2022). Integrating water quality index, GIS and multivariate statistical techniques towards a better understanding of drinking water quality. *Environmental Science and Pollution Research*, *29*(18), 26860–26876. https://doi.org/10.1007/s11356-021-17594-0

Mattson, S., & Wiklander, L. (1940) The laws of soil colloidal behavior: XXI A. The Amphoteric points, the pH, and the donnan equilibrium. *Soil Science, 49*(2), 109-154.

Meireles, A. C. M., Andrade, E. M. de, Chaves, L. C. G., Frischkorn, H., & Crisostomo, L. A. (2010). A new proposal of the classification of irrigation water. *Revista Ciência Agronômica*, *41*(3), 349–357. https://doi.org/10.1590/s1806-66902010000300005

Mendoza, J. A., & Barmen, G. (2006). Assessment of groundwater vulnerability in the Río Artiguas basin, Nicaragua. *Environmental Geology*, *50*(4), 569–580. https://doi.org/10.1007/s00254-006-0233-1

Mercado, A. (1976). Nitrate and chloride pollution of aquifers: A regional study with the aid of a single-cell model. *Water Resources Research*, *12*(4), 731–747. https://doi.org/10.1029/WR012i004p00731

Merkel, B. J., Planer-Friedrich, B., & Nordstrom, D. K. (2005). *Groundwater geochemistry: A practical guide to modeling of natural and contaminated aquatic systems*. Springer. https://doi.org/10.1007/b138774

Merwade, V., Cook, A., & Coonrod, J. (2008). GIS techniques for creating river terrain models for hydrodynamic modeling and flood inundation mapping. *Environmental Modelling and Software*, *23*(10–11), 1300–1311. https://doi.org/10.1016/j.envsoft.2008.03.005

Michael, H. A., & Voss, C. I. (2009). Controls on groundwater flow in the Bengal Basin of India and Bangladesh: Regional modeling analysis. *Hydrogeology Journal*, *17*(7), 1561–1577. https://doi.org/10.1007/s10040-008-0429-4

Miglani, P., Aggarwal, R., & Kaur, S. (2015). Groundwater Simulation Model for Sirhind

Canal Tract of Punjab. *Journal of Engineering & Technology*, 5(1).

Minhas, P. S., Qadir, M., & Yadav, R. K. (2019). Groundwater irrigation induced soil sodification and response options. *Agricultural Water Management*. *215,* 74-85. Elsevier B.V. https://doi.org/10.1016/j.agwat.2018.12.030

Mirzaei, R., & Sakizadeh, M. (2016). Comparison of interpolation methods for the estimation of groundwater contamination in Andimeshk-Shush Plain, Southwest of Iran. *Environmental Science and Pollution Research*, *23*(3), 2758–2769. https://doi.org/10.1007/s11356-015-5507-2

Misstear, B., Vargas, C. R., Lapworth, D., Ouedraogo, I., & Podgorski, J. (2022). A global perspective on assessing groundwater quality. *Hydrogeology Journal*. https://doi.org/10.1007/s10040-022-02461-0

Moreno-Gómez, M., Pacheco, J., Liedl, R., & Stefan, C. (2018). Evaluating the applicability of European karst vulnerability assessment methods to the Yucatan karst, Mexico. *Environmental Earth Sciences*, *77*(19). https://doi.org/10.1007/s12665-018-7869-5

Morio, M., Finkel, M., & Martac, E. (2010). Flow guided interpolation - A GIS-based method to represent contaminant concentration distributions in groundwater. *Environmental Modelling and Software*, *25*(12), 1769–1780. https://doi.org/10.1016/j.envsoft.2010.05.018

Mostaza-Colado, D., Carreño-Conde, F., Rasines-Ladero, R., & Iepure, S. (2018). Hydrogeochemical characterization of a shallow alluvial aquifer: 1 baseline for groundwater quality assessment and resource management. *Science of the Total Environment*, *639*, 1110–1125. https://doi.org/10.1016/j.scitotenv.2018.05.236

Mukherjee, A., & Fryar, A. E. (2008). Deeper groundwater chemistry and geochemical modeling of the arsenic affected western Bengal basin, West Bengal, India. *Applied Geochemistry*, 23(4), 863–894. https://doi.org/10.1016/j.apgeochem.2007.07.011

Murtaza, G., Rehman, M. Z., Qadir, M., Shehzad, M. T., Zeeshan, N., Ahmad, H. R., Farooqi, Z. R., & Naidu, R. (2021). High residual sodium carbonate water in the Indian subcontinent: concerns, challenges and remediation. *International Journal of Environmental Science and Technology, 18*, 3257–3272. https://doi.org/10.1007/s13762-020-03066-4

National Remote Sensing Centre. (2014). Technical Document on Land Use / Land Cover: Database for Dissemination through Bhuvan. https://bhuvan-app1.nrsc.gov.in/2dresources/thematic/LULC503/lulc.pdf.

Nayak, P., Mohanty, A. K., Samal, P., Khaoash, S., & Mishra, P. (2023). Groundwater Quality, Hydrogeochemical Characteristics, and Potential Health Risk Assessment in the Bhubaneswar City of Eastern India. *Water, Air, and Soil Pollution*, *234*(9). https://doi.org/10.1007/s11270-023-06614-z

Nelson, E.J., (1997). *WMS v5.0 Reference Manual*, Environmental Modeling Research Laboratory. Brigham Young University, Provo, Utah.

Nguyet, V. T. M., & Goldscheider, N. (2006). A simplified methodology for mapping groundwater vulnerability and contamination risk, and its first application in a tropical karst area, Vietnam. *Hydrogeology Journal*, *14*(8), 1666–1675. https://doi.org/10.1007/s10040-006-0069-5

Nikolaou, G., Neocleous, D., Christophi, C., Heracleous, T., & Markou, M. (2020). Irrigation groundwater quality characteristics: A case study of Cyprus. *Atmosphere*, *11*(3), 302. https://doi.org/10.3390/atmos11030302

Noori, A. R., & Singh, S. K. (2024). Assessment of seasonal groundwater quality variation employing GIS and statistical approaches in Kabul basin, Afghanistan. *Environment, Development and Sustainability*, *26* (2). https://doi.org/10.1007/s10668-022-02876-5

Olivera, F., Valenzuela, M., Srinivasan, R., Choi, J., Cho, H., Koka, S., & Agrawal, A. (2006). ArcGIS-SWAT: A geodata model and GIS interface for SWAT. *Journal of the American Water Resources Association*, *42*(2), 295–309. https://doi.org/10.1111/j.1752-1688.2006.tb03839.x

Padhi, S., Rangarajan, R., Rajeshwar, K., Sonkamble, S., & Venkatesam, V. (2017). Assessment of hydro-geochemical evolution mechanism and suitability of groundwater for domestic and irrigation use in and around Ludhiana city, Punjab, India. *The Journal of Indian Geophysical Union, 21*(4), 260-270.

Panagopoulos, G. P., Antonakos, A. K., & Lambrakis, N. J. (2006). Optimization of the DRASTIC method for groundwater vulnerability assessment via the use of simple statistical methods and GIS. *Hydrogeology Journal*, *14*(6), 894–911. https://doi.org/10.1007/s10040-005-0008-x

Panchabhai, R. C., & Mondal, N. C. (2024). Hydrochemical insights of groundwater for drinking, agriculture and potential nitrate threats in a part of Western India. *Environmental Earth Sciences*, *83*(15). https://doi.org/10.1007/s12665-024-11758-0

Pandey, A. K., Kumar, R., & Singh, M. K. (2018). Solution to advection–dispersion equation for the heterogeneous medium using Duhamel's principle. In *Lecture notes in mechanical engineering* (pp. 559–571). Springer. https://doi.org/10.1007/978-981-10-5329-0_42

Parween, S., Olbert, A. I., Bamal, A., Sajib, A. M., Diganta, M. T. M., Hasan, M. A., … Uddin, M. G. (2026). Advancing groundwater quality assessment in Siliguri City of India through the RMS-WQI model incorporating the data-driven approaches. *City and Environment Interactions*, *29*. https://doi.org/10.1016/j.cacint.2025.100270

Patil, S. B., & Chore, H. S. (2014). Contaminant transport through porous media: An overview of experimental and numerical studies. *Advances in Environmental Research*, *3*(1), 45–69. https://doi.org/10.12989/aer.2014.3.1.045

Petelet-Giraud, E., Dörfliger, N., & Crochet, P. (2000). RISKE: Méthode d'évaluation multicritère de la vulnérabilité des aquifères karstiques. Application aux systèmes des Fontanilles et Cent-Fonts (Hérault, Sud de la France). *Hydrogéologie, 4*, 71–88.

Pétré, M. A., Rivera, A., & Lefebvre, R. (2019). Numerical modeling of a regional

groundwater flow system to assess groundwater storage loss, capture and sustainable exploitation of the transboundary Milk River Aquifer (Canada – USA). *Journal of Hydrology*, *575*, 656–670. https://doi.org/10.1016/j.jhydrol.2019.05.057

Pavelic, P., Dillon, P. J., Narayan, K. A., Herrmann, T. N., & Barnett, S. R. (1997). Integrated groundwater flow and agronomic modelling for management of dryland salinity of a coastal plain in southern Australia. *Agricultural Water Management*, *35*(1–2), 75–93. https://doi.org/10.1016/S0378-3774(97)00027-9

Pinder, G. F. (2002). *Groundwater modeling using geographical information systems*. John Wiley & Sons.

Pinder, G. F., & Cooper, H. H. (1970). A Numerical Technique for Calculating the Transient Position of the Saltwater Front. *Water Resources Research*, *6*(3), 875–882. https://doi.org/10.1029/WR006i003p00875

Piper, A. M. (1944). A graphic procedure in the geochemical interpretation of water-analyses. *Eos, Transactions American Geophysical Union*, *25*(6), 914–928. https://doi.org/10.1029/TR025i006p00914

Plagnes, V., Théry, S., Fontaine, L., Bakalowicz, M., & Dörfliger, N. (2005). Karst vulnerability mapping: Improvement of the RISKE method. *Water Resources Environmental Problems in Karst.*

Polemio, M., Casarano, D., & Limoni, P. P. (2009). Karstic aquifer vulnerability assessment methods and results at a test site (Apulia, southern Italy). *Natural Hazards and Earth System Sciences*, *9*(4), 1461-1470. https://doi.org/10.5194/nhess-9-1461-2009

Pranville, J., Plagnes, V., Rejiba, F., & Trémoulet, J. (2008). Cartographie de la vulnérabilité sur la partie sud du causse de Gramat: application de la méthode RISKE 2. [Vulnerability mapping in the southern part of the Causse of Gramat: application of the method RISKE 2]. *Géologues*, 156, 44–48.

Prasun, A., & Singh, A. (2025). Assessment of groundwater contamination in Aurangabad, Bihar using WQI and geostatistical modeling. Stochastic Environmental Research and Risk Assessment, 39(2), 789–811. https://doi.org/10.1007/s00477-024-02901-1

Promilton, A. A. A., Ravindran, A. A., Pitchaimani, V. S., Kingston, J. V., & Karuppannan, S. (2025). Comprehensive hydrogeochemical characterization and seasonal water quality index analysis for sustainable groundwater management in Valliyur region, Southern Tamil Nadu, India. *Scientific Reports*, *15*(1), 33251. https://doi.org/10.1038/s41598-025-18285-3

Pusatli, O. T., Camur, M. Z., & Yazicigil, H. (2009). Susceptibility indexing method for irrigation water management planning: Applications to K. Menderes river basin, Turkey. *Journal of Environmental Management*, *90*(1), 341–347. https://doi.org/10.1016/j.jenvman.2007.10.002

Rajmohan, N., & Elango, L. (2004). Identification and evolution of hydrogeochemical processes in the groundwater environment in an area of the Palar and Cheyyar River Basins, Southern India. *Environmental Geology*, *46*(1), 47–61.

https://doi.org/10.1007/s00254-004-1012-5

Ram, A., Tiwari, S. K., Pandey, H. K., Chaurasia, A. K., Singh, S., & Singh, Y. V. (2021). Groundwater quality assessment using water quality index (WQI) under GIS framework. *Applied Water Science*, *11*(2), 46. https://doi.org/10.1007/s13201-021-01376-7

Ramos Leal, J. A., Noyola Medrano, C., & Tapia Silva, F. O. (2010). Aquifer vulnerability and groundwater quality in mega cities: Case of the Mexico Basin. *Environmental Earth Sciences*, *61*(6), 1309–1320. https://doi.org/10.1007/s12665-009-0434-5

Ranabhat, S., Awasthi, M. P., Phuyal, P., Khatri, S., Thapa, L. B., Yadav, R. K. P., & Pant, R. R. (2025). Hydrochemical modeling and water quality assessment of Chepe River (Nepal): Exploring the water-environment nexus. Environmental Earth Sciences, 84(13), 385. https://doi.org/10.1007/s12665-025-12384-0

Rao, V.V., & Sarma, P.B.S. (1993). Regional groundwater modelling using finite element method: a case study. In *Proc., International Conference on Hydrology and Water Resources*. The Netherlands: Kluwer Academic Publishers.

Ravbar, N., & Goldscheider, N. (2007). Proposed methodology of vulnerability and contamination risk mapping for the protection of Karst aquifers in Slovenia. *Acta Carsologica*, *36*(3), 397–411. https://doi.org/10.3986/ac.v36i3.174

Ravbar, N., & Goldscheider, N. (2009). Comparative application of four methods of groundwater vulnerability mapping in a Slovene karst catchment. *Hydrogeology Journal*, *17*(3), 725–733. https://doi.org/10.1007/s10040-008-0368-0

Reddy, K. R. (2008). Physical and Chemical Groundwater Remediation Technologies. In *Overexploitation and Contamination of Shared Groundwater Resources* (pp. 257–274). Springer Netherlands. https://doi.org/10.1007/978-1-4020-6985-7_12

Reed, P. M., Ellsworth, T. R., & Minsker, B. S. (2004). Spatial interpolation methods for nonstationary plume data. *Groundwater*, *42*(2), 190-202.

Reeve, A. S., Siegel, D. I., & Glaser, P. H. (2000). Simulating vertical flow in large peatlands. *Journal of Hydrology*, *227*(1–4), 207–217. https://doi.org/10.1016/S0022-1694(99)00183-3

Refsgaard, J. C., Thorsen, M., Jensen, J. B., Kleeschulte, S., & Hansen, S. (1999). Large scale modelling of groundwater contamination from nitrate leaching. *Journal of Hydrology*, *221*(3–4), 117–140. https://doi.org/10.1016/S0022-1694(99)00081-5

Reilly, T. E. (1987). *A conceptual framework for ground-water solute-transport studies with emphasis on physical mechanisms of solute movement*. (Report No. 87- 4191). Department of the Interior, US Geological Survey.

Reimann, C., & Filzmoser, P. (2000). Normal and lognormal data distribution in geochemistry: Death of a myth. Consequences for the statistical treatment of geochemical and environmental data. *Environmental Geology*, *39*(9), 1001–1014. https://doi.org/10.1007/s002549900081

Reimann, C., Filzmoser, P., & Garrett, R. G. (2002). Factor analysis applied to regional geochemical data: Problems and possibilities. *Applied Geochemistry*, *17*(3), 185–206. https://doi.org/10.1016/S0883-2927(01)00066-X

Reimann, C., Filzmoser, P., Garrett, R. G., & Dutter, R. (2008). Principal Component Analysis (PCA) and Factor Analysis (FA). In *Statistical Data Analysis Explained* (pp. 211–232). John Wiley & Sons, Ltd. https://doi.org/10.1002/9780470987605.ch14

Restrepo, J. I., Montoya, A. M., & Obeysekera, J. (1998). A wetland simulation module for the MODFLOW ground water model. *Ground Water*, *36*(5), 764–770. https://doi.org/10.1111/j.1745-6584.1998.tb02193.x

Rezaei, M., Nikbakht, M., & Shakeri, A. (2017). Geochemistry and sources of fluoride and nitrate contamination of groundwater in Lar area, south Iran. *Environmental Science and Pollution Research*, *24*(18), 15471–15487. https://doi.org/10.1007/s11356-017-9108-0

Rezig, A., Marinangeli, L., & Saggai, S. (2022). Comparative study for assessing vulnerability to pollution in El Asnam plain, North of Algeria. *Water Supply*, *22*(6), 5894–5914. https://doi.org/10.2166/ws.2022.216

Ribeiro, L., Pindo, J. C., & Dominguez-Granda, L. (2017). Assessment of groundwater vulnerability in the Daule aquifer, Ecuador, using the susceptibility index method. *Science of the Total Environment*, *574*, 1674–1683. https://doi.org/10.1016/j.scitotenv.2016.09.004

Rodell, M., Velicogna, I., & Famiglietti, J. S. (2009). Satellite-based estimates of groundwater depletion in India. *Nature*, *460*(7258), 999–1002. https://doi.org/10.1038/nature08238

Rundquist, D. C., Peters, A. J., Rodekohr, D. A., Ehrman, R. L., & Murray, G. (1991). Statewide groundwater-vulnerability assessment in nebraska using the drastic/GIS model. *Geocarto International*, *6*(2), 51–58. https://doi.org/10.1080/10106049109354307

Rustam, F., Ishaq, A., Kokab, S. T., de la Torre Diez, I., Mazón, J. L. V., Rodríguez, C. L., & Ashraf, I. (2022). An Artificial Neural Network Model for Water Quality and Water Consumption Prediction. *Water (Switzerland)*, *14*(21). https://doi.org/10.3390/w14213359

Saatsaz, M., & Eslamian, S. (2020). Groundwater modeling and its concepts, classifications, and applications for solute transport simulation in saturated porous media. In *Advances in Hydrogeochemistry Research*. https://doi.org/10.13140/RG.2.2.11923.71200

Saba, N.U., Umar, R., & Ahmed, S. (2016). Assessment of groundwater quality of major industrial city of Central Ganga plain, Western Uttar Pradesh, India through mass transport modeling using chloride as contaminant. *Groundwater for Sustainable Development*, *2–3*, 154–168. https://doi.org/10.1016/j.gsd.2016.08.002

Sadeqi, D. (2023). An integrated approach to address the temporal variation of geochemistry in groundwater of an arid region. *Environmental Monitoring and Assessment*, **195**,

251. https://doi.org/10.1007/s10661-022-10874-3

Sahoo, S., & Sahoo, B. (2019). A geomorphology-based integrated stream–aquifer interaction model for semi-gauged catchments. *Hydrological Processes*, *33*(9), 1362–1377. https://doi.org/10.1002/hyp.13406

Saidi, S., Bouri, S., & Dhia, H. B. (2010). Groundwater vulnerability and risk mapping of the hajeb-jelma aquifer (central Tunisia) using a GIS-based drastic model. *Environmental Earth Sciences*, *59*(7), 1579–1588. https://doi.org/10.1007/s12665-009-0143-0

Saitoh, S. I., Mugo, R., Radiarta, I. N., Asaga, S., Takahashi, F., Hirawake, Ishikawa, Y., Awaji T., In T., & Shima, S. (2011). Some operational uses of satellite remote sensing and marine GIS for sustainable fisheries and aquaculture. *ICES Journal of Marine Science*, *68*(4), 687–695. https://doi.org/10.1093/icesjms/fsq190

Saleem, M., Hussain, A., & Mahmood, G. (2016). Analysis of groundwater quality using water quality index: A case study of greater Noida (Region), Uttar Pradesh (U.P), India. *Cogent Engineering*, *3*(1). https://doi.org/10.1080/23311916.2016.1237927

Samper, J., Pisani, B., Alvares, D., & García, M. A. (2007). GIS-BALAN: un modelo hidrológico semi-distribuido acoplado a un sistema de información geográfica para la estimación de los recursos hídricos. *Estudios de la Zona no Saturada del Suelo*, *8*, 341-346.

Sankararamakrishnan, N., Sharma, A. K., & Iyengar, L. (2008). Contamination of nitrate and fluoride in ground water along the Ganges Alluvial Plain of Kanpur district, Uttar Pradesh, India. *Environmental Monitoring and Assessment*, *146*(1–3), 375–382. https://doi.org/10.1007/s10661-007-0085-5

Sarker, M. A. R., Chowdhury, M. A. H., Haque, M. T., Rahman, M. M., Meftaul, I. M., & Jubayer, M. F. (2025). From data to decision: leveraging machine learning and water quality index for groundwater quality evaluation. *Sustainable Water Resources Management*, *11*(5), 102. https://doi.org/10.1007/s40899-025-01276-7

Sarma, R., & Singh, S. K. (2021). Simulating contaminant transport in unsaturated and saturated groundwater zones. *Water Environment Research*, *93*(9), 1496-1509. https://doi.org/10.1002/wer.1555

Sarma, R., & Singh, S. K. (2022). A Comparative Study of Data-driven Models for Groundwater Level Forecasting. *Water Resources Management*, *36*(8), 2741–2756. https://doi.org/10.1007/s11269-022-03173-6

Sarma, R., & Singh, S. K. (2023). Assessment of groundwater quality and human health risks of nitrate and fluoride contamination in a rapidly urbanizing region of India. *Environmental Science and Pollution Research*, *30*(19), 55437–55454. https://doi.org/10.1007/s11356-023-26204-0

Sathe, S. S., and Mahanta, C. (2019). Groundwater flow and arsenic contamination transport modeling for a multi aquifer terrain: Assessment and mitigation strategies. *Journal of Environmental Management*, *231*, 166–181. https://doi.org/10.1016/j.jenvman.2018.08.057

Sauerwein, H. (1967). Numerical calculations of multidimensional and unsteady flows by the method of characteristics. *Journal of Computational Physics*, *1*(3), 406–432. https://doi.org/10.1016/0021-9991(67)90048-4

Sawyer, C. N., McCarty, P. L. & Parkin, G.E. (1994). *Chemistry for Environmental Engineering* (4th ed.). McGraw-Hill.

Schmoll, O., Howard, G., Clinton J. & Chorus, I. (Eds.). (2013). *Protecting Groundwater for Health: Managing the Quality of Drinking-water Sources*. IWA Publishing. https://doi.org/10.2166/9781780405810

Schoeller, H. (1965). Qualitative evaluation of groundwater resources. In *Methods and Techniques of Groundwater Investigations and Development* (pp.54-83). The United Nations Educational, Scientific and Cultural Organization.

Schofield, R.K. (1947). A ratio law governing the equilibrium of cations in the soil solution. *Proceedings of the 11th International Congress Pure Applied Chemistry, London, 3*, 257–261.

Secunda, S., Collin, M. L., & Melloul, A. J. (1998). Groundwater vulnerability assessment using a composite model combining DRASTIC with extensive agricultural land use in Israel's Sharon region. *Journal of Environmental Management*, *54*(1), 39–57. https://doi.org/10.1006/jema.1998.0221

Şener, Ş., Şener, E., & Davraz, A. (2017). Evaluation of water quality using water quality index (WQI) method and GIS in Aksu River (SW-Turkey). *Science of the Total Environment*, *584–585*, 131–144. https://doi.org/10.1016/j.scitotenv.2017.01.102

Sengupta, R., Bennett, D., & Wade, G. (1996). Agent mediated links between GIS and spatial modelling software using a model definition language. In proc., GIS/LIS'96—Annual conference and Exposition, p. 295–309.

Senthilkumar, M., & Elango, L. (2004). Three-dimensional mathematical model to simulate groundwater flow in the lower Palar River basin, southern India. *Hydrogeology Journal*, *12*(2), 197–208. https://doi.org/10.1007/s10040-003-0294-0

Seyedmohammadi, J., Esmaeelnejad, L., & Shabanpour, M. (2016). Spatial variation modelling of groundwater electrical conductivity using geostatistics and GIS. *Modeling Earth Systems and Environment*, *2*(4), 1-10. https://doi.org/10.1007/s40808-016-0226-3

Shaffer, M. J., Halvorson, A. D., & Pierce, F. J. (1991). Nitrate Leaching and Economic Analysis Package (NLEAP): Model Description and Application. In *Managing Nitrogen for Groundwater Quality and Farm Profitability* (pp. 285–322). Soil Science Society of America. https://doi.org/10.2136/1991.managingnitrogen.c13

Shamir, U., & Dagan, G. (1971). Motion of the Seawater Interface in Coastal Aquifers: A Numerical Solution. *Water Resources Research*, *7*(3), 644–657. https://doi.org/10.1029/WR007i003p00644

Shamrukh, M., Corapcioglu, M. Y., & Hassona, F. A. A. (2001). Modeling the effect of chemical fertilizers on ground water quality in the Nile Valley Aquifer, Egypt. *Ground*

Water, *39*(1), 59–67. https://doi.org/10.1111/j.1745-6584.2001.tb00351.x

Shanmuharajan, M. B., Aparna, S. B., & Vivek, S. (2023). Groundwater vulnerability assessment phenomenon using drastic & modified drastic modeling validated with nitrate concentration. *Global NEST Journal*, *25*(3), 153-163. https://doi.org/10.30955/gnj.004601

Shao, J.L., Zhao, Z.Z., Cui, Y.L., Wang, R., Li, C.Q., & Yang, Q.Q., (2009). Application of groundwater modeling system to the evaluation of groundwater resources in North China plain. *Resources Science*, 313, 361-367 (in Chinese). https://doi.org/10.1007/s00254-007-1095-x

Shirazi, S. M., Imran, H. M., Akib, S., Yusop, Z., & Harun, Z. B. (2013). Groundwater vulnerability assessment in the Melaka State of Malaysia using DRASTIC and GIS techniques. *Environmental Earth Sciences*, *70*(5), 2293–2304. https://doi.org/10.1007/s12665-013-2360-9

Shlomi, S., & Michalak, A. M. (2007). A geostatistical framework for incorporating transport information in estimating the distribution of a groundwater contaminant plume. *Water Resources Research*, *43*(3). https://doi.org/10.1029/2006WR005121

Sidhu B.S., Sharda R., & Singh S. (2020). A Study of Availability and Utilization of Water Resources in Punjab. *Current World Environment*, *15*(3), 18. http://dx.doi.org/10.12944/CWE.15.3.18

Sidhu, N., Kaur, L., Rishi, M. S., Din, S. N. U., Tewari, K., & Singh, P. (2024). Integrating multivariate hydrogeochemical analysis with human health risk assessment: An inverse geochemical and statistical modeling approach. Journal of Geochemical Exploration, 258, 107389. https://doi.org/10.1016/j.gexplo.2024.107389

Siegel, D. I. (1983). Ground Water and the Evolution of Patterned Mires, Glacial Lake Agassiz Peatlands, Northern Minnesota. *The Journal of Ecology*, *71*(3), 913. https://doi.org/10.2307/2259601

Silver, S. E. (2014). Getting Out of Squaresville: MODFLOW USG Tools for ArcGIS. In *ESRI international user conference*. http://proceedings.esri.com/library/userconf/proc14/papers/1071_188.pdf

Singh, A., Srivastav, S. K., Kumar, S., & Chakrapani, G. J. (2015). A modified-DRASTIC model (DRASTICA) for assessment of groundwater vulnerability to pollution in an urbanized environment in Lucknow, India. *Environmental Earth Sciences*, *74*(7), 5475–5490. https://doi.org/10.1007/s12665-015-4558-5

Singh, C. K., Kumar, A., Shashtri, S., Kumar, A., Kumar, P., & Mallick, J. (2017). Multivariate statistical analysis and geochemical modeling for geochemical assessment of groundwater of Delhi, India. *Journal of Geochemical Exploration*, *175*, 59–71. https://doi.org/10.1016/j.gexplo.2017.01.001

Singh, D. D., Sharma, M., Sahoo, S., & John, S. (2019a). Geospatial analysis of groundwater quality in Ludhiana, Punjab (India). *Journal of Geography, Environment and Earth Science International,* *20*(3), JGEESI.48345.

https://doi.org/10.9734/jgeesi/2019/v20i3 30105

Singh, G., Rishi, M. S., & Arora, N. K. (2019b). Integrated GIS-based modelling approach for irrigation water quality suitability zonation in parts of Satluj River Basin, Bist Doab region, North India. *SN Applied Sciences*, *1*(11). https://doi.org/10.1007/s42452-019-1405-4

Singh, R.B., & Punj, N.K. (1999). Quaternary geology and geomorphology of Ludhiana district, Punjab. *Gondwana Geological Magazine, 14*(2), 19-26.

Singh, R., Venkatesh, A. S., Syed, T. H., Reddy, A. G. S., Kumar, M., & Kurakalva, R. M. (2017). Assessment of potentially toxic trace elements contamination in groundwater resources of the coal mining area of the Korba Coalfield, Central India. *Environmental Earth Sciences*, *76*(16). https://doi.org/10.1007/s12665-017-6899-8

Singh, S. (2005). *Simulation Modeling for optimum use of water resources and nitrate pollution of groundwater in Punjab (Bist Doab tract)*. Ph.D Thesis. Panjab University.

Singh, S. K., & Noori, A. R. (2022). Groundwater quality assessment and modeling utilizing water quality index and GIS in Kabul Basin, Afghanistan. *Environmental Monitoring and Assessment*, *194*(10). https://doi.org/10.1007/s10661-022-10340-0

Smart, P.L., & Friedrich, H. (1986). Water movement and storage in the unsaturated zone of a maturely karstified carbonate aquifer, Mendip Hills, England. In Proc., Conf. Environmental Problems of Karst Terranes and Their Solutions, pp 59–87. NWWA, Dublin, Ohio.

Smith, P. N. (1997). Hydrologic data development system. *Transportation Research Record*, (1599), 118–127. https://doi.org/10.3141/1599-15

Snousy, M. G., Wu, J., Su, F., Abdelhalim, A., & Ismail, E. (2022). Groundwater Quality and Its Regulating Geochemical Processes in Assiut Province, Egypt. *Exposure and Health*, *14*(2), 305–323. https://doi.org/10.1007/s12403-021-00445-1

Sondhi, S. K., Rao, N. H., & Sarma, P. B. S. (1989). Assessment of groundwater potential for conjunctive water use in a large irrigation project in India. *Journal of Hydrology*, *107*(1–4), 283–295. https://doi.org/10.1016/0022-1694(89)90062-0

Steyaert, L. T., & Goodchild, M. F. (1994). Integrating geographic information systems and environmental simulation models: a status review. *Environmental Information Management and Analysis*, 333–355. https://doi.org/10.1201/9781482272505-34

Stoppiello, M. G., Lofrano, G., Carotenuto, M., Viccione, G., Guarnaccia, C., and Cascini, L. (2020). A comparative assessment of analytical fate and transport models of organic contaminants in unsaturated soils. *Sustainability (Switzerland)*, *12*(7). https://doi.org/10.3390/su12072949

Strassberg, G., Jones, N. L., & Lemon, A. (2010). Arc Hydro Groundwater Data Model and Tools: Overview and Use Cases. *AQUA Mundi*, *Am02014*, 101–114. https://doi.org/10.4409/Am-018-10-0014

Stylianoudaki, C., Trichakis, I., & Karatzas, G. P. (2022). Modeling Groundwater Nitrate Contamination Using Artificial Neural Networks. *Water (Switzerland)*, *14*(7). https://doi.org/10.3390/w14071173

Sui, D. Z., & Maggio, R. C. (1999). Integrating GIS with hydrological modeling: practices, problems, and prospects. *Computers, environment and urban systems*, *23*(1), 33-51.

Sun, R.J., Weeks, J.B., & Grubb, H.F., (1997). *Bibliography of Regional Aquifer System Analysis Program of the U.S. Geological Survey, 1978-1996*. (Report No. 97-4074). U.S. Geological Survey Water Resources, Austin, Texas.

Sunayana, Kalawapudi, K., Dube, O., & Sharma, R. (2020). Use of neural networks and spatial interpolation to predict groundwater quality. *Environment, Development and Sustainability*, *22*(4), 2801–2816. https://doi.org/10.1007/s10668-019-00319-2

Tait, N. G., Davison, R. M., Whittaker, J. J., Leharne, S. A., & Lerner, D. N. (2004). Borehole Optimisation System (BOS) - A GIS based risk analysis tool for optimising the use of urban groundwater. *Environmental Modelling and Software*, *19*(12), 1111–1124. https://doi.org/10.1016/j.envsoft.2003.11.014

Taşan, S. (2023). Estimation of groundwater quality using an integration of water quality index, artificial intelligence methods and GIS: Case study, Central Mediterranean Region of Turkey. *Applied Water Science*, *13*(1). https://doi.org/10.1007/s13201-022-01810-4

Tay, C. K., Kortatsi, B. K., Hayford, E., & Hodgson, I. O. (2014). Origin of major dissolved ions in groundwater within the Lower Pra Basin using groundwater geochemistry, source-rock deduction and stable isotopes of 2H and 18O. *Environmental Earth Sciences*, *71*(12), 5079–5097. https://doi.org/10.1007/s12665-013-2912-z

Thirumurugan, M., Manoj, S., Gowrisankar, G., & Elango, L. (2018). Hydrogeochemical characteristics and groundwater quality in a weathered rock aquifer in Northern Karnataka, India. *Geochemistry International*, *56*(9), 950–960. https://doi.org/10.1134/S0016702918090100

Todd, D.K., & Mays, L.W., (2005). *Groundwater Hydrology* (3rd ed.). John Wiley & Sons.

Tóth, J. (1963). A theoretical analysis of groundwater flow in small drainage basins. *Journal of Geophysical Research*, *68*(16), 4795–4812. https://doi.org/10.1029/jz068i016p04795

Toth, J. (1970). A conceptual model of the groundwater regime and the hydrogeological environment. *Journal of Hydrology,* 10, 164-176.

Toth, J. (1971). Groundwater discharge: a common generation of diverse geological and morphological phenomena. *Bulletin of the International Association of Scientific Hydrology XVI*, 9-24.

Toth, J. (1972). Properties and manifestations of regional groundwater movement. *In Proc., 24th International Geological Congress, Montreal,* Section 11, 153-163.

Tyson, H.N., & Weber, E.M. (1964). Use of electronic computer in the simulation of dynamic behaviour of groundwater basin. In *Proc., ASCE Water Resources Conference*, Milwaukee, Wisconsin, USA.

Uddin, M. G., Nash, S., & Olbert, A. I. (2021). A review of water quality index models and their use for assessing surface water quality. *Ecological Indicators*, *122*, 107218. https://doi.org/10.1016/j.ecolind.2020.107218

Uddin, M. G., Rana, M. S. P., Diganta, M. T. M., Bamal, A., Sajib, A. M., Abioui, M., ... & Olbert, A. I. (2024). Enhancing groundwater quality assessment in coastal area: A hybrid modeling approach. *Heliyon*, *10*(13). https://doi.org/10.1016/j.heliyon.2024.e33082

Ukah, B. U., Ameh, P. D., Egbueri, J. C., Unigwe, C. O., & Ubido, O. E. (2020). Impact of effluent-derived heavy metals on the groundwater quality in Ajao industrial area, Nigeria: an assessment using entropy water quality index (EWQI). *International Journal of Energy and Water Resources*, *4*(3), 231-244. https://doi.org/10.1007/s42108-020-00058-5

US Salinity Laboratory staff. (1954). *Diagnosis and improvement of saline and alkali soils* (L.A. Richards, ed.). United States Department of Agriculture, Agriculture Handbook no. 60.

Vaezihir, A., & Tabarmayeh, M. (2015). Total vulnerability estimation for the Tabriz aquifer (Iran) by combining a new model with DRASTIC. *Environmental Earth Sciences*, *74*(4), 2949–2965. https://doi.org/10.1007/s12665-015-4327-5

Vaiphei, S. P., Kurakalva, R. M., & Sahadevan, D. K. (2020). Water quality index and GIS-based technique for assessment of groundwater quality in Wanaparthy watershed, Telangana, India. *Environmental Science and Pollution Research*, *27*(36), 45041–45062. https://doi.org/10.1007/s11356-020-10345-7

Van Duijvenbooden, W., & Van Waegeningh, H. G. (Eds.). (1987). *Vulnerability of soil and groundwater to pollutants: Proceedings of the International Conference, Noordwijk aan Zee, The Netherlands, March 30–April 3, 1987* (Verslagen en Mededelingen, No. 38). TNO Committee on Hydrological Research

Van Stempvoort, D., Ewert, L., & Wassenaar, L. (1993). Aquifer vulnerability index: A gis - compatible method for groundwater vulnerability mapping. *Canadian Water Resources Journal*, *18*(1), 25–37. https://doi.org/10.4296/cwrj1801025

Velasco, V., Tubau, I., Vázquez-Suñè, E., Gogu, R., Gaitanaru, D., Alcaraz, M., & Sanchez-Vila, X. (2014). GIS-based hydrogeochemical analysis tools (QUIMET). *Computers and Geosciences*, *70*, 164–180. https://doi.org/10.1016/j.cageo.2014.04.013

Vetrimurugan, E., & Elango, L. (2015). Groundwater Chemistry and Quality in an Intensively Cultivated River Delta. *Water Quality, Exposure and Health*, *7*(2), 125–141. https://doi.org/10.1007/s12403-014-0133-7

Vetrimurugan, E., Senthilkumar, M., & Elango, L. (2017). Solute transport modelling for assessing the duration of river flow to improve the groundwater quality in an

intensively irrigated deltaic region. *International Journal of Environmental Science and Technology*, *14*(5), 1055–1070. https://doi.org/10.1007/s13762-016-1211-0

Vias, J. M., Andreo, B., Perles, J. M., Carrasco, F., Vadillo, I., & Jiménez, P. (2006). Proposed method for groundwater vulnerability mapping in carbonate (karstic) aquifers: the COP method. Application in two pilot sites in Southern Spain. *Hydrogeology Journal*, *14*, 912–925.

Vías, J., Andreo, B., Ravbar, N., & Hötzl, H. (2010). Mapping the vulnerability of groundwater to the contamination of four carbonate aquifers in Europe. *Journal of Environmental Management*, *91*(7), 1500–1510. https://doi.org/10.1016/j.jenvman.2010.02.025

Voutchkova, D. D., Schullehner, J., Rasmussen, P., & Hansen, B. (2021). A high-resolution nitrate vulnerability assessment of sandy aquifers (DRASTIC-N). *Journal of Environmental Management*, *277*. https://doi.org/10.1016/j.jenvman.2020.111330

Vrba, J. & Zaporozec, A. (Editors) (1994). *Guidebook on Mapping Groundwater Vulnerability*. IAH International Contribution for Hydrogeology, Volume 16/94, Heise, Hannover, pp 131.

Wagenet, R. J., & Hutson, J. L. (1986). Predicting the Fate of Nonvolatile Pesticides in the Unsaturated Zone. *Journal of Environmental Quality*, *15*(4), 315–322. https://doi.org/10.2134/jeq1986.00472425001500040001x

Wang, J. L., & Yang, Y. S. (2008). An approach to catchment-scale groundwater nitrate risk assessment from diffuse agricultural sources: A case study in the Upper Bann, Northern Ireland. *Hydrological Processes*, *22*(21), 4274–4286. https://doi.org/10.1002/hyp.7036

Wang, Y., Merkel, B. J., Li, Y., Ye, H., Fu, S., & Ihm, D. (2007). Vulnerability of groundwater in Quaternary aquifers to organic contaminants: A case study in Wuhan City, China. *Environmental Geology, 53*, 479–484. https://doi.org/10.1007/s00254-007-0669-y

Watkins, M. W. (2021). Step 4. In *A Step-by-Step Guide to Exploratory Factor Analysis with SPSS* (pp. 62–65). Routledge. https://doi.org/10.4324/9781003149347-9

Wei, M., Wu, J., Li, W., Zhang, Q., Su, F., & Wang, Y. (2022) Groundwater geochemistry and its impacts on groundwater arsenic enrichment, variation, and health risks in Yongning County, Yinchuan Plain of northwest China. *Exposure and Health*, *14*(2), 219-238. https://doi.org/10.1007/s12403-021-00391-y

Wilcox, L.V. (1955) Classification and use of irrigation waters. United States Department of Agriculture. Circular no. 969. 1955.

Wilcox, L.V., Blair, G.Y., & Bower, C.A. (1954). Effect of bicarbonate on suitability of water for irrigation. Soil Science. 77: 259-266. 1954

Winter, T. C. (1999). Relation of streams, lakes, and wetlands to groundwater flow systems. *Hydrogeology Journal*, *7*(1), 28–45. https://doi.org/10.1007/s100400050178

Wolfe, A. H., & Patz, J. A. (2002). Reactive nitrogen and human health: Acute and long-term

implications. *Ambio, 31*, pp. 120–125. https://doi.org/10.1579/0044-7447-31.2.120

Woo, M. K., & Winter, T. C. (1993). The role of permafrost and seasonal frost in the hydrology of northern wetlands in North America. *Journal of Hydrology*, *141*(1–4), 5–31. https://doi.org/10.1016/0022-1694(93)90043-9

World Bank. (2010). *Deep Wells and Prudence: Towards Pragmatic Action for Addressing Groundwater Overexploitation in India*. The International Bank for Reconstruction and Development/The World Bank.

Singh, G., Rishi, M. S., & Arora, N. K. (2019b). Integrated GIS-based modelling approach for irrigation water quality suitability zonation in parts of Satluj River Basin, Bist Doab region, North India. *SN Applied Sciences*, *1*(11). https://doi.org/10.1007/s42452-019-1405-4

Wu, J., Li, P., Wang, D., Ren, X., & Wei, M. (2020). Statistical and multivariate statistical techniques to trace the sources and affecting factors of groundwater pollution in a rapidly growing city on the Chinese Loess Plateau. *Human and Ecological Risk Assessment*, *26*(6), 1603-1621. https://doi.org/10.1080/10807039.2019.1594156

Wu, W., Yin, S., Liu, H., & Chen, H. (2014). Groundwater Vulnerability Assessment and Feasibility Mapping Under Reclaimed Water Irrigation by a Modified DRASTIC Model. *Water Resources Management*, *28*(5), 1219–1234. https://doi.org/10.1007/s11269-014-0536-z

Xu, D., Li, P., Chen, X., Yang, S., Zhang, P., & Guo, F. (2023). Major ion hydrogeochemistry and health risk of groundwater nitrate in selected rural areas of the Guanzhong Basin, China. *Human and Ecological Risk Assessment: An International Journal*. https://doi.org/10.1080/10807039.2022.2164246

Yadav, A. K., Khan, P., & Sharma, S. K. (2010). Water quality index assessment of groundwater in todaraisingh tehsil of Rajasthan State, India-A greener approach. *E-Journal of Chemistry*, *7*(S1), 419432. https://doi.org/10.1155/2010/419432

Yıldız, S., & Karakuş, C. B. (2020). Estimation of irrigation water quality index with development of an optimum model: a case study. *Environment, Development and Sustainability*, *22*(5), 4771–4786. https://doi.org/10.1007/s10668-019-00405-5

Yilma, M., Kiflie, Z., Windsperger, A., & Gessese, N. (2018). Application of artificial neural network in water quality index prediction: a case study in Little Akaki River, Addis Ababa, Ethiopia. *Modeling Earth Systems and Environment*, *4*(1), 175–187. https://doi.org/10.1007/s40808-018-0437-x

Zaman, M., Shahid, S. A., & Heng, L. (2018). *Guideline for Salinity Assessment, Mitigation and Adaptation Using Nuclear and Related Techniques*. *Guideline for Salinity Assessment, Mitigation and Adaptation Using Nuclear and Related Techniques*. Springer International Publishing. https://doi.org/10.1007/978-3-319-96190-3

Zhang, H., Yang, R., Wang, Y., & Ye, R. (2019). The evaluation and prediction of agriculture-related nitrate contamination in groundwater in Chengdu Plain, southwestern China.

Hydrogeology Journal, *27*(2), 785–799. https://doi.org/10.1007/s10040-018-1886-z

Zhang, J., Huang, W. W., Létolle, R., & Jusserand, C. (1995). Major element chemistry of the Huanghe (Yellow River), China - weathering processes and chemical fluxes. *Journal of Hydrology*, *168*(1–4), 173–203. https://doi.org/10.1016/0022-1694(94)02635-O

Zhao, Y., Lin, L., & Hong, M. (2019). Nitrobenzene contamination of groundwater in a petrochemical industry site. *Frontiers of Environmental Science and Engineering*, *13*(2), 29. https://doi.org/10.1007/s11783-019-1107-6

Zhao, Z., Gao, Z., Liu, J., Luo, Z., Sun, H., Wang, Y., & Li, F. (2024). Hydrochemical characterization and comprehensive water quality assessment of groundwater within the main stream area of Yishu River. Environmental Monitoring and Assessment, 196(6), 512. https://doi.org/10.1007/s10661-024-12669-0

Zhou, J., Li, G., Liu, F., Wang, Y., & Guo, X. (2010). DRAV model and its application in assessing groundwater vulnerability in arid area: A case study of pore phreatic water in Tarim Basin, Xinjiang, Northwest China. *Environmental Earth Sciences*, *60*(5), 1055–1063. https://doi.org/10.1007/s12665-009-0250-y

Zhou, Y., Li, P., Xue, L., Dong, Z., & Li, D. (2020). Solute geochemistry and groundwater quality for drinking and irrigation purposes: a case study in Xinle City, North China. *Geochemistry*, *80*(4), 125609. https://doi.org/10.1016/j.chemer.2020.125609

Zwahlen, F. (2004). *Vulnerability and risk mapping for the protection of carbonate (karst) aquifers, final report (COST action 620)*. European Commission, Directorate-General XII Science. Research and Development, Brussels.

Appendix I

List of Publications

A. Published Research Papers

- Goyal, D., Haritash, A. K., & Singh, S. K. (2021). A comprehensive review of groundwater vulnerability assessment using index-based, modelling and coupling methods. ***Journal of Environmental Management****, 296,* 113161. https://doi.org/10.1016/j.jenvman.2021.113161
- Goyal, D., Haritash, A. K., & Singh, S. K. (2023). Hydrogeochemical characterisation and geospatial analysis of groundwater for drinking water quality in Ludhiana district of Punjab, India. ***Environmental Monitoring and Assessment****, 195* (6), 653. https://doi.org/10.1007/s10661-023-11220-x
- Goyal, D., Haritash, A. K., & Singh, S. K. (2025). Predictive modeling and spatial analysis of irrigation water quality in a key agricultural region: An ANN-based approach. ***Water Environment Research***, 97 (7), e70147. https://doi.org/10.1002/wer.70147

B. Conference Proceeding

- Goyal, D., Haritash, A. K., Singh, S. K. (2024). A Comparative Assessment of the Water Footprint of Agricultural, Industrial and Domestic Practices in India. In: Nagabhatla, N., Mehta, Y., Yadav, B. K., Behl, A., Kumari, M. (Eds.) ***Recent Developments in Water Resources and Transportation Engineering. TRACE 2022***. *Lecture Notes in Civil Engineering, vol 353*. Springer, Singapore. https://doi.org/10.1007/978-981-99-2905-4_13

C. International Conferences

- Goyal, D., Haritash, A. K., Singh, S. K. (2022). 'A Comparative assessment of the water footprint of agricultural, industrial and domestic practices in India' in the 4th International Conference on Trends & Recent Advances in Civil Engineering (**TRACE-2022**) organized by Amity University Uttar Pradesh, Noida during 18th - 19th October, 2022.

- Goyal, D., Haritash, A. K., Singh, S. K. (2023). 'Analysis of groundwater for drinking water quality in Gurdaspur district of Punjab, India' in the 2nd International Conference on Innovations in Clean Energy Technologies (**ICET- 2023**) organized by National Institute of Technology, Bhopal, Madhya Pradesh during 8th - 10th April, 2023.

Appendix II

CURRICULUM VITAE

DEEPALI GOYAL
Email: deepali.goyal16@gmail.com

LinkedIn: linkedin.com/in/deepali-goyal-47210ba4
Google Scholar: scholar.google.com/citations?user=4RNWgm4AAAAJ&hl=en

---

EDUCATION

Ph.D. in Environmental Engineering
Delhi Technological University, New Delhi, India
***Research Title**:* Status of groundwater quality in Ludhiana district of Punjab, India

M.Tech in Water Science & Governance (2014 – 2016)
TERI University, New Delhi, India | CGPA: 8.29/10.0

B.Tech in Food Technology (Hons.) (2010 – 2014)
Punjab Agricultural University, Ludhiana, Punjab, India | CGPA: 7.8/10.0

Class 12th (2010)
DAV Public School, B.R.S. Nagar, Ludhiana, Punjab
Stream: Non-Medical | Marks: 89%

Class 10th (2008)
DAV Public School, B.R.S. Nagar, Ludhiana, Punjab
Marks: 92% | Mathematics: 100/100 (Top 0.1% nationally)

RESEARCH INTERESTS

Groundwater quality assessment | Hydrogeochemical characterization | Geospatial analysis | Water quality indexing | Multivariate statistical analysis | Groundwater modeling | Irrigation water quality | Artificial neural networks for water quality prediction

---

RESEARCH EXPERIENCE

Master's Research Projects (2014 – 2016)

Project 1: Impact assessment of River Rejuvenation Project
Vyakti Vikas Kendra India, The Art of Living International Centre, Bangalore
Duration: January – May 2016

- Documented impacts of Vedavathi River rejuvenation project
- Developed case studies for three villages in Lakya watershed
- Analyzed implementation challenges and lessons learned

Project 2: Water-Energy nexus in context of Water supply in Delhi
Department of Regional Water Studies, TERI University, New Delhi
Duration: June – November 2015

- Assessed energy footprint of water supply infrastructure in Delhi
- Analyzed electricity consumption across abstraction, treatment, transmission, and distribution
- Established interdependency between water and energy sectors

---

PROFESSIONAL CERTIFICATIONS

1. Introduction to GIS – IIT Roorkee (NPTEL) – Gold Certificate (Topper)
2. Digital Elevations Models and Applications – IIT Roorkee (NPTEL) – Gold Certificate (Topper)
3. Remote Sensing and Digital Image Processing – IIT Roorkee (NPTEL) – Gold Certificate (Topper)
4. Programming for Everybody (Python) – University of Michigan (Coursera)
5. Introduction to Programming with MATLAB – Vanderbilt University (Coursera)
6. Applied Groundwater Modeling – Mak Gurukul (2020)
7. Systems Thinking for Enhanced Water Security in Urban India – DTU (GIAN, 2018)
8. Demystifying Environmental and Sustainability Data – AAETI (2024)

AWARDS & HONORS

- Commendable Research Award – Delhi Technological University (2021, 2023)
- UGC-NET JRF – Qualified for Junior Research Fellowship in Environmental Science (January 2018)
- Top 0.1% in Mathematics – Featured for securing 100/100 marks in CBSE Class 10
- Award for Academic Excellence – Three-time recipient during school years
- Merit Scholarship – Seven-year scholarship holder during school education

---

WORK EXPERIENCE

Research Assistant (Volunteer)
@ River Rejuvenation and Projects Department, Vyakti Vikas Kendra India
The Art of Living International Centre, Bangalore
July 2016 – March 2017

Responsibilities:

- Prepared scientific action plans for groundwater recharge site identification using ArcGIS
- Analyzed rainfall data to determine groundwater recharge potential in targeted river basins
- Designed surveys and data collection protocols using SocialCops Collect tool
- Developed proposals for CSR (Corporate Social Responsibility) collaborations

- Collaborated with technical and research teams on comprehensive watershed management plans.

INDUSTRIAL TRAINING

S.S. Bonn Food Industries, Biscuit Plant, Ludhiana
Quality Executive Trainee
January – May 2014

- Worked in Procurement, Quality Control, and Production sections
- Conducted shelf-life stability studies of biscuits and cakes

---

ADDITIONAL ACTIVITIES

- Conducted Navchetna and Balchetna workshops for underprivileged communities
- Executed happiness quotient surveys (March–April 2014)
- Participated in "Volunteer for Better India" initiative
